

SPECTROSCOPIC PROPERTIES
OF
CONJUGATED SYSTEMS

A thesis submitted for the
Degree of Doctor of Philosophy
of The University of London

and

The Diploma of Membership
of Imperial College

by

John Charles Packer , B.Sc., A.R.C.S.

Department of Chemistry,
Imperial College,
London, S.W. 7 .

February 1968 .

Acknowledgments.

I would like to thank first my supervisors . The initial portion of the work which is presented here was carried out under the direction of Dr. John Walkley . The latter part has been under the supervision of Dr. John Avery, who has had to tolerate me for the greatest period. Particular thanks go to Dr. Avery for his kindness and encouragement at all times and in all things. The co-operation of Dr. Janos Ladik and his supporting group at the Hungarian Academy of Sciences, Budapest, must also be gratefully recognized. It was Dr. Ladik who initiated the study of the π -electron wave functions of polymeric analogues of DNA which are discussed here.

None of the work reported here would have been possible were it not for a supporting grant from the Scientific Research Council and a generous allocation of time on Imperial College's IBM 7090/1401 electronic computer . I also wish to acknowledge the research facilities provided by Imperial College Chemistry Department.

Finally , but by no means least , grateful thanks must go to my wife, family and friends for their forbearance.

(iii)

Abstract.

The resonance energy transfer of electronic excitation between two weakly coupled molecules is discussed. The energy transfer mechanism between an isolated ground state acceptor and an excited sensitizer is studied in the dipole-dipole approximation, and the limitations of this model noted. Using the single acceptor-sensitizer pair interaction the behaviour of a whole system of transferring species is investigated. A new cell-model is proposed for the statistical treatment of the transfer in solution, and the results of a computer simulation of a random solution presented. The effect of diffusion on the transfer rate is also theoretically investigated.

The time-dependent luminescence of a randomly distributed collection of sensitizer and acceptor molecules is discussed using a Green's function method when the exciting light is an arbitrary function of time. This theory is applied to the interpretation of phase-fluorimetry results.

Theoretical expressions describing the effect of light attenuation in fluorescing solutions are given, and a model for secondary fluorescence and the trivial effect is proposed and tested against experimental results. An account of an apparatus for the observation and measurement of resonance energy transfer is given, and the results of an experimental investigation presented.

The treatment of molecular π -electrons in the semi-

(iv).

empirical self-consistent field (SCF) approximation is discussed. A derivation of the Hartree-Fock SCF equations for both closed-shell ground states and half open-shell states is given. The nature and validity of the semi-empirical SCF approximation and the π - σ electron separability is considered. The Pople-Pariser-Parr approach is followed throughout .

The calculation of spectral properties from the π -electron SCF wave functions of molecules is discussed, and the spin properties of the open-shell methods considered. The application of a spin projection operator in the form of a single annihilator to obtain spin eigen states is also described.

A semi-empirical self-consistent treatment of the π -electrons in polymeric systems with simple translational symmetry is presented , using the crystal orbital Bloch approximation .

FORTTRAN IV computer programs of the SCF molecular and polymer treatments are included , with a description of their particular usage .Results obtained with these programs are finally presented. Theoretical predictions of π -electron properties in molecules and polymers are compared with experimental results. The band widths of helical analogues of DNA were calculated in the delocalized π -electron model.

Contents.

| <u>Chapter I .</u> | Page |
|--|------|
| <u>Resonance Energy Transfer and Related Phenomena.</u> | |
| (1) Introduction | 1 |
| (2) Time-Dependent Perturbation Theory | |
| (a) Introduction | 3 |
| (b) First-Order Perturbation | 5 |
| (c) Second-Order Perturbation | 13 |
| (d) The Perturbation Matrix Element, $ H'_{jk} $. | 15 |
| (3) Resonance Transfer via Dipole-Dipole Coupling | 18 |
| (4) The Break-Down of the Dipole-Dipole Approximation | 30 |
| (5) Resonance Transfer in Solution | |
| (a) Introduction | 35 |
| (b) Sensitizers | |
| (i) General Theory | 37 |
| (ii) The Cell Model: Sensitizers | 42 |
| (iii) Steady-State Illumination | 47 |
| (iv) Sensitizer Lifetimes | 49 |
| (c) Acceptors | |
| (i) General Theory | 50 |
| (ii) Cell Model:Acceptors | 55 |
| (iii) Acceptor Lifetimes | 58 |
| (6) Time-Dependent Fluorescence | 61 |
| (7) Phase-Fluorimetry | 64 |
| (8) Re-Absorption of Fluorescence:Time-Dependent Theory | 67 |
| (9) The Computer Simulation of a Random Solution with Energy Transfer | 70 |

| | Page |
|---|------|
| (10) The Effect of Diffusion on Resonance Transfer | |
| (a) Introduction | 74 |
| (b) The Diffusion Model | 78 |
| (c) Experimental Comparison with the Proposed Model | 94 |
| (11) Some Comments on Resonance Transfer | 95 |
| (12) Light Re-Absorption in Fluorescent Solutions | |
| (a) Primary Fluorescence | 97 |
| (b) Secondary Fluorescence | 106 |
| (c) Experimental Test of Model | 114 |
| (d) The Trivial Effect | 118 |
| (13) A Practical Investigation | |
| (a) Construction of Apparatus | 123 |
| (b) Experimental Investigation of a Transferring System, Fluorescein- Rhodamine-B | 134 |
| (c) Some Conclusions | 139 |

Chapter II .

The Calculation of the Properties of π -Electron Systems.

| | |
|---|-----|
| (1) Introduction | 142 |
| (2) The Schrödinger Wave Equation | 143 |
| (3) The Many-Particle Hamiltonian | 148 |
| (4) Many-Electron Wave Functions | 150 |
| (5) The Variation Principle | 156 |
| (6) The Molecular Orbital Approximation | 159 |
| (7) The σ - π Separation | 160 |

| | Page |
|--|------|
| (8) The Hartree-Fock Equations | 166 |
| (9) The Roothaan Equations | 175 |
| (10) The Goepfert-Mayer and Sklar Core Potential | 178 |
| (11) The Pople-Pariser-Parr Approximation to \bar{F} | 180 |
| (12) The Zero Differential Overlap Approximation | 182 |
| (13) The Parameters | |
| (a) Introduction | 187 |
| (b) The Valence State Ionization Energy, I_p^π | 188 |
| (c) The Core Resonance Integrals, β_{ij}^c | 189 |
| (d) The Two Centre Coulomb Integrals, $\langle ii jj \rangle$ | 191 |
| (14) Closed-Shell SCF Molecular Properties | |
| (a) Ground State Properties | 193 |
| (b) Excited States | |
| (i) Introduction | 199 |
| (ii) Ionization Potential and Electron Affinity | 199 |
| (iii) Optical Excited States | 204 |
| (iv) Configuration Interaction | 208 |
| (v) Intensities of Electronic Transitions | 216 |
| (15) Comments on the Pople-Pariser-Parr Method | 219 |
| (16) Correlation in the Closed-Shell Approximation | 222 |
| (17) Alternant Hydrocarbons and the Hückel Approximation | 227 |

| | Page |
|--|------|
| (18) Spin-Polarized Self-Consistent Field Theory | |
| (a) Introduction and derivation of SCF Conditions | 231 |
| (b) Spin Properties of Unrestricted Wave Functions | 240 |
| (c) Some Comments on the Spin- Polarized Method | 255 |
| (19) The Open-Shell Self-Consistent Theory of Roothaan | |
| (a) The SCF Conditions | 258 |
| (b) Open-Shell SCF Matrix Elements | 270 |
| (c) Comments on Roothaan's Open- Shell Method | 272 |
| (20) Self-Consistent Wave Functions for Polymeric Systems | 273 |
| <u>Chapter III .</u> | |
| <u>Four Semi-Empirical SCF Computer Programs.</u> | |
| (1) Introduction | 281 |
| (2) The Closed-Shell SCF Program, with Configuration Interaction for Excited States | 283 |
| (3) The Spin-Polarized SCF Program, with Spin Projection | 305 |
| (4) A Program of Roothaan's Open-Shell Procedure | 333 |
| (5) The Polymer SCF Program | 353 |

| <u>Chapter IV .</u> | Page |
|--|------|
| <u>Some Selected Results Obtained with the SCF Semi-Empirical Computer Programs.</u> | |
| (1) Introduction | 371 |
| (2) Selected Results | |
| (a) The Butadiene Molecule | 372. |
| (b) The trans-Butadiene Ion, $C_4H_4^+$ | 384 |
| (c) Benzene | 389 |
| (d) The Benzyl Radical, $C_7H_7^\bullet$ | 394 |
| (e) Naphthalene | 403 |
| (f) The Naphthalene Ions, $C_{10}H_8^+$ | 410 |
| (g) The Allyl Radical | 413 |
| (h) The Nucleotide Bases | 415 |
| (i) The Nucleotide Base-Pairs, G-C and A-T | 426 |
| (j) The Helical Polynucleotides, Poly(A-T), Poly(G-C), and Poly(U) | 436 |
| (3) Comments on the Results | 456 |
| <u>References.</u> | 460 |

CHAPTER I.

RESONANCE ENERGY TRANSFER AND RELATED PHENOMENA.

(I) Introduction.

The first observation of resonance energy transfer was made by Cario and Franck in 1922, (1). They studied the emission spectrum of a mixture of Mercury and Thallium vapour excited by a Mercury-resonance light source, and found it contained Thallium lines as well as the anticipated Mercury components. Since Thallium did not absorb any of the exciting light used, they concluded that the Thallium was indirectly excited by the Mercury atoms. This non-radiative transfer could not be attributed to trivial reabsorption, or collisional effects, and indicated a long-range transfer of excitation across space between the isolated atoms, with Mercury as the "donor" or "sensitizer" and Thallium as the "acceptor".

The mechanism for this transfer was first discussed by J. Perrin,(2), using a classical coupled-oscillator model. This theory was expressed in quantum mechanical terms by F. Perrin,(3), and Kallmann and London,(4). These treatments culminated in Th. Förster's discussion of resonance transfer between vibrationally relaxed sensitizer and acceptor molecules in solution, (5),(6).

In the extensive theoretical discussion which follows we shall consider the evaluation of the transfer rate using

time-dependent perturbation theory and the dipole-dipole approximation. The theory will be applied to bulk systems of acceptors and sensitizers. The time-dependence is explicitly considered, and a new model for the transfer is proposed. Finally we consider some of the experimental problems involved in the study of the phenomena, and illustrate these with an experimental investigation.

(2) Time-dependent Perturbation Theory.

(a) Introduction.

A quantum mechanical treatment of resonance energy transfer involves the use of time-dependent perturbation theory to evaluate the rate of inter-state transition under an applied perturbation.

In the following conventional development of time-dependent perturbation theory, (7), (8), we shall assume the part of the Hamiltonian * which varies with time is small in comparison to the time-independent part, H_0 . Thus we can write our total Hamiltonian as,

$$H(t) = H_0 + H'(t) \quad (\text{I-1})$$

Additionally we presume knowledge of the orthonormal eigenfunctions of the unperturbed time-independent Hamiltonian, H_0 ,

$$H_0 \phi_n = \epsilon_n \phi_n \quad (\text{I-2})$$

For the perturbation problem, as H is now a function of time, we must use the time-dependent Schrödinger equation,

$$i\hbar \frac{\partial \Psi}{\partial t} = H \Psi \quad (\text{I-3})$$

Where $\Psi(t)$ represents the total wave function of the system, and may be expanded in the stationary eigenfunctions of H_0 , except now the time-dependence of $\{\phi_n\}$ must be included,

$$\Psi(t) = \sum_n a_n(t) \phi_n e^{-\frac{\epsilon_n i t}{\hbar}} \quad (\text{I-4})$$

* See the section on Wave Mechanics, Chapter 2., for a fuller discussion of the concepts used here.

The expansion coefficients depend on time, representing the evolution of the new state from the state at $t=0$, (9), and the sum over n includes all the discrete set of eigenfunctions of H_0 together with a continuum for completeness. Substituting $\Psi(t)$ into the perturbed Schrödinger equation we find,

$$\sum_n \left[i\hbar \frac{\partial a_n}{\partial t} \phi_n e^{-\frac{E_n i t}{\hbar}} + a_n E_n \phi_n e^{-\frac{E_n i t}{\hbar}} \right] = \sum_n a_n [H_0 + H'] \phi_n e^{-\frac{E_n i t}{\hbar}} \quad (\text{I-5})$$

Multiplication by ϕ_k^* , followed by integration gives,

$$i\hbar \frac{\partial a_k}{\partial t} e^{-\frac{E_k i t}{\hbar}} = \sum_n a_n e^{-\frac{E_n i t}{\hbar}} \int \phi_k^* H' \phi_n d\tau \quad (\text{I-6})$$

Writing the integral on the left as,

$$\int \phi_k^* H' \phi_n d\tau = H'_{kn} \quad (\text{I-7})$$

where H'_{kn} is referred to as a matrix element of the perturbation and if we also use an angular frequency defined by ,

$$\omega_{kn} = \frac{E_k - E_n}{\hbar} \quad (\text{I-8})$$

then we have,

$$\frac{\partial a_k}{\partial t} = \frac{1}{i\hbar} \sum_n H'_{kn} a_n e^{i\omega_{kn} t} \quad (\text{I-9})$$

To find $a_k(t)$, we express these expansion coefficients as power series in λ ,

$$a_k = a_k(0) + \lambda a_k(1) + \lambda^2 a_k(2) + \dots \quad (\text{I-10})$$

and if we write H' as $\lambda H'$, we find,

$$\begin{aligned} & \frac{\partial a_k(0)}{\partial t} + \lambda \frac{\partial a_k(1)}{\partial t} + \lambda^2 \frac{\partial a_k(2)}{\partial t} + \dots \\ &= \frac{1}{i\hbar} \sum_n H'_{kn} \lambda [a_n(0) + \lambda a_n(1) + \lambda^2 a_n(2) + \dots] e^{i\omega_{kn}t} \end{aligned} \quad (\text{I-11})$$

On equating coefficients, and setting $\lambda = 1$ we have,

$$\begin{aligned} \frac{\partial a_k(0)}{\partial t} &= 0 \\ \frac{\partial a_k(1)}{\partial t} &= \frac{1}{i\hbar} \sum_n H'_{kn} a_n(0) e^{i\omega_{kn}t} \\ \frac{\partial a_k(s+1)}{\partial t} &= \frac{1}{i\hbar} \sum_n H'_{kn} a_n(s) e^{i\omega_{kn}t} \end{aligned} \quad (\text{I-12})$$

These equations can be integrated in principle to approximate for any desired order in the perturbation.

(b) First - Order Perturbation.

The zero - order coefficients, $a_k(0)$, are independent of time, as $\frac{\partial a_k(0)}{\partial t} = 0$, and are hence

constants, giving the initial conditions of the problem, specifying the state of the system before the perturbation is applied. This state may be represented by all but one of the $\{a_k(0)\}$ being zero, thus for a system initially in state j , represented by ϕ_j , then,

$$a_k(0) = \delta_{jk} \quad (\text{I-I3})$$

where δ_{jk} is the Kronecker Delta, defined by $\delta_{jk} = 0$ with $j \neq k$, $\delta_{jk} = 1$ with $j = k$

Hence substituting for $a_k(0)$ in our expression

for $a_k(t)$,

$$\begin{aligned} \frac{\partial a_k(t)}{\partial t} &= \frac{1}{i\hbar} \sum_n H'_{kn} \delta_{jn} e^{i\omega_{kn}t} \\ &= \frac{1}{i\hbar} H'_{kj} e^{i\omega_{kj}t} \end{aligned} \quad (\text{I-I4})$$

and,

$$a_k(t) = \int_0^t H'_{kj} e^{i\omega_{kj}t} dt \quad (\text{I-I5})$$

We have assumed the perturbation is "switched on", at

$t = 0$ and "turned off" at time t , then evaluating the integral at these limits we find,

$$a_k(t) = \frac{H'_{kj}}{\hbar \omega_{kj}} \cdot [e^{i\omega_{kj}t} - 1] \quad (\text{I-I6})$$

In this first - order theory we represent the probability

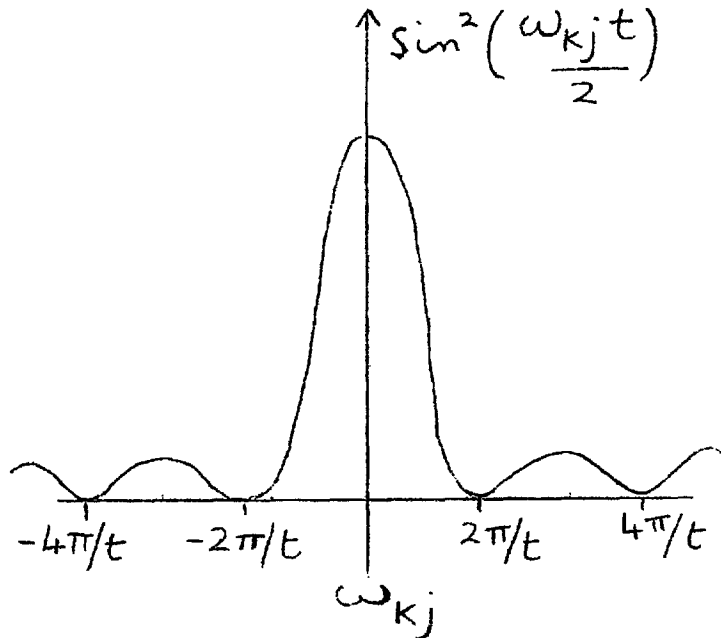
that after time t , under the influence of the perturbation H' , a transition from $\phi_j \rightarrow \phi_k$ will have been induced by $|a_{k(1)}|^2$

$$|a_{k(1)}|^2 = [a_{k(1)}^* a_{k(1)}] = |H'_{kj}|^2 \frac{[e^{i\omega_{kj}t} - 1][e^{-i\omega_{kj}t} - 1]}{\omega_{kj}^2} \quad (\text{I-17})$$

or, expressing the right hand side in terms of a real function,

$$|a_{k(1)}|^2 = 4 |H'_{kj}|^2 \frac{\sin^2 \left[\frac{\omega_{kj}t}{2} \right]}{\omega_{kj}^2} \quad (\text{I-18})$$

The predominance of the transitions with $\omega_{kj} \approx 0$ can be seen from evaluating $\frac{\sin^2(\omega_{kj}t)}{2}$ as a function of ω_{kj} ,



Hence we find the probability for a transition between

two sharp states k and j , represented by the ordinate depends on t^2 . This implies that the transition probability increases quadratically with time, which is not observed physically or expected intuitively. This ambiguity is removed by giving the final state K a finite width, with a density of states, $\rho(\epsilon_K)$. The requirement of a finite width of K is easily fulfilled in real systems as ϕ_K is not exactly stationary. Under the influence of unspecified interactions other than the perturbation, H' , it will be split. We shall assume K acquires the nature of a continuous distribution centred at ω_K , with $\rho(\epsilon_K)d\epsilon_K$ representing the number of K -states with energy between ϵ_K and $\epsilon_K + d\epsilon_K$. Additionally we shall take $\rho(\epsilon_K)$ to be only a weak function of ϵ_K . Then the transition probability per unit time for the transition j to K is given by,

$$P_{(j)} = \int_{-\infty}^{+\infty} |a_{Kj}(t)|^2 \rho(\epsilon_K) d\epsilon_K \quad (\text{I-19})$$

Then, since $H'_{Kj} \cdot \rho(\epsilon_K)$ varies little over the important range, $\epsilon_K \approx \epsilon_j$,

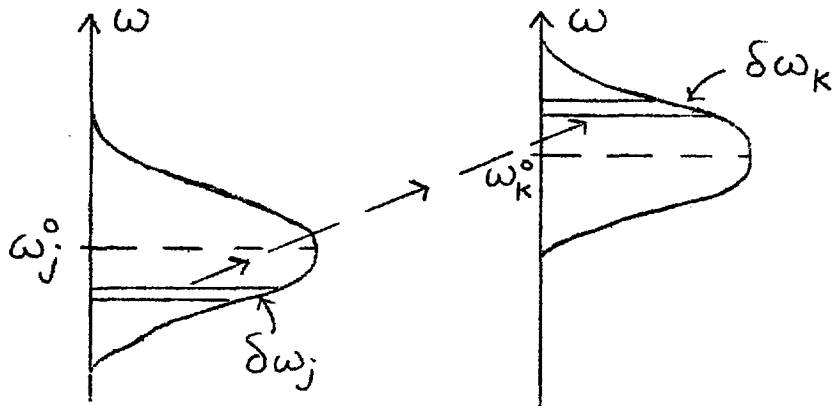
$$P_{(j)} = \frac{2\pi}{\hbar^2} \rho(\epsilon_K) \cdot |H'_{Kj}|^2 \quad (\text{I-20})$$

It will be noticed that the conservation of energy principle

for the transition $j \rightarrow k$ is automatically fulfilled, and does not have to be inserted as a special requirement.

The principle is however suitably modified by the uncertainty relation of Heisenberg, which gives an energy width of $\sim \frac{\hbar}{t}$. We have neglected transients from the "switching on" of the perturbation, and have obtained a probability which is constant per unit time, unlike the "sharp states" transition which increased with time.

Let us now consider transitions between two Lorentzian distributions, centred on ω_j^0 and ω_k^0 , representing the initial state j , and the final state k . The broadening of these corresponds to the coupling of the states with their environments.



We then find the total transfer probability per unit time, which according to our first-order perturbation treatment is given by equation (I-20),

$$P(\omega) = \int_{-\infty}^{+\infty} \frac{\Gamma_j / \pi d\omega_j}{((\omega_j^0 - \omega_j)^2 + \Gamma_j^2)} \int_{-\infty}^{+\infty} |H'_{kj}|^2 \frac{2\pi}{k} \cdot \frac{\Gamma_k / \pi d\omega_k}{((\omega_k^0 - \omega_k)^2 + \Gamma_k^2)} \quad (\text{I-21})$$

Further, on assuming, $\Gamma_j = \Gamma_k = \Gamma$, and also assuming that $|H'_{kj}|$ is not a strong function of ω_k and ω_j ,

$$P(\omega) = \left(\frac{\Gamma}{\pi}\right)^2 |H'_{kj}|^2 \frac{2\pi}{k^2} \iint_{-\infty}^{+\infty} \frac{d\omega_k d\omega_j}{((\omega_j^0 - \omega_j)^2 + \Gamma^2)((\omega_k^0 - \omega_k)^2 + \Gamma^2)} \quad (\text{I-22})$$

Without any further qualifications $P(\omega)$ may now be evaluated by Riemann integration, (8),

$$P(\omega) = \frac{|H'_{kj}|^2 4\Gamma}{k^2((\omega_k^0 - \omega_j^0)^2 + 4\Gamma^2)} \quad (\text{I-23})$$

This result can also be obtained by a simpler route — if we insert the conservation of energy principle, by using the Dirac delta function, $\delta(\omega_k - \omega_j)$. This function has the property,

$$\int_{-\infty}^{+\infty} f(\omega_k, \omega_j) \cdot \delta(\omega_k - \omega_j) d\omega_k = f(\omega_j, \omega_j) \quad (\text{I-24})$$

Hence,

$$\begin{aligned}
 P(1) &= \left(\frac{\Gamma}{\pi}\right)^2 |H'_{kj}|^2 \frac{2\pi}{\mathcal{R}^2} \int_{-\infty}^{+\infty} \frac{\delta(\omega_k - \omega_j) d\omega_k d\omega_j}{((\omega_k^0 - \omega_k)^2 + \Gamma^2)((\omega_j^0 - \omega_j)^2 + \Gamma^2)} \\
 &= \frac{2\Gamma^2}{\pi \mathcal{R}^2} |H'_{kj}|^2 \int_{-\infty}^{+\infty} \frac{d\omega_j}{((\omega_k^0 - \omega_j)^2 + \Gamma^2)((\omega_j^0 - \omega_j)^2 + \Gamma^2)}
 \end{aligned}$$

(I-25)

This is a much easier Riemann integral, and gives the same result as before, equation (I-23).

The case of $\omega_k^0 = \omega_j^0$, can be solved, using the conservation of energy principle, without recourse to complex integration, giving,

$$P(1) = \frac{2\Gamma}{\pi \mathcal{R}^2} |H'_{kj}|^2 \int_{-\infty}^{+\infty} \frac{d\omega_k}{((\omega_k^0 - \omega_k)^2 + \Gamma^2)^2} = \frac{|H'_{kj}|^2}{\Gamma \mathcal{R}^2}$$

(I-26)

It should be realised that these derivations of the transfer probability per unit time ignore initial transient effects from the "switching on" of the perturbation. This is shown by the more rigorous evaluation of the probability, which involves the determination of,

$$P_{(1)} = \frac{1}{t} \int_{-\infty}^{+\infty} \frac{\Gamma_j / \pi d\omega_j}{((\omega_j^0 - \omega_j)^2 + \Gamma^2)} \cdot \int_{-\infty}^{+\infty} \frac{\Gamma_k / \pi d\omega_k}{((\omega_k^0 - \omega_k)^2 + \Gamma^2)} |a_k(t)|^2$$

$$|a_k(t)|^2 = \frac{|H'_{kj}|^2}{\hbar^2} \cdot \frac{(e^{i\omega_{kj}t} - 1)(e^{-i\omega_{kj}t} - 1)}{\omega_{kj}^2} \quad (\text{I-27})$$

Using Riemann integration it is found, (8), with the assumption that $|H'_{kj}|$ is not dependent on ω_k and ω_j ,

$$P_{(1)} = \frac{|H'_{kj}|^2}{\hbar^2} \left\{ \frac{(1 - e^{-i(\omega_k^0 - \omega_j^0 - 2i\Gamma)t})}{(\omega_k^0 - \omega_j^0 - 2i\Gamma)^2} + \frac{(1 - e^{i(\omega_k^0 - \omega_j^0 + 2i\Gamma)t})}{(\omega_k^0 - \omega_j^0 + 2i\Gamma)^2} + \frac{4\Gamma}{((\omega_k^0 - \omega_j^0)^2 + 4\Gamma^2)} \right\} \quad (\text{I-28})$$

The first terms in the curly brackets are the transient terms, decaying rapidly with time, and leaving a constant probability per unit time represented by the last term. This will be recognised as the expression derived in the simpler procedure given earlier.

(c) Second - Order Perturbation.

In this section we are concerned with the magnitude of $a_k(2)$, the second non - zero term in the expansion for $a_k(t)$ given in equation (I-10).

For the transition $j \rightarrow k$, we have $a_k(0) = 0$, and $a_k(1)$ is determined as described in the last section.

The term $a_k(2)$ represents the contribution of second - order processes to the $j \rightarrow k$ transition. Using the recurrence relations for $\frac{\partial a_k(s+1)}{\partial t}$ with the result for $a_k(1)$ we obtain from equations (I-12) and (I - 16),

$$\frac{\partial a_k(2)}{\partial t} = \frac{1}{i\hbar^2} \sum_n \frac{H'_{kn} H'_{nj} (e^{i\omega_{nj}t} - 1) e^{i\omega_{kn}t}}{\omega_{nj}} \quad (\text{I-29})$$

If we have only one state n , with $n = \ell$ for which H_{kn} and H_{nj} are non - zero, on integration we find,

$$a_k(2) = \frac{1}{i\hbar^2} \frac{H'_{k\ell} H'_{\ell j} (e^{i\omega_{kj}t} - e^{i\omega_{k\ell}t})}{\omega_{\ell j}} \quad (\text{I-30})$$

This corresponds to the transition $j \rightarrow k$ passing through an intermediate state, ℓ , coupled to both the initial and final states. Thus it is a three - state interaction effect

which we are considering in the evaluation of these second-order coefficients.

Representing each of the states, $j \rightarrow \rho \rightarrow k$, as a Lorentzian distribution, we require the integral,

$$P(z) = \frac{1}{t} \int_{-\infty}^{+\infty} \int_{-\infty}^{+\infty} \frac{\Gamma_j / \pi d\omega_j}{((\omega_j^0 - \omega_j)^2 + \Gamma_j^2)} \cdot \frac{\Gamma_k / \pi d\omega_k}{((\omega_k^0 - \omega_k)^2 + \Gamma_k^2)} \cdot \frac{\Gamma_e / \pi d\omega_e}{((\omega_e^0 - \omega_e)^2 + \Gamma_e^2)} \cdot a_k(z) a_k^*(z)$$

(I-31)

This has been evaluated explicitly for the case where,

$\Gamma_k = \Gamma_j = \Gamma_e = \Gamma$, and, $\omega_k^0 = \omega_j^0 = \omega_e^0$, using Riemannian integration, (8).

$$P(z) = \frac{|H'_{ke} \cdot H'_{ej}|^2}{k^4 \Gamma^3}$$

(I-32)

This discussion of the second-order process is included so that we have an insight into what conditions militate for the breakdown of the simpler first-order perturbation transfer route. This will be discussed later.

(d) The Perturbation Matrix Element, $|H'_{jk}|$.

As we have established from the discussion of first-order perturbation theory, it is possible for a transition from the state j of a system to the state K to occur, so long as j and K both have the same energy, and are coupled via the perturbation matrix element, $|H'_{jk}|$.

Now we shall specifically concern ourselves with the case of resonance energy transfer between two species. Let S denote the sensitizer and A the acceptor. The initial state of the system j corresponds to an excited sensitizer in the neighbourhood of an acceptor, which is in the ground state.

This situation can be represented by the simple wave function,

$\psi_S^* \psi_A^0$ +. The final state, with the transfer to the acceptor having occurred can be written as, $\psi_S^0 \psi_A^*$. Competing radiative effects and non-radiative transitions are ignored for simplicity.

Then the matrix element required is;

$$\langle \psi_S^* \psi_A^0 | H' | \psi_S^0 \psi_A^* \rangle$$

The perturbation coupling the two states, without which an energy transfer is impossible, arises from the electronic interactions of the molecules. Normally we consider only the coupling of the excited valence electron on the

+ Note here antisymmetrization is ignored.

sensitizer with the corresponding ground state electron on the acceptor, but initially we must at least acknowledge the presence of all the others. Neglecting retardation and magnetic effects,(8), we represent our matrix element as,(I0),(I2),

$$|H'_{SA}| = \langle \psi_S^* \psi_A^0 | H' | \psi_S^0 \psi_A^* \rangle$$

$$= \iint \psi_S^* \psi_A^0 \sum_m \sum_n \frac{e^2}{(\vec{r}_{m,S} - \vec{r}_{n,A})} \psi_S^0 \psi_A^* d\tau_S d\tau_A$$

(I-33)

The sums involve all the electrons effected in the transition,

m referring to sensitizer electrons, and n to acceptor electrons. The integrals are over the coordinates of both electronic distributions. If the element is expanded in a Taylor Series, and we retain only the dipole-dipole term,(I0), (II),(I2),

$$|H'_{SA}| = \frac{1}{\epsilon} \left(\frac{\vec{d}_S \cdot \vec{d}_A}{R^3} - 3 \frac{(\vec{d}_S \cdot \vec{R})(\vec{d}_A \cdot \vec{R})}{R^5} \right)$$

(I-34)

where; $\vec{R} = \vec{X}_S - \vec{X}_A$, the distance vector between the centres of the sensitizer and the acceptor, and $\epsilon = n^2$, is the dielectric of the medium.

$$\vec{d}_S = e \int \psi_S^* \sum_m (\vec{r}_{m,S} - \vec{X}_S) \psi_S^0 d\tau_S.$$

$$\vec{d}_A = e \int \psi_A^* \sum_n (\vec{r}_{n,A} - \vec{X}_A) \psi_A^0 d\tau_A.$$

(I-35)

These are the transition dipoles between the ground and excited states for both the sensitizers and acceptors.

This "dipole - interaction" model is only an approximation, we usually consider only a single electron on both the sensitizer and the acceptor as being involved, and have totally neglected electron exchange. Also in the Taylor expansion we have ignored higher order interactions, such as dipole - quadrupole, and quadrupole - quadrupole (10). This is reasonable so long as this dipole - dipole term is non - vanishing. If it were not, higher order interaction would have to be used.

In the evaluation of the transfer probability we require the square of $|H'_{SA}|$, and from equation (I - 34), we obtain,

$$|H'_{SA}|^2 = \frac{1}{n^4 R^6} \left(\vec{d}_S \cdot \vec{d}_A - \frac{3}{R^2} (\vec{d}_S \cdot \vec{R})(\vec{d}_A \cdot \vec{R}) \right)^2$$

(I-36)

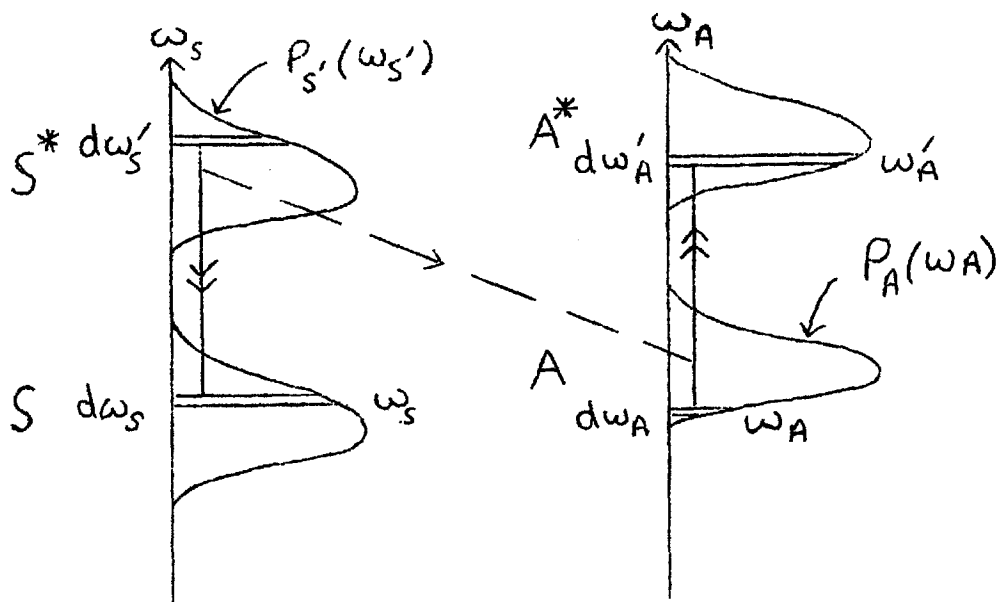
which immediately brings us to the familiar inverse - sixth power variation of the probability of resonance - energy transfer.

Clearly however we have ignored the specific angular properties of the transition dipole \vec{d}_S and \vec{d}_A in $|H'_{SA}|$ and only one pair of sensitizers and acceptors have been considered.

We shall particularly concern ourselves with the application of the principles discussed to the sensitizer - acceptor transfer for species with large band - widths in the next section, then it will be possible to proceed to the statistical problem of macro - ensembles of interacting molecules.

(3) Resonance - Transfer via Dipole - Dipole Coupling.

Now we shall consider the specific problem of energy transfer between two vibrationally relaxed species, (I4), (I5), (I0), (5), both with broad undefined energy levels. The two coupled transitions which give rise to the transfer are shown, ---



We have used $P_{S'}(\omega_{S'})$ and $P_A(\omega_A)$ to represent the vibrational energy - state distributions for the excited state of the sensitizer and the ground - state acceptor respectively. These distributions are normalized to unity,

$$\int_0^{\infty} P_{S'}(\omega_{S'}) d\omega_{S'} = 1 = \int_0^{\infty} P_A(\omega_A) d\omega_A \quad (\text{I-37})$$

It will be noted that we do not commit ourselves to any particular form of distribution - the Lorentzian distribution which was used to illustrate the first and second - order perturbation results, generally does not well represent the experimental spectra of molecules in solution. The wavefunctions applicable to the individual molecules in their initial states are normalised,

$$\int \Psi_{S'}(\omega_{S'}) \cdot \Psi_{S'}^*(\omega_{S'}) d\tau_S = 1$$

$$\int \Psi_A(\omega_A) \cdot \Psi_A^*(\omega_A) d\tau_A = 1$$

(I-38)

The final states , $\Psi_S(\omega_S)$ and $\Psi_{A'}(\omega_{A'})$ are not unique as are the starting states, the excited sensitizer may return to a band of states, and similarly the acceptor may

be excited to anywhere within a band of states, $\Delta \omega$.

Hence we normalize these states as for a continuum,

$$\frac{1}{\Delta \omega} \int_{\omega}^{\omega + \Delta \omega} d\omega_s \int \psi_s(\omega_s) \psi_s^*(\omega_s) d\tau_s = 1$$

$$\frac{1}{\Delta \omega} \int_{\omega}^{\omega + \Delta \omega} d\omega_{A'} \int \psi_{A'}(\omega_{A'}) \psi_{A'}^*(\omega_{A'}) d\tau_{A'} = 1 \quad (\text{I-39})$$

The integrations over $d\tau_s$ and $d\tau_{A'}$ involve all the electron coordinates of the appropriate molecules.

Antisymmetrizing the initial and final states, denoted by $\bar{\Psi}_I$ and $\bar{\Psi}_F$ respectively,

$$\bar{\Psi}_I(\omega_s', \omega_A) = \frac{1}{\sqrt{2}} \left(\psi_{S'}(\vec{\Gamma}_1, \omega_s') \psi_A(\vec{\Gamma}_2, \omega_A) - \psi_{S'}(\vec{\Gamma}_2, \omega_s') \psi_A(\vec{\Gamma}_1, \omega_A) \right)$$

$$\bar{\Psi}_F(\omega_s, \omega_{A'}) = \frac{1}{\sqrt{2}} \left(\psi_S(\vec{\Gamma}_1, \omega_s) \psi_{A'}(\vec{\Gamma}_2, \omega_{A'}) - \psi_S(\vec{\Gamma}_2, \omega_s) \psi_{A'}(\vec{\Gamma}_1, \omega_{A'}) \right)$$

Here \vec{r}_1 and \vec{r}_2 are the valence electron.

coordinates - here we have taken the simplest two electron model for the transition, (10). It will be seen overlap terms of the type,

$$\iint \psi_{S'}^*(\vec{r}_1, \omega_{S'}) \psi_A^*(\vec{r}_1, \omega_A) \psi_A(\vec{r}_2, \omega_A) \psi_{S'}(\vec{r}_2, \omega_{S'}) d\tau_S d\tau_A$$

have been ignored. It is reasonable to expect them to be small, especially within the dipole - dipole approximation, which is only valid for $R_{SA} \gg 5\text{\AA}$. If they were non - zero the $1/\sqrt{2}$ expansion coefficients in the antisymmetrization procedure would be affected. We write the dimensionless matrix - element between the initial and final states as,

$$\iint \psi_I H' \psi_F d\tau_S d\tau_A = \langle \omega_{S'}, \omega_A | H' | \omega_S, \omega_A' \rangle$$

Thus the transfer probability, in the first - order perturbation approximation can be written

as,

$$P_{S'A} = \frac{2\pi}{\hbar} \int d\omega_{A'} \int d\omega_S \int d\omega_A P_A(\omega_A) \dots$$

$$\dots \int d\omega_{S'} P_{S'}(\omega_{S'}) \cdot \left(\langle \omega_{S'}, \omega_A | H | \omega_S, \omega_{A'} \rangle \right)^2$$

(I-4I)

We have assumed the transition may only occur between two non - degenerate states. In order to integrate for $P_{S'A}$, we invoke the Frank - Condon Principle, that is we assume, $(\omega_{S'} - \omega_S) = (\omega_{A'} - \omega_A)$. This is an approximation which is analogous to the conservation of energy principle discussed in the section on first - order perturbations. Now, however, we have to take into account the fact that the two molecules are coupled to non - specified other systems, which give them such broad energy bands. The Frank - Condon principle also allows us to assume the jump $\Psi_I \rightarrow \Psi_F$ is much faster than any other external process, and as an isolated mechanism must conserve energy.

Hence in the expression for $P_{S'A}$ we can use the Dirac Delta function, $\delta((\omega_{S'} - \omega_S) - (\omega_{A'} - \omega_A))$. Integrating over ω_S , using the properties of the Delta function, (see equation (I -24)),

and with $E = \omega_{S'} - \omega_S = \omega_{A'} - \omega_A$,

$$P'_{SA} = \frac{2\pi}{\hbar} \int dE \int d\omega_A P_A(\omega_A) \int d\omega_{S'} P_{S'}(\omega_{S'}) \dots$$

$$\dots \left(\langle \omega_{S'}, \omega_A | H | \omega_{S'} - E, \omega_A + E \rangle \right)^2$$

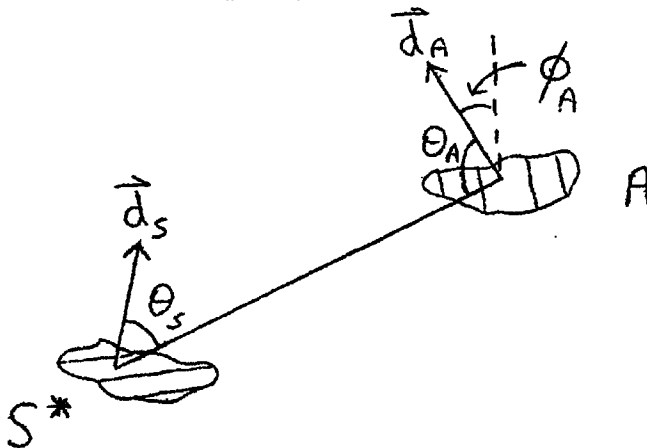
(I-42)

The perturbation matrix element is obtained using the conventional dipole - dipole approximation, considering only the single electrons on the acceptor and sensitizer explicitly involved in the transition. Unfortunately this term has an angular dependence, given by,

$$\Phi^2 = \left(\sin \theta_S \sin \theta_A \cos \phi_A - 2 \cos \theta_S \cos \theta_A \right)^2$$

(I-43)

arising from the coupling of the two transition dipoles,



Thus the transfer rate is dependent on the orientation of the two dipole vectors. If we assume our sensitizer and acceptor

are rotating at a speed much greater than $(1/P_S'A)$, then this angular dependence may be averaged out. To find the mean value of this angular term, $(\underline{\Phi}^2)_{\text{mean}}$, we have to integrate over all θ_S, θ_A and ϕ_A , with $\underline{\Phi}^2$ weighted by a suitable probability function,

$$P(\theta_S, \theta_A, \phi_A) = \frac{1}{8\pi} \sin \theta_S \sin \theta_A d\theta_S d\theta_A d\phi_A \quad (\text{I-44})$$

where P represents the probability that the dipoles are orientated with angles $\theta_S, \theta_A, \phi_A$. Hence we require,

$$(\underline{\Phi}^2)_{\text{mean}} = \int_{\theta_S=0}^{\pi} \int_{\theta_A=0}^{\pi} \int_{\phi_A=0}^{2\pi} \frac{1}{8\pi} \sin \theta_S \sin \theta_A \left(\sin \theta_S \sin \theta_A \cos \phi_A - 2 \cos \theta_S \cos \theta_A \right)^2 d\theta_S d\theta_A d\phi_A \quad (\text{I-45})$$

This gives, (6),

$$(\underline{\Phi}^2)_{\text{mean}} = 2/3.$$

Hence we can write,

$$\begin{aligned} & \left(\langle \omega_S', \omega_A | H' | \omega_S' - E, \omega_A + E \rangle^2 \right)_{\text{mean}} \\ &= \left(\frac{1}{n^4} \left(\frac{\vec{d}_S \cdot \vec{d}_A}{R^3} - \frac{(\vec{d}_S \cdot \vec{R})(\vec{d}_A \cdot \vec{R})}{R^5} \right)^2 \right)_{\text{mean}} \\ &= \frac{2}{3} \cdot \frac{1}{R^6 n^4} \left| \vec{d}_S(\omega_S', \omega_S' - E) \right|^2 \left| \vec{d}_A(\omega_A, \omega_A + E) \right|^2 \end{aligned} \quad (\text{I-46})$$

It is found that performing the averaging at this step, for only two molecules, yields an identical result to averaging at a later stage in the development of the statistical model, (I4). Thus we finally obtain,

$$P_{S'A} = \frac{4\pi}{3R R^6 n^4} \int_{E=0}^{\infty} dE \int_{\omega'_S=0}^{\infty} d\omega'_S P_S(\omega'_S) \cdot \left| \vec{d}_S(\omega'_S, \omega'_S - E) \right|^2 \dots$$

$$\dots \int_{\omega_A=0}^{\infty} d\omega_A P_A(\omega_A) \left| \vec{d}_A(\omega_A, \omega_A + E) \right|^2 \quad (I-47)$$

This is the full theoretical expression for $P_{S'A}$, and from it we might consider it would be simple to insert the various quantities to calculate $P_{S'A}$ in any given circumstances. Unfortunately the distributions $P_{S'}$ and P_A , and the moments \vec{d}_S and \vec{d}_A , are usually unavailable — or of low accuracy. The solution to this problem is, as shown by Förster (5), (10), to relate the triple integral directly to the extinction coefficients of the states, which are easily obtained experimentally. We shall follow this development and first we consider the coefficient for spontaneous emission of an excited species, this is the Einstein coefficient A , (I5),

Where N' is the number of molecules per millimole, 6.02×10^{20}

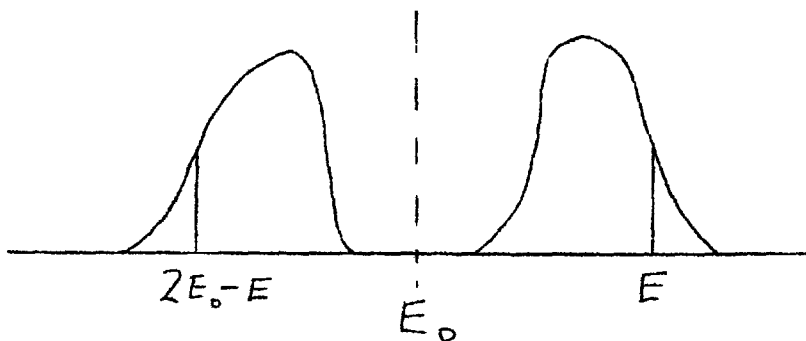
While it is experimentally quite simple to find \bar{B} from a measurement of $\epsilon(E)$, the corresponding measurement of \bar{A} for the emission spectrum is not so easy, and it is better to try and relate this to the absorption spectrum. This is possible if we assume the vibrational structure of the sensitizer is approximately the same in both the ground and the excited states,

$$\vec{d}_s(\omega_{s'}, \omega_{s'} - E) \approx \vec{d}_s(\omega_{s'} - E, \omega_{s'})$$

$$P_{s'}(\omega_{s'}) \approx P_s(\omega_s)$$

(I-51)

Then if in addition we use this "mirror symmetry", (I6), (I7), to relate the energies to the plane of symmetry, E_0 between the absorption and fluorescence bands.



Using the relations derived for \bar{A} and \bar{B} ,

$$\bar{A}(E) = \frac{n^3 (2E_0 - E)^3}{k^3 c^3 \pi^2} \cdot \bar{B}(2E_0 - E) \quad (\text{I-52})$$

Then,

$$\bar{A}(E) = \frac{n^3 (2E_0 - E)^2}{k^3 c^2 \pi^2 N'} \ln(10) \epsilon(2E_0 - E) \quad (\text{I-53})$$

From these relations (I-51), (I-53), and (I-47), we can now derive P'_{SA} in terms of integrals over extinction coefficients,

$$P'_{SA} = \frac{3}{4} \frac{k c^2 \ln(10)^2}{n^2 R^6 (N')^2 \pi^3} \cdot \int_{E=0}^{\infty} \frac{\epsilon_A(E) \epsilon_S(2E_0 - E) dE}{E (2E_0 - E)} \quad (\text{I-54})$$

With the reasonable approximation, $E_0 \approx E; E, E_0 > 0$, then,

$$P'_{SA} \approx \frac{3}{4} \frac{k c^2 \ln(10)^2}{n^2 R^6 (N')^2 E_0^2} \cdot \int_0^{\infty} \epsilon_A(E) \epsilon_S(2E_0 - E) dE \quad (\text{I-55})$$

Hence the rate of transfer is obtained as a function of easily observable parameters, and involves a special type of "overlap integral" over the absorption bands of the transferring molecules. This is the same type of integral that

occurs in the discussion on the trivial effect, however it must be remembered that here it represents the possible coupling between two states - not the possibility of photon emission and reabsorption processes. The usual working definition of transfer probability is, (5), (6), (9),

$$P'_{SA} = \frac{1}{\tau_s} \left(\frac{R_0}{R} \right)^6 \quad (\text{I-56})$$

where τ_s is the radiative lifetime of the sensitizer in solution. Thus the radius parameter R_0 , often called the "critical radius", (5), (6), is given by,

$$R_0 = \sqrt[6]{\frac{3k c^2 \tau_s J}{4\pi^3 E_0^2 (N')^2 n^2}} \quad (\text{I-57})$$

where J is the overlap integral,

$$J = (\ln 10)^2 \int_{E=0}^{E=\infty} \epsilon_A(E) \epsilon_S(2E_0 - E) dE \quad (\text{I-58})$$

Most experiments in the field of energy transfer are aimed towards a determination of R_0 , rather than the direct confirmation of a calculated R_0 , (I9), (I8).

The correlation between calculated R_0 and their experimental values is not always good, this is due to many causes - the approximate nature of the statistics used in solution, the inherent failings of the dipole - dipole approximation, and finally the value of the integral J is not always very accurately known.

(4) The Break - down of the Dipole - Dipole Approximation.

Here we shall discuss the breakdown of the approximations used to derive the transfer rate given in the last section. Apart from various minor assumptions in the derivation of P_{SA}' , the major basis of the theory is the use of first - order perturbation, and the retention of only the dipole- dipole term in the multipole expansion of the perturbation matrix element. Considering first the perturbation approximation, we must recognise the basic differences between the various orders of perturbation. In first - order perturbation induced transitions we picture energy transitions between sensitizers and acceptors as being a series of single jumps, no intermediate states are involved in the transition across space between the two molecules. Representing the initial and final states as Lorentzian distributions, with the same band - width, and centred at the same point, we found $P(1) \approx |H'_{kj}|^2 / \Gamma^2 R^2$. (See equations (I-20), to (I-28)). The transfer of excitation through an intermediate state is described by the magnitude

of the second-order perturbation term. Here we can regard the sensitizer as passing its energy to the acceptor via a third molecule, acting as an intermediary in the transition. This transition is however a concerted one, and the intermediate has only a transitory existence. The probability for this transition was found to be,

$$P(2) = |H'_{KL} \cdot H_{Lj}|^2 / R^4 \Gamma^3$$

Thus the ratio of the squares of the perturbation expansion coefficients is given by,

$$\frac{P(2)}{P(1)} = \frac{|H'|^2}{R^2 \Gamma^2}$$

assuming, $H'_{KL} \approx H'_{Lj} \approx H'_{Kj} = H$, and for the perturbation series to converge we must require, $H < R \Gamma$, (II).

This corresponds to a "weak coupling" model, (6), (20), where the perturbation must be small compared with the band-width of the states, Γ . When the reverse holds, and $P(2) \approx P(1)$, then we can no longer consider the excitation as localized between jumps, it is essentially delocalized, and may transfer through a number of intermediate states. This is the "strong coupling" case, and certainly is not appropriately described by any of the foregoing theory. For this case the exciton model is used, (2I), (8).

Coupling criteria have been discussed by Förster, (6), who proposes three categories, strong, medium, and weak. Our

"weak coupling" corresponds to that of Förster's, and he distinguishes the higher couplings by whether or not resonance exists between individual vibronic levels in both molecules. The situation in molecular crystals, such as benzene, where the transfer has to "wait" for the correct vibration before transferring, is referred to as a "medium interaction" case in Förster's nomenclature. For this mechanism we regard the excitation as being only slightly delocalized, in the "strong coupling" limit, delocalization is complete. Here the interaction is so strong that the vibronic levels of the two species are in resonance and vibrational quantization may be neglected. For two "strongly coupled" molecules we find an oscillation of excitation between the two centres. Considering the time dependent functions for the sensitizer and acceptor, we can write two antisymmetric functions representing the exciton splitting, (2I),

$$\begin{aligned} \Psi_1 &= \frac{1}{\sqrt{2}} (\psi_S^* \psi_A + \psi_S \psi_A^*) e^{-i \frac{(E_0 - H')t}{\hbar}} \\ \Psi_2 &= \frac{1}{\sqrt{2}} (\psi_S^* \psi_A - \psi_S \psi_A^*) e^{-i \frac{(E_0 + H')t}{\hbar}} \end{aligned} \quad (\text{I-59})$$

If the system is in the state $\psi_S^* \psi_A$ at time $t = 0$ the time dependent wave function is given by,

$$\Psi = \frac{1}{\sqrt{2}} (\Psi_1 + \Psi_2) \quad (\text{I-60})$$

Squaring $\bar{\Psi}$ we find,

$$|\bar{\Psi}|^2 = |\psi_S^* \psi_A|^2 \cos^2\left(\frac{H't}{R}\right) + |\psi_S \psi_A^*|^2 \sin^2\left(\frac{H't}{R}\right)$$

(I-6I)

Thus the transfer is a purely oscillatory process between the sensitizer and acceptor, and the excitation is effectively delocalized with a rate of $\sim 2H'/\pi R$. It is this delocalized excitation spreading over the whole system of molecules involved in an aggregate which is referred to as an exciton,(22). In both of these last two cases, the absorption and fluorescence bands are effected by this strong coupling, although for the medium coupling the effect may only be slight, the molecules in an aggregate retaining their individuality. With strong coupling the bands are very distorted, and we must consider states of the system rather than the individual molecular excited states.

Hence our "resonance transfer" theory applies only to weakly coupled systems, with essentially localized excitation. These conditions are however likely to break down at high concentrations of acceptors and sensitizers, when the interaction term, H' , becomes large, with the increased likelihood of close proximity, ($\sim 5 \text{ \AA}$), of acceptors and sensitizers.

We assumed the interaction between the two molecules

is purely Coulombic in form, representing the interaction of the electrons on each molecule as, $\sum_i \sum_j \frac{e^2}{(\vec{r}_{i,S} - \vec{r}_{j,A})^3}$, (see equation (I-33)). This neglects all magnetic, exchange and retardation effects,(8), the exchange omission seems reasonable at large separations. The other omissions may however be more important. The Breit Interaction, which has been discussed elsewhere,(8), helps remove some of these criticisms, and a residual term in $I./R$ appears in the multipole expansion, so the use of a better interaction term may be very important. Also in the multipole expansion of the interaction we only retain the dipole-dipole terms, this approximation is reasonable, except of course for non-polar states where dipole-quadrupole terms are vital. All these expansions are based on the "single electron" model, but as we see from the SCF descriptions of molecules, the representation of the excited states of molecules by single electron transitions is inadequate. We should really concern ourselves with the total state wave functions, dependent on all the molecular electrons.

Finally we should note that with the simple dipole-dipole expression transitions are only possible between singlet states, and zero rate is predicted for singlet-triplet transfer,(23),(24), when the intermolecular overlap integrals vanish. However, if the Breit Interaction is used in place of the Coulomb interaction, the theory predicts that resonance transfer of triplet excitation energy can compete

effectively with spontaneous photon emission over distances as large as 30 Å ,(8).

(5) Resonance Transfer in Solutions.

(a) Introduction.

After discussing the preliminary theory, aimed at deriving the transfer rate between an isolated acceptor-sensitizer pair, let us now consider the problem of an assembly of such sensitizers and acceptors. Our specific concern is solutions, and we assume our approximation concerning the mutual orientation of the species is valid, and that they are rotating rapidly in solution. We shall develop our theory towards explaining the enhancement of the acceptor, and the quenching of the sensitizer fluorescence, as this is the major experimental technique employed for the study of resonance transfer in solution,(18),(19). The luminescence of a system of sensitizers and acceptors in solution is made up of the individual contributions of each species, with each molecule in its own exclusive environment. Thus the physical model used to explain the phenomena of sensitized fluorescence must make some assumptions concerning the distribution of molecules in solution. We shall always regard the solvent as just a medium for the solute molecules, and these molecules are taken as being randomly distributed throughout the bulk of solvent. This random distribution was assumed by Förster,(5), after a preliminary lattice theory, and he assumed that the molecular positions were constant over the

lifetime of the excitation in solution. Since the development of Förster's original theory the effect of Brownian Motion on the transfer has been investigated—with some evidence for a slight diffusional effect at low viscosities, (25), (26). We shall have more to say about this later, when a rather oversimplified model including diffusion is proposed. In moderately viscous media however, the Förster model seems well established, and confirmed by many experimental results, (18), (35), (36), (32), (33). In our discussion we shall consider the sensitizers and acceptors separately, and the applicability of a new simplified model will be investigated. Throughout our treatment we shall assume the inverse-6 power law for the transfer rate,

$$n_{S'A} = \frac{1}{\tau_s} \left(\frac{R_0}{R_{S'A}} \right)^6 \quad (I-62)$$

where τ_s is the lifetime of the sensitizer in solution alone, and $R_{S'A}$ is the distance between the sensitizer and acceptor pair. We shall not consider explicitly other random processes competitive with resonance transfer, such as internal quenching and radiative decay, (27). These are all contained within the lifetime term τ_s , where $1/\tau_s$ is the rate of decay of the sensitizers in the absence of acceptors, (19), (28).

The random nature of all these competing processes, and their consequent constant probabilities with time, always results in pure exponential decay, (27), so long as no resonance transfer occurs.

This is observed experimentally, using direct pulse scintillation measurements of fluorescence decay, (30),(31). Also it should be noted any possibility of back-transfer from acceptors to sensitizers is ignored, in any case the Stokes Shift,(I6),(29), helps make this unlikely.

(b) Sensitizers.

(i) General Theory.

We shall consider the decay of the excited sensitizers with time, in the presence of acceptors. The excited sensitizers are assumed to be randomly distributed throughout solution,(I4), having been excited by a flash of radiation at time , $t = 0$. Then if we let $S_j(t)$ represent the probability that the j -th sensitizer is still excited at time t , we have,(8),(5),

$$\frac{dS_j}{dt} = -\frac{1}{\tau_s} \left(1 + \sum_K^{NA} \left(\frac{R_0}{R_{jK}} \right)^6 \right) S_j \quad (I-63)$$

The sum over K gives the total de-excitation probability due to the acceptors at various distances R_{jK} from the j -th sensitizer. Thus we obtain;

$$S_j(t) = S_j(0) e^{-\frac{t}{\tau_s} \left(1 + \sum_K \left(\frac{R_0}{R_{jK}} \right)^6 \right)} \quad (I-64)$$

We shall assume that the initial excitation probability, $S_j(0)$, is independent of j , so that $S_j(0) = S(0)$. Then the total excitation probability of a sample containing N_s sensitizers

is given by,

$$S(t) = S(0) \sum_{j=1}^{N_s} \left(e^{-\frac{t}{\tau_s}} \left(1 + \sum_{k=1}^{N_A} \left(\frac{R_0}{R_{jk}} \right)^6 \right) \right) \quad (I-65)$$

But the observed sensitizer fluorescence intensity, $I_s(t)$, is proportional to $S(t)$,

$$I_s(t) = \frac{S(t)}{\tau_s} = \frac{S_0}{\tau_s} \sum_j e^{-\frac{t}{\tau_s}} \left(1 + \sum_k \left(\frac{R_0}{R_{jk}} \right)^6 \right) \quad (I-66)$$

Although it is easy to write an expression for $I_s(t)$ as in (I-66), it is not so simple to evaluate it as a function of time. The presence of the sums over j and k forces us either to propose a distribution for the species in solution, so as to obtain an integrable function in place of the sums, or to set up a simulation of a small representative volume of a "random solution", and watch the probability decay with time. This latter more direct evaluation of $I_s(t)$ is possible using a computer simulation. However we shall first consider simpler statistical models involving the use of distribution functions. Förster, (5), (18), (32), assuming a completely random distribution of acceptors and sensitizers in solution, obtained the result,

$$I_s(t) = e \left(-\frac{t}{\tau_s} - \sqrt{\pi} N \left(\frac{R_0}{R_g} \right)^3 \sqrt{\frac{t}{\tau_s}} \right)$$

with, $R_g^3 = \frac{3}{4\pi} V$ (I-67)

Here N is the number of acceptors contained within the

volume V , R_0 and τ_s have been previously defined.

This expression for the decay of the sensitizer luminescence is clearly not purely exponential since it involves $\sqrt{t/\tau_s}$.

This is what we would anticipate. Sensitizers in particularly unfavourable environments, with the close proximity of acceptors, will be quickly de-excited leaving those in more favourable sites to decay almost unaffected by acceptors. The method used by Förster, (18), (32), (33), (19), to obtain this expression for $I_s(t)$ was to assume a distribution function for the acceptors around each sensitizer and replace the sum over acceptors by an integration.

Thus he evaluated the integral,

$$I_s(t) = e^{-\frac{t}{\tau_s}} \prod_{K=1}^{NA} \int_0^{R_0} e^{-\left(\frac{R_0}{R_K}\right)^6 \frac{t}{\tau_s}} \cdot \omega(R_K) dR_K \quad (I-68)$$

where $\omega(R)$ represents the distribution function. The result was independent of the sensitizer concentration, and depended only on the concentration of acceptors, which provided the environment for each sensitizer, the number of sensitizers considered was only important from a statistical point of view in giving an "average" result. This is seen in the full expression for the intensity, given in equation (I-66), where the sum over j only serves to add up all the sensitizers contributions, whilst the sum over K represents the energy-transfer contribution, depending on the number of acceptors in solution. It will also be noted that we cannot factor the expression, $(1 + \sum_K \left(\frac{R_0}{R_{jk}}\right)^6)$

out of the sum over j . This would only be possible if all sensitizers were in identical environments, and then purely exponential decay of excitation would occur. Thus it is the non-uniformity of the environments in solution which gives rise to non-exponential decay.

Unfortunately the quantity $I_s(t)$ is usually unmeasurable because the lifetimes of excitation in solution are of the order 10^{-8} to 10^{-9} sec. Recently however, the decay has been observed directly with the use of special techniques. These are usually pulse scintillation methods, (31), (30), (34), in which a pulse of X-rays is used to excite the molecules, and then the output observed on a travelling beam oscilloscope. This work is difficult because the duration of the exciting pulse and the response time of the photo-multiplier are all of the same magnitude as the lifetimes under investigation. For this reason one is lead to seek for a more easily measured parameter, derived from $I_s(t)$. Such a quantity is the Quantum Yield, (37), (19), (32), defined by,

$$\left[\frac{\eta}{\eta_0} \right]_s = \frac{1}{\tau_s} \int_0^{\infty} I_s(t) \cdot dt$$

(I-69)

The quantum yield represents the total output quanta in the

presence of acceptors, divided by the quanta which would have been emitted in the absence of acceptors. This is the ratio,

$$\left(\frac{\eta}{\eta_0}\right)_s = \frac{\int_{t=0}^{\infty} \frac{S(t)}{\tau_s} \sum_{j=1}^{N_s} \left(e^{-t/\tau_s} \left(1 + \sum_{K=1}^{N_A} \left(\frac{R_0}{R_{jk}} \right)^6 \right) \right) dt}{\int_{t=0}^{\infty} \frac{S(t)}{\tau_s} \sum_{j=1}^{N_s} e^{-t/\tau_s} dt}$$

$$\left(\frac{\eta}{\eta_0}\right)_s = \frac{1}{N_s} \sum_j \left(1 / \left(1 + \sum_K \left(\frac{R_0}{R_{jk}} \right)^6 \right) \right). \quad (\text{I-70})$$

Using Förster's expression for $I_s(t)$ we find (I9), (32),

$$\left(\frac{\eta}{\eta_0}\right)_s = 1 - \sqrt{\pi} q e^{q^2} (1 - \Phi(q)) \quad (\text{I-71})$$

where,

$$\Phi(q) = \frac{2}{\sqrt{\pi}} \int_q^{\infty} e^{-x^2} dx$$

and,

$$q = \frac{\sqrt{\pi}}{2} \cdot N \cdot \left(\frac{R_0}{R_g} \right)^3 = (c/c_0)$$

with,

$$c_0 = 3 / 2 \sqrt{\pi^3} N' R_0^3$$

Often when discussing a particular example of resonance - transfer we refer to it's efficiency $\hat{\eta}_A$. Remembering the

definition of $(\eta/\eta_0)_s$, (equation I-69), we are able to express the transfer efficiency as $1 - (\eta/\eta_0)_s$. Also we may define,

$$(\eta/\eta)_A = 1 - (\eta/\eta_0)_s \quad (\text{I-72})$$

$(\eta/\eta_0)_A$ represents the efficiency of the transfer to the acceptors - and may be alternatively defined as,

$$\left(\frac{\eta}{\eta_0}\right)_A = \frac{\int_0^{\infty} I_a(t) dt}{\int_0^{\infty} I_A^{\circ}(t) dt} \quad (I-73)$$

where $I_A^{\circ}(t)$ represents the yield of the acceptors, when all the energy absorbed by the sensitizers is passed on to the acceptors.

Förster's expressions are in good agreement with experimental results. However, his model does not allow a discussion of the acceptor luminescence as a function of time. For this reason a simpler alternative model is now proposed.

(ii) The Cell Model: Sensitizers.

In this model (38), we allow each acceptor to dominate a volume of solution given by N_A / V , where V is the total volume of solution. This "sphere of action" in which the acceptor can act is assumed spherical, with radius $(\sqrt{\pi}/2C_A)^{1/3}$ measured in units of R_0 . Here reduced units of acceptor concentration C_A are used, giving the concentration in units of Förster's C_0 , $C_0 = \frac{3}{2\sqrt{\pi}^3 N' R_0^3}$. Thus our idealized solution consists of N_A spheres, each with a dominating acceptor at its centre. These acceptors are regularly distributed throughout the solution, for example

they might be arranged in a regular hexagonal lattice. Now we add sensitizers to the solution, and an average n_s fall inside each sphere of influence - then the distribution function for the sensitizers inside each "average" acceptor volume is given by,

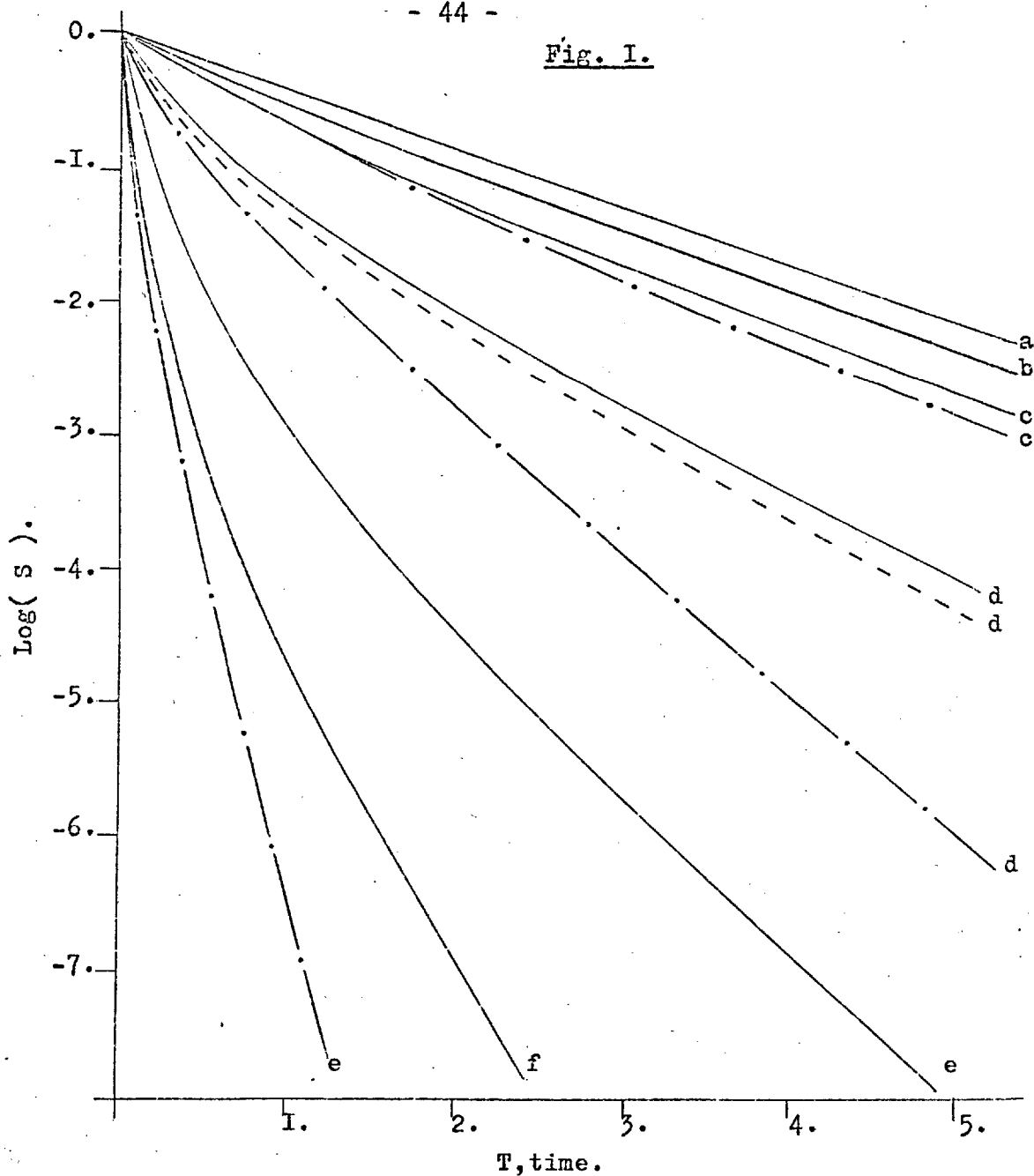
$$\omega(R) dR = n_s \frac{4\pi R^2 dR}{V_e} = n_s \frac{6CA}{\sqrt{\pi}} R^2 dR \quad (I-74)$$

where V_e is the volume of the spheres. Using this distribution function in equation (I-66) we lose the sum over K , as we only consider the single acceptor, and the \sum_j becomes a definite integral. The total intensity is given by,

$$I_s(t) \sim \frac{S(0)}{\tau_s} \cdot N_s \cdot \frac{6CA}{\sqrt{\pi}} \int_0^{(\sqrt{\pi}/2CA)^{1/3}} R^2 e^{-\frac{t}{\tau_s} \left(1 + \frac{1}{R^6}\right)} dR. \quad (I-75)$$

R is in units of Förster's R_0 , and $(n_s NA)$ is just the total number of sensitizers N_s . When this function is evaluated numerically for various concentrations, (see Fig. I), it is found to be almost identical with that of Förster's at low concentrations, however larger deviations occur at high concentrations. This is only to be expected of such a simple model, but as we shall see later it does have the great advantage of yielding analytic functions where Förster's model does not (I9).

Fig. 1.



The decay of sensitizer luminescence as a function of time. The abscissa represents time in units of τ_s , the ordinate the log of the excitation probability for an individual sensitizer excited at $T=0$. The letters on the curves refer to the acceptor concentration C_A measured in units of C_0 , $a=.001, b=.1, c=.3, d=1.0$, and $f=5.0$. The solid lines show Förster's function, the dotted line the computer simulation, and the dashed curves show the cell model. At $C_A \leq .3$, the first two are identical, at $C_A \ll 1$ all are.

We can easily calculate the quantum yield in this formalism, with

$$\left(\frac{\eta}{\eta_0}\right)_s = \frac{6 C_A}{\sqrt{\pi}} \frac{1}{\tau_s} \int_0^{\infty} dt \int_0^{\infty} dR e^{-\frac{t}{\tau_s} \left(1 + \frac{1}{R^6}\right)} R^2. \quad (\text{I-76})$$

On reversing the order of integration, integrating first over t , and then changing variables, and integrating over R we obtain,

$$\left(\frac{\eta}{\eta_0}\right)_s = 1 - \frac{2 C_A}{\sqrt{\pi}} \tan^{-1} \left(\frac{\sqrt{\pi}}{2 C_A} \right) \quad (\text{I-77})$$

This tends towards the same low concentration result as does Förster's expression, on expanding \tan^{-1} we obtain, with $C_A \ll 1$

$$\left(\frac{\eta}{\eta_0}\right)_s = 1 - \sqrt{\pi} \cdot C_A \quad (\text{I-78})$$

At high concentrations however the results deviate, on the model proposed here with $C_A \gg 1$ we find,

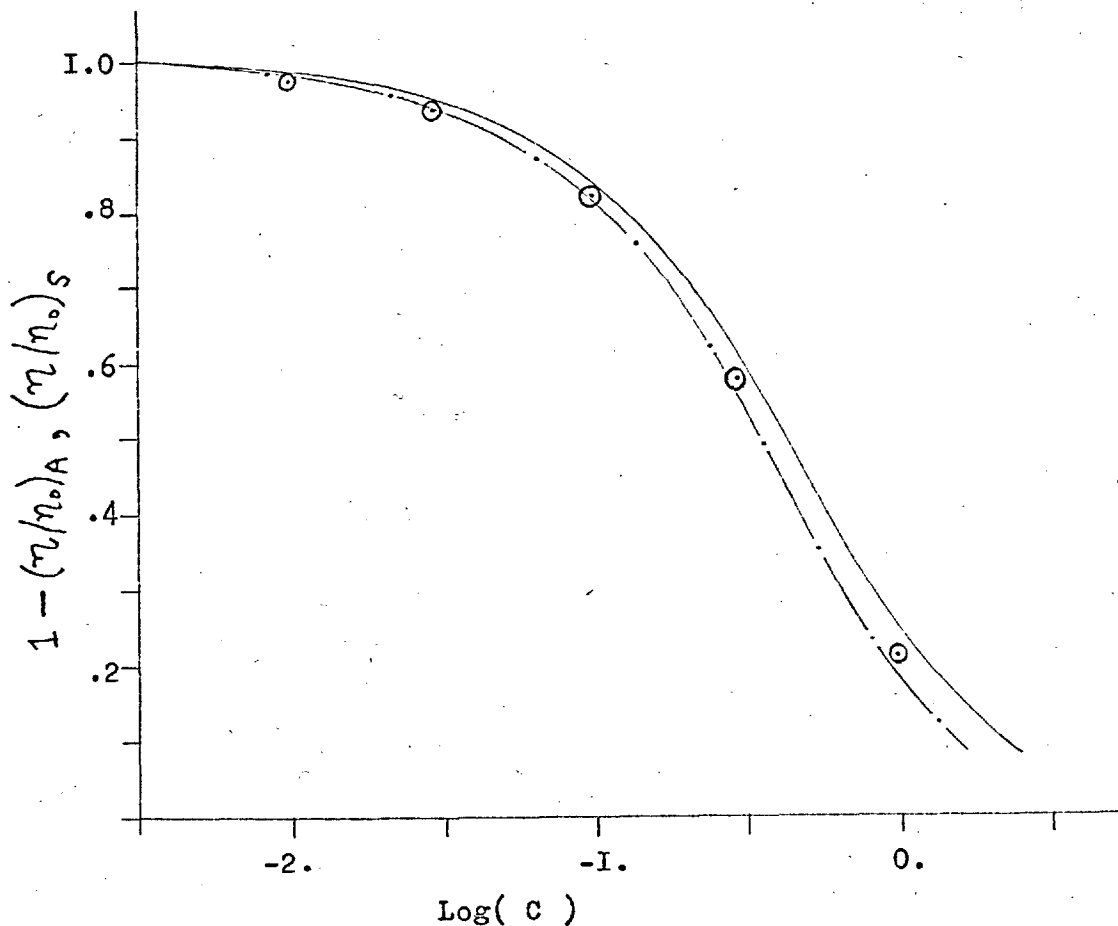
$$\left(\frac{\eta}{\eta_0}\right)_s = \pi / 12 C_A^2 \quad (\text{I-79})$$

For the identical requirement, $C_A \gg 1$, Förster obtains,

$$\left(\frac{\eta}{\eta_0}\right)_s = 1/2 C_A^2 \quad (\text{I-80})$$

Over the region where effective measurement of $\left(\frac{\eta}{\eta_0}\right)_s$ is possible the differences in the predictions of the two models is quite small. The form of $\left(\frac{\eta}{\eta_0}\right)_s$ is shown in Fig.2.

Fig. 2.



Quantum efficiencies as a function of reduced acceptor concentration, C_A/C_0 . The ordinate shows the sensitizer quantum efficiency $(\eta/\eta_0)_S$, this is the same as $1 - (\eta/\eta_0)_A$ where $(\eta/\eta_0)_A$ is the efficiency of the transfer. The solid line shows the results of Förster's statistics, the dashed line is obtained from the cell-model, and the points are from the computer simulation.

(iii) Steady - State Illumination.

All of our discussion until now has been based on the "flash - excitation" model as used by Förster, (I9), Galanin (I3) and others, where we have sought to describe the decay of an initially random array of excited sensitizers. The reason we say "initially. random" is that after the time $t = 0$, those sensitizers in close proximity to acceptors will be quickly de - excited, whilst those in effective "holes" in the acceptor distribution will decay relatively unaffected by resonance transfer (I4). Thus after a time there is a correlation between the distribution of excited sensitizers and the distribution of acceptors - the sensitizers in the "holes" predominate. Experimentally however, instead of watching directly the decay of species in solution by a sophisticated technique mentioned earlier, we normally observe steady state fluorescent intensities, excited by a constant incident intensity.

Thus we must now consider the steady state situation, where the fluorescent intensity is no longer time - dependent. As we now show, in the case of the sensitizers, we obtain the same result as for "flash - excitation" and the mode of excitation is unimportant. By assuming low concentrations of excited acceptors and sensitizers, we are able to preserve the requisite of a random distribution of excited species. Then we obtain the excitation probability from the "driven"

differential equation,

$$\frac{dS_j}{dt} = -\frac{1}{\tau_s} \left(1 + \sum_K^{N_A} \left(\frac{R_{0j}}{R_{jk}} \right)^6 \right) S_j + I \sigma_j \quad (\text{I-81})$$

where; I is the incident intensity, independent of time, and

σ_j represents the capture cross-section for the j -th sensitizer. At a steady state, $\sum_j \frac{dS_j}{dt} = 0$, hence;

$$\sum_j^{N_s} S_j = \sum_j^{N_s} I \sigma_j \tau_s / \left(1 + \sum_K \left(\frac{R_{0j}}{R_{jk}} \right)^6 \right) \quad (\text{I-82})$$

With no transfer occurring, the probability is given by;

$$\sum_j^{N_s} S_j^0 = \sum_j^{N_s} I \sigma_j \tau_s \quad (\text{I-83})$$

Thus we find the quantum efficiency, given as;

$$\left(\frac{\eta}{\eta_0} \right)_s = \frac{\sum_j S_j}{\sum_j S_j^0} = \frac{1}{N_s} \sum_j^{N_s} 1 / \left(1 + \sum_K^{N_A} \left(\frac{R_{0j}}{R_{jk}} \right)^6 \right) \quad (\text{I-84})$$

This expression for $\left(\eta/\eta_0 \right)_s$ is identical with that obtained for flash excitation in equation (I-70). Thus as we would expect, the efficiency of transfer is unchanged by the mode of excitation — we could have represented our steady state illumination just as easily by a series of flashes, but this interesting point is left until we consider explicitly time dependent excitations.

(iv) Sensitizer Life - times.

Until now we have been concerned mainly with the probability that a sensitizer is still excited after a certain time - lapse from it's initial excitation. Here we shall consider the "mean - life" of the excitation on the sensitizers.

Many definitions of mean - life are possible, but we shall use that proposed by Inokuti, (37), writing the mean-life as τ_m ,

$$\tau_m = \frac{\int_0^{\infty} t I(t) dt}{\int_0^{\infty} I(t) dt} \quad (I-85)$$

Thus for pure sensitizers we have,

$$\tau_s^m = \frac{\int_0^{\infty} t e^{-t/\tau_s} dt}{\int_0^{\infty} e^{-t/\tau_s} dt} = \tau_s \quad (I-86)$$

To evaluate the mean - life τ_s' , of sensitizers in the presence of acceptors using the cell - model we require,

$$\tau_s' = \frac{\int_0^{\infty} dt \int_0^{\infty} R^2 e^{-\frac{t}{\tau_s} (1 + 1/R^6)} dR}{\int_0^{\infty} dt \int_0^{\infty} \frac{\sqrt{\pi}/2CA}{R^2} e^{-\frac{t}{\tau_s} (1 + 1/R^6)} dR} \quad (I-87)$$

Normally we write τ_s' as a ratio of the mean - life in

absence of any transfer χ_s , hence on integration we find,

$$\frac{\chi_s'}{\chi_s} = \frac{\left(1 + \frac{1}{2(1 + \pi/4C_A^2)} - \frac{3C_A}{\sqrt{\pi}} \tan^{-1}\left(\frac{\sqrt{\pi}}{2C_A}\right)\right)}{\left(1 - \frac{2C_A}{\sqrt{\pi}} \tan^{-1}\left(\frac{\sqrt{\pi}}{2C_A}\right)\right)} \quad (\text{I-88})$$

At low concentrations, $C_A \ll 1$, the above equation reduces to;

$$\frac{\chi_s'}{\chi_s} = 1 - \frac{\sqrt{\pi}}{2} C_A \quad (\text{I-89})$$

This is the same result as that obtained by Galanin, (13), in the low concentration limit using the Förster model.

The form of $\frac{\chi_s'}{\chi_s}$ obtained with this simple cell model deviates quite appreciably from that derived from Förster's $I_s(t)$ using numerical integration, see fig. 3. In fig. 4 a comparison of the cell model $\frac{\chi_s'}{\chi_s}$ and the experimental data of Schmillen, (39), is given.

Having considered the sensitizers in some detail we shall now turn to the recipients of the transferred energy, the acceptors. In this field there is much less experimental and theoretical work available for comparison.

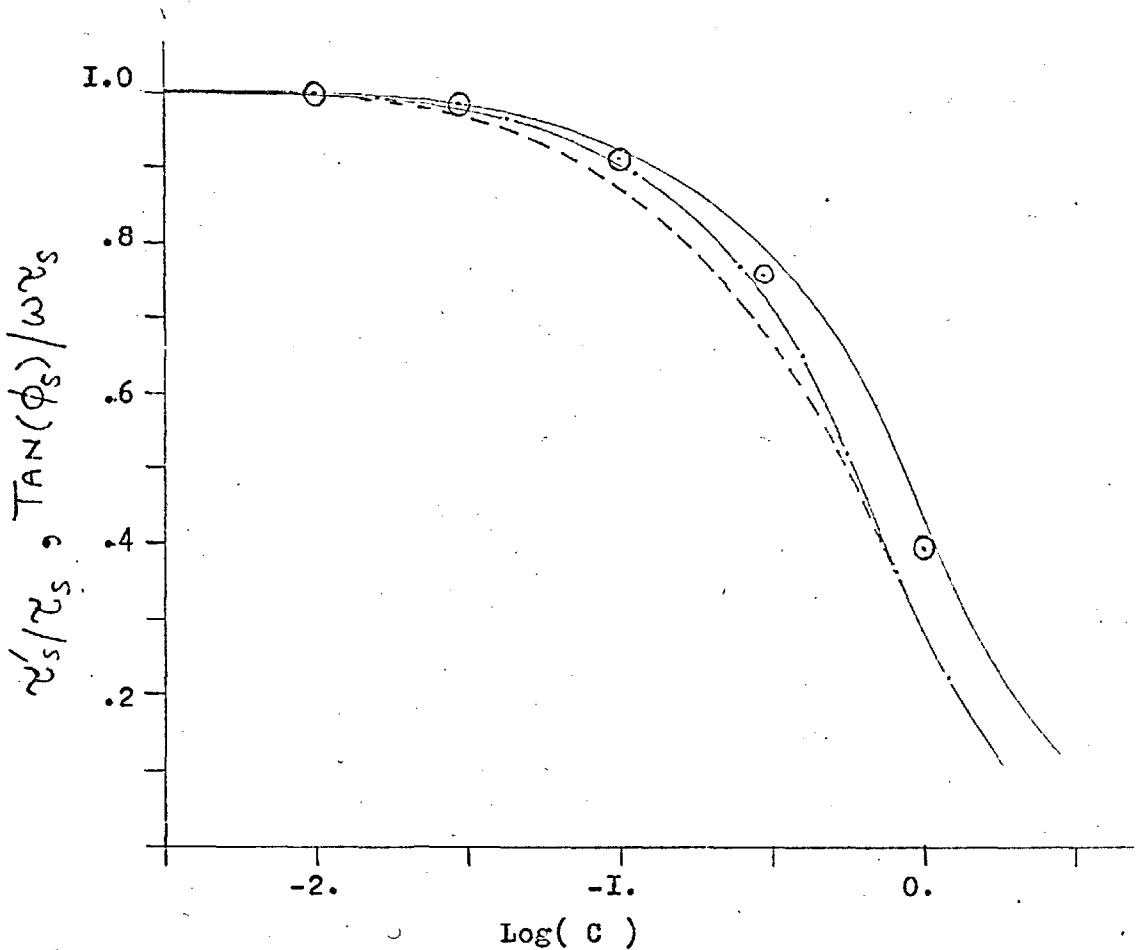
(c) Acceptors.

(i) General Theory.

As in the case of the sensitizers we shall first consider "flash-excitation" of the solution of acceptors and sensitizers at time, $t=0$. Then the decay of the acceptors is described by the differential equation,

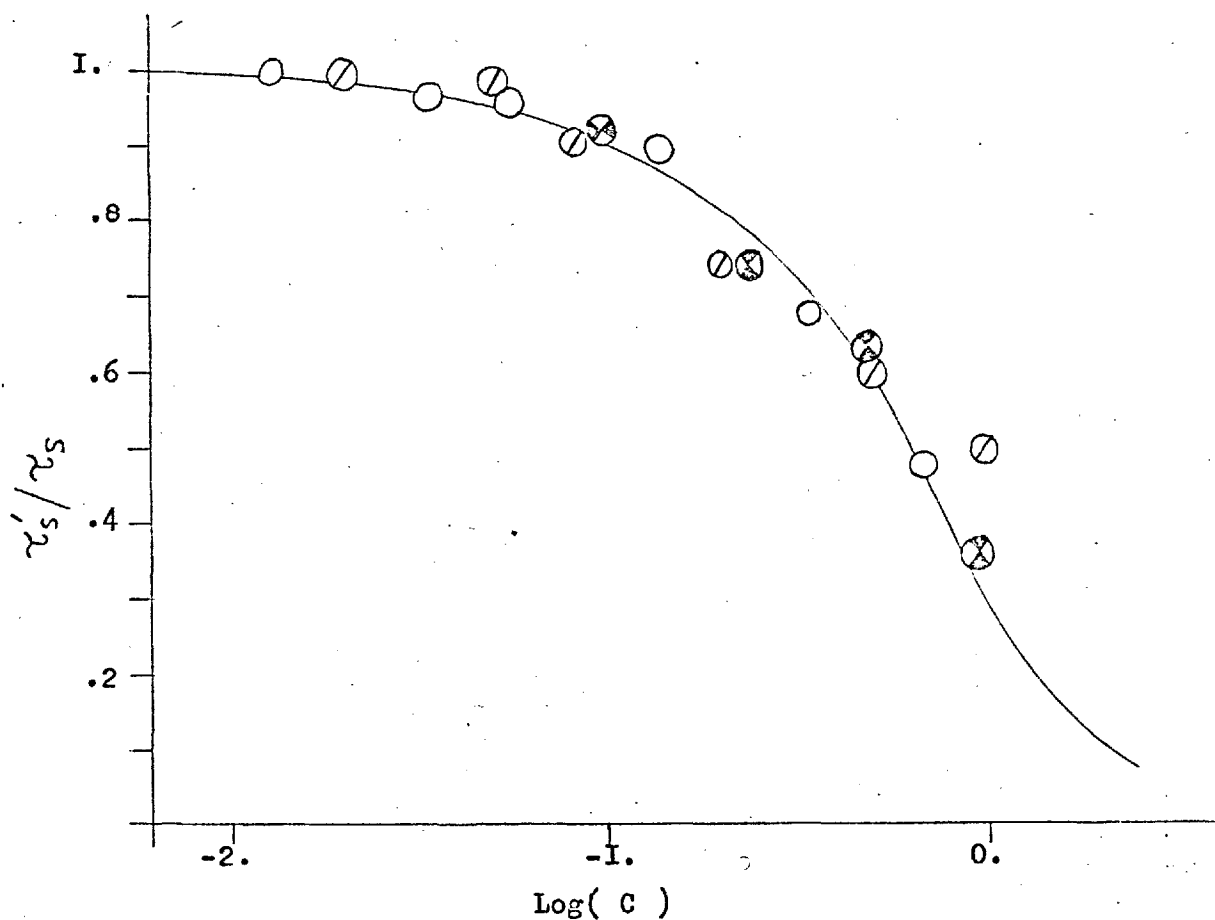
$$\frac{dA_k}{dt} = -\frac{1}{\chi_A} A_k(t) + \frac{1}{\chi_s} \sum_j^{N_s} \left(\frac{R_0}{R_{jk}}\right)^6 S_j(t) \quad (\text{I-90})$$

Fig. 3.



The dependence of sensitizer lifetime and phase angle on acceptor concentration. The concentration is measured in units of C_0 . The solid line shows τ'_s/τ_s obtained from Förster's decay function, the points were obtained from the computer simulation of $S(T)$. The dashed line gives the function $\frac{\text{TAN}(\phi_s)}{\omega\tau_s}$ for $\omega\tau_s = .04$, which is identical to τ'_s/τ_s derived from the cell-model. With $\omega\tau_s = 1.33$, the form of $\frac{\text{TAN}(\phi_s)}{\omega\tau_s}$ is shown by the dotted line. At $C_A \gg 1$ the functions $\frac{\tau'_s}{\tau_s}$ and $\frac{\text{TAN}(\phi_s)}{\omega\tau_s}$ are the same, even with $\omega\tau_s \approx 1$.

Fig. 4.



Sensitizer lifetime as a function of acceptor concentration. C is the reduced acceptor concentration, measured in units of C_0 . The solid line represents the cell-model function, the various points are experimental results of Schmitten, (39). Different points are used for the differing transferring systems; ○ = Trypaflavin/Rhodamine-B, ⊗ = Trypaflavin/Rhodamine-6G, ⊗ = Fluorescein/Erythrosin.

Where $A_k(t)$ is the probability that the k -th acceptor is excited at time t , and $S_j(t)$ the corresponding quantity for the sensitizers. Making use of the $S_j(t)$ derived previously in equation (I-65), and integrating we have,

$$A_k(t) = A_k(0) e^{-t/\tau_A} + S(0) \sum_{j=1}^{N_s} \frac{(R_0/R_{jk})^6}{1 - \tau_s/\tau_A + \sum_k (R_0/R_{jk})^6} \left(e^{-t/\tau_A} - e^{-t/\tau_s} \left(1 + \sum_k \frac{(R_0/R_{jk})^6}{1 - \tau_s/\tau_A + \sum_k (R_0/R_{jk})^6} \right) \right) \quad (I-91)$$

$A_k(0)$ represents the probability that the k -th acceptor

is excited at $t = 0$, before any transfer can have occurred, and is the result of direct excitation. Hence the total intensity at any time t will be given by,

$$I_A(t) = \frac{1}{\tau_A} A(0) \sum_{k=1}^{N_A} e^{-t/\tau_A} + \frac{1}{\tau_A} S(0) \sum_{j=1}^{N_s} \sum_{k=1}^{N_A} \frac{\left(\frac{R_0}{R_{j'k'}} \right)^6 \dots \left(e^{-t/\tau_A} - e^{-t/\tau_s} \left(1 + \sum_{k'=1}^{N_A} \frac{(R_0/R_{j'k'})^6}{1 - \tau_s/\tau_A + \sum_{k'} (R_0/R_{j'k'})^6} \right) \right)}{1 - \tau_s/\tau_A + \sum_{k'} (R_0/R_{j'k'})^6} \quad (I-92)$$

Here we have assumed all the $A_k(0)$ and $S_j(0)$ are equal, corresponding to the initial random excitation requirement.

This expression describes the acceptor fluorescent intensity as a function of time for flash-excitation. The first term on the right corresponds to the direct excitation decay, and the second to the transfer contribution donated by the sensitizers. From this equation we may derive an expression for the transfer efficiency, the ratio of the quanta received by the acceptors

via resonance transfer to the quanta absorbed by the sensitizers,

$$\left(\frac{\eta}{\eta_0}\right)_A = \frac{1}{N_S \tau_A} \int_0^{\infty} dt \sum_K^{N_A} \sum_j^{N_S} \frac{\left(\frac{R_0}{R_{jk}}\right)^6 \left(e^{-\frac{t}{\tau_A}} - e^{-\frac{t}{\tau_S}} \left(1 + \sum_{K'} \left(\frac{R_0}{R_{jK'}}\right)^6 \right) \right)}{1 - \tau_S/\tau_A + \sum_{K'} \left(\frac{R_0}{R_{jK'}}\right)^6}$$

The number of quanta which are absorbed by the sensitizer and (I-93)

which may be transferred to the acceptors, is given by, $S(0) \cdot N_S$.

Integrating gives us the quantum efficiency,

$$\left(\frac{\eta}{\eta_0}\right)_A = \frac{1}{N_S} \sum_K \sum_j \frac{\left(\frac{R_0}{R_{jk}}\right)^6}{1 + \sum_{K'} \left(\frac{R_0}{R_{jK'}}\right)^6} \quad (\text{I-94})$$

This efficiency does of course refer to flash-excitation conditions,

however it can be shown to apply equally well to steady-state

systems, under constant incident exciting light. Under these

conditions we have, for the K -th acceptor,

$$\frac{dA_K}{dt} = -\frac{1}{\tau_A} A_K + \frac{1}{\tau_S} \sum_{j=1}^{N_S} \left(\frac{R_0}{R_{jk}}\right)^6 \frac{I \sigma_j \tau_S}{1 + \sum_{K'} \left(\frac{R_0}{R_{jK'}}\right)^6} \quad (\text{I-95})$$

Since $\sum_{K=1}^{N_A} \frac{dA_K}{dt} = 0$, and the quanta absorbed by the sensitizers per unit time is $I \sigma_j N_S$, then,

$$\sum_{K=1}^{N_A} A_K = \tau_A \sum_j^{N_S} \sum_K^{N_A} \left(\frac{R_0}{R_{jk}}\right)^6 \frac{I \sigma_j}{\left(1 + \sum_{K'} \left(\frac{R_0}{R_{jK'}}\right)^6\right)} \quad (\text{I-96})$$

and,

$$\left(\frac{\eta}{\eta_0}\right)_A = \frac{\frac{1}{\tau_A} \sum_K A_K}{I \sigma_j N_S} = \frac{1}{N_S} \sum_K \sum_j \left(\frac{R_0}{R_{jk}}\right)^6 / \left(1 + \sum_{K'} \left(\frac{R_0}{R_{jK'}}\right)^6\right) \quad (\text{I-97})$$

Thus the quantum efficiency is the same regardless of the excitation mode, and in passing we confirm that our equations obey the conservation of energy principle, (see equation (I-72)),

$$\begin{aligned}
 (\eta/\eta_0)_S + (\eta/\eta_0)_A &= \frac{1}{N_S} \left(\sum_j \frac{1}{(1 + \sum_K (R_0/R_{jk})^6)} \right. \\
 &\quad \left. + \sum_K \sum_j \frac{(R_0/R_{jk})^6}{(1 + \sum_{K'} (R_0/R_{jk'})^6)} \right) = 1 \quad \text{(I-98)}
 \end{aligned}$$

(ii) The Cell Model: Acceptors.

In this section we shall utilize the cell model as proposed for the sensitizers, and develop it to account for the behaviour of the acceptors.

We now have to consider the excitation of the acceptor in the centre of its cell by the sensitizers contained in the "sphere of influence", radius $(\sqrt{\pi}/2C_A)^{1/3}$. Following the arguments used before, we have N_A such cells, each containing n_S sensitizers, with $n_S N_A = N_S$. Thus we lose the sums over j and K in equation (I-92) and obtain,

$$\begin{aligned}
 I_A(t) &= \frac{N_A}{\tau_A} \cdot A(0) e^{-t/\tau_A} \\
 &+ \frac{6C_A}{\sqrt{\pi}} \cdot \frac{(N_A \cdot n_S)}{\tau_A} S(0) \int_0^{(\sqrt{\pi}/2C_A)^{1/3}} \frac{(1/R^6) (e^{-t/\tau_A} - e^{-t/\tau_S \cdot (1+1/R^6)}) R^2 dR}{1 - \tau_S/\tau_A + 1/R^6} \quad \text{(I-99)}
 \end{aligned}$$

By setting $A(0) = 0$, we derive the expression when no acceptors are directly excited, and their excitation is all the result of energy transfer from the sensitizers,

$$I_A(t) = \frac{N_s}{\tau_A} \cdot \frac{6C_A}{\sqrt{\pi}} \cdot S(0) \int_0^{(\sqrt{\pi}/2C_A)^3} \frac{(1/R^6) (e^{-t/\tau_A} - e^{-t/\tau_s(1+1/R^6)}) R^2 dR}{1 - \tau_s/\tau_A + 1/R^6} \quad (I-100)$$

The form of $I_A(t)$ has been evaluated for various τ_s/τ_A ratios, and concentrations, as is shown in fig.5.

If we have $C_A \gg 1$, and $\frac{1}{R^6} \gg 1$, at high concentrations then we obtain,

$$I_A(t) = \frac{N_A A(0)}{\tau_A} e^{-\frac{t}{\tau_A}} + \frac{N_s S(0)}{\tau_A} \cdot \frac{6C_A}{\sqrt{\pi}} \int_0^{(\sqrt{\pi}/2C_A)^3} e^{-\frac{t}{\tau_A}} \cdot R^2 dR$$

$$= \frac{e^{-t/\tau_A}}{\tau_A} (N_A \cdot A(0) + N_s \cdot S(0)) \quad (I-101)$$

Thus the energy absorbed by the sensitizer is apparently instantaneously transferred from sensitizer to acceptor.

However, this transfer does need a finite time, for when we put $t = 0$ in the original expression for $I_A(t)$ we find,

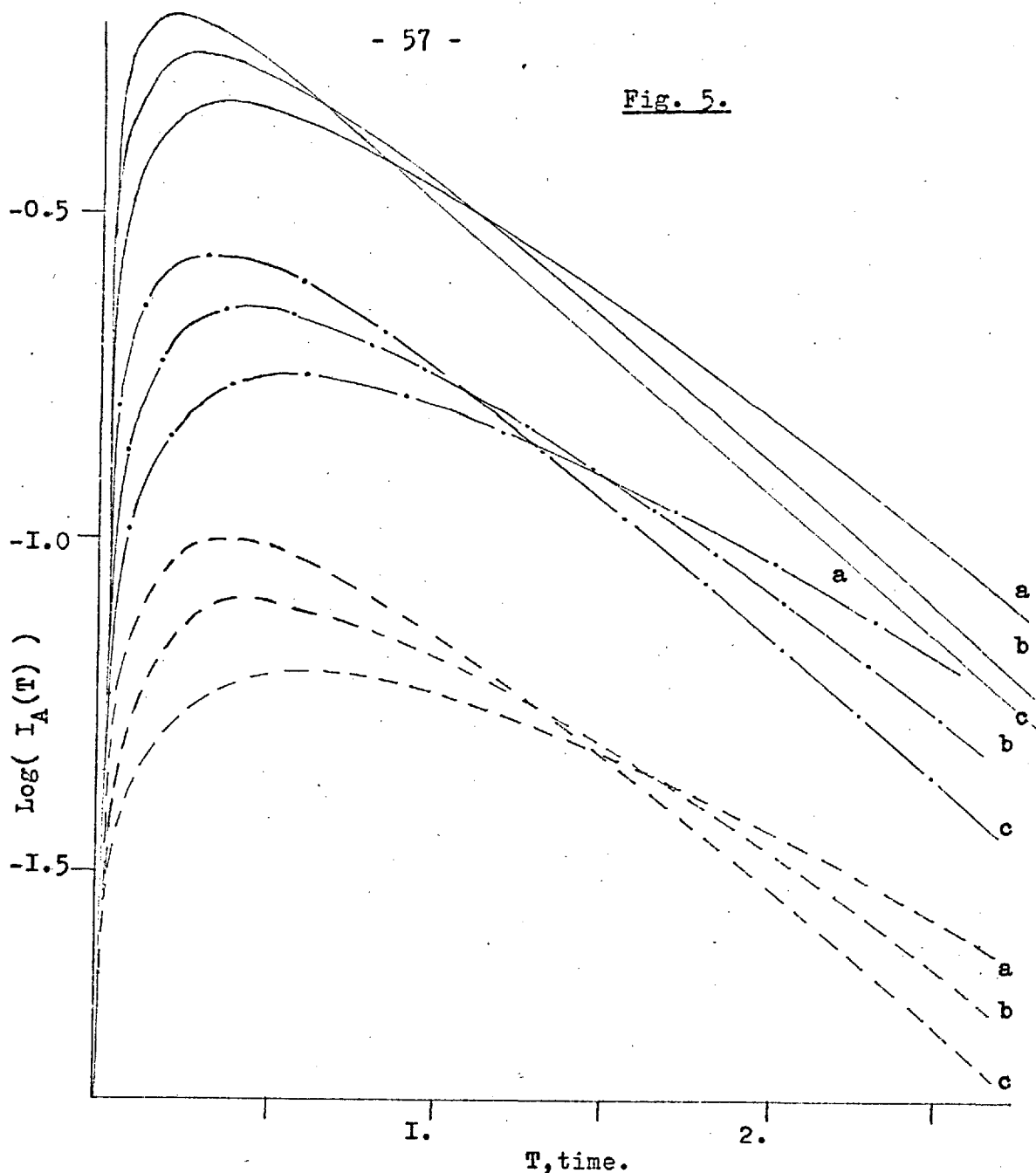
$$I_A(0) = N_A \cdot A(0) / \tau_A \quad (I-102)$$

The factors controlling the energy flow from sensitizers to acceptors are the ratio τ_s/τ_A and the reduced concentration,

C_A . Clearly any transfer is helped by higher concentrations, and also if the sensitizer has a long radiative lifetime, τ_s .

Now let us turn to the quantum efficiency of the transfer. As we

Fig. 5.



Acceptor luminescence as a function of time. The ordinate represents the excitation probability of an acceptor initially in the ground-state at $T=0$. Time is measured in units of . The letters on the curves show the values of the parameters used in their evaluation; $a=0.5, b=1.0, c=2.0$. The solid lines show the function for reduced concentration, $C_A=1.0$, the dashed line, $C_A=0.3$, and the dotted line, $C_A=0.1$.

have seen, the yield is the same for either flash or steady-state conditions, so applying our cell model we obtain,

$$\left(\frac{\eta}{\eta_0}\right)_A = \frac{6CA}{\sqrt{\pi}} \int_0^{\left(\frac{\sqrt{\pi}}{2CA}\right)^{1/3}} \frac{R^2}{(1+1/R^6)} \cdot \left(\frac{1}{R^6}\right) dR = \frac{2CA}{\sqrt{\pi}} \tan^{-1}\left(\frac{\sqrt{\pi}}{2CA}\right) \quad (\text{I-103})$$

This could have been obtained directly from $(\eta/\eta_0)_s$, using equation (I-72).

(iii) Acceptor Lifetime.

Using the definition of "mean - life" mentioned earlier, (37), we obtain with the cell model the ratio of the relative lifetimes,

$$\frac{\tau_A'}{\tau_A} = \frac{\int_0^\infty A(0) t e^{-\frac{t}{\tau_A}} dt + \frac{6CA S(0)}{\sqrt{\pi}} \int_0^\infty t dt \int_0^{\left(\frac{\sqrt{\pi}}{2CA}\right)^{1/3}} \frac{R^2 \left(e^{-\frac{t}{\tau_A}} - e^{-\frac{t}{\tau_s} \left(1 + \frac{1}{R^6}\right)} \right) dR}{\left(1 - \tau_s/\tau_A + 1/R^6\right) R^6}}{\int_0^\infty A(0) e^{-\frac{t}{\tau_A}} + \frac{6CA S(0)}{\sqrt{\pi}} \int_0^\infty dt \int_0^{\left(\frac{\sqrt{\pi}}{2CA}\right)^{1/3}} \frac{R^2 \left(e^{-\frac{t}{\tau_A}} - e^{-\frac{t}{\tau_s} \left(1 + \frac{1}{R^6}\right)} \right) dR}{\left(1 - \tau_s/\tau_A + 1/R^6\right) R^6}} \quad (\text{I-104})$$

This expression may be easily integrated to give,

$$\frac{\tau_A'}{\tau_A} = \frac{1 + \frac{2CA S(0)}{\sqrt{\pi}} \cdot \frac{\tau_s}{\tau_A} \left(\frac{1}{2} \tan^{-1}\left(\frac{\sqrt{\pi}}{2CA}\right) - \frac{\sqrt{\pi}/2CA}{2(1 + \pi/4CA^2)} \right)}{A(0) + \frac{2CA}{\sqrt{\pi}} S(0) \tan^{-1}\left(\frac{\sqrt{\pi}}{2CA}\right)}$$

Here τ_A represents the lifetime of the acceptors in solution, with no resonance transfer occurring. At high concentrations with $C_A \gg 1$, we obtain $\tau'_A/\tau_A = 1$. This is as we would anticipate, because if the excitation is transferred instantaneously from sensitizers to acceptors we might as well excite the acceptors directly. At the other limit, with $C_A \ll 1$, we find with $A(0) = 0$, $\tau'_A/\tau_A = 1 + \tau_s/2\tau_A$. Without $A(0) = 0$, then we have, with $C_A \ll 1$, $\tau'_A/\tau_A = 1$. This latter result would explain why Schmillen, (39), and Galanin, (13), both observed lives tending to τ_A at low concentrations as well as at high concentrations of acceptor. In any experimental set up using filters or even monochromators it is unlikely that $A(0)$ would be zero, and the acceptors would undoubtedly absorb directly some of the incident light. When τ'_A/τ_A is evaluated as a function of acceptor concentration a maximum occurs whose position is determined by the ratio, $A(0)/S(0)$. This is shown in fig. 6. The effect of the transfer is to increase the lifetime of the excitation in solution. At moderate concentrations the excitation lives on the sensitizers until it is passed to the acceptors where it acquires a new lease of life, so that $\tau'_A \geq \tau_A$. In contrast, with increasing transfer probability the excitation's life on the sensitizers becomes successively curtailed with $\tau'_s \leq \tau_s$. All the foregoing concerns decay after flash excitation, we do not have to consider an input intensity which is time-dependent. However, most experimental measurements of lifetimes in solution

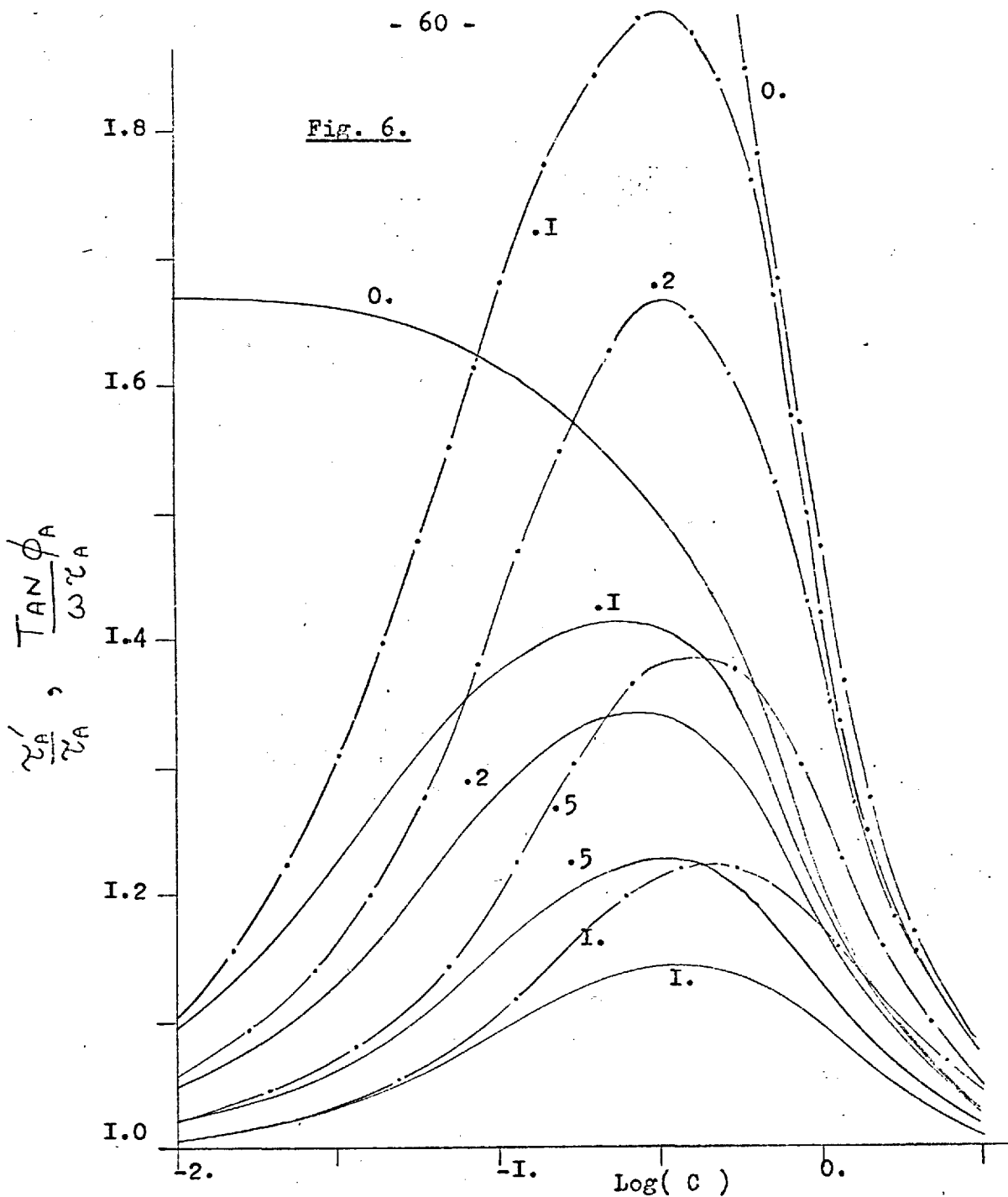


Fig. 6.

The dependence of acceptor lifetime and phase angle on concentration. The solid lines show $\frac{\tau_A'}{\tau_A}$ against reduced concentration, C , with $\tau_A = 1.33$. The ratio $S(0)/A(0)$ is shown on the curves. Function $\frac{\tan \phi_A}{\omega \tau_A}$ with $\omega \tau_A = 1$, $\omega \tau_A = 1.33$, is given by the dashed lines. When, $\omega \tau_A, \omega \tau_A \ll 1$, the functions $\frac{\tan \phi_A}{\omega \tau_A}$, $\frac{\tau_A'}{\tau_A}$, become the same.

involve the use of modulated input light, (39), (40), (41), (42), and we shall now turn to the problem of fluorescence excited by time-dependent illumination.

(6) Time-Dependent Fluorescence.

Here we shall be concerned explicitly with the fluorescence emitted by a solution of acceptors and sensitizers under excitation by a time-dependent incident intensity. Previously we have had either a constant incident beam, or a flash-excitation with the form of a Dirac Delta function. The treatment given now is perfectly general, both the case of steady illumination and the case of flash excitation can be derived as special examples. In this Green's Function method, (38), we consider first the function,

$$S_j(t) = \int_{-\infty}^{\infty} dt' I(t') G_j(t-t') \quad (\text{I-I06})$$

where,

$$G_j(t-t') = \sigma_s u(t-t') e^{-\frac{(t-t')}{\tau_s} \left(1 + \sum_k \left(\frac{R_0}{R_{jk}}\right)^6\right)}$$

and $u(t-t')$ is a step function,

$$u(t-t') = \begin{cases} 0, & t < t' \\ 1, & t > t' \end{cases}$$

$I(t)$ and σ_s are the illumination intensity and sensitizer capture cross-section respectively.

It can easily be shown that this function $S_j(t)$, is a solution to the "driven differential equation" expressing the

time-dependence of S_j , equation (I-8I), since we have,

$$\left(\frac{d}{dt} + \frac{1}{\tau_S} \left(1 + \sum_K \left(\frac{R_0}{R_{jK}} \right)^6 \right) \right) G_j(t-t') = \sigma_S \delta(t-t') \quad (\text{I-IO7})$$

so that,

$$\begin{aligned} & \left(\frac{d}{dt} + \frac{1}{\tau_S} \left(1 + \sum_K \left(\frac{R_0}{R_{jK}} \right)^6 \right) \right) S_j(t) \\ &= \int_{-\infty}^{\infty} dt' I(t') \left(\frac{d}{dt} + \frac{1}{\tau_S} \left(1 + \sum_K \left(\frac{R_0}{R_{jK}} \right)^6 \right) \right) G_j(t-t') \\ &= \int_{-\infty}^{\infty} dt' I(t') \sigma_S \delta(t-t') = \sigma_S I(t) \end{aligned} \quad (\text{I-IO8})$$

Similarly, the differential equation governing the excitation probability of the acceptors under time-dependent illumination,

$$\frac{dA_K}{dt} = -\frac{A_K}{\tau_A} + \frac{1}{\tau_S} \sum_j \left(\frac{R_0}{R_{jK}} \right)^6 S_j + \sigma_A I(t) \quad (\text{I-IO9})$$

has, as a solution,

$$A_K(t) = \int_{-\infty}^{\infty} dt' I(t') G_K(t-t') \quad (\text{I-III0})$$

with,

$$G_K(t-t') = U(t-t') \left(\sigma_A e^{-t'/\tau_A} + \sigma_S \sum_j \left(\frac{R_0}{R_{jK}} \right)^6 \left(e^{-t'/\tau_A} - e^{-t'/\tau_S} \left(1 + \sum_K \left(\frac{R_0}{R_{jK}} \right)^6 \right) \right) \right) / \left(1 - \tau_S/\tau_A + \sum_K \left(\frac{R_0}{R_{jK}} \right)^6 \right)$$

It can be seen that on replacing $I(t')$ by a delta function, $\delta(t-t')$, to give the case of flash-excitation the results for $S_j(t)$ and $A_K(t)$ assume the same form as we have derived previously.

We can now use our cell model to help evaluate the

function $\sum_{j=1}^{N_S} G_j(t-t')$, which we need to interpret the bulk properties of the solution. In this model we consider the acceptors dominating their own particular "sphere of influence", which contains n_s sensitizers, with $N_A \cdot n_s = N_S$. Thus the sum over j , $1 \leq j \leq N_S$, reduces to a sum over n_s , all the sensitizers in our averaged cell. Normalizing the result we obtain,

$$\frac{1}{n_s} \sum_{j=1}^{n_s} G_j(t-t') = G_s(t-t') = \sigma_s U(t-t') e^{-\frac{(t-t')}{\tau_s}} \frac{6CA}{\sqrt{\pi}} \int_0^{(\sqrt{\pi}/2CA)^{1/3}} R^2 e^{-\frac{t}{\tau_s}} \left(1 + \frac{1}{R^6}\right) dR \quad (\text{I-III})$$

Hence we find the total emission of the sensitizers,

$$I_s(t) = \frac{N_S}{n_s} S(t) = \frac{N_S}{n_s} \int_{-\infty}^{\infty} dt' I(t') G_s(t-t') \quad (\text{I-II2})$$

Using the same model for the acceptor function $\sum_{k=1}^{N_A} G_k(t-t')$ we find,

$$I_A(t) = \frac{N_A}{n_A} \int_{-\infty}^{\infty} dt' I(t') G_A(t-t') \quad (\text{I-II3})$$

where,

$$G_A(t-t') = U(t-t') \left(\sigma_A e^{-t/\tau_A} + \dots \right)$$

$$\dots \sigma_s \frac{N_s}{N_A} \frac{6CA}{\sqrt{\pi}} \int_0^{(\sqrt{\pi}/2CA)^{1/3}} \left(\frac{1}{R^6} \right) \frac{R^2 \left(e^{-t/\tau_A} - e^{-\frac{t}{\tau_s}} \left(1 + \frac{1}{R^6}\right) \right) dR}{1 - \tau_s/\tau_A + 1/R^6}$$

It will be noted that either of these expressions could easily be modified to apply to transfer processes which were not governed by the inverse-6 law, all that would be necessary would be to replace $1/R^6$ by $F(R)$. The evaluation of the

integrals at later stages might not however be so straight forward as with the $1/R^6$.

(7) Phase-Fluorimetry.

Most experimental methods used to measure the lifetimes of fluorescing species observe the phase-shift between the modulated input light and the appropriately time-dependent fluorescent output, (13),(39),(40),(41),(42),(43). The only methods not involving the measurement of this steady phase-shift are those using pulse scintillation techniques,(30),(31),(34). These methods follow the decay of excitation in solution, and hence determine τ_A and τ_S directly from the observed $I_A(t)$ and $I_S(t)$. We shall consider the special case where the intensity of the beam illuminating the sample is a sinusoidally modulated function of time * ,

$$I(t) = I_0 \cos(\omega t) + I_B = \text{Re}(I_0 e^{i\omega t} + I_B) \quad (\text{I-II4})$$

Here I_B is the constant background intensity, and ω is the frequency of modulation.

Then the function $S(t)$ is given by using equation (I-II2),

$$S(t) = \text{Re} \left(\int_{-\infty}^{\infty} dt' (I_0 e^{i\omega t'} + I_B) G_S(t-t') \right) \quad (\text{I-II5})$$

* By, $\text{Re}(f)$, the real part of function f , is implied, for example, $\text{Re}(x + iy) = x$.

Hence,

$$S(t) = \text{Re} \left(\int_{-\infty}^{\infty} dt' (I_0 e^{i\omega t'} + I_B) \sigma_s U(t-t') \dots \right. \\ \left. \dots e^{-\frac{(t-t')}{\tau_s}} \frac{\sqrt{\pi}}{2CA} \int_0^{\left(\frac{\sqrt{\pi}}{2CA}\right)^{\frac{1}{3}}} \left(\frac{1}{R^6}\right) e^{-\frac{(t-t')}{\tau_s}} R^2 dR \right) \quad (\text{I-II6})$$

Using the relation,

$$\int_{-\infty}^{\infty} dt' U(t-t') e^{-\frac{(t-t')}{\tau_s}} \beta = \tau_s / \beta$$

we have,

$$S(t) = \sigma_s \tau_s \frac{\sqrt{\pi}}{2CA} \int_0^{\left(\frac{\sqrt{\pi}}{2CA}\right)^{\frac{1}{3}}} R^2 dR \left(I_0 \left[\frac{(1+1/R^6) \cos \omega t + \tau_s \omega \sin \omega t}{(1+1/R^6)^2 + (\omega \tau_s)^2} \right] \right. \\ \left. + I_B / (1+1/R^6) \right). \quad (\text{I-II7})$$

Similarly, from equation (I-II3),

$$A(t) = I_B \left(\sigma_A \tau_A + \frac{\sqrt{\pi}}{2CA} \sigma_s \tau_A \int_0^{\left(\frac{\sqrt{\pi}}{2CA}\right)^{\frac{1}{3}}} \left(\frac{1}{R^6}\right) \frac{R^2 dR}{\left(1 - \frac{\tau_s / \tau_A}{1 + 1/R^6}\right)} \right) / \left(1 - \frac{\tau_s}{\tau_A} + \frac{1}{R^6}\right) \\ + I_0 \tau_A \cos \omega t \left(\frac{\sigma_A}{1 + (\omega \tau_A)^2} + \frac{\sqrt{\pi}}{2CA} \sigma_s \int_0^{\left(\frac{\sqrt{\pi}}{2CA}\right)^{\frac{1}{3}}} \left(\frac{1}{R^6}\right) \frac{R^2 dR}{1 - \tau_s / \tau_A + 1/R^6} \dots \right. \\ \left. \dots \left[\frac{1}{1 + (\omega \tau_A)^2} - \frac{\tau_s / \tau_A (1 + 1/R^6)}{(1 + 1/R^6)^2 + (\omega \tau_s)^2} \right] \right) + \omega \tau_A^2 I_0 \sin \omega t \left(\dots \right. \\ \left. \dots \frac{\sigma_A}{1 + (\omega \tau_A)^2} + \frac{\sqrt{\pi}}{2CA} \sigma_s \int_0^{\left(\frac{\sqrt{\pi}}{2CA}\right)^{\frac{1}{3}}} \left(\frac{1}{R^6}\right) \frac{R^2 dR}{1 - \tau_s / \tau_A + 1/R^6} \left[\frac{1}{1 + (\omega \tau_A)^2} - \frac{(\tau_s / \tau_A)^2}{(1 + 1/R^6)^2 + (\omega \tau_s)^2} \right] \right) \quad (\text{I-II8})$$

For these equations the corresponding phase-shift, ϕ_S and ϕ_A , of the fluorescent light of the two species with respect to the sine-wave input is given by,

$$\frac{\tan \phi_S}{\omega \tau_S} = \frac{\int_0^{\infty} \frac{(\sqrt{\pi}/2CA)^{1/2} R^2 dR}{(1 + \nu R^6)^2 + (\omega \tau_S)^2}}{\int_0^{\infty} \frac{(\sqrt{\pi}/2CA)^{1/2} R^2 dR}{(1 + \nu R^6)^2 + (\omega \tau_S)^2}} \quad (\text{I-II9})$$

and,

$$\frac{\tan \phi_A}{\omega \tau_A} = \left(\frac{\sigma_A}{1 + (\omega \tau_A)^2} + \frac{\sqrt{\pi}}{2CA} \sigma_S \int_0^{\infty} \left(\frac{L}{R^6} \right) \frac{R^2 dR}{1 - \tau_S/\tau_A + \nu R^6} \left[\frac{1}{1 + (\omega \tau_A)^2} - \frac{(\tau_S/\tau_A)^2}{(1 + \nu R^6)^2 + (\omega \tau_S)^2} \right] \right) / \left(\frac{\sigma_A}{1 + (\omega \tau_A)^2} + \frac{\sqrt{\pi}}{2CA} \sigma_S \int_0^{\infty} \left(\frac{L}{R^6} \right) \frac{R^2 dR}{(1 - \tau_S/\tau_A + \nu R^6)} \left[\frac{1}{1 + (\omega \tau_A)^2} - \frac{\tau_S/\tau_A (1 + \nu R^6)}{(1 + \nu R^6)^2 + (\omega \tau_S)^2} \right] \right) \quad (\text{I-I20})$$

Usually in the interpretation of phase fluorimetry results the relation $\tan \phi = \omega \tau$ is used to relate lifetimes to observed phase-shifts, (39), (40), (43). As we have shown above this is not exactly correct in a sensitizer/acceptor system except with $\omega \tau_S \ll 1$ and $\omega \tau_A \ll 1$, when we find,

$$\frac{\tan \phi_S}{\omega \tau_S} = \tau_S' / \tau_S \quad (\text{I-I21})$$

and,

$$\frac{\tan \phi_A}{\omega \tau_A} = \tau_A' / \tau_A \quad (\text{I-I22})$$

Thus the relationship between the phase-angle and the lives is very simple, so long as the inequalities given are fulfilled.*

(8) Reabsorption of Fluorescence. Time-Dependent Theory.

Much experimental evidence concerning the effects of secondary fluorescence comes from results of lifetime studies of single-component solutions as a function of concentration, (13). Because these results are obtained using phase-fluorimeters we must once again consider the time-dependence of the problem in deriving a phase-angle to approximately describe the contributions of primary and secondary fluorescence.

First we shall start with some relations expressing the decay of higher order fluorescence in solution. Considering a solution of pure sensitizer, initially excited at $t=0$, then with time the total probability decays from its value $S(0)$ at $t=0$, so that at any time t ,

$$I_1(t) \sim S(t) = S(0) e^{-t/\tau_S} \quad (\text{I-I23})$$

The rate of loss of probability at any time, t' , is given by,

$$\frac{dS}{dt}(t') = - \frac{S(0)}{\tau_S} e^{-t'/\tau_S} \quad (\text{I-I24})$$

If we imagine the radiative fraction of this probability to be reabsorbed, then the increment $\delta S(t')$ gives rise to the new " $S(0)$ "

* See figs. 3 and 6, where equations (I-II9) and (I-I20) have evaluated for various defining parameters.

term for secondary fluorescence. Thus we find,

$$I_2(t) \sim \frac{S(0)}{\tau_s} \eta_s \int_{t'=0}^{t'=t} e^{-\frac{t'}{\tau_s}} e^{-\frac{(t-t')}{\tau_s}} dt' = \frac{S(0)}{\tau_s} \eta_s e^{-\frac{t}{\tau_s}} t \quad (\text{I-I25})$$

From this expression for $I_2(t)$ we find the lifetime of secondary fluorescence, τ_{s2} , using definition (I-85),

$$\tau_{s2} = \int_{t=0}^{\infty} t^2 e^{-\frac{t}{\tau_s}} dt / \int_0^{\infty} t e^{-\frac{t}{\tau_s}} dt = 2\tau_s \quad (\text{I-I26})$$

So, as we might have anticipated, the lifetime of reabsorbed light in solution is exactly twice that of the simple primary fluorescence.

Also we observe that $I_2(t)$ reaches it's maximum value at τ_s .

A similar treatment for tertiary fluorescence, assuming two complete re-absorptions before eventual emission gives,

$$I_3(t) = \frac{S(0)}{\tau_s^2} \cdot \eta_s^2 \cdot e^{-\frac{t}{\tau_s}} \cdot \frac{t^2}{2} \quad (\text{I-I27})$$

With a maximum at $2\tau_s$, and a lifetime of $3\tau_s$.

In these equations we have assumed complete reabsorption occurring, rather than the partial effects we would expect to observe, so the total intensity could be better represented as,

$$I_T(t) = I_1(t) + I_2(t) + I_3(t) + \dots$$

Hence,

$$I_T(t) = S(0) \left(e^{-\frac{t}{\tau_s}} f_1 + e^{-\frac{t}{\tau_s}} \eta_s \frac{t}{\tau_s} f_2 + e^{-\frac{t}{\tau_s}} \frac{\eta_s^2}{\tau_s^2} \frac{t^2}{2} f_3 + \dots \right) \quad (\text{I-I28})$$

Where $f_1, f_2, f_3, f_4, \dots, f_i$, are the appropriate coefficients representing the proportions of the various orders of fluorescence. In order to simplify our problem we shall consider only primary and secondary fluorescence, neglecting higher-order effects,

$$I_T(t) = f_1 I_1(t) + f_2 I_2(t) \quad (\text{I-I29})$$

Using I_1 and I_2 , given by equations (I-I23) and (I-I25), and applying the time-dependent theory discussed in the last section, we find the total intensity I_T as a function of time, excited by a modulated input, $f_{ex}(t)$.

$$I_T(t) = S(0) e^{-\frac{t}{\tau_s}} \left(f_1 \int_{t'=t}^{t'=t} f_{ex}(t') e^{t'/\tau_s} dt' + \eta_s \frac{f_2}{\tau_s} \int_{t'=-\infty}^{t'=t} f_{ex}(t') e^{\frac{t'}{\tau_s}} (t-t') dt' \right) \quad (\text{I-I30})$$

If we ignore any constant background term in the modulated input, and write $f_{ex}(t) = \cos \omega t$, then we obtain,

$$I_T(t) = \tau_s S(0) \left(\cos \omega t \left[f_1 + \eta_s f_2 (1 - (\omega \tau_s)^2) + f_1 (\omega \tau_s)^2 \right] + \sin \omega t \left[f_1 \omega \tau_s + f_1 (\omega \tau_s)^3 + \eta_s f_2 (2 \omega \tau_s) \right] \right) \quad (\text{I-I31})$$

Hence we can find the phase-shift between the input and the output light, ϕ , with,

$$\frac{\tan \phi}{\omega \tau_s} = \frac{[f_1(1 + (\omega \tau_s)^2) + 2 \eta_s f_2]}{[f_1(1 + (\omega \tau_s)^2) + \eta_s f_2(1 - (\omega \tau_s)^2)]} \quad (\text{I-I32})$$

Results of phase-fluorimetry studies are usually expressed in terms

of lifetimes derived from the equation, $\tan \phi = \omega \tau$, so on rewriting our expression with $(f_2 \tau_s / f_1) = R$, the ratio of the lifetimes with secondary fluorescence is given as,

$$\frac{\tan \phi}{\omega \tau_s} = \frac{\tau_s'}{\tau_s} = \frac{[(1 + (\omega \tau_s)^2) + 2R]}{[(1 + (\omega \tau_s)^2) + R(1 - (\omega \tau_s)^2)]} \quad (\text{I-I32})$$

The ratio f_2/f_1 is obtained simply from the relative intensities of secondary and primary fluorescence, F_2/F_1 , under steady illumination, and may be calculated theoretically as we shall see later.

(9) The Computer Simulation of a Random Solution with Energy Transfer.

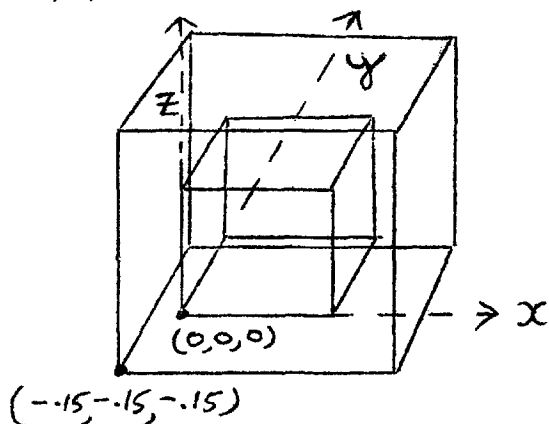
This computer simulation of a system of sensitizers and acceptors was directed at the explicit evaluation of equation (I-65). The species in the sample are allocated coordinates to give an appropriate random distribution, and then the sums over j and K may be evaluated. The purpose of this simulation was to test the validity of Förster's assumptions, as well as those in the similar proposed cell model. The statistics of the transfer were studied by simulating a small volume of solution with random acceptor and sensitizer coordinates, and the decay function of the sensitizers obtained in this microscopic system. The treatment includes the same basic assumptions as those proposed before in alternative statistical treatments. Apart from

the basic premise of the form $I_s(t)$, the particles were assumed to have no finite size, and may be represented as points, without any intermolecular attractive/repulsive potential, and with a random distribution in solution.

The practical application of the simulation was limited to fairly small sample solutions of only about 500 sensitizers and 500 acceptors. Any increase over 1000 total particles resulted in a disproportionate increase in computer time, the evaluation of the R_{jk} matrix becoming prohibitive. Fortunately the $1/R^6$ dependence of the transfer rate means that long-range transfers are unlikely and that the behavior of the small sample closely corresponds to that of a large one. While the size of the sample is not important from the point of view of the transfer rate, as long as it is above a certain critical size, it is important that enough sensitizers should be taken to give a good statistical sample.

The position coordinates of the molecules were allocated by three numbers from a pseudo-random number series, (44). These numbers, with a normal distribution between 0 and 1, were generated from a truncated Log function. The sensitizers were given coordinates in the range 0 to 1, while the acceptors were assigned with coordinates between -.15, and 1.15, the distribution of the pseudo-random series had to be renormalized for this last step. The sensitizers are contained in a unit cube, with origin at (0,0,0),

while the acceptors occupy a larger cube, surrounding the inner one containing the sensitizers. This cube has its origin at $(-.15, -.15, -.15)$, with a side of 1.3 units,



This procedure, imposing a larger acceptor environment on the sensitizers in the inner cube, was followed to eliminate "edge-effects": that is to say all the sensitizers were placed in reasonable environments. If acceptors were contained only in the inner box, the sensitizers at the sides would feel a marked edge effect, having only half an effective environment. This correction was especially needed as the initial sample was so small, and consequently the cube had a high proportion of side for it's volume, $(\text{Surface Area}/\text{Volume})_{\text{cube}} = 6/L$. The ratio of concentrations, $C_S/C_A = N_S/N_A = 500/200$, was chosen, but as we had to consider the acceptors occupying the larger cube, we were involved in dealing with 439 of them also, $(200 \cdot 1.3^3)$, although only 200 were in the inner cube. Hence each final result represented the average for 500 sensitizer environments.

For one particular random set of acceptor and sensitizer coordinates the box size was scaled by appropriate factors for each acceptor concentration investigated. Thus the same sums over K could be re-used with scale factors and they did not need to be constantly re-evaluated. While this was not so satisfactory from a statistical point of view, since a new random distribution was not generated for each new concentration, it certainly was very effective in saving large amounts of computer time.

As well as evaluating $\bar{I}_S(t)$ for the micro-solution the program also calculated the quantum efficiency of the transfer and the lifetimes, using direct numerical integration of the results for \bar{I}_S at the various times. Also some read-outs of individual environments were used to investigate the concept of the "average environment".

The program was run using various random number series, and the results evaluated over a range of concentrations. The results, however, were rather "noisy". This could have been due to poor random numbers. However the pseudo-random numbers used passed several standard tests for "randomness", (44). The most likely cause was the small size of the sample taken, but by taking 10 total "configurations" of acceptors and sensitizers, that is sampling the environments of 5,000 sensitizers, the average was considered to have settled down sufficiently to give acceptable consistency. The deviations from the average results

were most marked, as we would expect, at high concentrations, when the interaction distances of the sensitizers and acceptors were tending to approach the sample size.

Comparing the results obtained from this simulation with those of Förster, (see Table I and fig. 2), it is found there is little deviation. This deviation is however of significant size, and reflects the validity of the approximations in Förster's model, which apply less rigorously as concentration increases. The differences are of the magnitude of typical experimental errors, and often in experimental work results are fitted to the $(n/A_0)_s$ plot to obtain R_0 , and no direct comparison is made using the theoretical expression for R_0 . Hence discrepancies would be hard to confirm experimentally. Perhaps the greatest hope of an experimental check is at high concentrations. In the main, the statistical theory of Förster is validated by our computer simulation, including its rather unexpected dependence on \sqrt{t} in the exponential.

(IO) The Effect of Diffusion on Resonance Transfer.

(a) Introduction.

In all our considerations of resonance energy transfer we have assumed the interacting sensitizers and acceptors ~~to~~ occupy fixed positions throughout the lifetime of the excitation in solution. Thus we have taken the rate of energy transfer as being much faster than any variation in intermolecular

Table I .

Comparison of Computer Simulation Results and those of Förster.

| C_A * | $(\eta/\eta_0)_S^f$ | $(\eta/\eta_0)_S^c$ | $I_S(I)^{\oplus}$ | $I_S(I)^c$ | $I_S(5)^f$ | $I_S(5)^c$ |
|---------|---------------------|---------------------|-------------------|------------|------------|------------|
| 1.0 | .248 | .215 | 24.8 | 19.2 | .039 | .021 |
| 0.3 | .617 | .587 | 100.9 | 98.6 | .881 | .754 |
| 0.1 | .848 | .829 | 150.7 | 148.9 | 2.154 | 2.087 |
| 0.03 | .955 | .939 | 173.4 | 172.4 | 2.945 | 2.921 |
| 0.01 | .989 | .975 | 180.3 | 179.9 | 3.222 | 3.204 |

* Reduced acceptor concentration, measured in units of C_0 .

$\oplus I_S(T)$ gives the number of sensitizers still excited in a sample of 500 at time T after the initial excitation.

This time T is measured in units of τ_S .

f This indicates the Förster Model.

c Indicates the Computer Simulation.

distances. The diffusion, or Brownian Motion of the solute molecules was only involved to the extent of producing a random solution, which was necessary for the statistical treatment of the transfer.

Despite the omission of diffusional effects the treatments of both Förster, (18), (19), and Galanin, (13), have been shown to be in quite good agreement with experimental investigations of the transfer phenomena. Several studies have, however, been specifically directed towards the detection of a diffusional effect, (48), (45), both Weinreb, (46), and Feitelson, (26), obtained evidence in favour of the diffusional enhancement of the resonance transfer rate. However a contradictory result was obtained by Hardwick, (47), who concluded that the effect was negligible.

To some extent these differing results may perhaps be explained by the experimental problems involved. In order to change the diffusional parameters of two solutes in a solvent it is inevitable that either the temperature or the solvent must be altered, (46). The obvious disadvantage is that both methods would also effect the resonance transfer rate quite appreciably. In the first method the change in solvent viscosity, η , with temperature, T , is relied on to change the diffusion coefficient, which is proportional to $\frac{1}{\eta}$. There is, however, some evidence that viscosity may effect the fluorescent efficiency of the individual molecules in solution,

Bowen,(49),(50), found that the return of the excited-state to the ground-state seems to require certain amplitudes of vibration to be reached against the solvent viscosity. Also we must always remember we are considering the bulk macroscopic viscosity , which may not necessarily be applicable on a molecular scale.

The use of temperature changes to obtain different diffusional parameters is also suspect since changes in thermal energy may alter the vibrational populations of the systems concerned, and these populations are directly involved in the transfer probability. Thus any band changes with temperature indicate a shift in the resonance conditions. Attempts have been made to allow for all these variations experimentally,(46), and to isolate the diffusional effects, but often the corrective factors involved are relatively large.

Variation in the solvent has also been applied to alter the mobility of species in solution. Solutions are investigated and then polymerized,(48),(51),(52),(53),(54),(55), or the system's viscosity changed by adding various proportions of other solvents to the main solvent,(46).

While these methods are valid for the Förster mechanism, assuming no band shape changes and no solvent-solute interaction effects, one should remember that if the transfer goes even partially through excited states of the medium any solvent change may alter the whole process. This may be a serious

objection to the polymerization method, where the whole mechanism of the transfer may be altered. We may have virtual excited-states in the solid phase, or even exciton delocalization

Most evidence seems to point to the fact that if a mechanism of transfer is essentially of the single-jump variety, with localized excitations, the diffusional effect is not too large, and the model is one of the Förster type rather than the essentially diffusion controlled quenching discussed by Bowen,(49),(50), such as oxygen quenching of organic dyes in solution obeying the Smoluchowski rate,

$$K_D = 8 a R T / 3000 \eta$$

where a = a molecular dimension.

A theoretical treatment of the effects of diffusion on the Förster model has been attempted by Feitelson,(26), using a mean displacement approximation. This method seems rather fallacious however. The idea of allowing for diffusion by taking a term appearing in Förster's statistics, and then allowing this " average distance " term to change with time seems questionable. We shall now consider an alternative to this model.

(b) The Diffusion Model.

Solving Fick's second law,(58),

$$\frac{\partial c}{\partial t} = D \nabla^2 c \quad (\text{I-I34})$$

for spherical symmetry, we find the probability function of the

diffusing particle, initially at $r=0$ at $t=0$,

$$p(r) dr = \frac{1}{(4\pi Dt)^{3/2}} e^{-\frac{r^2}{4Dt}} \cdot 4\pi r^2 dr \quad (\text{I-I35})$$

where D is the diffusion coefficient. The function $p(r)$ expresses the probability of finding the particle between a radius of r and $r+dr$ from its starting point after a time t . The mean displacement of the particle is given by \bar{r}^2 ,

$$\bar{r}^2 = \frac{\int_0^{\infty} r^2 p(r) dr}{\int_0^{\infty} p(r) dr} = 2Dt \quad (\text{I-I36})$$

Clearly if we had taken the mean value \bar{r} , we would have obtained zero.

We shall use this mean displacement instead of integrating over $p(r)dr$, in order to simplify the mathematical treatment used later. The meaning of $p(r)dr$ and $\sqrt{\bar{r}^2}$ can be understood as the statistical average of the Random Walks or Brownian Motions of a large number of particles, all started at $r=0$ and $t=0$.

Before considering the interactions of a whole system of acceptors and sensitizers with diffusion, we shall first consider the pair interaction for an excited sensitizer and an acceptor separated by a distance R_{jk} . The rate of transfer is given by equation (I-62), but for our time-dependent problem

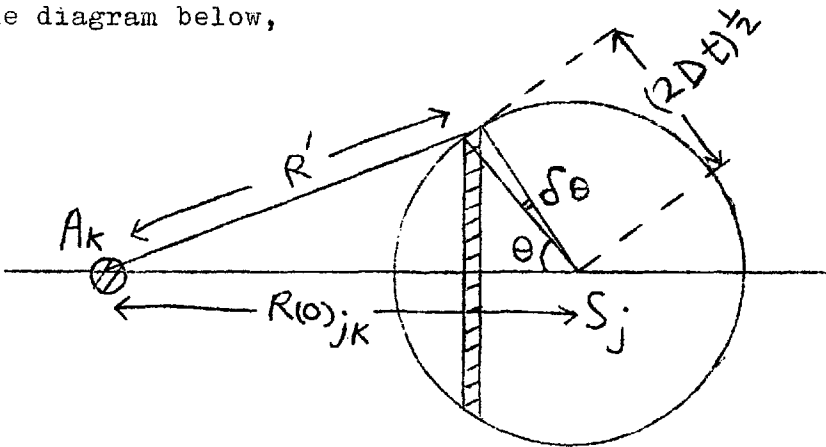
we must rewrite this,

$$\eta_{jk}(t) = \frac{1}{\tau_s} \frac{R_0^6}{(R_{jk}(t))^6} \quad (\text{I-I37})$$

Let us simplify the situation by fixing the acceptor, and allowing the sensitizer to diffuse, with a diffusion coefficient, D , given by (17),

$$D = D_A + D_S \quad (\text{I-I38})$$

Then the rate η_{jk} at any time t can be obtained using the diagram below,



and we find,

$$\eta_{jk}(t) = \frac{1}{\tau_s} \frac{R_0^6}{2} \int_0^\pi \frac{\sin(\theta) d\theta}{(R_{(0)_{jk}}^2 - 2(2Dt)^{1/2} R_{(0)_{jk}} \cos \theta + 2Dt)^3} \quad (\text{I-I39})$$

Note here that we have used the mean displacement model for simplicity, the probability the sensitizer is at radius R' and angle θ being given by,

$$\frac{\sin \theta (2Dt) 2\pi d\theta}{4\pi (2Dt)}$$

On integration we find,

$$\eta_{jk}(t) = \frac{R_0^6}{\tau_s} \frac{(R_{(0)jk}^2 + 2Dt)}{(R_{(0)jk}^2 - 2Dt)^4} \quad (\text{I-I40})$$

This result represents the averaged time-dependence of the transfer rate over a large number of systems, started with $R_{jk} = R_{(0)jk}$ at $t=0$.

This result corresponds to that obtained by Feitelson, (26), however we must observe, as Feitelson did not, that $\eta_{jk}(t)$ has a discontinuity at $t = \frac{R_{(0)jk}^2}{2D}$, that is when $R_{(0)jk}^2 = 2Dt$.

The reason for this incongruity is obvious, in either the mean displacement or the full distribution model we must always have this problem. For at $t = \frac{R_{(0)jk}^2}{2D}$ on the mean displacement model we place a small probability of excited sensitizer on the acceptor, which since the R_{jk} term is now zero, results in the discontinuity. Similarly, on the distribution model we have the same trouble, except here it occurs at any time t , with $t \neq 0$, as there will always be some probability, however low, of the sensitizer sitting on top of the acceptor. Fortunately this problem can be circumvented quite simply by allowing the acceptors and sensitizers to have a certain collision size, and this will be discussed in more detail later. Now, however, we turn to the basic differential equation, expressing the decay of the sensitizer luminescence as a function of time, although now we allow for time dependent coordinates,

$$- \frac{dI_j}{dt} = \frac{1}{\tau_s} \left(1 + \sum_K \left(\frac{R_0}{R_{jK}(t)} \right)^6 \right) I_j(t) \quad (\text{I-I41})$$

Replacing the time-dependent term sum, $\frac{1}{\tau_s} \sum_k \left(\frac{R_0}{R_{jk}(t)} \right)^6$ by $\eta_j(t)$, and integrating over time we obtain,

$$I_j = I_j(0) \exp\left(-\left(\frac{t}{\tau_s} + \int_0^t \eta_j(t) dt\right)\right) \quad (\text{I-I42})$$

I_j representing the decay of the j -th sensitizer in the vicinity of the acceptors, $\eta_j(t)$ has been defined earlier, and the meaning of its integral is perhaps best understood on the Brownian Motion model.

Although after a time t , the mean displacement of the sensitizer is represented as $(2Dt)^{1/2}$ the molecule will in fact have moved very much further than this, having performed many short random walks in solution. If we denote each "infinitely fast" jump by \dot{i} , and give a residency time of τ_i after each \dot{i} -th jump, then we may write for the total possibility transfer has occurred,

$$P_j(t) = \sum_k \sum_{i=1}^N \frac{1}{\tau_s} \left(\frac{R_0}{R_{jk}(i)} \right)^6 \tau_i \quad (\text{I-I43})$$

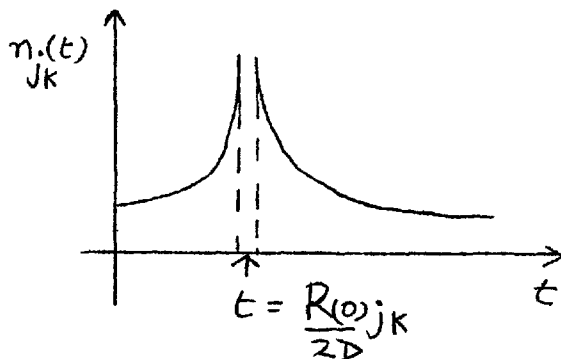
where $\sum_i \tau_i = t$, N jumps occurring in time t . Clearly in the limit when τ_i is small this reduces to,

$$P_j(t) \rightarrow \int_0^t \frac{1}{\tau_s} \left(\frac{R_0}{R_{jk}(t)} \right)^6 dt = \int_0^t \eta_j(t) dt \quad (\text{I-I44})$$

To obtain our final total intensity, $\sum_{j=1}^{N_s} I_j(t)$, we shall use the cell model already proposed, thus dropping the sum over K in $\eta_j(t)$, $\eta_j(t) = \frac{1}{\tau_s} \left(\frac{R_0}{R_{jk}} \right)^6$ as we are only concerned with one single acceptor occupying its own isolated cell, hence we have to evaluate,

$$I_j(t) = I_j(0) e^{-\left(\frac{t}{\tau_s} + \int_0^t \eta_j(t) dt \right)} \quad (\text{I-I45})$$

before we can find the total intensity function. Unfortunately in obtaining the integral over t of $\eta_j(t)$ we immediately run into the problem of the discontinuity, with $t \geq \frac{R_0^2}{2D} k_j$.



However, as mentioned briefly before, we can easily remove this problem by assigning the sensitizer/acceptor distance R_{jk} a certain minimum value, $R_{jk} \geq R_c$. This is physically reasonable, for apart from the physical size of the two molecules, there is the solvation shell of each to consider.

Thus in the time range $\frac{(R_0 - R_c)^2}{2D} \leq t \leq \frac{(R_0 + R_c)^2}{2D}$, that is as $\sqrt{\tau^2}$ passes from $\frac{R_0 - R_c}{jk}$ to $\frac{R_0 + R_c}{jk}$ the rate of transfer

is taken as constant, with the value of $n_j \left(\frac{(R_{(0)jk} - R_c)^2}{2D} \right)$, outside this range we integrate normally. Hence we have three domains to consider the evaluation of $\int_0^t n_j(t) dt$ over. We shall use the notation,

$$I_n(t) = \int_0^t n_j(t) dt = \frac{1}{\tau_s} \int_0^t R_0^6 \frac{(R_{(0)jk}^2 + 2Dt)}{(R_{(0)jk}^2 - 2Dt)^4} dt \quad (I-I46)$$

and omit the zero in the radius at $t=0$ term, $R_{(0)jk} \rightarrow R_{jk}$.

(a). With $0 \leq t < \frac{(R_{jk} - R_c)^2}{2D}$

On evaluation of the integral as a function of time we obtain,

$$I_n(t) = \frac{R_0^6}{2D\tau_s} \left(\frac{2}{3} \cdot \frac{R_{jk}^2}{(R_{jk}^2 - 2Dt)^3} - \frac{1}{2} \frac{1}{(R_{jk}^2 - 2Dt)^2} - \frac{1}{6R_{jk}^4} \right) \quad (I-I47)$$

(b). With $\frac{(R_{jk} - R_c)^2}{2D} \leq t \leq \frac{(R_{jk} + R_c)^2}{2D}$

The total probability is regarded as constant in this range, where the discontinuity occurs, and set equal to $I_n \left(\frac{(R_{jk} - R_c)^2}{2D} \right)$. Thus we have,

$$I_n(t) = \frac{1}{\tau_s} \frac{R_0^6}{2D} \left(\frac{2}{3} \frac{R_{jk}^2}{(2R_{jk}R_c - R_c^2)^3} - \frac{1}{2} \frac{1}{(2R_{jk}R_c - R_c^2)^2} - \frac{1}{6R_{jk}^4} \right) + \frac{R_0^6}{R_c^4 \tau_s} \frac{(2R_{jk}^2 + R_c^2 - 2R_{jk}R_c)}{(2R_{jk} - R_c)^4} \left(t - \frac{(R_{jk} - R_c)^2}{2D} \right) \quad (I-I48)$$

(c). With $t > \frac{(R_{jk} + R_c)^2}{2D}$

For this, the final domain we have,

$$I_n(t) = \frac{1}{\tau_s} \frac{R_0^6}{2D} \left(\frac{2}{3} \left(\frac{R_{jk}^2}{(R_{jk}^2 - 2Dt)^3} + \frac{R_{jk}^2}{(R_c^2 + 2R_{jk}R_c)} \right) - \frac{1}{2} \left(\frac{1}{(R_{jk}^2 - 2Dt)^2} - \frac{1}{(R_c^2 + 2R_{jk}R_c)^2} \right) \right) + \frac{R_0^6}{R_c^4 \tau_s} \frac{(2R_{jk} + R_c^2 - 2R_{jk}R_c)}{(2R_{jk} - R_c)^4} \cdot \left(\frac{(R_{jk} + R_c)^2 - (R_{jk} - R_c)^2}{2D} \right) + \frac{R_0^6}{2D \tau_s} \left(\frac{2}{3} \cdot \frac{R_{jk}^2}{(2R_{jk}R_c - R_c^2)^3} - \frac{1}{2} \cdot \frac{1}{(2R_{jk}R_c - R_c)^2} - \frac{1}{6} \frac{1}{R_{jk}^4} \right)$$

These integrated rates may be inserted into the cell (I-I49) model, using the appropriate $I_n(t)$ depending on, t with the modification of the "closest approach" distance R_c . Thus we find our total decay represented as,

$$I_s(t) = \frac{3 e^{-\frac{t}{\tau_s}}}{(\sqrt{\pi}/2CA - R_c^3)} \int_{R=R_c}^{R = (\sqrt{\pi}/2CA)^{1/3}} \exp(-I_n(t)) R^2 dR \quad (I-I50)$$

Where the radius of the cell, R , is measured in units of R_0 .

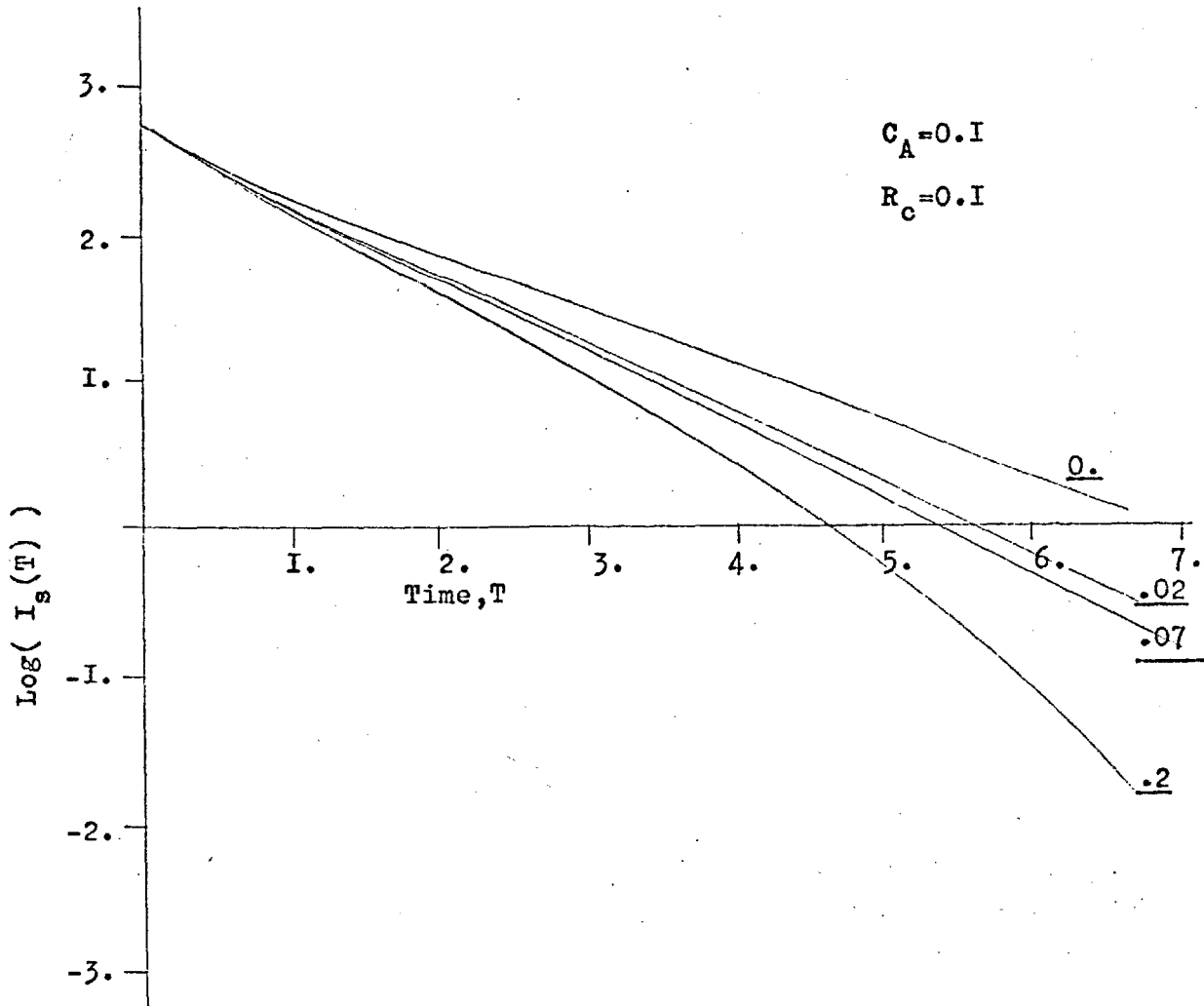
Hence $I_s(t)$ may be obtained by numerical integration at each time t as required, using the appropriate form of $I_n(t)$ given by the equations (I-I47 to I-I49) for each combination of (R, t) in the integral (I-I50).

From $I_s(t)$ for a given concentration of acceptors C_A , and a reduced diffusion coefficient D^* , with $D^* = \frac{D \nu_s}{R_c^2}$, the quantum efficiency and the lifetime were calculated from numerical integration of $I_s(t)$ itself. It was found the results were not critically dependent on R_c , so the value of R_c was standardized in all calculations at 0.1 units of R_0 , that is 3-4 Å.

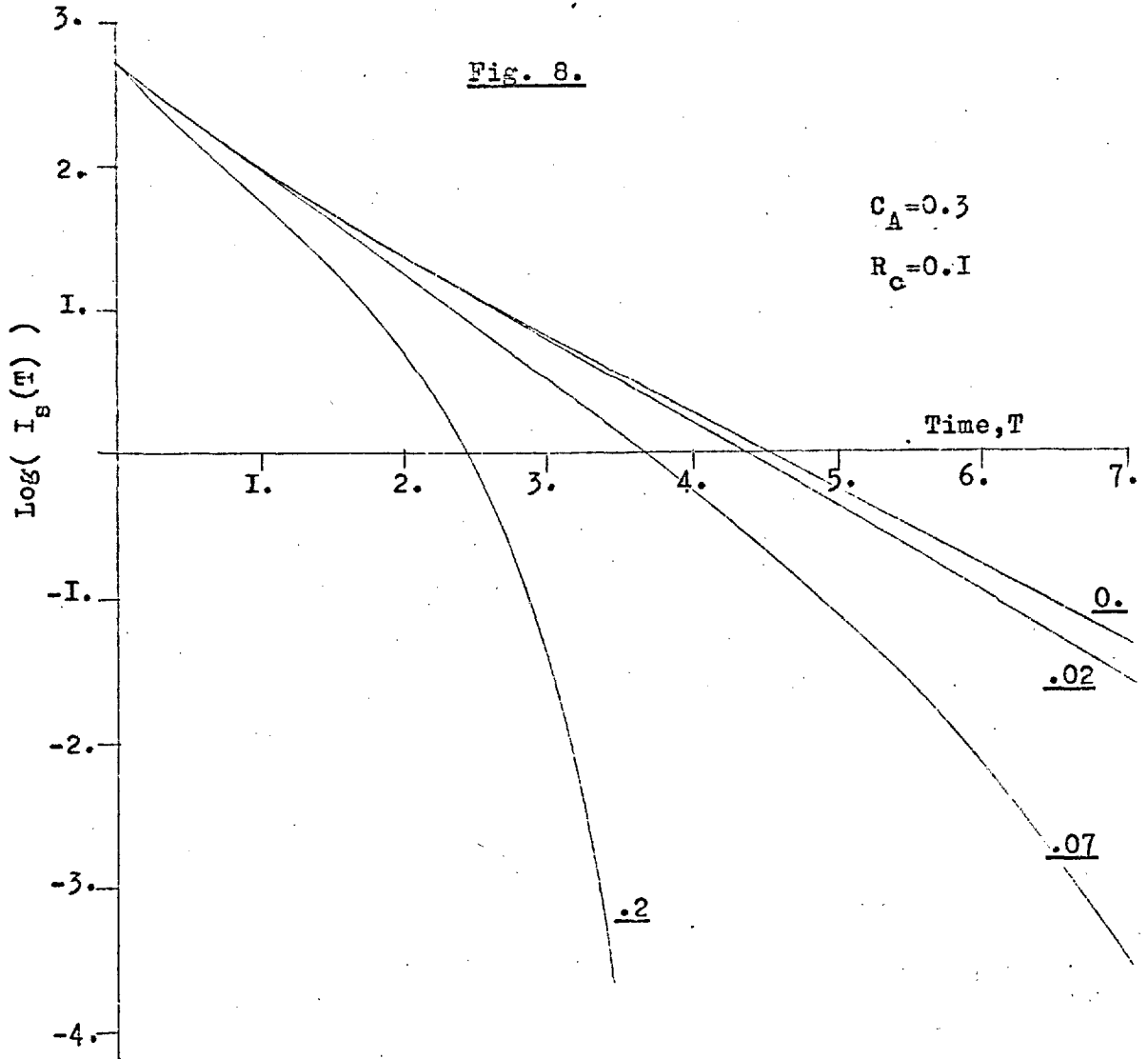
The results of evaluating $I_s(t)$ and $(\eta/n_0)_s$, ν'_s/ν_s , as functions of concentration and reduced diffusion coefficient, shown in figs. 7 to 12, indicate as we might have expected that diffusion has its greatest effects at intermediate concentrations. At high concentrations the transfer of excitation is so fast that diffusion hardly has time to occur and affect the issue. At low concentrations the radiative decay of excitation predominates any non-radiative effects, and the separations between sensitizers and acceptors are so large that diffusion does little to favour transfer within the lifetime of the excitation in solution.

As we would expect, the most sensitive parameter to diffusion is $I_s(t)$, whilst unfortunately the least sensitive is $(\eta/n_0)_s$, which is the usual experimentally measured quantity. Thus although we do find a diffusive effect it would be hard to detect, as often we fit experimental $(\eta/n_0)_s$ to obtain our values of R_0 and C_0 , and as we can see the transposing of the various functions with differing viscosities, could be done in such a way that they could all approximate to the function $(\eta/n_0)_s$ with $D^* = 0$.

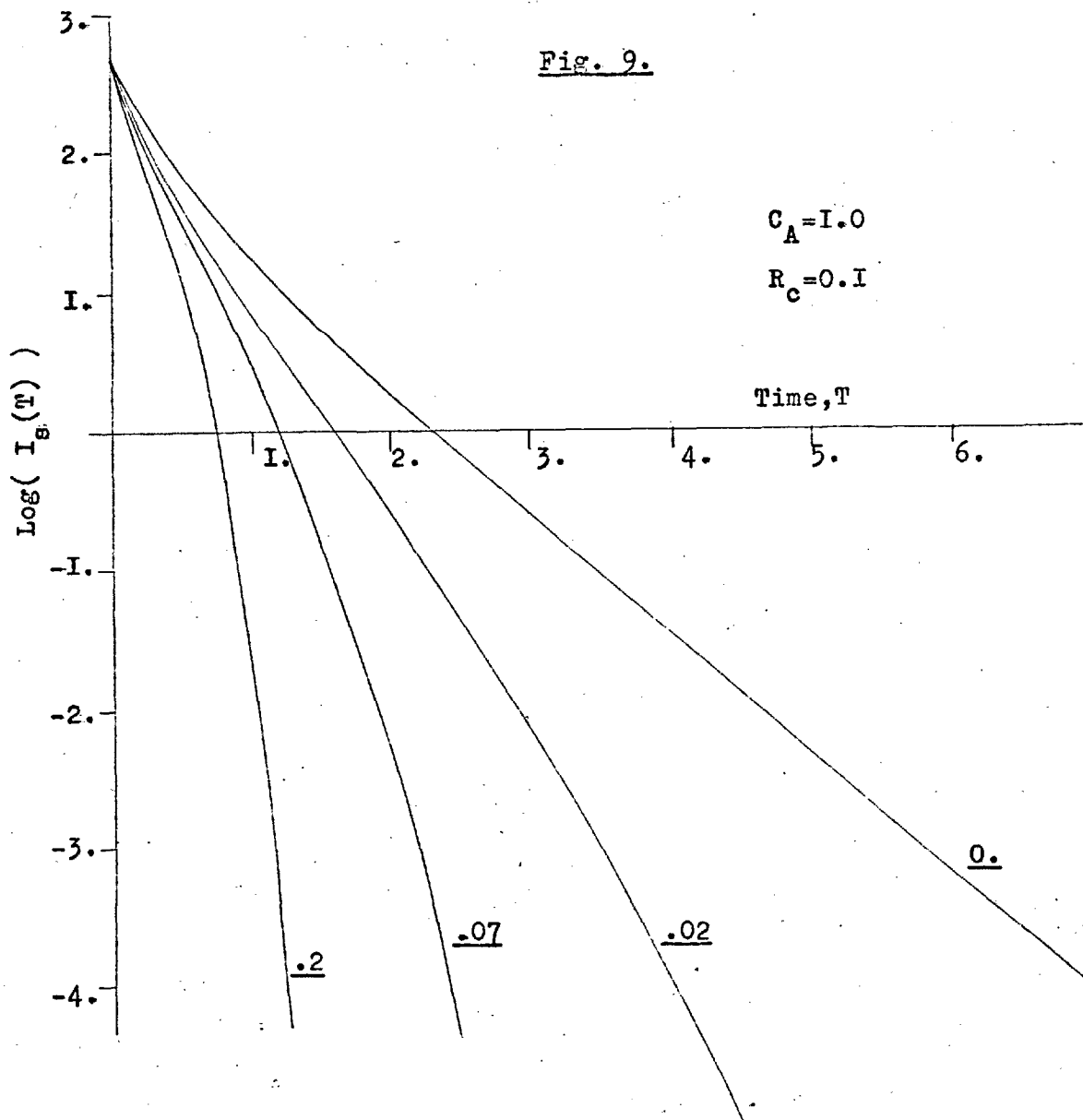
Fig. 7.



The diffusion model: the decay of a sample of 500 sensitizers with a reduced acceptor concentration, $C_A = 0.1$. Time is measured in units of τ_s . The critical radius for the sensitizers is $R_c = 0.1$. The appropriate reduced diffusion coefficients, D_c^* , are shown underlined on the curves.

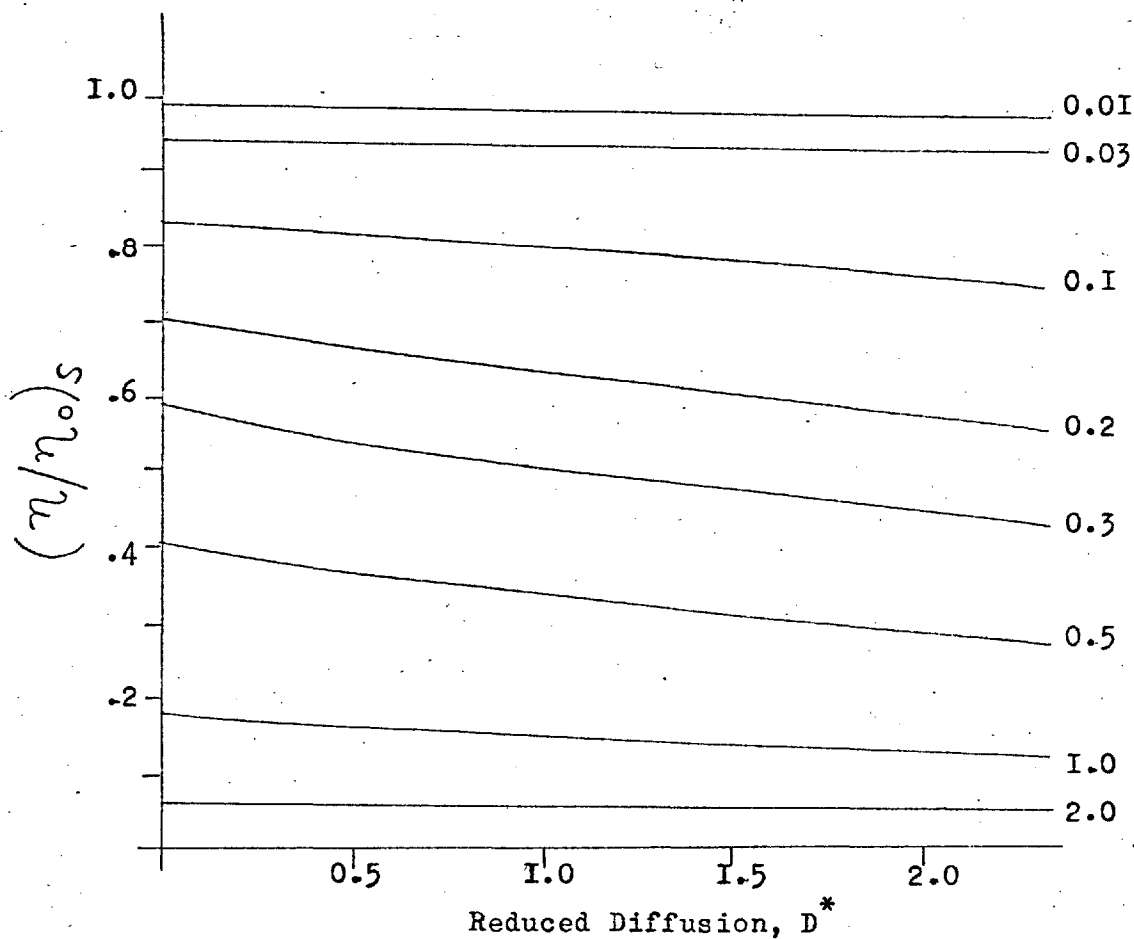


The diffusion model: The decay of a sample of 500 sensitizers with a reduced acceptor concentration, $C_A = 0.3$. Time is measured in units of τ_s . The critical radius for the sensitizers is $R_C = 0.1$. The appropriate reduced diffusion coefficients, D_c^* , are shown underlined on the curves.

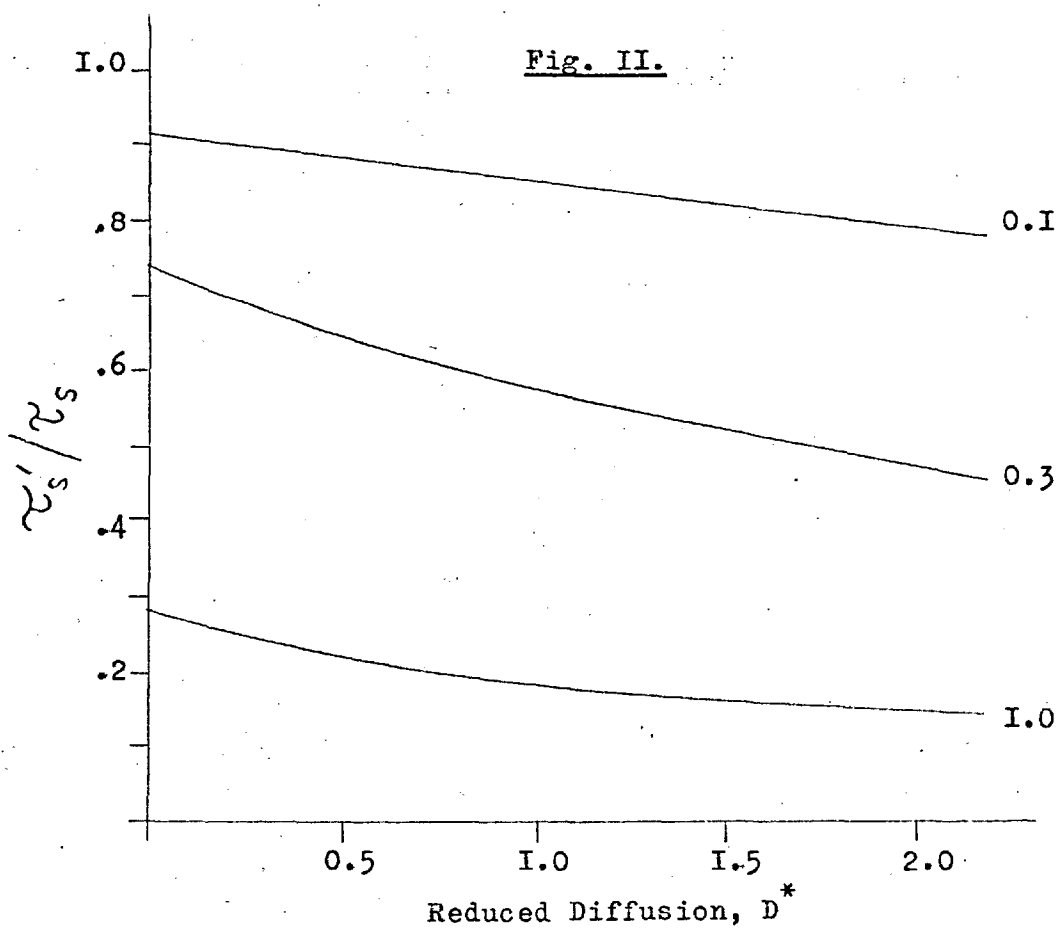


The diffusion model: The decay of a sample of 500 sensitizers with a reduced acceptor concentration, $C_A = 0.3$. Time is measured in units of τ_s . The critical radius for the sensitizers is $R_c = 0.1$. The appropriate reduced diffusion coefficients, D^{*c} , are shown underlined on the curves.

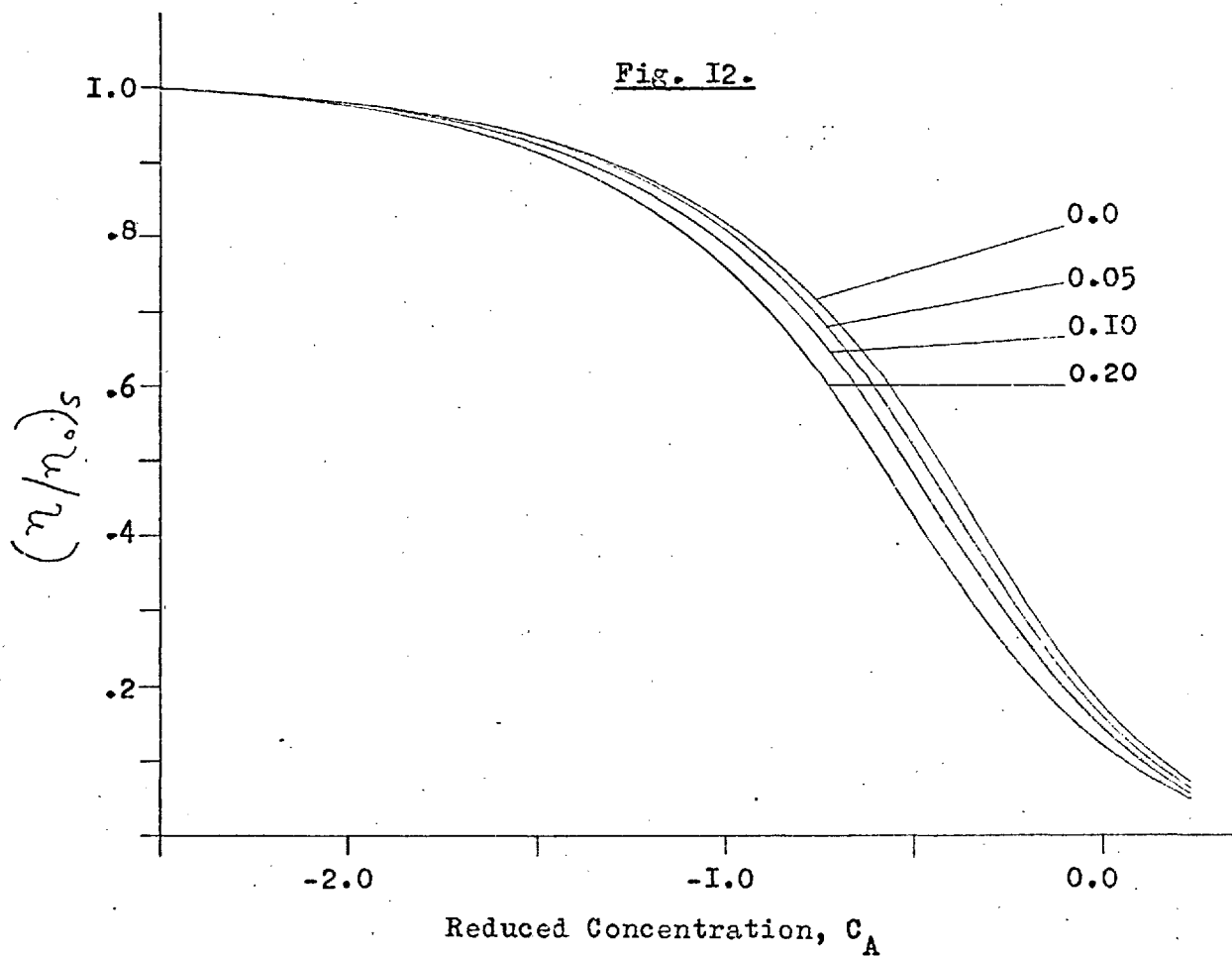
Fig. 10.



The Diffusion Model: The effect of diffusion on sensitizer quantum efficiency, $(\eta/\eta_0)_s$, at various acceptor concentrations. Diffusion coefficients are expressed in reduced units, as are the acceptor concentrations marked on the right by their respective curves. The critical radius $R_c=0.1$.



The Diffusion Model: The effect of diffusion on sensitizer lifetime, τ_s'/τ_s , at various acceptor concentrations. The critical radius of the sensitizers, $R_c = 0.1$. Both diffusion coefficients and acceptor concentrations shown on the curves are in reduced units.



The Diffusion Model: The effect of several rates of diffusion on sensitizer quantum efficiency, $(\eta/\eta_0)_s$, as a function of reduced acceptor concentration, C_A . The reduced diffusion coefficients appropriate to the various curves are shown on the right. Again the critical radius, $R_c=0.1$.

We see the relatively small effect of diffusion on the apparent values of R_0 , the coupling parameter in Table 2. These results were obtained by calculating the various concentrations, C_A , which with the diffusion coefficients given, D^* , give the same quantum yield as with $C_A = 0.3$, and $D^* = 0$. The apparent R_0 values are obtained on an arbitrary assumption that $R_0 = 30 \text{ \AA}$ with no diffusion.

Table 2.

| C_A | D^* | R_0 |
|-------|-------|-------|
| 0.30 | 0.0 | 30.0 |
| 0.26 | 0.05 | 31.0 |
| 0.24 | 0.10 | 32.5 |
| 0.20 | 0.20 | 34.5 |

The interaction distance could be theoretically derived from the absorption spectra of the species concerned, but as these are not always exactly known R_0 would be indeterminate within several \AA units. So direct theoretical/experimental comparisons of R_0 would be a very unfavourable way of attempting to isolate a diffusional effect. We may note that for a $D^* = .1$, R_0 changes from $D^* = 0$ to $D^* = 0.1$ by only 2.5 \AA , and yet in the lifetime of the excitation the sensitizer could have diffused $\sim 13. \text{\AA}$. This illustrates the relative unimportance of the diffusional effect, as it only begins to change the

distribution in solution after the initial decay or transfer has occurred.

(c) Experimental Comparison with Proposed Model.

There are unfortunately few sources of data suitable to test these approximations. The results obtained certainly agree with Weinreb's rather qualitative pulse scintillation data, (25), which showed an increase in decay constant, $1/\tau_s$, with decreasing viscosity.

Some earlier results of Weinreb, (46), are more suited to test the theory. He measured the efficiency of transfer of Naphthalene to Anthracene in paraffin oil as a function of temperature, correcting for all non-diffusional effects, thus obtaining $(\eta/\eta_0)_s$ as a function of the diffusion parameter, T/η . Using $\tau_s = 5.2 \times 10^{-9}$ sec., (59), and $R_0 = 40$ Å. obtained from his $D^* = 0$. results, and the viscosity as a function of temperature $\eta(T)$ for paraffin oil he quoted, it was possible to find the reduced diffusion coefficients for various temperatures. The equation used was,

$$D = kT/6\pi\eta a \quad (I-151)$$

with T taken as constant over the small range of temperature involved, $T = 295$ °K and $a = 2.5$ Å. Then $D^* = D_A^* + D_S^* \approx 1.7/\eta$ with η in centipoise, this agrees with Feitelson, (26).

With these parameters a reasonable correspondance with

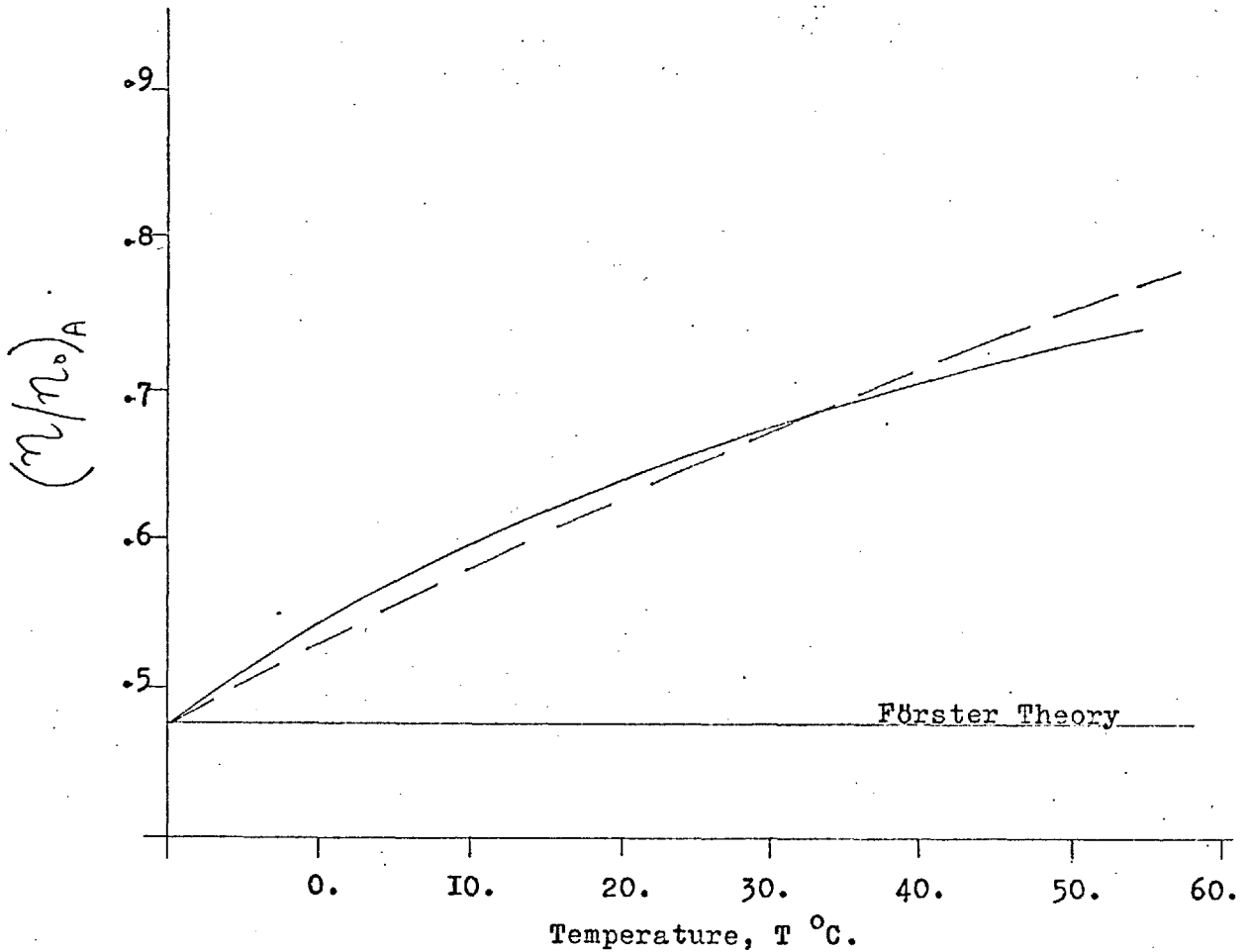
the experimental results was obtained, see fig. 13, using the model previously discussed. However a similar comparison attempted for the Toluene/Anthracene system in paraffin oil did not give such good results, but as Weinreb concluded this system did not appear to be of Förster type mechanism, the lack of correspondence is not surprising.

(II) Some Comments on Resonance-Transfer.

We must first acknowledge that the original Förster transfer mechanism and statistical treatment was, and still is, perfectly satisfactory in explaining experimental singlet/singlet transfer phenomena in solution. The neglect of diffusion has been largely validated, and the effect of averaging over all the possible orientations of the dipoles shown to be the same, irrespective of at what stage in the statistics this averaging is carried out, (14). Even the statistical treatment of the solution problem has been shown to be basically correct by the use of a computer simulation.

Thus it would appear to all intents that the Förster model is well established, and until much more accurate experimental results are available it would seem unlikely to be dropped in favour of a more sophisticated model. We have only to remember all the difficulties in the discussion of secondary fluorescence and other reabsorption effects to realize that any increase in experimental accuracy would be quite difficult. A full discussion of these reabsorption effects is given in the next section.

Fig. 13.



The variation of transfer efficiency, $(n/n_0)_A$, with temperature for the system Naphthalene/Anthracene in paraffin oil is shown by the solid line. These results were obtained by Weinreb, (46). The diffusion model prediction is given by the dashed line. The Förster model is independent of diffusion parameters, and hence is invariant under temperature changes.

In fact , in view of the inaccuracy of most results, the cell model proposed would seem of sufficient accuracy, and is certainly useful for deriving physical quantities as analytic functions, rather than as numerical integration problems, as often occurs with the Förster model.

As we have stated previously the mechanism is well established but has nothing to say in the "allowing" of transitions between states of different multiplicities, essentially the singlet/triplet transfer problem,(24),(60). For this situation a more complex interaction term is needed, (8).

The break-down of the dipole-dipole approximation at high concentrations is again difficult to confirm experimentally , because this is just where the output intensities of solutions are at their lowest, and where reabsorption processes tend to dominate any possible measurements.

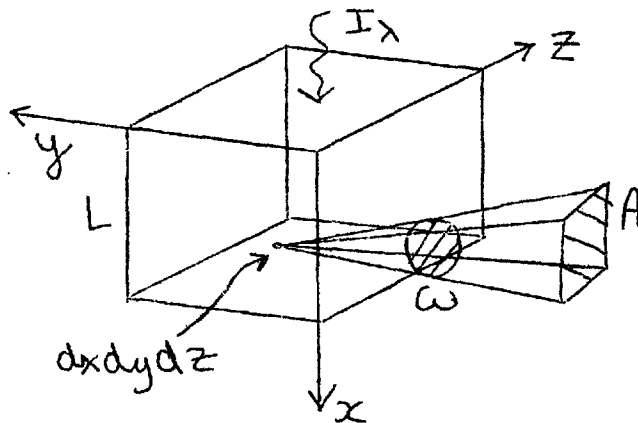
(I2) Light Reabsorption in Fluorescent Solutions.

Before any treatment of the reabsorption of fluorescence we first consider the phenomena of primary fluorescence, ignoring contributions from secondary fluorescence following light reabsorption in solution.

(a). Primary Fluorescence.

The evaluation of the intensity of primary fluorescence is essentially a geometric problem, (61),(62). We are vitally concerned with the spatial arrangement of the cell containing the sample and the system used to excite and detect the

fluorescent light. In the following treatment we consider the effect of exciting a fluorescent sample, in the form of a cube of side L , with parallel monochromatic light of constant wavelength, λ , and intensity I_λ . The coordinates (x,y,z) are chosen with the light incident parallel to the x -axis, and perpendicular to the face formed by the z and y -axes.



The fluorescence emitted by an incremental volume of solution, $dx dy dz$, at (x,y,z) is obtained using Beer's Law, (I7),

$$dF = I_\lambda \epsilon_\lambda c e^{-\epsilon_\lambda c x} \cdot \eta_\lambda dx dy dz \quad (\text{I-152})$$

where c is the concentration, and ϵ_λ the extinction of the fluorescing species. The factor η_λ is the quantum efficiency of the subsequent fluorescence process, that is the fluorescent conversion ratio,

$$\eta_\lambda = (\text{fluorescent quanta/absorbed incident quanta})$$

This increment of the total fluorescence is emitted in all directions, as in solution all the molecules are randomly
However in leaving the solution this intensity suffers

attenuation by reabsorption given by the extinction of the solution for the fluorescent light $\epsilon_{\lambda'}$ *. The intensity is also distributed throughout the fluorescent spectrum of the species concerned, hence the output in the range λ' to $\lambda'+\Delta\lambda'$ is given by $dF f(\lambda') d\lambda'$, where f is the normalized intensity function,

$$\int_{\lambda=0}^{+\infty} f(\lambda) d\lambda = 1$$

In most practical investigations the intensity of fluorescence is observed through the use of some detector of effective area A . The area A may represent a monochromator slit, an appropriate filter or lens, in any case it will, (especially in the case of the monochromator), only be sensitive to a certain "pass-band" of radiation, and will subtend a certain solid angle, ω , at each volume increment of solution. Hence the proportion of fluorescence in the band $\Delta\lambda'$ incident on area A , positioned parallel to any of the sides of the cell will be given by,

$$dF_{SD} = \int_{\lambda''=\lambda'-\Delta\lambda'/2}^{\lambda''=\lambda'+\Delta\lambda'/2} I_{\lambda} \cdot \eta_{\lambda} \epsilon_{\lambda} c e^{-\epsilon_{\lambda} c x} e^{-\epsilon_{\lambda''} c y} \frac{A}{4\pi r^2} \dots \dots f(\lambda'') d\lambda'' dx dy dz \quad (I-153)$$

In order not to complicate the solid angle term, $\frac{A}{4\pi r^2}$, and the attenuation term, $\exp(-\epsilon_{\lambda''} c y)$, we have assumed $r \gg L$. The total output incident on A in the band $\Delta\lambda'$ is given by

* Although we "allow" reabsorption, we do not take account of any subsequent re-emission contributions to dF here.

further integrating dF_{SD} over x, y and z , giving,

$$F_{SD} = \bar{\Phi} \eta_{\lambda} \epsilon_{\lambda} c L \left(\frac{1}{\epsilon_{\lambda} c} (1 - e^{-\epsilon_{\lambda} c L}) \right) \dots \dots \left(\frac{1}{\epsilon_{\lambda}' c} (1 - e^{-\epsilon_{\lambda}' c L}) \right) \quad (I-154)$$

This involves the further restriction that ϵ_{λ}' is not a strong function of λ' in the range, $\Delta\lambda'$,

$$\int_{\lambda''} f(\lambda'') e^{-\epsilon_{\lambda}'' c x} dx \approx e^{-\epsilon_{\lambda}'' c x} \int_{\lambda''} f(\lambda'') d\lambda'' \quad (I-155)$$

$\bar{\Phi}$ is a constant for a given spatial arrangement and fixed incident and fluorescent wavelengths.

$$\bar{\Phi} = \bar{I}_{\lambda} \frac{A}{4\pi r^2} \int_{\lambda'' = \lambda' - \frac{\Delta\lambda'}{2}}^{\lambda'' = \lambda' + \frac{\Delta\lambda'}{2}} f(\lambda'') d\lambda'' \quad (I-156)$$

With $\epsilon_{\lambda} c L \ll 1$ and $\epsilon_{\lambda}' c L \ll 1$, we obtain the linear form,

$$F_{SD}' = \bar{\Phi} \epsilon_{\lambda} c \eta_{\lambda} L^3 \quad (I-157)$$

This is equivalent to the extension of Beer's Law into fluorescence, with F_{SD}' directly proportional to $\epsilon_{\lambda}, c, \eta_{\lambda}$, and sample size L^3 . At the other limit, with $\epsilon_{\lambda} c L \gg 1$ and $\epsilon_{\lambda}' c L \gg 1$,

$$F_{SD}'' = \bar{\Phi} \eta_{\lambda} L / \epsilon_{\lambda}' c \quad (I-158)$$

The "straight-through" fluorescence, which is observed from the

face opposite to that illuminated by the incident light, may be obtained in an analogous manner,

$$F_{ST} = \Phi \cdot \eta_{\lambda} \cdot \epsilon_{\lambda} c L^2 e^{-\epsilon_{\lambda}' c L} \left(\frac{1 - e^{-(\epsilon_{\lambda} - \epsilon_{\lambda}') c L}}{(\epsilon_{\lambda} - \epsilon_{\lambda}') c} \right) \quad (I-I59)$$

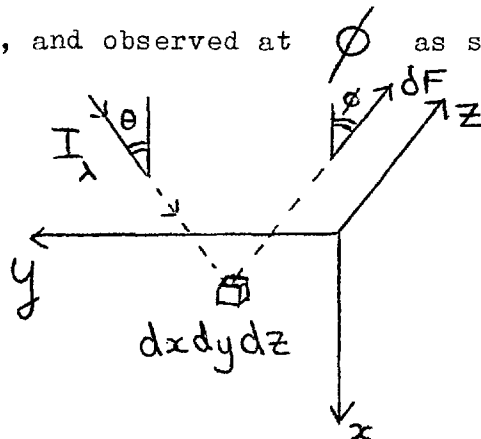
This equation includes all the assumptions given previously for side viewing.

In the case where $\epsilon_{\lambda} c L \ll 1$ and $\epsilon_{\lambda}' c L \ll 1$ we obtain the same result as given in equation (I-I57), the limiting expression for side viewing. At the other extreme however, with $\epsilon_{\lambda} c L \gg 1$, $\epsilon_{\lambda}' c L \gg 1$, and $\epsilon_{\lambda} > \epsilon_{\lambda}'$ we find,

$$F_{ST}'' = \Phi \eta_{\lambda} \frac{\epsilon_{\lambda}}{(\epsilon_{\lambda} - \epsilon_{\lambda}')} \cdot L^2 \cdot e^{-\epsilon_{\lambda}' c L} \quad (I-I60)$$

It will be noted how much faster F_{ST}'' decreases after reaching a maximum than F_{SD}'' , the latter only falling as the reciprocal of concentration.

The final case we have to consider for our cubic sample is "forward viewing", observation from the same side as excitation. We shall consider the case with light incident at an angle θ , and observed at ϕ as shown.



Refraction effects on leaving and entering the solution through any glass cell wall are neglected. Allowing for the new geometry, but with the same approximations as before, we find,

$$F_F = \bar{\Phi} \eta_\lambda \epsilon_\lambda c L^2 \left(\frac{1 - e^{-cL \left(\frac{\epsilon_\lambda}{\cos \theta} + \frac{\epsilon_\lambda'}{\cos \phi} \right)}}{c \left(\frac{\epsilon_\lambda}{\cos \theta} + \frac{\epsilon_\lambda'}{\cos \phi} \right)} \right) \quad (\text{I-I6I})$$

With the appropriate conditions for weakly absorbing solutions,

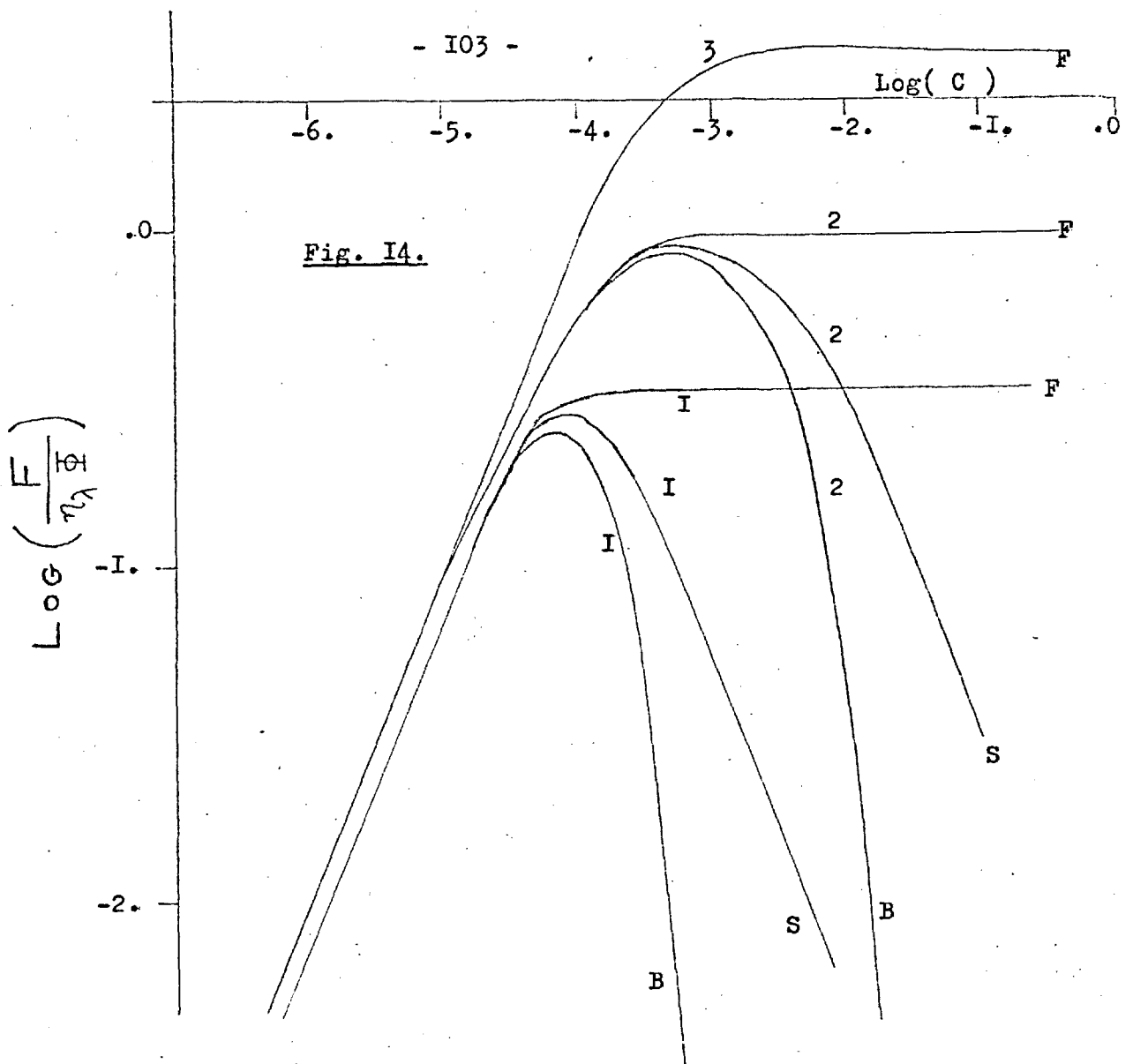
$(\epsilon_\lambda / \cos \theta + \epsilon_\lambda' / \cos \phi) c L \ll 1$, we again obtain the result (I-I57).

At the other extreme, $(\epsilon_\lambda / \cos \theta + \epsilon_\lambda' / \cos \phi) c L \gg 1$, we find;

$$F_F'' = \bar{\Phi} \eta_\lambda \epsilon_\lambda L^2 / \left(\frac{\epsilon_\lambda}{\cos \theta} + \frac{\epsilon_\lambda'}{\cos \phi} \right) \quad (\text{I-I62})$$

Thus at high optical densities the output observed becomes concentration independent, all the incident light is absorbed by the solution and a constant proportion re-emitted. The analogy with the straight through high optical density result can be clearly seen by using, $\theta = 0^\circ$, and, $\phi = 180^\circ$, then the $e^{-\epsilon_\lambda' c L}$ term in equation (I-I60) represents the additional attenuation of the fluorescence, due to passage through the bulk of the solution. The expressions (I-I54), (I-I59), and (I-I6I) have been evaluated with typical parameter values and are shown in fig. I4.

All of these equations describe the movement of the fluorescing volume from the whole solution to the front face, nearest the illuminating source. This transition between "homogenous" and "localized fluorescence" is governed by the

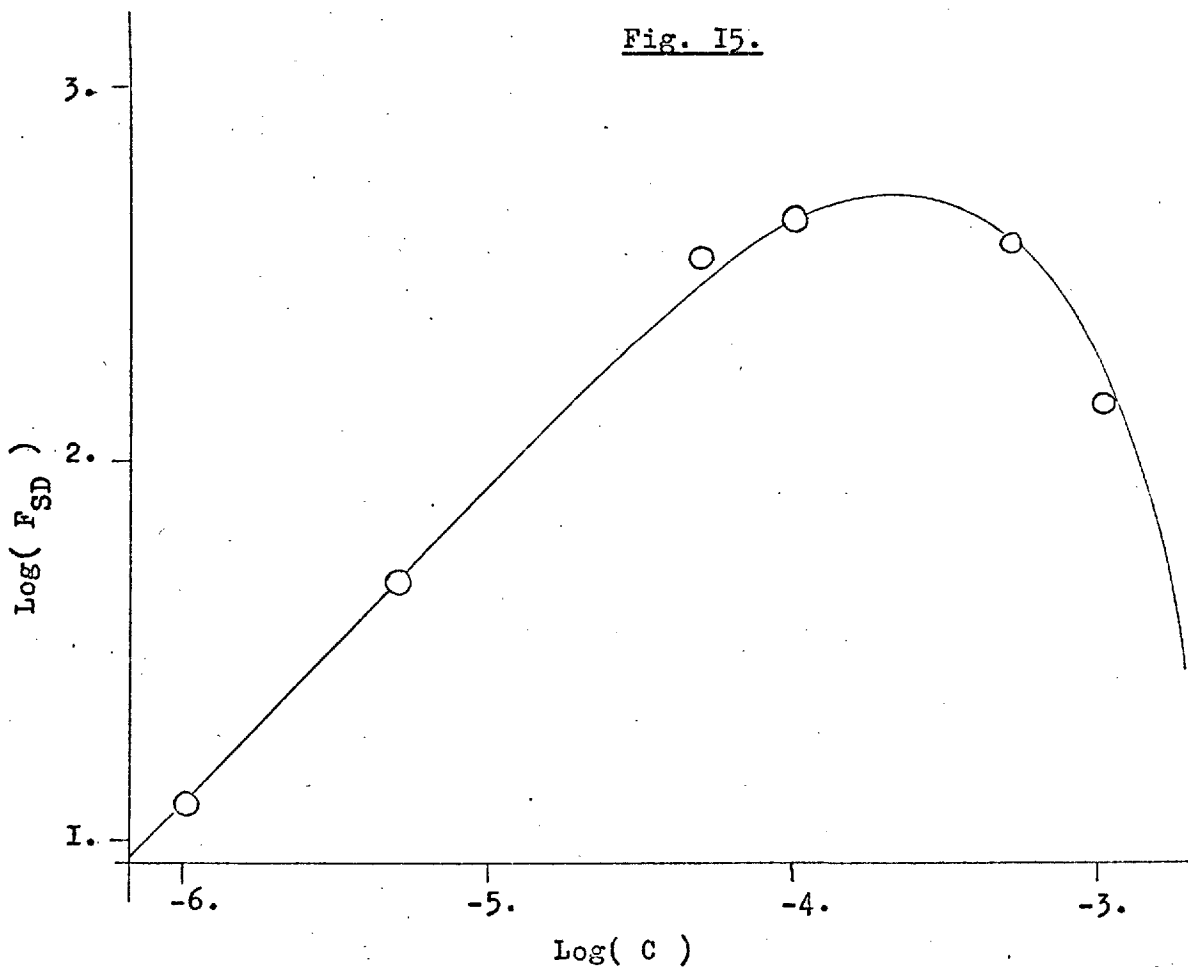


Fluorescence Attenuation: The fluorescent intensity of a 1. cm. cube observed from various directions as a function of concentration, C . F=front viewing, equation(I-161), S=side viewing, equation(I-154), B=back viewing, equation(I-159). For the set of curves I, the parameters used were, $\epsilon_{\lambda} = 7500$, $\epsilon'_{\lambda} = 300$; whilst for curves 2, $\epsilon_{\lambda} = 10000$, $\epsilon'_{\lambda} = 20000$. Curve 3 was obtained using the same extinction parameters as for 2, except a .1cm. sample thickness was used, the overall volume however was still 1ml. . This illustrates the value of front viewing of thin samples.

optical density terms, with $| > \epsilon_{\lambda} c L > |$, the transition occurring at $\epsilon_{\lambda} c L \approx |$. At low optical density the solution absorbs only weakly, and hence each incremental volume fluoresces equally, being subjected to an incident intensity which is virtually independent of position (x, y, z) . Thus in this situation the output fluorescence intensity is the same in all directions, and proportional to $L^3, \epsilon_{\lambda}, \eta_{\lambda}$ and concentration as expected. At high optical densities however, light is strongly absorbed on entering the solution, and the fluorescence becomes essentially localized at the illuminated face.

Although we have considered the effects of reabsorption, by assigning a value ϵ_{λ}' to the extinction coefficient for the fluorescent light, we have not considered any re-emission as a result of this absorption. This is reasonable for low optical densities, or if η_{λ} is small, and in fig. 15 we see that experiment and the model proposed do agree quite well. Also it will be noticed we have only considered one-species solutions, in mixtures fluorescence may be reabsorbed by several different types of molecule, and hence the fluorescence of additional species is observed, although it was anticipated only from that which absorbed the exciting light directly. All these considerations bring us to the problem of secondary fluorescence.

Fig. 15.



Test of the theoretical fluorescence intensity function, F_{SD} .

Experimental points are shown as circles, whilst the solid line represents the fitted function F_{SD} .

The points were obtained for Trypaflavin solutions, viewed from the side using a Farrand Spectrofluorimeter.

(b) Secondary Fluorescence.

This is usually considered in qualitative terms only, (63), and is only observable indirectly, such as in the apparent increase in lifetimes of fluorescing species as measured using a phase-fluorimeter, (13), or in polarization investigations, (64). The measured intensity of fluorescence is the sum of all orders of fluorescence,

$$F_T = \sum_{n=1}^{\infty} F_n(c) \quad (I-163)$$

where; $F_1(c)$ = primary fluorescence contribution, $F_2(c)$ = secondary contribution, arising from the reabsorption of F_1 , and $F_3(c)$ = tertiary component, as a result of reabsorption of F_2 , and so on.....

The form of $F_1(c)$ has been dealt with already, and the model we shall use here to approximate $F_2(c)$ is just a simple extension of that used for $F_1(c)$. We consider the reabsorption of primary fluorescence emitted from an incremental volume $dx_i \cdot dy_i \cdot dz_i$ at (x_i, y_i, z_i) by another volume $dx_j \cdot dy_j \cdot dz_j$ at (x_j, y_j, z_j) , followed by its subsequent re-emission as secondary fluorescence. As in the discussion of primary fluorescence, the coordinates used have their origin at one corner of the cubic sample, with the exciting light incident parallel to the x-axis. The fluorescence of the i -th incremental volume, emitted in all directions, and distributed throughout the entire fluorescence

spectrum is given by equation (I-152). The proportion of this primary fluorescence in the wave band $d\lambda''$ incident on the

j -th cell, at a distance r_{ij} is given by,

$$dI_i = I_\lambda \epsilon_\lambda c \eta_\lambda e^{-\epsilon_\lambda c x_i} e^{-\epsilon_\lambda'' c r_{ij}} A_j f(\lambda'') d\lambda'' \frac{dx_i dy_i dz_i}{4\pi r_{ij}^2} \quad (\text{I-164})$$

A_j is the area of the j -th element in the direction \vec{r}_{ij} , and $f(\lambda)$ the intensity distribution. From the derivative of the above equation with respect to r_{ij} , and ignoring the contribution from the purely geometric term arising from the solid angle, we find the intensity absorbed by the j -th element as,

$$dI_j' = I_\lambda \epsilon_\lambda \epsilon_\lambda'' c^2 \eta_\lambda e^{-\epsilon_\lambda c x_i} e^{-\epsilon_\lambda'' c r_{ij}} \dots \frac{A_j}{4\pi r_{ij}^2} f(\lambda'') d\lambda'' dr_{ij} dx_i dy_i dz_i \quad (\text{I-165})$$

Hence the total intensity absorbed by the j -th element is given by, $\int_{\lambda''=0}^{\lambda''=\infty} dI_j'$ and the total secondary fluorescence emitted by the incremental volume is,

$$dF_2^j = I_\lambda \epsilon_\lambda c^2 \eta_\lambda^2 e^{-\epsilon_\lambda c x_i} \frac{A_j}{4\pi r_{ij}^2} dr_{ij} dx_i dy_i dz_i \dots \int_0^\infty e^{-\epsilon_\lambda'' c r_{ij}} f(\lambda'') d\lambda'' \quad (\text{I-166})$$

Here we have assumed that η_λ , the quantum efficiency does not depend on λ .

As the light has still to leave the bulk of solution, we need a further attenuation factor, and for the case of side viewing in the fluorescence wave band $\Delta\lambda'$ we derive,

$$dF_z^j = I_\lambda \epsilon_\lambda c^2 n_\lambda^2 e^{-\epsilon_\lambda c x_i} \frac{A_j}{4\pi r_{ij}^2} \cdot \frac{A}{4\pi F^2} \dots$$

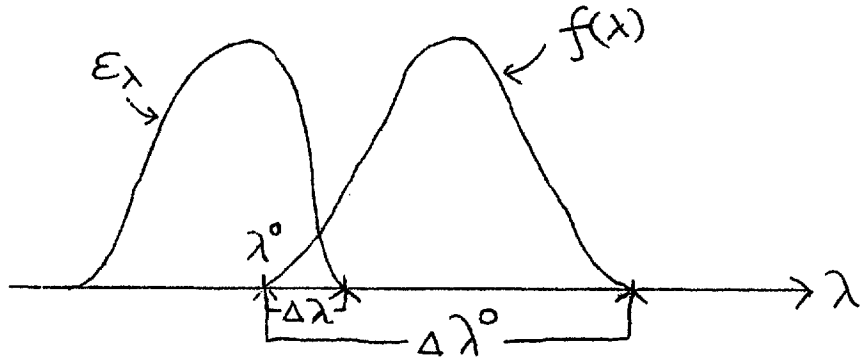
$$\dots dr_{ij} dx_i dy_i dz_i \int_{\lambda''=0}^{\infty} \epsilon_{\lambda''} e^{-\epsilon_{\lambda''} c r_{ij}} f(\lambda'') d\lambda'' \int_{\lambda'''=\lambda' - \frac{\Delta\lambda'}{2}}^{\lambda' + \frac{\Delta\lambda'}{2}} e^{-\epsilon_{\lambda'''} c y_i} f(\lambda''') d\lambda''' \quad (1-167)$$

This represents the secondary fluorescence intensity emitted by incremental volume j in the y direction within the wave band $\Delta\lambda'$. The expression needs further multiplication by a factor of $A/4\pi F^2$, where A is the area of the detector, distant F from the solution, but this may all be included in a machine constant, Φ , later, (see equation (1-156)).

Now we shall turn our attention to the integral over $d\lambda''$ contained in equation (1-167),

$$I = \int_{\lambda''=0}^{\infty} \epsilon_{\lambda''} e^{-\epsilon_{\lambda''} c r_{ij}} f(\lambda'') d\lambda''$$

First we must consider the absorption and emission bands of the fluorescing species.



$\Delta\lambda$ measures the emission/absorption overlap interval, and $\Delta\lambda^\circ$ the band width of the fluorescence, hence the integral over

λ'' can be split into domains, and using the assumptions;

$$\begin{aligned} \epsilon_\lambda = 0 & \dots \{ \lambda^\circ + \Delta\lambda \leq \lambda \} & f(\lambda) = 0 & \dots \{ \lambda^\circ > \lambda > \lambda^\circ + \Delta\lambda \} \\ \epsilon_\lambda \neq 0 & \dots \{ \lambda^\circ \leq \lambda < \lambda^\circ + \Delta\lambda \} \end{aligned}$$

we retain only one term in ρ ,

$$\rho = \int_{\lambda'' = \lambda^\circ}^{\lambda^\circ + \Delta\lambda} \epsilon_{\lambda''} e^{-\epsilon_{\lambda''} c \tau_{ij}} f(\lambda'') d\lambda''$$

Thus we finally derive,

$$\begin{aligned} dF_2^j &= \Phi \epsilon_\lambda c^2 \eta_\lambda^2 e^{-\epsilon_\lambda c x_i} e^{-\epsilon_\lambda c y_j} \frac{A_j}{4\pi r_{ij}^2} \\ &\dots d\tau_{ij} dx_i dy_i dz_i \int_{\lambda'' = \lambda^\circ}^{\lambda^\circ + \Delta\lambda} \epsilon_{\lambda''} e^{-\epsilon_{\lambda''} c \tau_{ij}} f(\lambda'') d\lambda'' \end{aligned}$$

Where, $\Phi = \frac{I_\lambda A}{4\pi r^2} \int f(\lambda'') d\lambda''$ and we have assumed $\epsilon_{\lambda'}$ does not vary much across the instrument pass band, $\Delta\lambda'$. In addition if we place $A_j d\tau_{ij} = dx_j dy_j dz_j$, the total output of secondary fluorescence is given by,

$$F_2^{SD} = \Phi \int_{\lambda''=\lambda^0}^{\lambda^0+\Delta\lambda} f(\lambda'') d\lambda'' \int_{x_i, y_i, z_i=0}^L dx_i dy_i dz_i \int_{x_j, y_j, z_j=0}^L dx_j dy_j dz_j \frac{1}{4\pi r_{ij}^2} \dots \epsilon_{\lambda''} \epsilon_\lambda c^2 n_\lambda^2 e^{-\epsilon_{\lambda''} c \tau_{ij}} e^{-\epsilon_\lambda c x_i} e^{-\epsilon_{\lambda'} c y_j} \quad (I-I69)$$

Now we consider the integration over λ'' , involving the term,

$$\int_{\lambda''=\lambda^0}^{\lambda^0+\Delta\lambda} \epsilon_{\lambda''} e^{-\epsilon_{\lambda''} c \tau_{ij}} f(\lambda'') d\lambda''$$

This integral over the distribution function, f , is the mean value, $\overline{\epsilon_{\lambda''} e^{-\epsilon_{\lambda''} c \tau_{ij}}}$, assuming τ_{ij} is approximately constant. This is reasonable as $0 < \tau_{ij} \ll L$, whilst $0 \leq \epsilon_\lambda \leq 10^4$, and as a further simplification we approximate,

$$\overline{\epsilon_{\lambda''} e^{-\epsilon_{\lambda''} c \tau_{ij}}} \approx \overline{\epsilon_{\lambda''}} e^{-\overline{\epsilon_{\lambda''}} c \tau_{ij}} \quad (I-I70)$$

with, $\overline{\epsilon_{\lambda''}} \approx \frac{1}{\Delta\lambda} \cdot \int \epsilon_{\lambda'} d\lambda'$. Thus $\overline{\epsilon_{\lambda''}}$ assumes the form of a semi-empirical parameter, only approximated by the actual mean overlap extinctions. Substituting this into the equation for F_2^{SD} , (I-I69), changing coordinates and integrating, we obtain,

$$\begin{aligned}
 F_2^{SD} &= \Phi \epsilon_\lambda \bar{\epsilon}_{\lambda''} \eta_\lambda^2 c^2 L \left(\frac{1 - e^{-\epsilon_\lambda c L}}{\epsilon_\lambda c} \right) \dots \\
 &\dots \left(\frac{1 - e^{-\epsilon_{\lambda'} c L}}{\epsilon_{\lambda'} c} \right) \frac{1}{4\pi} \int_0^{2\pi} d\phi \int_0^\pi \frac{2 \sin \theta d\theta}{c(\epsilon_\lambda \sin \theta \cos \phi + 2\bar{\epsilon}_{\lambda''} - \epsilon_{\lambda'} \cos \theta)} \\
 &\dots \left(1 - \exp\left(-\frac{cL}{4} [\epsilon_\lambda \sin \theta \cos \phi + 2\bar{\epsilon}_{\lambda''} - \epsilon_{\lambda'} \cos \theta]\right) \right) \quad \text{(I-171)}
 \end{aligned}$$

If we write secondary fluorescence as a ratio of primary output, the expression is simplified, for side viewing to,

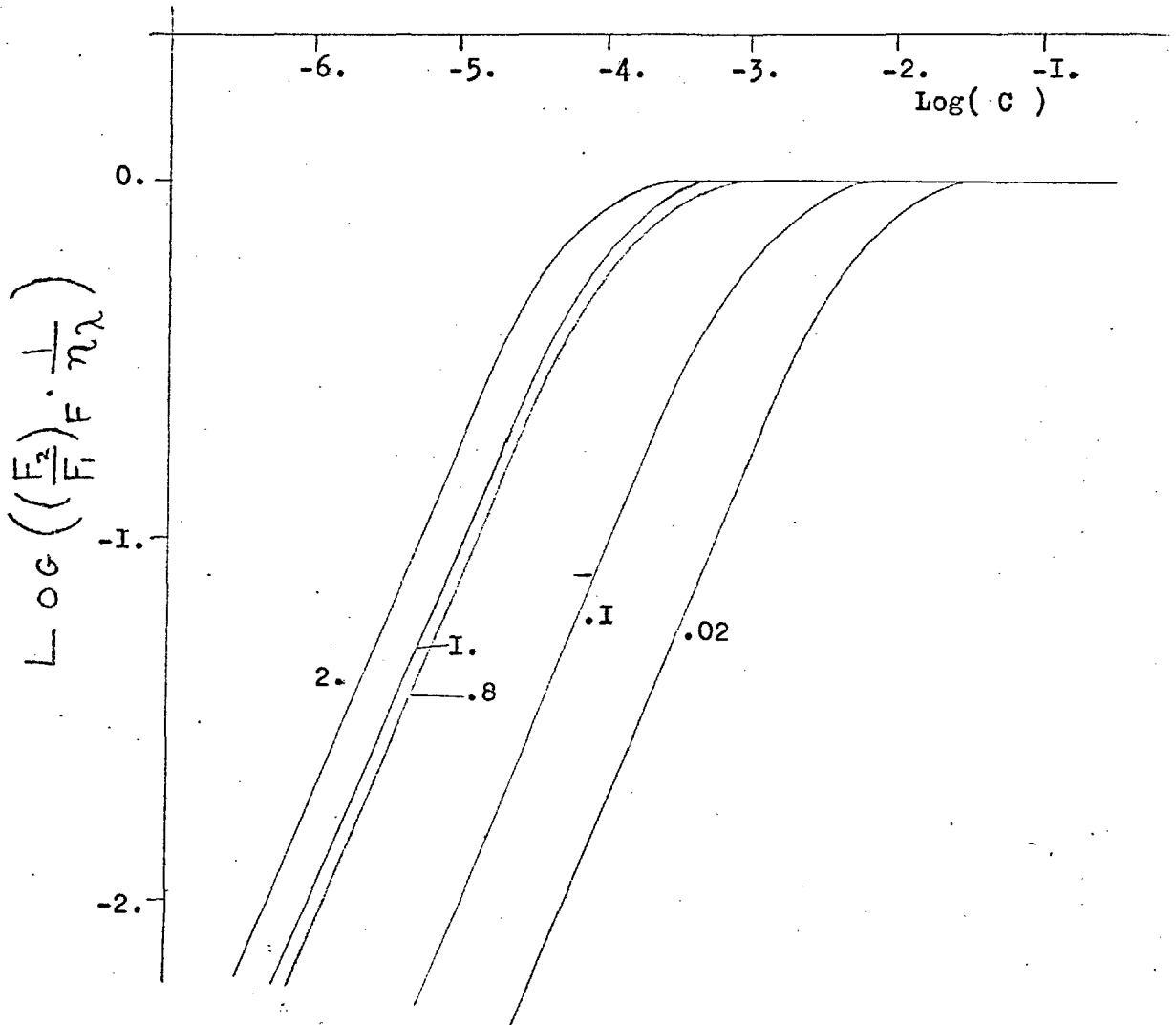
$$\begin{aligned}
 \left(\frac{F_2}{F_1} \right)_{SD} &= \frac{\eta_\lambda \bar{\epsilon}_{\lambda''} c}{4\pi} \int_0^{2\pi} d\phi \int_0^\pi \frac{2 \sin \theta d\theta}{c(\epsilon_\lambda \sin \theta \cos \phi + 2\bar{\epsilon}_{\lambda''} - \epsilon_{\lambda'} \cos \theta)} \\
 &\dots \dots \left(1 - \exp\left(-\frac{cL}{4} [\epsilon_\lambda \sin \theta \cos \phi + 2\bar{\epsilon}_{\lambda''} - \epsilon_{\lambda'} \cos \theta]\right) \right) \quad \text{(I-172)}
 \end{aligned}$$

This function is shown in fig.16, evaluated using typical parameters.

A similar method may be used to find the ratio, $\left(\frac{F_2}{F_1} \right)_F$, for forward viewing, which is found to be,

$$\begin{aligned}
 \left(\frac{F_2}{F_1} \right)_F &= \frac{\eta_\lambda \bar{\epsilon}_{\lambda''} c}{4\pi} \int_0^{2\pi} d\phi \int_0^\pi \frac{2 \sin \theta d\theta}{c([\epsilon_\lambda - \epsilon_{\lambda'}] \sin \theta \cos \phi + 2\bar{\epsilon}_{\lambda''})} \\
 &\dots \left(1 - \exp\left(-\frac{cL}{4} [(\epsilon_\lambda - \epsilon_{\lambda'}) \sin \theta \cos \phi + 2\bar{\epsilon}_{\lambda''}]\right) \right) \quad \text{(I-173)}
 \end{aligned}$$

Fig. 16.



Secondary Fluorescence: The ratio of secondary to primary fluorescence as a function of concentration and sample thickness. The sample is observed from the front, and the various thicknesses are shown on the curves. The extinction parameters used were, $\epsilon_{\lambda} = 7500$, $\overline{\epsilon}_{\lambda}'' = 20000$, $\epsilon_{\lambda}' = 300$.

At low optical densities, or sample sizes, with,

$$\frac{cL}{4} (\epsilon_{\lambda} \sin \theta \cos \phi + 2 \overline{\epsilon_{\lambda}''} - \epsilon_{\lambda} \cos \theta) \ll 1$$

and the corresponding condition for front viewing,

$$\frac{cL}{4} ([\epsilon_{\lambda} - \epsilon_{\lambda}'] \sin \theta \cos \phi + 2 \overline{\epsilon_{\lambda}''}) \ll 1$$

the results for both directions of observation are analogous,

$$\left(\frac{F_2}{F_1}\right)'_{SD} = \left(\frac{F_2}{F_1}\right)'_F = \eta_{\lambda} c \overline{\epsilon_{\lambda}''} \frac{L}{2} \quad (I-I74)$$

In the other extreme, with high overlap extinction, $\overline{\epsilon_{\lambda}''} \gg \epsilon_{\lambda}$,

$\overline{\epsilon_{\lambda}''} \gg \epsilon_{\lambda}'$, and $\frac{\overline{\epsilon_{\lambda}''} cL}{2} \gg 1$ we find,

$$\left(\frac{F_2}{F_1}\right)''_{SD} = \left(\frac{F_2}{F_1}\right)''_F = \eta_{\lambda} \quad (I-I75)$$

The approximated forms of F_2 and F_1 are progressively less reliable as they depart from linearity at high optical densities. These are all rather empirical formulae, employing many approximations, and the value of $\overline{\epsilon_{\lambda}''}$, the overlap extinction is hard to evaluate, but as experiments involving the direct measurement of F_2 are impossible we do not need a highly sophisticated model to interpret the meagre experimental results available. Secondary fluorescence is often observed by it's effect on the apparent excitation lives of fluorescing species in solution, when it is found the lifetimes derived are functions of concentration and sample geometry.

In order to test the validity of the foregoing theory, and the expression derived earlier for the life of excitation in

solution with reabsorption , equation (I-133) , some experimental comparisons are now given.

(c) Experimental Test of Model.

(i). Galanin's Results.

Galanin, (13), using a phase-fluorimeter, was able to measure directly the dependence of fluorescent lifetime, τ'_s , of fluorescein on the thickness of the sample taken. The exciting light was of wavelength 436 $m\mu$., and modulated at $1.47 \cdot 10^8$ c/s, with the samples viewed from the same side as the incident exciting light. The value of τ_s , the lifetime at high dilution was taken as $4 \cdot 10^{-9}$ sec. , the shortest life observed. Hence we find , for equation (I-133),

$$\frac{\tau'_s}{\tau_s} = \frac{1.35 + 2R}{1.35 + 0.65R}$$

The values of R , $R = \frac{F_2}{F_1} \cdot \eta$, were obtained assuming $\eta = .8$, (I7) and using $\overline{\epsilon}_\lambda = 2 \cdot 10^4$ and $\epsilon_\lambda = 7500$ to derive F_2/F_1 as a function of sample thickness, we can compare the experimental and theoretical quantities, see Table 3.

Table 3.

| Sample thickness cm. | Conc. = .0001 gm/ml | | Conc. = .001 gm/ml | |
|-------------------------|------------------------|--------|------------------------|--------|
| | expt. τ'_s/τ_s | theory | expt. τ'_s/τ_s | theory |
| 0.8 | 1.38 | 1.49 | 1.52 | 1.58 |
| 0.1 | 1.25 | 1.17 | 1.48 | 1.44 |
| 0.02 | 1.0 | 1.04 | 1.30 | 1.29 |
| 0.04 | 1.0 | 1.00 | 1.05 | 1.08 |

(ii). Schmillen's Results.

The lifetimes of various organic dyes in solution were also measured by Schmillen, (39), using a phase-fluorimeter. This time however a lower modulation frequency was used. With $\omega\tau_s \ll 1$, we can use the relation (I-133) to obtain,

$$\tau_s'/\tau_s = \frac{1 + 2R}{1 + R}$$

With the values found from the absorption spectrum of Trypaflavin for the extinction parameters, $E_\lambda = 7500$, and $\overline{E}_\lambda'' = 3000$, with $\eta_\lambda = .37$, (17), we show in Table 4 the corresponding values of τ_s'/τ_s found.

Table 4.

| Log(concn) | τ_s'/τ_s expt. | τ_s'/τ_s theory |
|------------|------------------------|-------------------------|
| -5.0 | 1.02 | 1.01 |
| -4.4 | 1.05 | 1.02 |
| -4.0 | 1.12 | 1.05 |
| -3.7 | 1.16 | 1.09 |
| -3.3 | 1.25 | 1.18 |
| -3.0 | 1.27 | 1.23 |

At concentrations greater than $\sim 10^{-3}M$. self-quenching begins, and the function defining the ratio F_2/F_1 becomes unrealistic, so this was taken as the upper limit of testing the theory. For a similar treatment of Fluorescein, using the same parameters as in the duplication of Galanin's results the comparison

is shown in Table 5 .

Table 5.

| Log(concn) | τ'_s/τ_s expt. | τ'_s/τ_s theory |
|--------------|------------------------|-------------------------|
| -5.0 | 1.0 | 1.07 |
| -4.5 | 1.0 | 1.18 |
| -3.8 | 1.22 | 1.38 |
| -3.6 | 1.39 | 1.42 |
| -3.2 | 1.55 | 1.44 |

(iii). Bailey and Rolleson's Results.

Bailey and Rolleson (43), made another phase-fluorimeter study, although this time a large 2 cm. sample was used. The use of such a thick sample was rather unfortunate in view of the increased possibilities of reabsorption distorting the lifetimes observed. Fluorescein was studied, so the same parameters as used before were applied, and also because $\omega\tau_s \ll 1$, the simplified equation could be used. The results obtained are given in Table 6, above Log(C) = -3.7 the value of R is unity and the theory breaks down.

Table 6.

| Log(concn) | τ'_s/τ_s expt | τ'_s/τ_s theory |
|--------------|-----------------------|-------------------------|
| -5.8 | 1.02 | 1.02 |
| -5.1 | 1.02 | 1.11 |
| -5.0 | 1.11 | 1.12 |
| -4.1 | 1.40 | 1.39 |
| -4.0 | 1.47 | 1.41 |
| -3.7 | 1.55 | 1.44 |

(iv). Conclusions.

The first comment that seems valid is to wonder at the quite reasonable degree of accuracy in the theoretical predictions considering all the uncertainties involved. The situation is helped by the fact that all the experimental results lie in the range where $\frac{\tau_3'}{\tau_3}$ is between 1.0 and 1.6, but even so the fit is quite satisfactory considering the rather lengthy theoretical digressions and approximations involved in the calculation of the ratio F_2/F_1 and in the application of the time-dependent theory. In any case the results do illustrate the need for understanding the large effects reabsorption can have on the measured lives of species in reabsorbing media.

Now we can appreciate the reasons for the often wide discrepancies in the values of τ_3 ascribed by different workers to the same compound. The case of anthracene is particularly bad, with a large choice of "accurate" τ_3 possible, all varying with the subdivision of the solid sample. Clearly care is needed in reaching conclusions based on lifetimes in bulk media.

Finally we must recognize the many assumptions in our theory, the neglect of competing effects such as resonance transfer, self-quenching, all effecting secondary fluorescence. Also the approximation of the modulation of the exciting light by a sine wave may not be very good, it might perhaps be better represented as a chopped beam.

(d) The Trivial Effect.

From our treatment of secondary fluorescence we are now in a position to estimate the magnitude of the radiative transfer of energy between a system of sensitizers and acceptors, known as the "trivial effect". In studies of resonance transfer it is important to exclude the radiative process as a competing mechanism of energy transfer. Thus we must compare the magnitude of this reabsorption process with the efficiency of radiationless energy transfer, written as the ratio $(\eta/\eta_0)_A$, given by equation (I-97). This ratio tells us the fraction of quanta absorbed by the sensitizers which are passed onto the acceptors, to reappear as acceptor fluorescence. The transfer of these quanta by the trivial effect would occur through sensitizer emission followed by the reabsorption and re-emission of quanta by the acceptors. Resonance transfer however occurs via the coupling of the sensitizer and acceptor dipoles as we have seen, and no emission and reabsorption processes are involved.

Until now we have regarded the acceptors and sensitizers as different species, this need not be the case, they could well be different molecules of the same type. This is the situation we shall consider, so as not to complicate matters further by having to extend the secondary fluorescence theory to cater for two species in solution. Such an extension is simple, but results in more complex expressions.

The trivial quantum efficiency can be defined as ,

$$\left(\frac{\eta}{\eta_0}\right)_T = \frac{\text{(Quanta reabsorbed by solution)}}{\text{(Quanta absorbed from exciting intensity)}} = \frac{Q_{RA}}{Q_A} \quad \text{(I-176)}$$

For the upper term we shall only consider a single reabsorption of radiation; that is the absorption which leads to secondary fluorescence. Higher order cascade effects are neglected. The lower term , representing the quanta absorbed from the incident exciting beam may be easily derived using Beer's Law ,(see equation (I-152)). Considering the usual sample cube , of side L , and with coordinate origin at one of the corners, we find,

$$Q_A = I_0 (1 - e^{-\epsilon_\lambda c L}) \cdot L^2 \quad \text{(I-177)}$$

where I_0 , the intensity incident in the x-dir~~ection~~ is in units of quanta/sec/area. We have assumed the incident exciting light is monochromatic. The calculation of the primary fluorescence intensity absorbed by the bulk of the solution can be handled in an analogous manner to that used for secondary fluorescence, and we find,

$$Q_{RA} = I_0 \epsilon_\lambda \bar{\epsilon}_\lambda'' c^2 L^2 \eta_\lambda \left(\frac{1 - e^{-\epsilon_\lambda c L}}{\epsilon_\lambda c} \right) \dots$$

$$\dots \int_0^{2\pi} d\phi \int_0^\pi \frac{2 \sin \theta d\theta}{c(\epsilon_\lambda \sin \theta \cos \phi + 2 \bar{\epsilon}_\lambda'')} \cdot \left(1 - e^{-\frac{cL}{4} (\epsilon_\lambda \sin \theta \cos \phi + 2 \bar{\epsilon}_\lambda'')} \right)$$

(I-178)

Hence we have ,

$$\left(\frac{\eta}{\eta_0}\right)_T = \frac{Q_{RA}}{Q_A} = \frac{\overline{E}_\lambda'' c \eta_\lambda}{4\pi} \dots$$

$$\dots \int_0^{2\pi} d\phi \int_0^\pi \frac{2 \sin \theta d\theta}{c(E_\lambda \sin \theta \cos \phi + 2\overline{E}_\lambda'')} \cdot \left(1 - e^{-\frac{cL}{4}(E_\lambda \sin \theta \cos \phi + 2\overline{E}_\lambda'')}\right)$$

(I-I79)

Where \overline{E}_λ'' is the semi-empirical mean overlap extinction previously discussed, equation (I-I70) . In fig. I7 the results of evaluating equation (I-I79) with the appropriate parameters are compared with experimental measurements of Birks (65) of the trivial effect in TPB/polystyrene glasses.

At low optical densities, $\overline{E}_\lambda'' cL \ll 1$ and $E_\lambda cL \ll 1$,

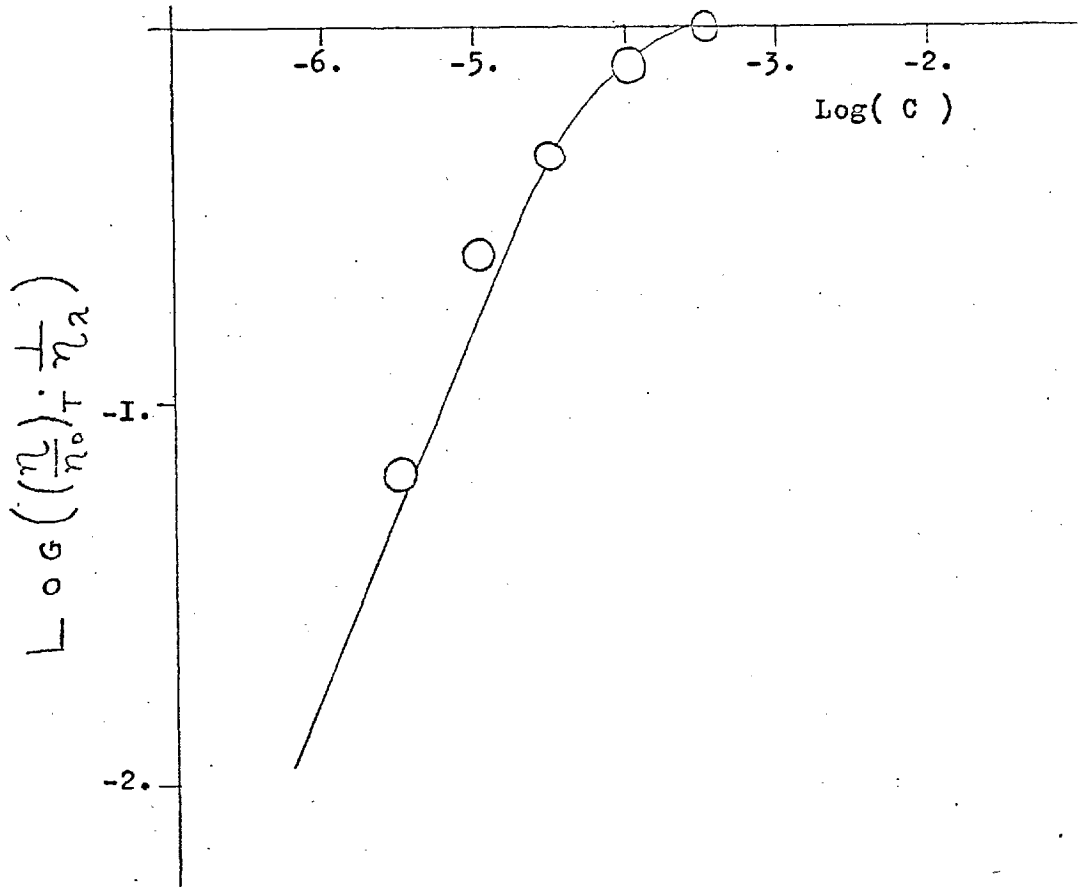
$$\left(\frac{\eta}{\eta_0}\right)'_T = \eta_\lambda \overline{E}_\lambda'' \frac{Lc}{2} \tag{I-I80}$$

This is exactly the same as (F_2/F_1) , the primary/secondary fluorescence ratio at low concentrations , equation (I-I74) .

The linear dependence of the trivial effect on these parameters is as might have been anticipated. Now we can compare the magnitude of this effect with that of resonance transfer. For the latter mechanism we have an efficiency at low concentrations given by equation (I-78),

$$\left(\frac{\eta}{\eta_0}\right)_A = \sqrt{\pi} \frac{c}{c_0} \tag{I-I81}$$

Fig. 17.



The Trivial Effect: Comparison of theory and experiment.

The experimental results shown are those of Birks, (65), obtained for the trivial effect in TPB/Polystyrene glasses.

The solid line was obtained from equation(I-179) with; $L=1.0$, $\overline{\epsilon_\lambda} = 40000$, $\epsilon_\lambda' = 300$, $\epsilon_\lambda = 7500$, and the quantum efficiency of polystyrene, $\eta_\lambda \approx .16$.

Where C^0 is the critical concentration, $\approx 10^{-4}M$.

Hence as $\frac{1}{C^0} \approx \bar{\epsilon}_\lambda \approx 10^4$, the ratio of the two concentration proportionality constants for the two processes is, $[2\sqrt{\pi}/\eta_\lambda L]$ and as $\eta_\lambda L \approx .5$, we finally conclude that the trivial effect should only be about one seventh of the non-radiative effect.

This is only an approximate result, dependent on the individual parameters for any situation, but it serves to give a reasonable basis for the omission from consideration of the trivial effect in typical resonance energy transfer experiments. At concentrations where $(\eta/\eta_0)_A$ is not small the factor η_λ in equation (I-179) should be written as $(1 - (\eta/\eta_0)_A)\eta_\lambda$, so that as the resonance transfer efficiency increases, the corresponding trivial efficiency is reduced. At the other limit, with $\bar{\epsilon}_\lambda C L \gg 1$, with high overlap and extinction, we find,

$$(\eta/\eta_0)_T = \eta_\lambda$$

Thus we find the maximum transfer efficiency by the trivial process is η_λ , whilst it is 1. by the non-radiative route. The reduced efficiency of the former is due to the requirement of fluorescent light emission by the sensitizer, this requires internal conversion within the excited state. In the resonance coupling required for radiationless transfer the sensitizer does not have to be in a potential fluorescing state.

(I3) A Practical Investigation.

(a) Construction of Apparatus

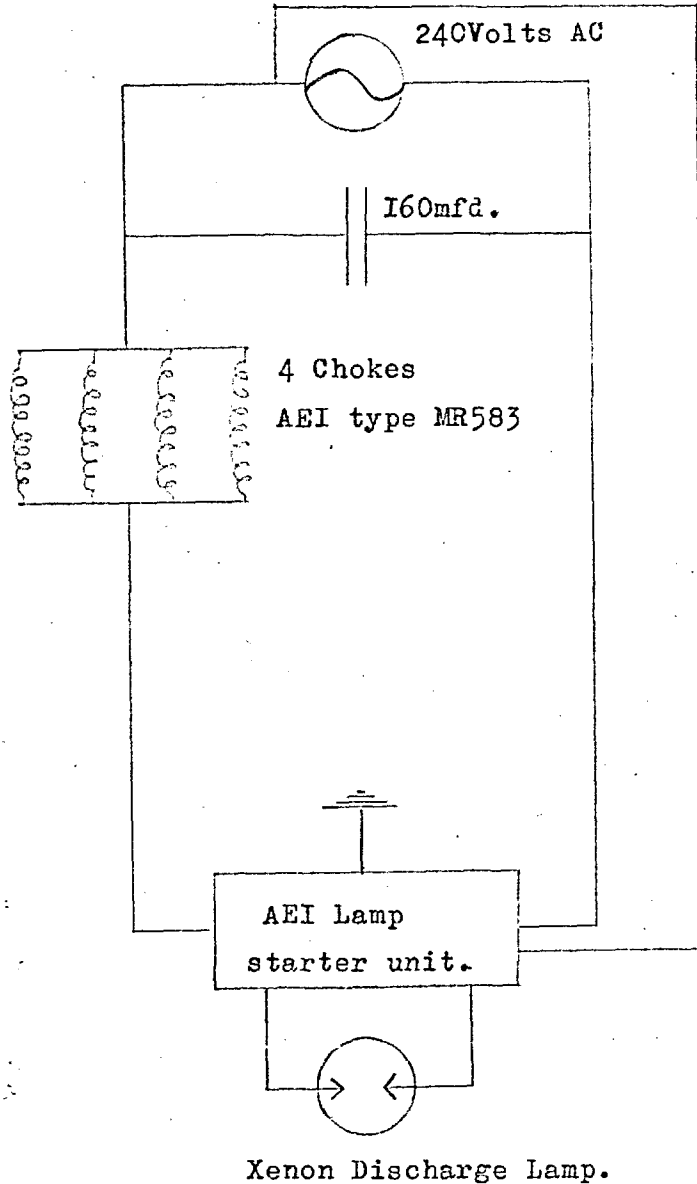
An experimental system for the investigation of fluorescence spectra was built. It consisted essentially of four basic units , with which the sample under test was positioned, excited, and its fluorescence detected and displayed.

(i) Exciting System

The sample molecules are excited to a fluorescing state by the absorption of light quanta from an incident light beam. The lamp used was of the Xenon Discharge type (AEI-Mazda, 250 Watt.) operating off the 240 Volts AC mains via an inductive ballast, see fig. I8 . This Xenon lamp provides a very intense light source , with a continuous spectrum in the near ultra-violet, visible , and near infra-red. The powerful emission at the high frequency limit particularly suits the lamp to the study of conjugated molecules, which generally absorb in this region. The AC arc between the tungsten electrodes in the pressurized Xenon atmosphere is struck initially by the use of the appropriate AEI lamp starter unit, which generates a potential of 20 Kv. Due to this very high voltage the lamp has to be well insulated to prevent "striking" to earth, rather than across the electrodes.

To increase lamp life and improve stability a centrifugal cooling fan was used to blow a powerful current of air directly onto the lamp and its mountings. These mountings were

Fig. I8.



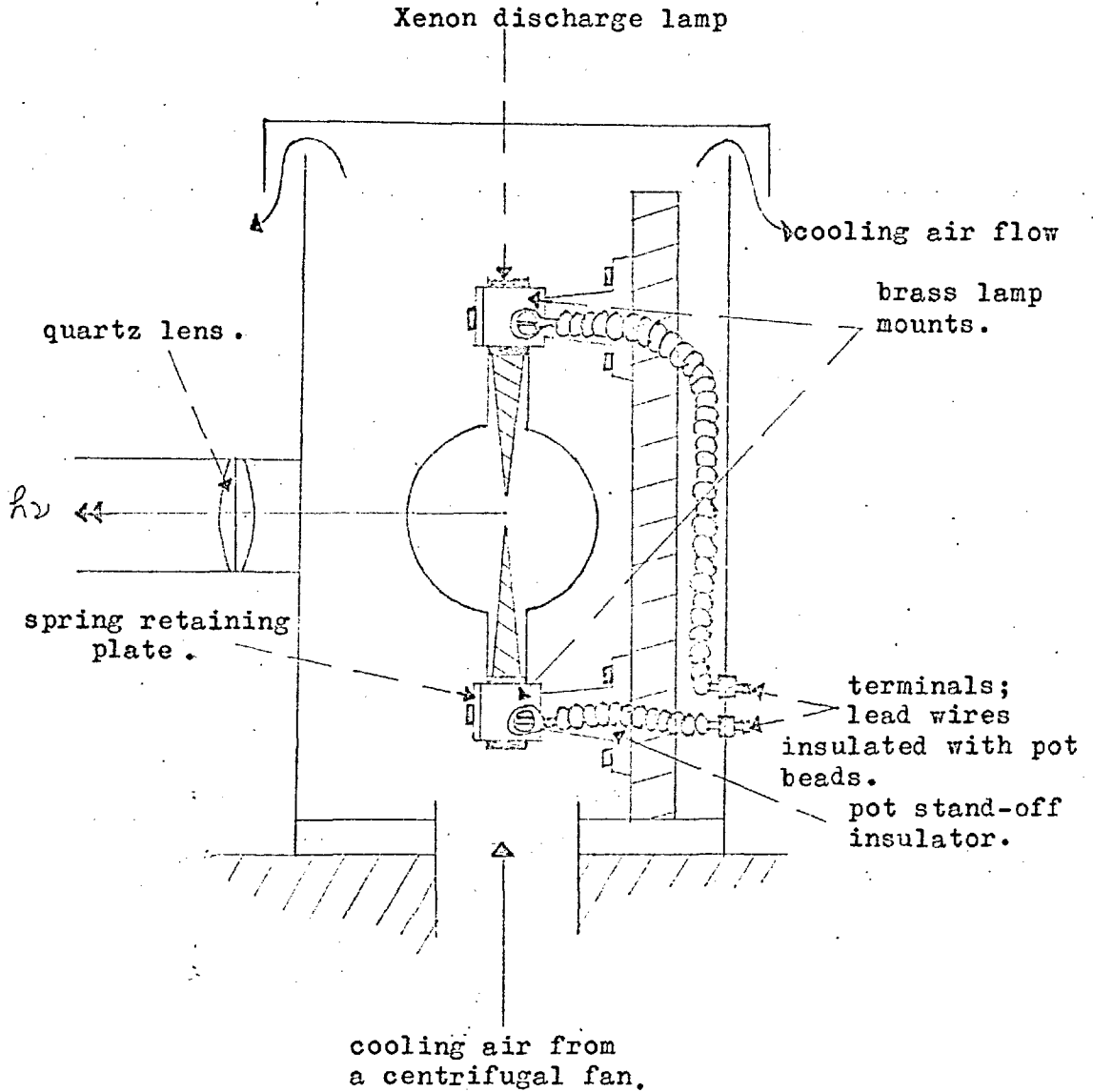
The diagram above shows the Xenon Discharge Lamp control circuit, the lamp being a 250Watt AC type.

specially designed to hold the lamp without strain by the two brass caps at it's extremities, and to allow for differential expansion during the warming and cooling down periods. Throughout the operation of the lamp, and when it was cooling down after switching off, the fan was kept in use. The lamp assembly is shown in Fig. 19.

The output from the lamp was focused by a quartz lens (1.in diameter, $f=1.5in.$), onto the entrance slit of a Beckmann GM-II39 Monochromator. From the exit slit of this instrument a further quartz lens focuses the monochromatic light onto the sample. This monochromator uses a replica diffraction grating, with higher order radiation removed by filters selected automatically as the wavelength scale is scanned. Both the entrance and exit slits are variable, a 0.95mm combination gives a half intensity bandwidth of $\sim 10m\mu$. These slits are co-linear, and hence the instrument operates as a highly selective filter.

For the production of excitation spectra a Smiths synchronous motor can be used to drive the monochromator across its range. This motor did not require a clutch or reverse gear, as after scanning the whole range, 250 to $700m\mu$, the machine is automatically ready to re-scan again commencing at $250m\mu$.

Fig. 19.



(ii). The Sample Holder.

This was a thermostated brass block, with water circulated through it from a temperature controlled bath by a Stewart-Turner rotary water pump. This maintains the sample at a predetermined temperature throughout an experiment. This block, adjustable in the vertical plane, pivots about a vertical axis perpendicular to the exciting beam from the input monochromator. The holder, shown in Fig. 20, was suitable for ordinary 5mm and 10mm cells, and also RIIIC uV-OI thin layer cells, allowing both front and back viewing. The most frequently utilized position was oblique front viewing.

(iii). The Detection System.

The arrangement of the physical units used for the observation of the sample fluorescence depended on the chosen experimental geometry. For straight through viewing the cell was positioned perpendicular to the exciting beam, and a lens used at an angle to this beam to focus the fluorescence onto the output monochromator, see Fig. 2Ia. The choice of angle α is such as to avoid the cone of scattered incident intensity.

For reasons discussed in the section on light attenuation this experimental geometry is not very favourable, more useful is front viewing, with oblique illumination and observation of the cell, as shown in Fig. 2Ib. Again the angles have to be chosen to avoid the reception of large amounts of

Fig. 20.

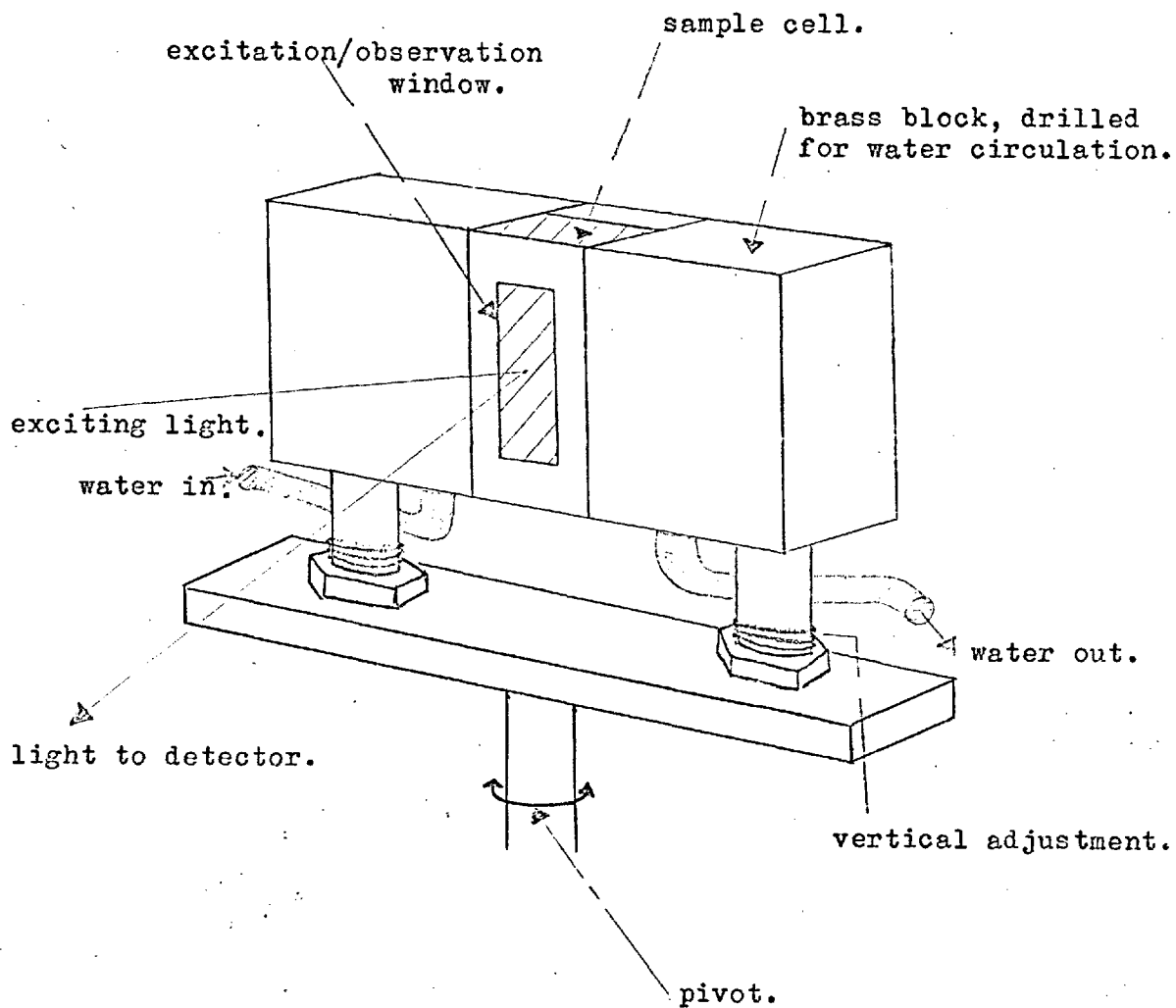


Fig. 2I(a).

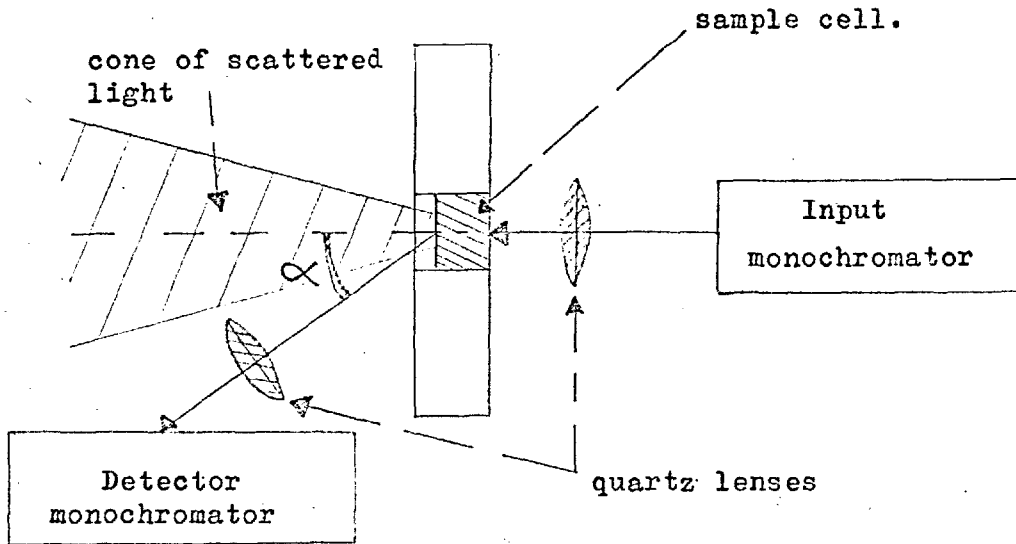
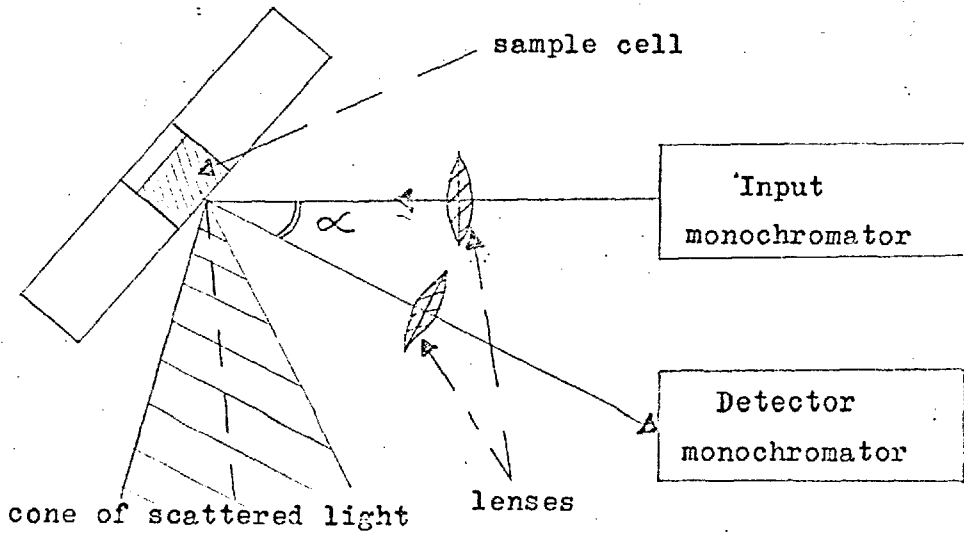


Fig. 2I(b).



scattered light by the detector.

The fluorescent light emitted by the sample in any particular geometry is focused onto the slit of the output monochromator, another Beckmann Grating Monochromator, GM-II39. As with the input instrument, this could be driven across its scale by a synchronous motor, which in conjunction with the display system enabled fluorescence emission spectra to be run.

Against the exit slit of this monochromator was the detector, a RCA IP-28 photomultiplier. This nine-stage phototube was directly attached to the monochromator, with its dynode chain resistors housed in a separate container, connected to the phototube by a multicore cable.

The ripple-free ($< .01\%$ RMS) stabilized DC power-supply used to provide the phototube potential via the dynode resistor chain was an AEI type R-II84, with a stabilized range of 300 to 1100 Volts DC, at 2. Ma. The quartz glass envelope of the IP-28 was covered with an electrostatic shield, connected to the same potential as the photocathode, with a 10 Meg Ω resistor to reduce leakage. This "noise" reducing shield had a window for the light incident from the monochromator onto the photocathode.

Unfortunately the coarse scale divisions on the power supply rendered accurate and reproducible readings of it's output impossible, so a 50Meg. resistor in series with a

Pye Scalamp mirror galvanometer was connected across the anode and the 5-th dynode. The galvanometer reading was then used as a direct measure of the DC potential across the phototube, and could be read to $\sim 1\%$ accuracy. The circuit of the dynode chain and the phototube is shown in Fig.22.

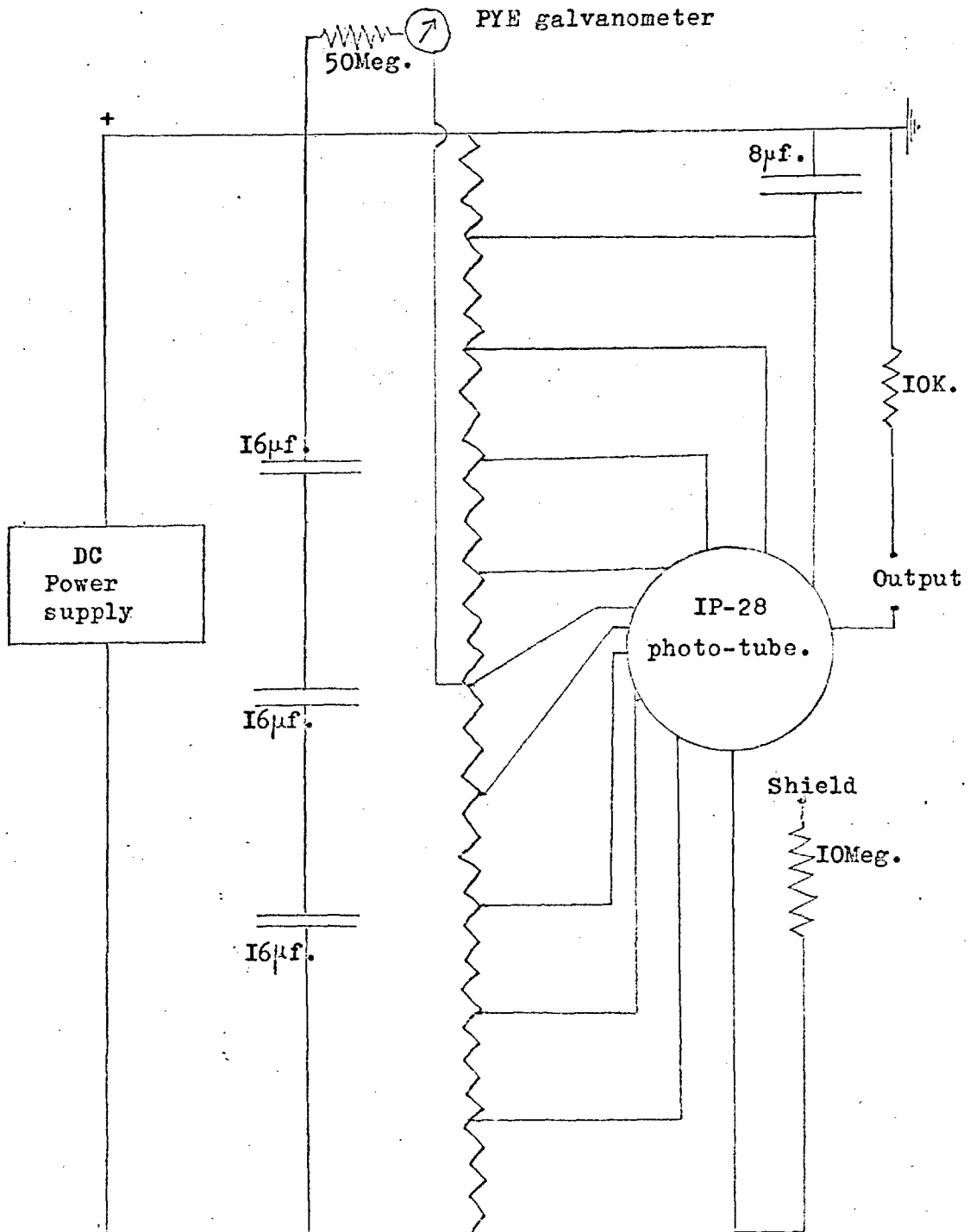
(iv). Display.

The output from the phototube could be displayed directly on a RCA Ultra-Sensitive DC Microammeter, MV-84C, connected in series to the tube output. Alternatively the micro-ammeter can be used to provide an amplified signal for feeding into a 10 mV Honeywell-Brown Electronic Chart Recorder, Elektronik 5015. Together with this recorder and the motor driving either of the monochromators, both fluorescence and absorption spectra could be obtained. The six scales on the microammeter, and the power supply to the dynode chain, provide easily obtained variations in sensitivity.

There was a facility for "backing off" the phototube dark-current from the chart recorder, this is important at high sensitivities when the dark-current is quite a large proportion of the signal. In addition it was found useful, except for very strong signals, to place a damping capacitor across the phototube output, usually in the range .1 to .01 μ F, to smooth out random noise.

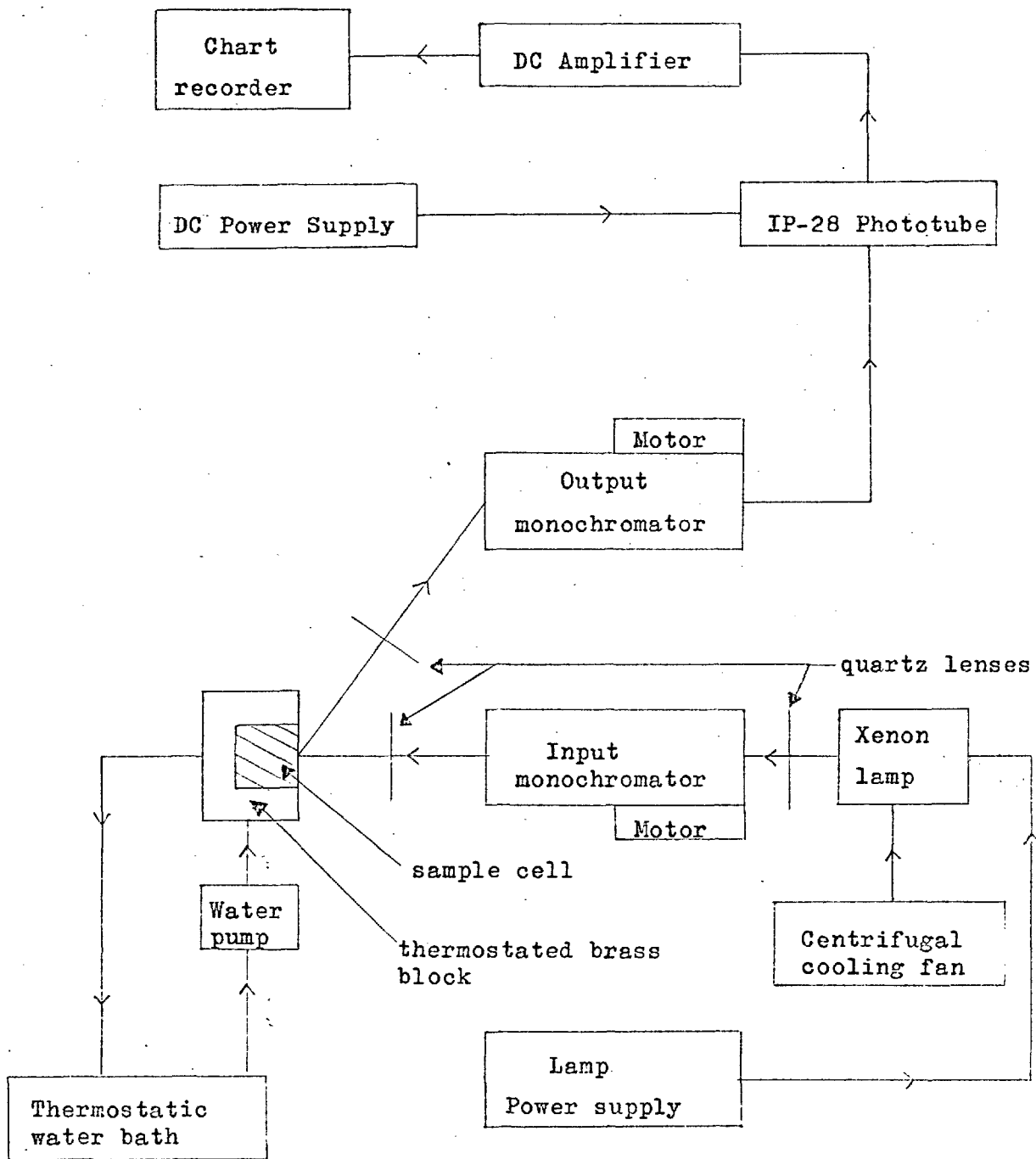
A simplified block diagram of the whole system is given in Fig. 23.

Fig. 22.



Each of the resistors in the Dynode chain is 50K. .
There are 10 such resistors for the 9-stage IP-28 .

Fig. 23.



(v)Calibration.

The sensitivity of the apparatus was calibrated against the potential supplied to the phototube by using a fluorescent sample, excited and observed at fixed wavelengths. This overall sensitivity independent of wavelength, is shown plotted against the monitoring galvanometer current, which is directly proportional to the applied voltage; see Fig. 24.

No attempt was made to calibrate the system for relative sensitivity as a function of wavelength, and thus all spectra obtained have to be examined bearing this in mind. The phototube response is a function of the incident wavelength, the IP-28 has a pronounced peak in the ultra-violet. Also the lamp intensity and monochromator performance are all wavelength dependent. If however readings are taken at a fixed excitation and emission combination, comparisons can be made directly, knowing the overall sensitivity for various phototube potentials.

Finally reproducibility; this was good to $\sim 1\%$, except when the lamp was warming up, or over long time periods, when the lamp intensity varied with the mains voltage, as the supply circuit had no constant-voltage mains transformer.

(b)Experimental Investigation of a Transferring System,
Fluorescein/Rhodamine-B.

To underline the effect of attenuation, which has previously been investigated at length, and self-quenching, both dependent on concentration, the fluorescence signal of

Fig. 24.

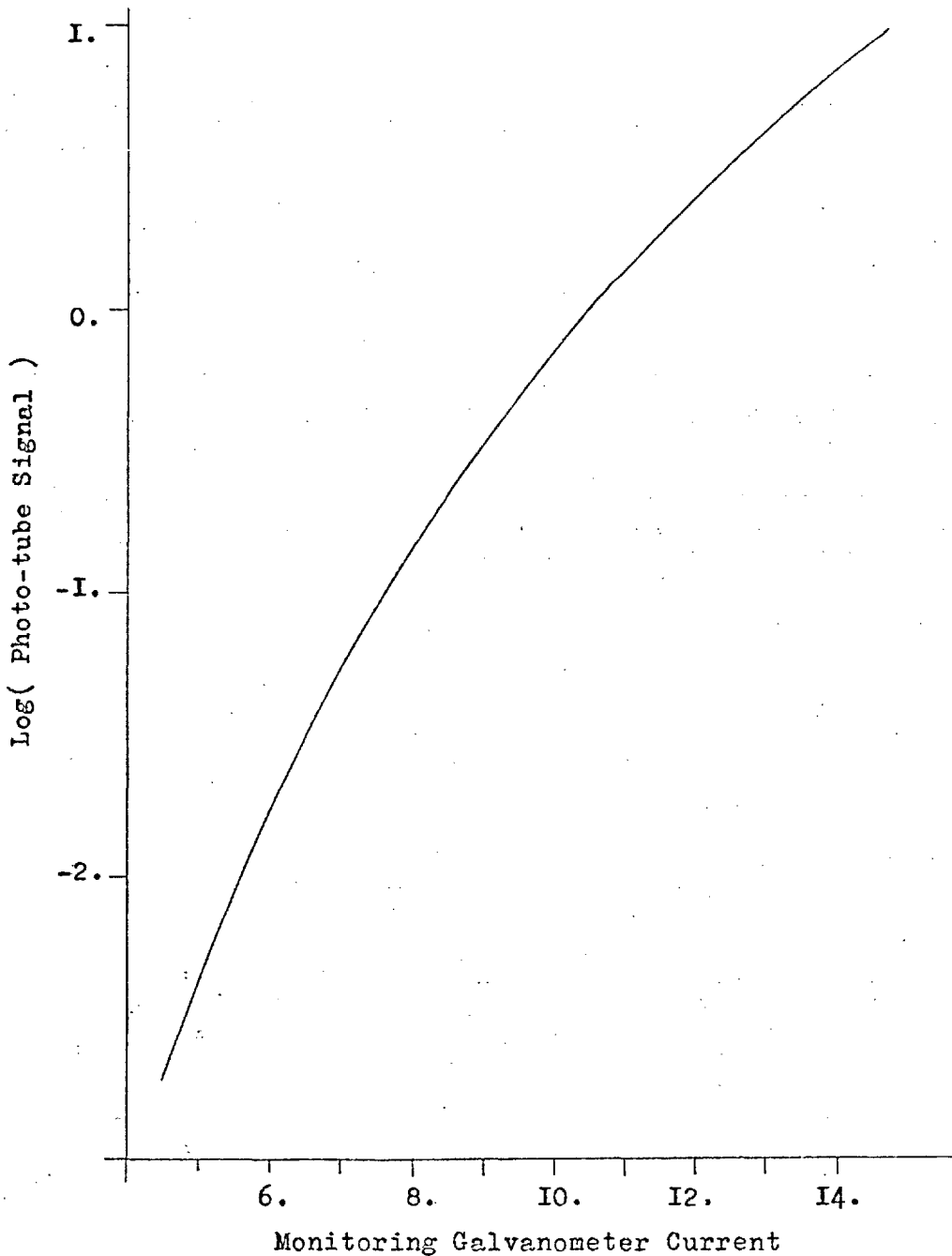


Photo-tube Sensitivity: The log of photo-tube response as a function of the applied potential for a constant input light intensity. This potential is directly proportional to the monitoring galvanometer current.

Fluorescein was followed as a function of concentration. As may be seen in Fig. 25, at low concentrations the plot is linear. However at high concentrations as attenuation becomes important instead of giving a constant signal as all the exciting light is absorbed, as we would expect for front viewing, the yield decreases under the influence of self quenching.

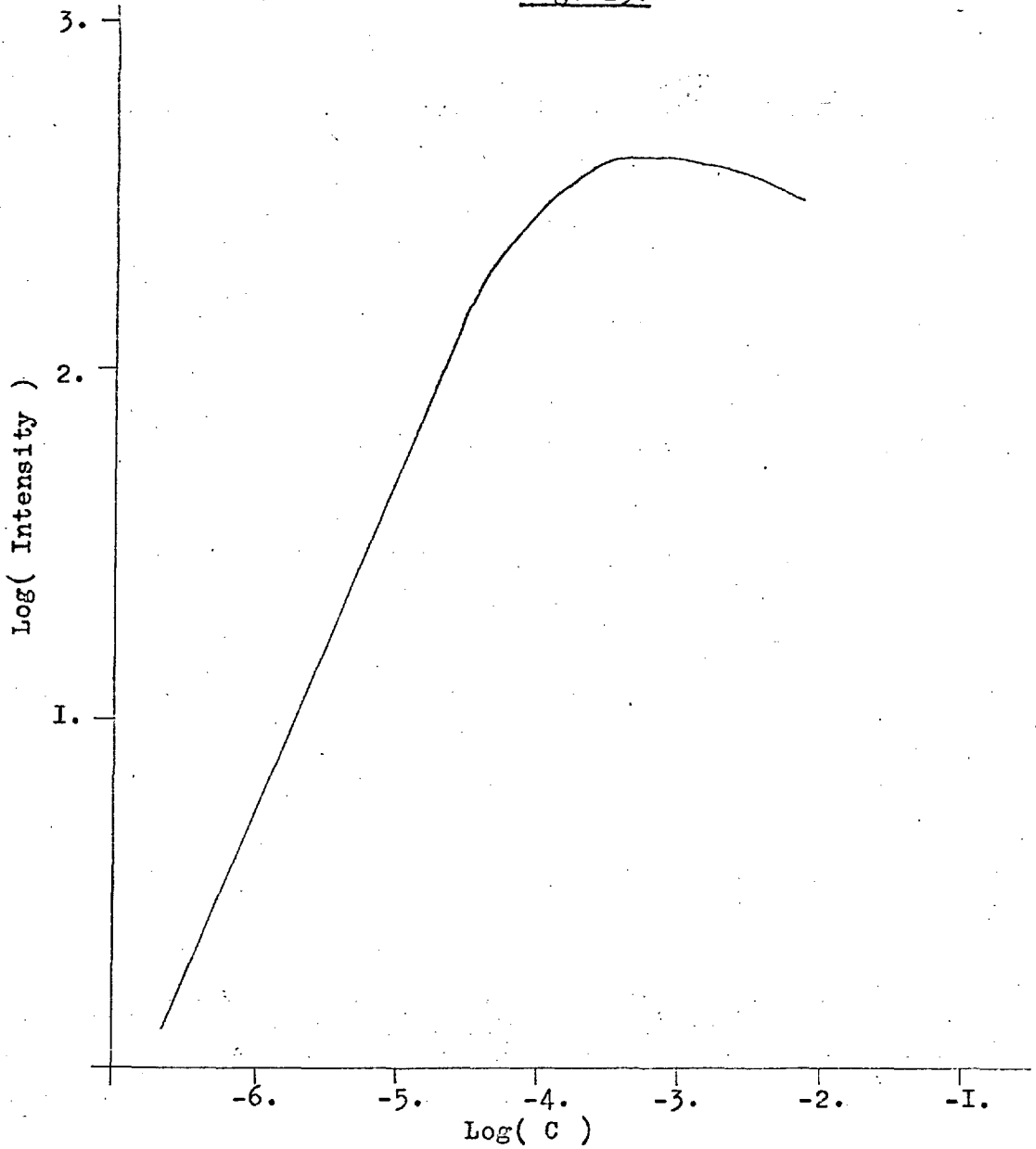
Also it was interesting to observe the effect of self-absorption on the position of the maximum fluorescence intensity. As may be seen, Fig. 26, this effect is very large for back viewing with a 5mm cell, although it is diminished appreciably by the use of a thin layer of material, as shown by the results for the .Imm layer.

All this helps to experimentally emphasize the problems which have already been discussed in theoretical terms concerning the measurement of radiationless transfer in the presence of appreciable attenuation effects.

The way we may partially circumvent these problems was first mentioned by Förster, (18). We must first use only forward viewing, then the fluorescence of A in the presence of B is given by,

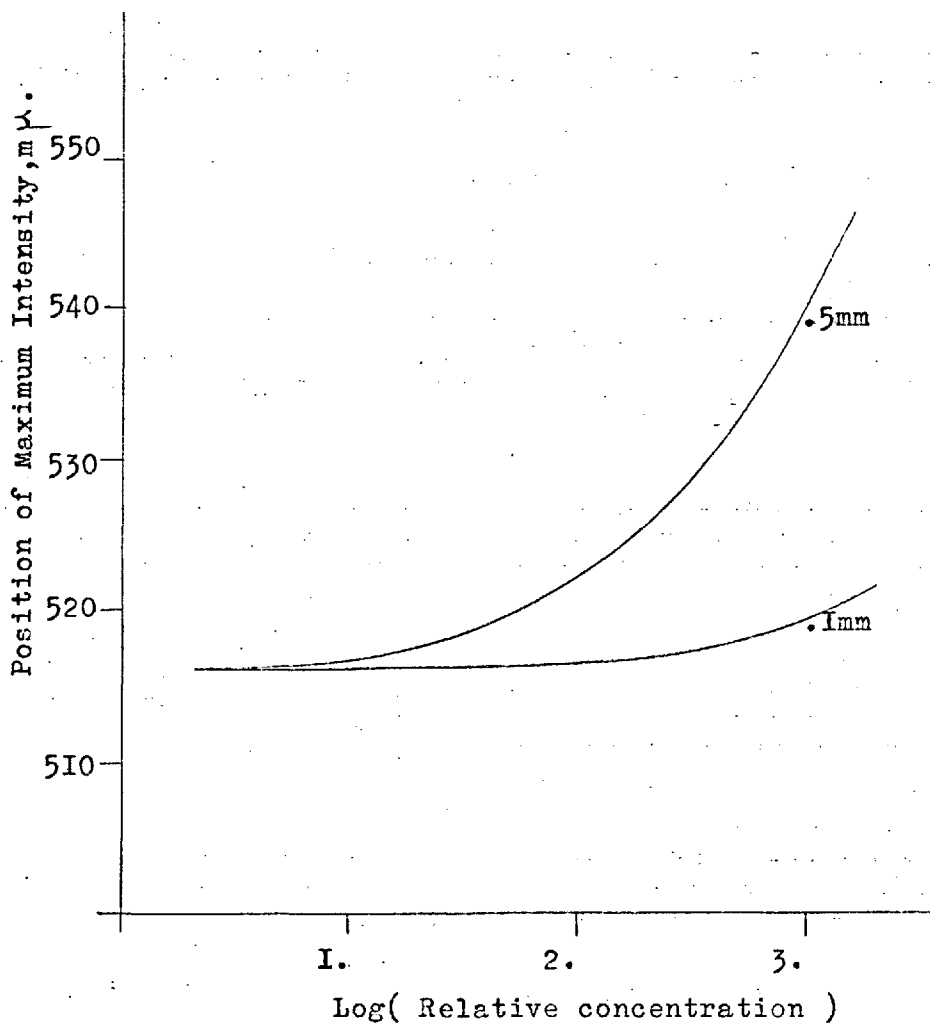
$$F_F^A = \bar{\Phi} \eta_{\lambda} E_{\lambda}^A C_A L^2 \dots \left(\frac{1 - \exp(-L [C_A (E_{\lambda}^A / \cos \theta + E_{\lambda}' / \cos \phi) + C_B (E_{\lambda}^B / \cos \theta + E_{\lambda}' / \cos \phi)])}{\cos \phi (C_A [E_{\lambda}^A / \cos \theta + E_{\lambda}' / \cos \phi] + C_B [E_{\lambda}^B / \cos \theta + E_{\lambda}' / \cos \phi])} \right)$$

Fig. 25.



The fluorescent intensity of a Fluorescein sample as a function of concentration . Forward viewing was used, with excitation in a .5mm cell by 450m μ light .

Fig. 26.



The wavelength at maximum fluorescence intensity of Fluorescein samples as a function of concentration and cell thickness.

The sample was viewed in the straight through position, and the advantage of a thin cell is clear. Cell thickness is shown on the curves, and concentration is in units of $3.86 \cdot 10^{-5} M$.

Then at high optical densities with,

$$C_A [E_{\lambda}^A / \cos \theta + E_{\lambda}'^A / \cos \phi] + C_B [E_{\lambda}^B / \cos \theta + E_{\lambda}'^B / \cos \phi] \gg 1$$

we find,

$$F_F^A = \frac{\Phi \eta_{\lambda} E_{\lambda}^A L^2}{[E_{\lambda}^A / \cos \theta + E_{\lambda}'^A / \cos \phi] + \frac{C_B}{C_A} [E_{\lambda}^B / \cos \theta + E_{\lambda}'^B / \cos \phi]}$$

(I-183)

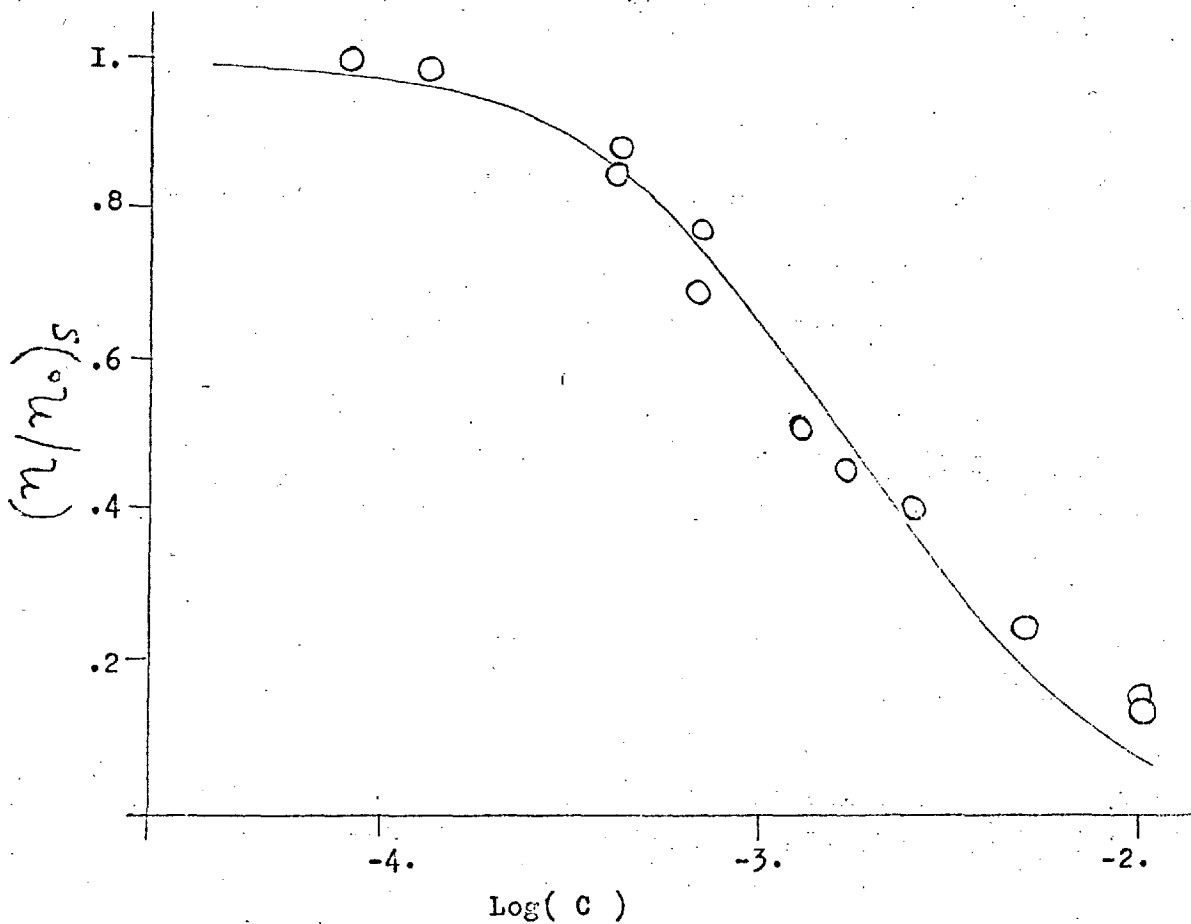
That is, so long as C_B/C_A is constant, the effect of attenuation on the fluorescence of A will be constant. The validity of this expression clearly depends on the inequality holding at a given concentration of A and B . For solutions of Rhodamine-B and Fluorescein the condition is obeyed at concentrations greater than $\sim 10^{-4}$ M., and so this enables the investigation of transfer between the two species in solution to be carried out in a straight forward manner, ignoring attenuation effects at these concentrations.

With this assumption results confirm the Förster theory within experimental error, see Fig.27, except that deviations appear to occur at high concentrations. From the results the value of Förster's parameter, the critical concentration is obtained as $C^0 = 2.8 \cdot 10^{-3}$ M. (See Förster's result, $C^0 = 2.3 \cdot 10^{-3}$ M. for the system Trypaflavin/Rhodamine-B, (32).)

(c) Some Conclusions.

From this experimental work, and the work of others, which confirm the already discussed theoretical treatment,

Fig. 27.



The quenching of sensitizer fluorescence as a function of acceptor concentration for the system Fluorescein/Rhodamine-B. Points are experimental values, the solid line represents the fitted Förster function, $(\eta/\eta_0)_S$.

it seems we must recognize two basic points;

(a). The impossibility of obtaining results of high accuracy, approaching 1%, due to attenuation effects, lamp instability and other sources of error. Thus these and similar experiments seem inappropriate for the investigation of various theoretical models for the transfer mechanism.

(b). If, instead of studying the integral properties of the systems, their time-dependent behaviour is studied, perhaps much more could be learnt. It would seem more relevant to investigate the decay of the excitation on the acceptors and sensitizers directly, measuring the intensity decay of systems as a function of time. Hence the transfer mechanism could be investigated at first-hand, rather than through insensitive integrals appropriate to steady-state conditions. This time-dependent method is however the most difficult experimentally, requiring quite sophisticated electronic techniques, but it seems the most likely area for "critical experiments" at the present time.

CHAPTER 2.

THE CALCULATION OF THE PROPERTIES OF Π -ELECTRON SYSTEMS.

(I.) Introduction.

At the end of the 19-th Century the discovery of the electron by Thomson and the deductions of Rutherford concerning the nature of the positive nucleus paved the way for the "classical" quantum mechanics of Max Planck (1900), and Niels Bohr (1913). The idea of discrete stationary states for electrons introduced by Bohr gave non-radiating states for an electron in a central field, unlike classical mechanics.

Bohr also proposed that the structure of many electron atomic systems could be represented, to a good approximation, by regarding each electron as being in a stationary state in the field of the nucleus and the charge distributions of all the other electrons.

The use of three quantum numbers (n,l,m) to describe electronic levels in atoms proved only partially successful for atoms heavier than Hydrogen. Experimental results indicated the need for a fourth quantum number, and this was introduced as spin with the Pauli Exclusion Principle.

A decisive step forward came with the inception of Wave and Matrix Mechanics by Schrödinger and Heisenberg in 1925. Schrödinger's mechanics was based on much earlier work by Hamilton, who established a formal analogy between mechanics

and optics. The new wave nature ascribed to the electron confirmed Heisenberg's Uncertainty Principle and De Broglie's investigations into the wave properties of matter. This important advance however led to the loss of the simple classical idea of an electron orbit, electrons lost their identity as all measurable quantities had to be symmetric functions of particle coordinates. This "exchange phenomena" is very important in the transition from one electron to many electron systems.

The final stage in the basic development of quantum mechanics was the evolution of Relativistic Quantum Mechanics by Dirac, who removed discrepancies in Schrödinger's mechanics, using a four-component wave function and relativistic operators.

(2.) The Schrödinger Wave Equation.

The general time-dependent form of the Schrödinger equation for a one electron system in a conservative field is given as, (66),(67),(7),

$$i \hbar \frac{\partial \Psi}{\partial t} = H \Psi \quad (2-1)$$

The quantum mechanical Hamiltonian, H , represents, as in classical mechanics, the sum of kinetic and potential energy, except now to form the quantum operator we transform linear

momentum; $\vec{p}_x \rightarrow \frac{\hbar}{i} \frac{\partial}{\partial x}$

Hence we have for the Hamiltonian,

$$H = V(\vec{r}) - \frac{\hbar^2}{2m} \nabla^2 \quad (2-2)$$

Where; $V(\vec{r})$ = the potential energy of the system.

$$\nabla^2 = \text{the Laplacian Operator, } \frac{\partial^2}{\partial x^2} + \frac{\partial^2}{\partial y^2} + \frac{\partial^2}{\partial z^2} .$$

The time dependence of the wave function Ψ is represented as,

$$\Psi(t) = \Psi(0) e^{\frac{Eit}{\hbar}} \quad (2-3)$$

$\Psi(0)$ being the wave function of the system at $t=0$.

Hence for a stationary state, with E not dependent on time, we obtain the time-independent form of the Schrödinger equation,

$$\left[-\frac{\hbar^2}{2m} \nabla^2 + V(\vec{r}) \right] \Psi = H \Psi = E \Psi \quad (2-4)$$

Without any further detailed consideration of H and Ψ

some general conclusions can be reached as to the properties of solutions of the equation above with a given Hamiltonian.

For a solution representing a particular stationary state, $E_i, \Psi_i \rightarrow 0$ and $\int_0^{\infty} |\Psi_i|^2 dr$ converges as $r \rightarrow \infty$

The set of energy values, $\{E_i\}$, the "eigenvalues", for which the equation has solutions, have corresponding "eigenfunctions",

$\{\Psi_i\}$, which are finite and single valued throughout space.

Usually the convention is adopted that $V \rightarrow 0$ as $r \rightarrow \infty$, so the values of E_i for stationary states are negative.

It is clear for the form of the Schrödinger equation that if Ψ_i is a solution, for the system with energy E_i ,

then so is any constant multiple $a \psi_i$, thus it is convenient to normalize the function, so that* $\int \psi_i^* \psi_i d\tau = 1$. For two different normalized solutions ψ_i and ψ_j it can be shown that, $\int \psi_i^* \psi_j d\tau = \delta_{ij}$; where δ_{ij} is the Kroenecker Delta. This is expressed by saying ψ_i and ψ_j are orthogonal and the set of solutions, $\{\psi_i\}$, is said to be "orthonormal".

If the state of energy E_i is degenerate, and can be represented by two eigenfunctions ψ_{i1} and ψ_{i2} , the Schrödinger equation does not force ψ_{i1} and ψ_{i2} to be orthogonal. We could however use any combination, $a\psi_{i1} + b\psi_{i2}$, as a solution for energy E_i , so we just chose two orthogonal ones from the infinite set. This imposes no additional restrictions, and enables us to preserve the orthogonality principle. A similar procedure may be followed for roots with higher degeneracy.

Finally we must consider the vectorial interpretation of the Schrödinger equation. In the matrix mechanics of Heisenberg we represent wave functions as vectors, and operators, (such as the Hamiltonian,) as matrices. This transformation from the differential form of Schrödinger's wave equation is easily followed if we expand our prospective solution to the wave equation, ψ_i , in terms of a complete

* Integration over all electronic coordinates is implied when no limits appear in an integral. ψ_i^* is the complex conjugate of ψ_i .

set of orthonormal basis functions, $\{\phi_j\}$,

$$\psi_i = \sum_j c_{ij} \phi_j \quad (2-5)$$

Then we have,

$$H \sum_j c_{ij} \phi_j = \epsilon_i \sum_j c_{ij} \phi_j \quad (2-6)$$

On multiplying this equation by the complex conjugate of one of our basis set, say ϕ_k^* , and integrating we obtain,

$$\sum_j c_{ij} \left[\int \phi_k^* H \phi_j d\tau \right] = \epsilon_i c_{ik} \quad (2-7)$$

If we use $k=1, \dots, i, j, \dots$, covering our entire basis set, it can be seen we obtain a matrix equation of the form,

$$H C_i = \epsilon_i C_i \quad (2-8)$$

Where C_i is a column vector, representing $\sum_j c_{ij}$, with the coefficients c_{ij} giving the components of the basis functions appropriate to eigenvalue ϵ_i . This expansion technique of solving eigenvalue problems is a special case of a method first proposed by Ritz, (76).

The matrix equivalent of the Hamiltonian, H , has elements, $H_{ij} = \int \phi_i^* H \phi_j d\tau$. Such matrix equations may be easily manipulated and solved using conventional matrix methods.

Thus we can regard our wave function, ψ_i , as a vector, with components, c_{ij} , of the orthonormal basis set, $\{\phi_j\}$. The action of the Hamiltonian operator matrix representative

on such a vector, if it is an eigenfunction of the system, is to give a parallel vector, of length ϵ_j compared to the original unit length of the eigenfunction. The normalization of this eigenfunction is expressed by,

$$\int \psi_i^* \psi_i d\tau = \sum_{j,j'} c_{ij'}^* c_{ij} \int \phi_{j'}^* \phi_j d\tau = \sum_j c_{ij}^* c_{ij} = 1. \quad (2-9)$$

The orthogonality of the eigenvectors corresponding to different eigenvalues, ϵ_i and ϵ_k , can be written in a similar manner,

$$\int \psi_k^* \psi_i d\tau = \sum_{j,j'} c_{kj'}^* c_{ij} \int \phi_{j'}^* \phi_j d\tau = \sum_j c_{kj}^* c_{ij} = 0. \quad (2-10)$$

Thus this integral can be considered as the scalar product of two vectors at right angles to each other. In the more compact vector notation we summarize these properties as, *

$$C_k^+ C_j = \delta_{jk} \quad (2-II)$$

The complex vector space we are considering is referred to as Hilbert Space, and in this space the eigenvectors of the wave equation are all perpendicular, and such that $\epsilon_i C_i$ gives another vector parallel to C_i , with length representing the eigenvalue, ϵ_i .

In this consideration of the properties of the Schrödinger equation no approximations have been made, this however is certainly not the case in it's solution for many electron problems. The question of importance here is what approximations are valid in a given context.

* C_k^+ is the complex conjugate transpose of column vector C_k

(3) The Many-Particle Hamiltonian.

For an interacting system of N nuclei, labeled j and j' , and n electrons i and i' , by neglecting spin terms and only considering two-body potentials, the Hamiltonian may be written as,

$$H = - \left\{ \frac{\hbar^2}{2} \sum_{j=1}^N \frac{\nabla_j^2}{M_j} + \frac{\hbar^2}{2m_e} \sum_{i=1}^n \nabla_i^2 \right\} + \sum_{j,j' > j}^N \frac{z_j z_{j'}}{r_{jj'}} + \sum_{i,i' > i}^n \frac{e^2}{r_{ii'}} - \sum_{i,j}^{n,N} \frac{z_j e}{r_{ij}} \quad (2-12)$$

Where M_j are the nuclear masses, m_e the electronic mass,

z_j and e are the nuclear and electronic charges respectively. The potential terms result from nuclear-nuclear and electron-electron repulsion, and the electron-nucleus attraction. With $\frac{M_j}{m_e} \gg 1840$, it seems reasonable to assume that the nuclei are essentially fixed in space, as long as we are not concerned with vibrational problems. This omission of the kinetic energy of the nuclei from the Hamiltonian is the famous Born-Oppenheimer Approximation, (68).

If we assume the separability of the electronic and vibrational components of our wave function, the Schrödinger equation for the electronic wave function, Ψ_{el} , can be written,

$$\left(- \frac{\hbar^2}{2m_e} \sum_i \nabla_i^2 + \sum_{j,j' > j} \frac{z_j z_{j'}}{r_{jj'}} + \sum_{i,i' > i} \frac{e^2}{r_{ii'}} + \dots - \sum_{i,j} \frac{z_j e}{r_{ij}} \right) \cdot \Psi_{el}(1,2,\dots,n) = E \cdot \Psi_{el}(1,2,\dots,n) \quad (2-13)$$

The fixed nuclear framework over which the electrons move enters the Hamiltonian as a parameter. This nuclear repulsion term $\sum_{j,j'} \frac{z_j z_{j'}}{r_{jj'}}$ is constant for a fixed nuclear conformation so we may omit it from the electronic energy, (67),

$$E_{el} = E - \sum_{j,j' > j} \frac{z_j z_{j'}}{r_{jj'}} \quad (2-I4)$$

Hence we finally obtain, using units of electronic mass and charge,

$$\left(\left[-\frac{1}{2} \sum_i \nabla_i^2 - \sum_{i,j} \frac{z_j}{r_{ij}} \right] + \sum_{i,i' > i} \frac{1}{r_{ii'}} \right) \psi_{el} = E_{el} \psi_{el} \quad (2-I5)$$

The inner brackets enclose a sum of single electron operators, $-\frac{1}{2} \nabla_i^2 - \sum_j \frac{z_j}{r_{ij}}$, describing the motion of each electron in the field of the nuclei alone. These are often referred to as the "core operators", (67), (69),

$$H_i^c = -\frac{1}{2} \nabla_i^2 - \sum_{i,j} \frac{z_j}{r_{ij}} \quad (2-I6)$$

Hence,

$$\left(\sum_i H_i^c + \sum_{i,i' > i} \frac{1}{r_{ii'}} \right) \psi_{el} = E_{el} \psi_{el} \quad (2-I7)$$

Thus we may represent our many-electron Hamiltonian by two components, the core-electron and electron-electron interaction terms.

Several other general properties of the Hamiltonian are important, first the Hamiltonian is a linear operator as it contains only derivatives and multipliers.

$$H(\psi_i + \psi_j) = H\psi_i + H\psi_j \quad (2-18)$$

Also it is a Hermitian operator ,

$$\int \psi_i^* H \psi_j d\tau = \int \psi_j H^* \psi_i^* d\tau \quad (2-19)$$

Hence the diagonal elements of the matrix $H_{ii} = H_{ii}^*$ are real, and also, $H_{ij} = H_{ji}^*$. This compactly expressed in the matrix notation gives, $H = H^\dagger$. The invariance of H under any permutation operator is very important. If we represent the interchange of electrons i and j by P_{ij} , then, $P_{ij}(H) = H$. This equation holds since H is symmetric in both electron coordinates and momenta, as can be seen from equation (2-15).

(4) Many-Electron Wave Functions.

For the single electron in the Hydrogen atom we have only nucleous-electron interactions to consider, however with any problem involving two or more electrons we have to consider in addition the electron-electron repulsion terms. Thus any wave function used to describe a many-particle system should take these electron correlations into account.

Consider a two electron system, with the coordinates of electron 1 denoted by \vec{r}_1 and electron 2 by \vec{r}_2 , (70).

The total wave function $\Psi(\vec{r}_1, \vec{r}_2)$ is given by,

$$\left(-\frac{1}{2} [\nabla_1^2 + \nabla_2^2] + V(\vec{r}_1, \vec{r}_2) \right) \Psi(\vec{r}_1, \vec{r}_2) = E \Psi(\vec{r}_1, \vec{r}_2) \quad (2-20)$$

The potential term can be written as,

$$V(\vec{r}_1, \vec{r}_2) = V_1(\vec{r}_1) + V_2(\vec{r}_2) + V_{12}(\vec{r}_1 - \vec{r}_2) \quad (2-21)$$

the last component, V_{12} , is the relative position contribution.

If we ignore inter-electron interaction and set, $V_{12} = 0$, then the force on electron 1, $-\frac{\partial V}{\partial \vec{r}_1}$, is independent of \vec{r}_2 , so we can write our separable wave function corresponding to each electron moving independently as,

$$\Psi(\vec{r}_1, \vec{r}_2) = \phi_1(\vec{r}_1) \phi_2(\vec{r}_2) \quad (2-22)$$

The one electron wave functions ϕ_1 and ϕ_2 represent the motions of each individual electron in the potential field, and the corresponding energies E_1 and E_2 are the independent one electron energy levels.

However, when the electrons are allowed to interact with $V_{12} \neq 0$, $-\frac{\partial V}{\partial \vec{r}_1}$ depends on \vec{r}_1 and \vec{r}_2 , and the two electron wave function is no longer separable into one electron components. Only the two electrons together are in a stationary state of constant total energy. The individual electrons can no longer be assigned independently to particular one electron levels.

This inseparability is basic, even though we may often

use a product wave function as an approximation for the total wave function. When using such a product function the motion of each electron in the field of the nuclei and all the other electrons is considered to derive the approximate one electron function. Clearly however, in such a case the energy associated with this one electron wave function is meaningless without recognition of the interdependence of the whole set of electrons.

The product wave function approximation was implied in some of Bohr's work, (71), where electrons were considered to occupy levels given by quantum numbers, the levels being singly occupied in accordance to Pauli's Exclusion Principle. We may write such a product function as ,

$$\bar{\Phi} = \phi_{\alpha}(1) \phi_{\beta}(2) \phi_{\gamma}(3) \dots \phi_{\pi}(n) \quad (2-23)$$

where, $\alpha, \beta, \gamma, \dots, \pi$, are the one electron wave function labels, and $1, 2, \dots, n$ are electron labels, standing for space and spin coordinates. The function $\bar{\Phi}$, dependent on the coordinates of all electrons, is not implied to be a solution of the Schrödinger equation appropriate to the system. It may however be used as a flexible function which through variations in the set $\{\phi_{\alpha}\}$ can become a reasonable approximation to the real solution, ψ .

In the function $\bar{\Phi}$, the individual orbitals give an average charge density for the j -th electron , $|\phi_{\alpha}(j)|^2$,

suggesting that each of the functions, $\{\phi_\alpha\}$, should be determined as a solution to Schrödinger's equation for one electron in the field of the nuclei and all the other electronic distributions. This quickly leads to the idea of "Self-Consistent Field" orbitals, (72), where a product wave function is used, and the set $\{\phi_\alpha\}$ varied to give a function Φ the closest possible to the correct solution, Ψ .

The multiple product approximation does not however fulfill a very important requirement for a wave function, it is not antisymmetric with respect to electron exchange. This may be illustrated by considering a solution E_0 with eigenfunction Ψ_0 . If the coordinates of electrons i and j are exchanged in Ψ_0 , we represent the new function as, $P_{ij}\Psi_0$, where P_{ij} is the appropriate permutation operator. The Hamiltonian of the system is unchanged by P_{ij} , $P_{ij}H=H$ so if Ψ_0 is a solution to the wave equation, then so is $P_{ij}\Psi_0$, for any i and j . As long as E_0 is non-degenerate then P_{ij} must be a constant multiple of Ψ_0 , $P_{ij}\Psi_0 = c_{ij}\Psi_0$. But since $P_{ij}P_{ij} = I$, $\Psi_0 = c_{ij}P_{ij}\Psi_0$, and $c_{ij} = \pm 1$. For a function with $c_{ij} = +1$, $P_{ij}\Psi_0 = \Psi_0$, and Ψ_0 is termed a "symmetrical" wave function. With $c_{ij} = -1$, $P_{ij}\Psi_0 = -\Psi_0$, and Ψ_0 is an "anti-symmetrical" wave function.

It is found that the only valid form of wave functions derived from the Schrödinger equation are the anti-symmetric ones. This is the wave mechanical foundation of the

Pauli Principle for particles of half integer spin.

To conform to this requirement we must represent our wave function as a series of products giving a final antisymmetric form. The prescription for this is to represent our state, one particular electronic configuration, as a determinant. We use this form as a determinant has the correct properties. It is antisymmetric with respect to electron exchange, column interchange in the determinant, and becomes zero if the Pauli Principle is not obeyed, with two identical columns in the determinant. Hence for our total many electron wave function, $\bar{\Phi}$, we write,

$$\bar{\Phi} = \frac{1}{\sqrt{n!}} \begin{vmatrix} \phi_{\alpha}(1) & \phi_{\alpha}(2) & \phi_{\alpha}(3) & \dots & \phi_{\alpha}(n) \\ \phi_{\beta}(1) & \phi_{\beta}(2) & \dots & \dots & \phi_{\beta}(n) \\ \vdots & \vdots & \vdots & \vdots & \vdots \\ \phi_{\pi}(1) & \dots & \dots & \dots & \phi_{\pi}(n) \end{vmatrix} \quad (2-24)$$

In this function all permutations of electrons are equally possible, the sign to be taken with each permutation depends on the parity of the particular permutation, (1, 2, ..., p, ..., n). The normalizing factor $1/\sqrt{n!}$ ensures that, $\int \bar{\Phi} \bar{\Phi}^* d\tau = 1$, and assumes the $\{\phi_{\alpha}\}$ are individually normalized and orthogonal. Also the determinant is unaltered by writing, $\phi_{\beta} \rightarrow \phi_{\beta} + A \phi_{\alpha}$, so the orthogonality requirement for the set $\{\phi_{\alpha}\}$ imposes no additional restrictions upon the determinant. These representations are often known as Slater Determinants, (74).

An alternative notation is possible in the antisymmetrization of many electron wave functions. Instead of writing the total wave function in determinantal form we use an antisymmetrizing projection operator, (69),(75),

$$A_{as} = \frac{1}{\sqrt{n!}} \sum_P (-1)^P P \quad (2-25)$$

on the wave function. P is a permutation operator acting on all electron coordinates, and P is the parity of the particular permutation. The result of applying the operator to the wave function, $A_{as} \Phi$, is exactly the same as expanding out the Slater determinant in the equivalent notation.

We must remember that this concept of electron exchange only arises as a result of the indistinguishability of the electrons involved in any particular configuration. The idea of "exchange energy" has no physical meaning, in our approximations all the energy is essentially coulombic, (73).

Up to now, except in so much as we have adhered to the generalized Pauli Principle, electron spin has not been explicitly involved in our wave functions. All the orbitals used, $\{\phi_\alpha\}$, are spin-orbitals, involving spin as well as spatial coordinates, $\phi = f(x, y, z, s)$. The spin coordinate s , is usually taken as the projection of the intrinsic moment of the electron onto an arbitrary Z-axis, $\pm \frac{\hbar}{2}$. Hence we can represent the spin possibilities either in a single function, $\phi(x, y, z, s)$, where $s = \pm \frac{1}{2}$, or as a pair

of functions, $\phi(x, y, z)$ and $\overline{\phi}(x, y, z)$. The "barred" function indicating $S = -\frac{1}{2}$.

If we neglect spin-orbit interaction, that is we ignore any variation of $\phi(x, y, z)$ under spin effects, then the spin component of our wave function may be factored out to give, $\phi(x, y, z) \chi(s)$. Usually we write $\chi(s = \frac{1}{2}) = \alpha$ and $\chi(s = -\frac{1}{2}) = \beta$, thus in this approximation an electron j in orbital ϕ_i with $S = +\frac{1}{2}$ is represented as $\phi_i(j) \alpha(j)$. If $S = -\frac{1}{2}$ for the electron of opposite spin, we have $\phi_i(j) \beta(j)$. Note in this approximation we assume our two possible spin orbitals are spatially degenerate, that is we have essentially "paired" orbitals. These spin functions are normalized and orthogonal,

$$\begin{aligned} \int \alpha^{(1)} \alpha^{*(1)} d\tau_1 &= 1 & \int \beta^{(1)} \beta^{*(1)} d\tau_1 &= 1 \\ \int \alpha^{(1)} \beta^{*(1)} d\tau_1 &= 0 \end{aligned} \quad (2-26)$$

With this notation we may represent a doubly occupied system of $2p$ electrons by the determinant,

$$\Phi = \frac{1}{\sqrt{(2p)!}} \begin{vmatrix} \phi_{\alpha}^{(1)} \alpha^{(1)} & \phi_{\alpha}^{(2)} \beta^{(2)} & \dots & \phi_{\pi}^{(2p)} \beta^{(2p)} \end{vmatrix} \quad (2-27)$$

or using the nomenclature, $\phi_{\alpha}^{(1)} \alpha^{(1)} = \overline{\phi}_{\alpha}^{(1)}$, $\phi_{\alpha}^{(2)} \beta^{(2)} = \overline{\phi}_{\beta}^{(2)}$ it may be expressed in equivalent form,

$$\overline{\Phi} = \frac{1}{\sqrt{(2p)!}} \begin{vmatrix} \overline{\phi}_{\alpha}^{(1)} & \overline{\phi}_{\alpha}^{(2)} & \overline{\phi}_{\beta}^{(3)} & \overline{\phi}_{\beta}^{(4)} & \dots & \overline{\phi}_{\pi}^{(2p)} \end{vmatrix} \quad (2-28)$$

Further spin properties involved in wave functions will be explained as they are met in later sections.

(5) The Variation Principle.

As we have considered some valid approximations for the wave function of a system of nuclei and electrons, it is important to introduce the variational theorem, which allows the optimization of a variable wave function, Φ , with a given Hamiltonian, H . This theorem is of general importance in quantum theory, but we shall be specially concerned with it in the setting up of a series of secular equations for molecular orbitals. Even time-dependent perturbation theory can be derived from the principle as a special case, (70).

If we consider the case of an exact wave function, Ψ , which describes a stationary state, E_0 , then we have,

$$H \Psi = E_0 \Psi \quad (2-29)$$

Now we consider the quantity E' , usually referred to as the "expectation energy", and defined by,

$$E' = \frac{\int \Phi^* H \Phi d\tau}{\int \Phi^* \Phi d\tau} \quad (2-30)$$

To find how E' depends on Φ , which is not in general a solution of the wave equation, variational calculus is used, and it is found, (70):

(i). If Φ is an exact solution to the Hamiltonian, H , that is $\Phi \equiv \Psi$, then E' is stationary, with $\Delta E' = 0$

to first order for any variation, $\Delta \bar{\Phi}$. Thus if $\bar{\Phi}$ is an approximation to the exact solution ψ , $\bar{\Phi} \approx \psi$, then E' is a better approximation to the exact energy, E_0 , than $\bar{\Phi}$ is to ψ .

(ii). If E' is stationary, that is $\Delta E' = 0$ for any $\Delta \bar{\Phi}$, then this $\bar{\Phi}$ is a solution, ψ , of the wave equation, and $E' = E_0$.

It can be shown that for the lowest energy state attainable by a system, E' is an absolute minimum. Hence the value of E' can be used to compare various approximations to the wave function of the ground state. The "best" wave function being regarded as the one to give the lowest E' and as of course we do not know the exact solution this is a useful criterion. The fact that a given wave function is the "best" to describe the ground state energy does not necessarily mean it is the best to describe other physical properties of the system. Other approximations may be much better for other properties, but as it seems no one criterion can judge the appropriateness of a given wave function, the energy one appears the most useful, (77), (78), (79).

It has been shown by Fock, (81), and also Slater, (82), that the variational principle applied to many electron wave functions of product or determinantal form leads to effective eigenvalue equations for the component single electron functions

of either the product or its antisymmetrized form. Thus the wave function of equation (2-27), can be reduced to a series of equations of the type,

$$H \phi_{\alpha}(1) = E_{\alpha} \phi_{\alpha}(1) \quad (2-31)$$

by the use of the variational principle, $\delta \langle \Phi^* | H | \Phi \rangle = 0$.

These eigenvalue problems can then be solved using matrix mechanics. We expand the function ϕ_{α} in terms of a basis set, $\{\chi_i\}$, and obtain the eigenvectors of this set appropriate to ϕ_{α} by solving,

$$E_{\alpha} = C_{\alpha}^{\dagger} H C_{\alpha} \quad (2-32)$$

This equation should be compared with equation (2-8).

The analogy between the right hand side of this equation, and the right of (2-30) is obvious. By solving for $E_{\alpha}, E_{\beta}, \dots$ we can find the component one electron eigenvectors, $C_{\alpha}, C_{\beta}, \dots$, with which the wave function is constructed. Thus we see the basic nature of the variational principle, and it's contribution to self-consistent field theory which we shall be considering later.

Results (i) and (ii) of the variational principle apply to excited states as well as to ground states, except here the stationary E' for the excited state need not be an absolute minimum. Thus the energy minimum criterion is certainly no good in evaluating the degree of accuracy in an excited

state wave function. Also it is possible that in searching for the excited state, the class of function we have chosen to vary may not contain a combination giving a stationary value of E' near the excited state.

(6) The Molecular Orbital Approximation.

Until now we have only been concerned with generalities concerning molecular systems, now we are going to consider the various methods available for the calculation of molecular properties in π -electron conjugated systems. We shall use exclusively the molecular orbital, (MO), approach originated by Mulliken, (80), (83), where the MO is constructed from a basis set of atomic orbitals centred on the various atoms in the molecule. This approach is not the only one possible, although it is now well established as the most convenient for molecular studies.

Two possible alternatives are the Valence Bond, (VB), (84), and Free Electron, (FE), methods, (85). These fall either side of the MO model in their degree of electron delocalization. In VB the electrons are localized in the bonds of the various canonical structures, while in the FE method the electrons move entirely freely in a potential groove.

These three methods, different as they seem, can be shown to be equivalent in many ways. They all emphasize different aspects of the same problem, Slater has studied the connection between the VB and MO methods, (86), and the

MO/FE comparison has also been made. We have only to remember the transformation properties of orbitals to realize that under suitable unitary transformations the invariant total wave functions of molecules can be made up in very different manners, all of which are in fact equivalent, (88).

The MO treatment has proved to be the most useful up to the present time, the electronic spectrum of a molecule is simply interpreted as transitions between empty and filled orbitals, and the MO obtained is generally symmetry adapted to the molecule in question. Also the effect of electron/electron repulsions is easily introduced, and additionally the problem of which orbitals are the "best" for a given electronic configuration can be solved with the use of self-consistent field theory.

(7) The σ - π Separation.

The first additional approximation we have to make before further investigation is to assume that we need only consider π -electrons explicitly. This step is justified by experimental observation, and to differing degrees by various theoretical calculations.

It has long been realized from experimental work that the π -electrons in a conjugated molecule are those which are involved in many physical properties such as, optical transitions, magnetic properties, and it is these electrons which give rise to the characteristic "conjugated" properties.

Thus we may feel we are justified in only considering the movement of the π -electrons over the core of the σ -electrons and nuclei.

This formal separation was first proposed by Hückel in 1931, (89), and has been used ever since, with various degrees of success. Even so it was soon realized that such a separation did not remove the question of the σ - π interaction, (90), which may be treated in various rather empirical ways. Normally the π -electrons are considered explicitly, and the σ -electrons regarded as effecting the potential they move in.

Various attempts have been made to treat systems allowing direct σ - π interaction. Altmann, (91), treated Ethylene using a VB method, taking the σ - π resonance effect into account, and concluded that the π -approximation was not valid. The σ - π interaction was found especially important for excited states. A contradictory result was found by Moser, (92), who used an 8-electron MO treatment on Ethylene, and found σ -excitations had little effect on the ground state. A similar treatment of Acetylene by Ross, (93), agreed with Moser's conclusions. Some levels were found to be purely π in nature, and the ones of mixed σ - π character were at least 22.6ev. above the ground state. The situation became worse as R_{c-c} increased, but it was found as long as $R_{c-c} \leq 1.5 \text{ \AA.}$, the effect of σ electrons on the π -levels

was unimportant. Finally evidence in favour of the separation was given by Parks and Parr, (94), who studied Formaldehyde as a 6-electron problem, and adjusted the π and σ functions to each other until self-consistency was reached. Their conclusion was that a fixed σ -contribution leads only to small errors in energy, but is not always good in determining wave functions.

The exact nature of the separation theorem is best understood by considering the $\sigma + \pi$ problem, and then simplifying to just the treatment of π -electrons, (95). The essential idea behind the π -approximation in a many electron problem is that some electrons can be treated separately from the rest. We shall represent the σ -core as $\Psi_{\sigma}(1, 2, \dots, n_{\sigma})$ and the π -shell as $\Psi_{\pi}(n_{\sigma}+1, \dots, n_{\sigma}+n_{\pi})$, where both of these many electron wave functions are antisymmetrized. Then the total wave function for the system of σ and π -electrons is approximated by the antisymmetrized product of Ψ_{σ} and Ψ_{π} ,

$$\underline{\Psi} = P_{\sigma\pi} \Psi_{\sigma} \Psi_{\pi} \quad (2-33)$$

Where $P_{\sigma\pi}$ is an appropriate antisymmetrizer, accounting for $\sigma-\pi$ exchange. Here we have represented our two groups of electrons by two many electron functions, and it has been shown in such systems that the inter-group correlation is much less important than the intra-group correlation, (96).

Our total wave function can be written in determinantal form,

$$\bar{\Psi} = \frac{1}{\sqrt{(n_\sigma + n_\pi)!}} \begin{vmatrix} \sigma_1(1) & \dots & \sigma_1(n_\sigma + n_\pi) \\ \vdots & & \vdots \\ \sigma_{n_\sigma}(n_\sigma) & \sigma_{n_\sigma+1}(n_\sigma+1) & \dots \\ \vdots & & \vdots \\ \pi_{n_\pi}(1) & \dots & \pi_{n_\pi}(n_\sigma + n_\pi) \end{vmatrix} \quad (2-35)$$

Hence $\bar{\Psi}$ satisfies the Pauli Principle, and σ - π exchange has been taken into account. These terms, ensuring the antisymmetry of the two group wave functions, are in the upper right hand side and the lower left of the determinant. If the factorization into two groups of electrons is valid then it is very important to know whether we may apply the Variational Principle to one of the groups individually. Justification of the application of the theorem to π -electrons using a π -electron operator has been given by Lykos and Parr, (97).

We can write the total Hamiltonian for the molecule

as,

$$H = \sum_{i=1}^{n_\sigma} \left(-\frac{1}{2} \nabla_i^2 - \sum_{\alpha} \frac{Z_{\alpha}}{r_{\alpha i}} + \sum_{j>i}^{n_\sigma} \frac{1}{r_{ij}} \right) + \sum_{i=1}^{n_\sigma} \sum_{j=n_\sigma+1}^{n_\sigma+n_\pi} \frac{1}{r_{ij}} + \sum_{i=n_\sigma+1}^{n_\sigma+n_\pi} \left(-\frac{1}{2} \nabla_i^2 + \sum_{\alpha} \frac{Z_{\alpha}}{r_{\alpha i}} + \sum_{j>i}^{n_\sigma+n_\pi} \frac{1}{r_{ij}} \right) \quad (2-35)$$

The central term is the σ -core electron/ π -electron interaction term, the other bracketed quantities are the kinetic energy, electron/core and electron/electron terms

for the σ and π -electron groups alone. Thus the total energy of the system can be represented as ,

$$E_T = E_\sigma + E_{\sigma\pi} + E_\pi \quad (2-36)$$

The cross-term, $E_{\sigma\pi}$, can be removed into an effective π -Hamiltonian,

$$E_T = E_\sigma + E'_\pi \quad (2-37)$$

with,

$$E'_\pi = \int \Psi_\pi^* H_\pi \Psi_\pi d\tau \quad (2-38)$$

H_π is an operator depending on the coordinates of the σ and π -electrons, while E_σ depends directly only on the σ -coordinates.

$$H_\pi = \sum_{i=n_\sigma+1}^{n_\sigma+n_\pi} \left\{ H_{(i)}^c + \sum_{j,i}^{n_\sigma+n_\pi} \frac{1}{r_{ij}} \right\} \quad (2-39)$$

Where,

$$H_{(i)}^c = -\frac{1}{2} \nabla_i^2 - \sum_\alpha \frac{Z_\alpha}{r_{\alpha i}} + G_\sigma(i) \quad (2-40)$$

and we have ignored nuclear/nuclear terms, α and β being nuclear indices;

$$H_{nuc} = \sum_\alpha \sum_{\beta, \beta > \alpha} \frac{Z_\alpha Z_\beta}{r_{\alpha\beta}} \quad (2-41)$$

$G_\sigma(i)$ is an operator accounting for the σ - π coupling between the i -th π -electron in MO π_i , and the n_σ electrons their orbitals, $\{\sigma_j\}$;

$$G_{\sigma}(i) \pi_i = \sum_{j=1}^{n_{\sigma'}} \int \sigma_j^{(1)} \sigma_j^{(1)*} \frac{1}{r_{12}} \pi_i^{(2)} - \sum_{j=1}^{n_{\sigma'}} \int \sigma_j^{(1)} \sigma_j^{(2)*} \frac{1}{r_{12}} \pi_i^{(1)} \quad (2-42)$$

The first term is the coulomb expression, and the second the exchange, (see later). Thus it is possible to define an energy operator H_{π} for the π -electrons alone, so that it's expectation value over an antisymmetrized product wave function for the π -electrons alone includes the σ - π coulomb and exchange interactions.

Such a method was used by Parks and Parr ,(94), in varying the σ and π groups in turn to achieve a consistent result, but as Stewart has shown, (98), the "best" wave function can only be obtained by varying the total energy E_T , not just E_{σ} or E'_{π} .

A different approach to the σ - π problem was followed by Coulson, (99), who calculated the electron density in Benzene 0.35 Å. above the molecular plane. This was a direct test of Hückel's argument that the σ -electrons and π -electrons have little overlap, due to the π -nodes being at the nucleus. From the separately computed results for the σ and π densities, it was found the largest overlap, as expected, was over the carbon atoms, where the σ and π densities were about equal. Thus there appeared considerable σ - π overlap, and thus the separation hypothesis becomes

rather doubtful .

However in the final analysis, quite good results can be obtained using the $\sigma-\pi$ factorizability, and it seems until the procedure is positively invalidated, this approach will continue to be used.

(8) The Hartree-Fock Equations.

Now we shall follow the development of the perfectly general Hartree-Fock scheme for a closed-shell state through various stages of its specialization for calculating π -molecular orbitals using the semi-empirical Pople-Pariser-Parr method. By a closed-shell state it is meant all electrons are spin paired, the orbitals occurring in spatially degenerate pairs. As a consequence the molecule is in a singlet state, with $\langle S_z \rangle = 0$.

The total wave function of the molecular state, Ψ_0 , is assumed to be a normalized Slater determinant, with doubly occupied orbitals,

$$\Psi_0 = \frac{1}{\sqrt{(2n)!}} \left| \phi_1(1) \bar{\phi}_1(2) \phi_2(2) \bar{\phi}_2(3) \dots \phi_n(2n-1) \bar{\phi}_n(2n) \right| \quad (2-43)$$

The set of $2n$ occupied orbitals, $\{\phi_i, \bar{\phi}_i\}$, is constructed from a complete set of n space orbitals, $\{\phi_i\}$

The differing spin functions are just indicated by a "bar",

$$\phi_i(1) = \phi_i(1) \alpha(1) \quad \bar{\phi}_i(1) = \phi_i(1) \beta(1) \quad (2-44)$$

The set is mutually orthogonal and normalized,

$$\int \phi_i(1) \phi_j(1) d\tau_1 = \delta_{ij} \quad (2-45)$$

$$\langle \phi_i | \bar{\phi}_i \rangle = \langle \phi_i | \phi_i \rangle \langle \alpha | \beta \rangle = 0 \quad (2-46)$$

The use of these n spin-paired orbitals ensures that the final total wave function is a pure spin state, that is an eigenfunction of both S_z and S^2 .

The expectation energy of our system with Hamiltonian, H , can be written,

$$E_0 = \frac{1}{(2n)!} \int |\phi_1(1) \bar{\phi}_1(2) \dots \bar{\phi}_n(2n)| H |\phi_1(1) \bar{\phi}_1(2) \dots \bar{\phi}_n(2n)| \dots d\tau. \quad (2-47)$$

From the Variational Principle, the best set, $\{\phi_i, \bar{\phi}_j\}$, for approximating the closed-shell state will be that which gives no first order change in total energy, E_0 , when the orbitals, $\{\phi_i, \bar{\phi}_j\}$ are subjected to a small variation whilst still preserving their orthogonality.

From equation (2-47), and taking the Hamiltonian in its core plus electrons form as in equation (2-17), we find,*

$$E_0 = \langle \phi_1(1) \bar{\phi}_1(2) \dots \bar{\phi}_n(2n) | \sum_i^{2n} H^c(i) | \phi_1(1) \bar{\phi}_1(2) \dots \bar{\phi}_n(2n) \rangle + \langle \phi_1(1) \bar{\phi}_1(2) \dots \bar{\phi}_n(2n) | \sum_{i,j > i} \frac{1}{r_{ij}} | \phi_1(1) \bar{\phi}_1(2) \dots \bar{\phi}_n(2n) \rangle \quad (2-48)$$

and,
$$E_0 = \sum_{i=1}^n 2 \epsilon_i^c + \sum_i^n \sum_j^n (2 J_{ij} - K_{ij}) \quad (2-49)$$

with,
$$\epsilon_i^c = \langle \phi_i(1) | H^c(1) | \phi_i(1) \rangle \quad (2-50)$$

*Using the convenient modified Dirac notation, and remembering that the wave functions are still determinants. Integration is implied.

Thus these ϵ_i^e are the mono-electronic energies in the field of the nuclei ; the J_{ij} and K_{ij} are Coulomb and Exchange integrals respectively,

$$J_{ij} = \iint \phi_i^{(1)} \phi_i^{*(1)} \frac{1}{r_{12}} \phi_j^{(2)} \phi_j^{*(2)} d\tau_1 d\tau_2 \quad (2-51)$$

$$K_{ij} = \iint \phi_i^{(1)} \phi_j^{(1)} \frac{1}{r_{12}} \phi_i^{*(2)} \phi_j^{*(2)} d\tau_1 d\tau_2 \quad (2-52)$$

It will be seen use has been made of the space function equivalence of each electron pair in an orbital to reduce the sums limits to n instead of $2n$. This result for the total energy, E_0 , given in equation (2-49), is quite easy to find using special methods developed for determinant algebra, (100), (70), (101).

The first order variation in an orbital, ϕ_j , can be written, (67),

$$\phi_j \rightarrow \phi_j + \sum_{K, K \neq j}^N c_{jK} \phi_K \quad (2-53)$$

For ϕ_j and ϕ_i to be orthonormal to the first order we find,*

$$c_{ij} = -c_{ji} \quad (2-54)$$

This holds for $1 \leq i, j \leq n$; that is only for occupied orbitals.

In the expansion (2-53), K ranges over the complete set, not just $1 \leq K \leq n$, and now the set includes $\{\phi_{k+1} \dots \phi_N\}$. For a complete set $N \rightarrow \infty$ may occur, (66), (103).

* The wave functions are assumed real from here onwards.

$$\phi_j = \phi_j^* \quad (2-55)$$

Now we investigate the effect of a first order variation in the occupied orbitals on the total energy, examining the change in each term in the total energy expression in turn. We retain only first order terms in all series, then,

$$\varepsilon_i^c \rightarrow \varepsilon_i^c + 2 \sum_{k, \neq i}^N c_{ik} \varepsilon_{ik}^c + \dots \quad (2-56)$$

where,

$$\varepsilon_{ik}^c = \int \phi_i(\omega) H(\omega) \phi_k(\omega) d\tau_1 \quad (2-57)$$

The Coulomb and Exchange terms become,

$$J_{ij} \rightarrow J_{ij} + 2 \sum_{k, \neq i}^N c_{ik} \xi_{jj}^{ik} + 2 \sum_{e, \neq j}^N c_{je} \xi_{je}^{ii} + \dots \quad (2-58)$$

$$K_{ij} \rightarrow K_{ij} + 2 \sum_{k, \neq i}^N c_{ik} \xi_{kj}^{ij} + 2 \sum_{e, \neq j}^N c_{je} \xi_{ie}^{ij} + \dots \quad (2-59)$$

with;

$$\xi_{ke}^{ij} = \iint \phi_i(\omega) \phi_j(\omega) \frac{1}{r_{12}} \phi_k(\omega_2) \phi_e(\omega_2) d\tau_1 d\tau_2 \quad (2-60)$$

Hence for a first order variation in orbitals the energy becomes,

$$\begin{aligned} E \rightarrow E + 4 \sum_{i, k, \neq i} c_{ik} \varepsilon_{ik}^c + 2 \sum_{i, j}^n \left[\sum_{k, \neq i}^N c_{ik} (2 \xi_{jj}^{ik} - \xi_{kj}^{ij}) \right. \\ \left. + \sum_{e, \neq j}^N c_{je} (2 \xi_{je}^{ii} - \xi_{ie}^{ij}) \right] \\ = E + 4 \sum_{i, k, \neq i}^n c_{ik} \left[\varepsilon_{ik}^c + \sum_{j=1}^n (2 \xi_{jj}^{ik} - \xi_{kj}^{ij}) \right] \end{aligned} \quad (2-61)$$

where $1 \leq i, j \leq n$, are the indices of occupied orbitals,

$1 \leq k \leq N$, this index covers the entire basis set.

Thus applying the Variation Principle and requiring the first order change in energy to be zero we find,

$$\sum_{\substack{i, N \\ i, k \neq i}}^{n, N} C_{iK} \left[\epsilon_{iK}^c + \sum_{j=1}^n (2 \xi_{jj}^{iK} - \xi_{Kj}^{ij}) \right] = 0 \quad (2-62)$$

In this double sum occur terms of the type,

$$\begin{aligned} \dots C_{iK} \left[\epsilon_{iK}^c + \sum_j (2 \xi_{jj}^{iK} - \xi_{Kj}^{ij}) \right] \dots \\ \dots + C_{Ki} \left[\epsilon_{Ki}^c + \sum_j (2 \xi_{jj}^{Ki} - \xi_{ij}^{Kj}) \right] \dots \end{aligned}$$

which, since $C_{iK} = -C_{Ki}$ for $1 \leq K, i \leq n$, from the orthonormality requirements (2-54), and from the definitions of the functions, (2-60), we can see,

$$\epsilon_{iK}^c + \sum_j (2 \xi_{jj}^{iK} - \xi_{Kj}^{ij}) = \epsilon_{Ki}^c + \sum_j (2 \xi_{jj}^{Ki} - \xi_{ij}^{Kj})$$

Thus all these terms give no contribution to the sums in equation (2-62). (2-63)

Hence for self-consistency in our orbitals we require,

$$\sum_{i=1}^n \sum_{K=n+1}^N C_{iK} \left[\epsilon_{iK}^c + \sum_{j=1}^n (2 \xi_{jj}^{iK} - \xi_{Kj}^{ij}) \right] = 0 \quad (2-64)$$

so, as in general we cannot expect $C_{iK} = 0$ for $1 \leq i \leq n$ and $n+1 \leq K \leq N$ then we must assume,

$$\epsilon_{iK}^c + \sum_{j=1}^n (2 \xi_{jj}^{iK} - \xi_{Kj}^{ij}) = 0 \quad (2-65)$$

This expression may be rewritten in terms of some special operators, \bar{J}_j and K_j , and we have, so long as $1 \leq i, j \leq n$, and $n+1 \leq K \leq N$,

$$\int \phi_k \left\{ H^c + \sum_{j=1}^n (2J_j - K_j) \right\} \phi_i d\tau = 0 \quad (2-66)$$

The Coulomb and Exchange operators are defined by,

$$J_j^{(1)} \phi_i(z) = \int \phi_j(1) \phi_j(1) \frac{1}{r_{12}} \phi_i(z) d\tau_1 \quad (2-67)$$

and,

$$K_j^{(1)} \phi_i(z) = \int \phi_j(1) \phi_j(z) \frac{1}{r_{12}} \phi_i(1) d\tau_1 \quad (2-68)$$

Now we can derive the effective Hamiltonian for use in SCF treatments by applying the operator, $H^c + \sum_j (2J_j - K_j)$, to an orbital ϕ_i . The result can be expressed in terms of the complete set, $\{\phi_k\}$,

$$\left[H^c + \sum_{j=1}^n (2J_j - K_j) \right] \phi_i = \sum_{k=1}^N \epsilon_{ik} \phi_k \quad (2-69)$$

Multiplying each side by ϕ_k and integrating,

$$\int \phi_k \left[H^c + \sum_{j=1}^n (2J_j - K_j) \right] \phi_i d\tau = \epsilon_{ik} \quad (2-70)$$

Thus, in conjunction with equation (2-66) we find, $\epsilon_{ik} = 0$,

for $n+1 \leq k \leq N$ and $1 \leq i \leq n$. Hence our expansion over a

complete set, $\{\phi_1, \dots, \phi_n, \dots, \phi_N\}$, reduces just to that involving

the occupied orbitals, $\{\phi_1, \dots, \phi_n\}$, and,

$$\left[H^c + \sum_{j=1}^n (2J_j - K_j) \right] \phi_i = \sum_{k=1}^n \epsilon_{ik} \phi_k \quad (2-71)$$

This is often written,

$$F \phi_i = \sum_{k=1}^n \epsilon_{ik} \phi_k \quad (2-72)$$

Where F is the Hartree-Fock Hamiltonian, $F = H^c + \sum_j (2J_j - K_j)$.

The set of coefficients, $\{\epsilon_{ik}\}$, can be shown to be a matrix of Lagrangian Multipliers by using a more rigorous approach to the Hartree-Fock Hamiltonian where variational calculus results in the introduction of these multipliers, (103).

These coefficients serve to ensure the orthogonality of the orbitals, $\{\phi_i\}$, despite first order variations.

Clearly it would be very advantageous to have a diagonal matrix, so that we would have a set of effective eigenvalue problems for the self-consistent orbitals, $\{\phi_i\}$,

$$F\phi_i = \epsilon_i \phi_i \quad (2-73)$$

This is possible, for the basis set used, $\{\phi\}$, can be transformed into another set, $\{\phi'\}$, using any suitable unitary transform, for example,

$$\phi'_i = \sum_j u_{ji} \phi_j \quad (2-74)$$

Or for the whole set, using matrix notation;

$$\Phi' = \Phi U \quad (2-75)$$

Both the total many electron wave function, equation (2-43), and the Hartree-Fock operator are invariant with this change in basis set, $\{\phi\}$, to, $\{\phi'\}$. With appropriate choice of the transformation, U , the off-diagonal elements in \mathcal{E} vanish and the effective Hamiltonian, F , gives a simple eigenvalue problem, equation (2-73), which ensures the self-consistent orbitals form an orthogonal set.

The invariance of the Fock operator and the total wave function can be seen by considering the effect of the unitary transform, $\{\phi\}$ to $\{\phi'\}$, on these quantities.

In the operator F the core term H^c is unaffected by choice of basis set, the inter-electron term, $\sum_j (2J_j - K_j)$, is also independent. This may be shown by expanding $\sum_j J_j$, now expressed in terms of the new basis, $\{\phi'\}$, in terms of the original set, $\{\phi\}$, then,

$$\begin{aligned} \sum_j J_j \{\phi'\} &= \sum_j \int \phi'_j(1) \phi'_j(1) \frac{1}{r_{12}} d\tau_1 \\ &= \sum_{j,k,l} u_{jk} u_{jl} \int \phi_k(1) \phi_l(1) \frac{1}{r_{12}} d\tau_1 \end{aligned}$$

But since $\sum_j u_{jk} u_{jl} = [u^+ u]_{k,l}$, and using the property of unitary transforms, that $u^+ u = [1]$ we find, (2-76)

$$\sum_j J_j \{\phi'\} = \sum_k \int \phi_k(1) \phi_k(1) \frac{1}{r_{12}} d\tau_1 = \sum_k J_k \{\phi\} \quad (2-77)$$

Similar arguments apply to $\sum_j K_j \{\phi'\}$.

The total antisymmetrized wave function, Ψ_0 , may also be shown to be unchanged in the transformation using another property of unitary matrices,

$$\Psi_0 \{\phi'\} = \frac{1}{\sqrt{(2n)!}} \left| \phi'_1(1) \overline{\phi'_1(2)} \dots \overline{\phi'_n(2n)} \right| = \frac{1}{\sqrt{(2n)!}} |u| \cdot \left| \phi_1(1) \overline{\phi_1(2)} \dots \overline{\phi_n(2n)} \right| \quad (2-78)$$

Now as $|u| = |1|$, then, $\Psi_0 \{\phi'\} = \Psi_0 \{\phi\}$ and our total wave function is unaltered.

Thus having shown neither the F operator or the total state function, ψ_0 , to be changed by the transformation, $\{\phi\}$ to $\{\phi'\}$, then we just have to chose U so as to diagonalize the matrix \mathcal{E} , that is ,

$$U^T \mathcal{E} U = \mathcal{E}' \quad (2-79)$$

where \mathcal{E}' is the new diagonalized matrix of Lagrangian Multipliers.

This choice of orbitals which diagonalize the Lagrangian matrix is clearly just a matter of mathematical convenience, to give an eigenvalue problem easily solved using conventional methods. The idea of a "molecular orbital" is thus not invariant and such orbitals can be subjected to any suitable unitary transformations. Delocalized MO's can be transformed so as to produce the loges of localized bonds, (73), thus we are able to understand the essential similarity of the VB and MO approach.

One fundamental property of the molecular orbitals of any molecule is that they should automatically reflect the symmetry of the molecule under consideration,(75). The Hartree-Fock functions obtained by solving (2-72) have been shown to be symmetry adapted to their nuclear framework. Thus the SCF MO's form a basis for the irreducible representations of the molecule, and do correspond to a specific total energy minimum,(134). This energy may not however be the absolute minimum, a lower energy may be obtained from a wave function

which is not necessarily symmetry adapted. This question of the overall symmetry of the total wave function of a molecule will be met again in discussions on the application of Spin-Polarized SCF to calculate ground state properties. In these cases lower energy ground state wave functions are obtained than for the corresponding spin-paired wave functions by the removal of the symmetry restriction of electron pairing. This problem is however resolved by the use of a spin projection operator, which in effect re-introduces spin-paired orbitals.

(9) The Roothaan Equations.

In the development of the Hartree-Fock equations we considered a complete basis set of orbitals, $\{\phi_1, \dots, \phi_n, \dots, \phi_N\}$. If only a limited number of basis functions are used, $\{\phi_1, \dots, \phi_m\}$, which are themselves constructed from a restricted set, $\{\chi\}$, then the Roothaan equations result, (103).

With n doubly occupied orbitals, and a basis set of m components, $m \geq n$, the first order variation of an orbital now becomes,

$$\phi_i \rightarrow \phi_i + \sum_{k_j \neq i}^m c_{ik} \phi_k \quad (2-80)$$

and the self-consistent conditions become,

$$\int \phi_k \left[H^c + \sum_{j=1}^n (2J_j - K_j) \right] \phi_i d\tau = 0 \quad (2-81)$$

with $1 \leq i, j \leq n$ and $n+1 \leq k \leq m$.

The molecular orbitals, ϕ_k and ϕ_i , and ϕ_j , are expanded by the Ritz technique, (76), using a basis set, $\{\chi\}$, of m components,

$$\begin{aligned} \phi_k &= \sum_{p=1}^m c_{kp} \chi_p & \phi_i &= \sum_{q=1}^m c_{iq} \chi_q \\ \phi_j &= \sum_{r=1}^m c_{jr} \chi_r = \sum_{s=1}^m c_{js} \chi_s \end{aligned} \quad (2-82)$$

In the well known LCAO-MO method, the set $\{\chi\}$ consists of atomic orbitals localized at the various atomic centres of the molecule. The π -electron approximation limits the set further, it only contains the $2p_z$ orbitals of the constituent atoms. Substituting equations (2-82) into our Hartree-Fock operator, for the matrix element, F_{ki} , we obtain,

$$\begin{aligned} \langle \phi_k | F | \phi_i \rangle &= \sum_{p,q}^m c_{kp} c_{iq} \{ \langle \chi_p | H^c | \chi_q \rangle \\ &+ \sum_{j=1}^n \sum_{r,s}^m c_{jr} c_{js} [2 \langle p q | r s \rangle - \langle p r | s q \rangle] \end{aligned} \quad (2-83)$$

Thus we have for the element F_{pq} of our Hartree-Fock matrix using a limited basis set,

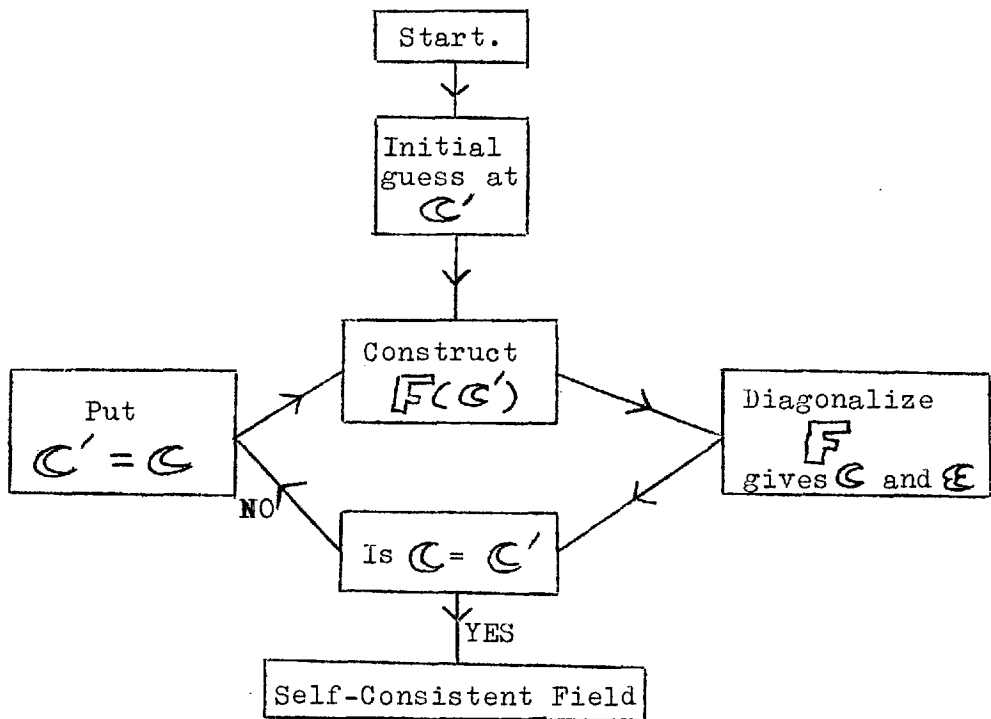
$$F_{pq} = \langle \chi_p | H^c | \chi_q \rangle + \sum_{j=1}^n \sum_{r,s}^m c_{jr} c_{js} \{ 2 \langle p q | r s \rangle + \langle p r | s q \rangle \} \quad (2-84)$$

The core integrals, $\langle \chi_p | H^c | \chi_q \rangle$, are often written as β_{pq}^c , with the diagonal element $\alpha_p^c = \langle \chi_p | H^c | \chi_p \rangle$.

To solve this self-consistent problem we have to diagonalize F , which is constructed using some initial guess at the eigenvectors, C_j ,

$$F(C_j) \cdot C_i = \epsilon_i C_i \quad (2-85)$$

Then we use the resulting eigenvectors C_i to repeat the process, and this is carried through until the required degree of consistency is achieved. This may be illustrated in a diagrammatic form;



This all assumes we can construct the F matrix, but this unfortunately is difficult to do exactly and approximations are often used in the evaluation of $\langle \chi_p | H^c | \chi_q \rangle$ and integrals such as $\langle p q | r s \rangle$. We shall now discuss these approximations.

(IO) The Goeppert-Mayer and Sklar Core Potential.

This approximation to the core Hamiltonian, H^c , was first used in a famous paper treating Benzene, (IO4). The potential was originally introduced for use in the treatment of Hydrocarbons, but we shall consider it's generalized extension into hetero-atomic π -systems. To find the potential we require the following,

(i). Hydrogen nuclei and surrounding electrons are regarded as giving no potential contribution to the core. These nuclei are regarded as completely screened by the electronic distributions.

(ii). The potential contribution from an individual nucleus and surrounding electrons is approximated as the potential due to the atom in its valence state, less the charge distribution of Z_K π -electrons delocalized in the MO.

Z_K is the effective nuclear charge when the $2p_z$ electrons contributing to a MO are removed.

(iii). Exchange terms are neglected.

This potential has the form,

$$H^c(i) = \frac{1}{2} \nabla^2(i) + \sum_K u_K^+(i) \quad (2-86)$$

the summation of K extends over all the atomic cores, with $u_K^+(i)$ the potential of the K -th ionized core.

Writing u_K for the potential due to a neutral valence state atom,

$$u_K(i) = u_K^+(i) + Z_K \int \frac{\pi_K^2(2)}{r_{12}} d\mathcal{V}_2 \quad (2-87)$$

Hence,

$$H^c(1) = -\frac{1}{2} \nabla^2(1) + \sum_K (u_K(1) - \frac{z_K}{r_{12}} \langle KK | \frac{1}{r_{12}} \rangle) \quad (2-88)$$

The diagonal term, $\alpha_p^c = \langle p | H^c(1) | p \rangle$, becomes,

$$\alpha_p^c = \langle \phi_p | -\frac{\nabla^2(1)}{2} + \sum_K (u_K(1) - \frac{z_K}{r_{12}} \langle KK \rangle) | \phi_p \rangle \quad (2-89)$$

and, with rearrangement,

$$\alpha_p^c = \langle \phi_p | -\frac{\nabla^2(1)}{2} + u_p^+(1) | \phi_p \rangle + \sum_{K, \neq p} \langle p | u_K^+ | p \rangle \quad (2-90)$$

From the definition of u_K^+ , we would expect the approximate ionization energy, I_K^π , of the valence state π -electron to be given by,

$$\left(-\frac{1}{2} \nabla^2(1) + u_K^+(1)\right) \phi_K(1) = -I_K^\pi \phi_K(1) \quad (2-91)$$

Hence for the core term we find,

$$\alpha_p^c = -I_p^\pi + \sum_{K, \neq p} (\langle p | u_K(1) | p \rangle - z_K \langle KK | PP \rangle) \quad (2-92)$$

The first terms in the sum over K are usually termed the penetration integrals,

$$\langle p | u_K(1) | p \rangle = \iiint u_K(1) \frac{1}{r_{12}} \phi_p(2) \phi_p(2) d\tau_1 d\tau_2 \quad (2-93)$$

giving the mutual potential energy between a neutral atom in its valence state, and the charge distribution represented by $\langle p | p \rangle$.

A full discussion of the values to use for the ionization potential, the Coulomb and penetration integrals will be given later. Also it will be noted $\beta_{pq}^c = \langle \chi_p | H^c | \chi_q \rangle$ has not

been discussed, this is because it will be used as a semi-empirical parameter.

(II) The Pople-Pariser-Parr Approximation to F .

This semi-empirical form of SCF theory was developed by Pople, (I05), from the Roothaan equations, using assumptions similar to Pariser and Parr, (I06), in their treatment of Ethylene and Benzene. . It was introduced after the results obtained by non-empirical solution of the SCF equations proved rather disappointing.

The Goeppert-Mayer and Sklar Potential is substituted into the diagonal element of the Hartree-Fock matrix, F ,

$$F_{pp} = -I_p^\pi + \sum_{k, \neq p} \{ \langle p | u_k^{(1)} | p \rangle - z_k \langle k k | p p \rangle \} + \sum_j^n \sum_{r, s} c_{jr} c_{js} (2 \langle p p | r s \rangle - \langle p r | s p \rangle) \quad (2-94)$$

If we neglect differential overlap everywhere,

$$\chi_i \chi_j^* = \chi_i \chi_i^* \delta_{ij} \quad (2-95)$$

we obtain,

$$F_{pp} = -I_p^\pi + \sum_j^n \sum_{r, \neq p}^m \langle p p | r r \rangle \{ 2 c_{jr} c_{jr} - z_r \} + \sum_j^n c_{jp} c_{jp} \langle p p | p p \rangle + \sum_{k, \neq p}^n \langle p | u_k | p \rangle \quad (2-96)$$

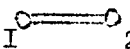
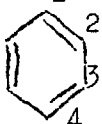
The diagonal element is,

$$F_{pq} = \beta_{pq}^c - \sum_j^n c_{jp} c_{jq} \langle q q | p p \rangle \quad (2-97)$$

The neglect of overlap will be fully discussed in the next section.

The difficulty of evaluating $\langle p|u_k|p \rangle$, the penetration terms, is avoided by neglecting them completely. This is justified by the fact that they are generally small, or probably since the term is constant, can be added to the effective value of the ionization energy used. Some numerical examples of penetration integrals taken from Ohno, (69), are given in table 7.

Table 7.

| Molecule | p | k | Penetration integrals: $\langle p u_k p \rangle$ |
|--|---|---|--|
| Ethylene  | I | 2 | -0.989 ev. |
| Benzene  | I | 2 | -0.856 ev. |
| | I | 3 | -0.013 ev. |
| | I | 4 | -0.003 ev. |

If we use the substitution for the two centre Coulomb integrals,

$$\langle i|i|j \rangle = \delta_{ij} \quad (2-98)$$

and define a charge and bond-order matrix,

$$P_{ij} = 2 \sum_{k=1}^n c_{ki} c_{kj} \quad (2-99)$$

Then, neglecting penetration integrals, we obtain the matrix elements,

$$F_{pp} = -I_p^\pi + \sum_{r \neq p}^m (P_{rr} - Z_r) \delta_{pr} + \frac{1}{2} P_{pp} \delta_{pp} \quad (2-I00)$$

$$F_{pq} = \beta_{pq}^c - \frac{1}{2} P_{pq} \delta_{pq} \quad (2-I01)$$

In matrix notation this can be written as ,

$$\mathbf{F} = \mathbf{H} + \mathbf{Z} \mathbf{J} - \mathbf{K} \quad (2-I02)$$

with the matrix elements given by , (I07),

$$\begin{aligned} H_{pp} &= -I_p^\pi - \sum_{r \neq p}^m Z_r \delta_{pr} \\ H_{pq} &= \beta_{pq}^c \\ J_{pq} &= \delta_{pq} \frac{1}{2} \sum_r P_{rr} \delta_{rp} \\ K_{pq} &= -\frac{1}{2} P_{pq} \delta_{pq} \end{aligned} \quad (2-I03)$$

(I2) The Zero Differential Overlap Approximation.

The Pariser and Parr approximation of assuming zero differential overlap, equation (2-95), is of primary importance in reducing the difficulties in the evaluation of the \mathbf{F} matrix elements. In this approximation all four centre two electron integrals, $\langle pq | rs \rangle$, so long as $p \neq q$, $r \neq s$, and thus only the relatively simple two centre Coulomb integrals are left.

The fact that such a sweeping approximation does not jeopardize the success of the Pople-Pariser-Parr method in molecular predictions indicates this neglect of overlap has

a real physical basis. This may be shown by expanding our molecular orbitals in a basis of Löwdin orthogonalized atomic orbitals, (I08). Each Löwdin orbital is a linear combination of atomic π -orbitals containing one main term from the atom in question, and a small amount from the others to ensure orthogonality.

To find these Löwdin orbitals we must reconsider our expansion of solutions of the wave equation in terms of an orthogonal set, as used in equation (2-8). If instead we use a more general non-orthogonal set, such as could be constructed from the atomic orbitals in any molecule, then from the n components of this basis set, $\{\chi_i\}$, we can build a non-diagonal overlap matrix, S , with elements,

$$S_{ij} = \int \chi_i^{(1)} \chi_j^{*(1)} d\tau, \quad (2-I04)$$

Now to obtain a diagonal overlap matrix we require a n component set, $\{\eta_i\}$, such that,

$$\int \eta_i^{(1)} \eta_j^{*(1)} d\tau = \delta_{ij} \quad (2-I05)$$

If we construct this orthogonal set from our non-orthogonal one,

$$\eta_i = \sum_{k=1}^n u_{ki} \chi_k \quad (2-I06)$$

then the orthogonality condition, equation (2-I05), gives,

$$\begin{aligned} \sum_{k,L} u_{ki} u_{Lj}^* \int \chi_k^{(1)} \chi_L^{*(1)} d\tau \\ = \sum_{k,L} u_{ki} u_{Lj}^* S_{KL} = \delta_{ij} \end{aligned} \quad (2-I07)$$

In the equivalent matrix notation this becomes,

$$U^T S U = [1] \quad (2-I08)$$

where $[1]$ is the unit matrix, $[1]_{ij} = \delta_{ij}$.

Hence we can construct our orthogonalized atomic orbital set using any suitable transformation matrix U in equation(2-I08).

To simplify matters it is reasonable to chose U such that $U^T = U$, and hence we find,

$$U = S^{-\frac{1}{2}} \quad (2-I09)$$

So we can represent our transform from the basis, $\{\chi_i\}$, to, $\{\eta_i\}$,

by,

$$\eta = \chi S^{-\frac{1}{2}} \quad (2-II0)$$

where η and χ are row matrices, corresponding to the the respective orbital sets $\{\eta_i\}$ and $\{\chi_i\}$.

The wave equation stated in matrix form for the evaluation of eigenvectors, C , in terms of a non-orthogonal basis set is,

$$H C = S C E \quad (2-III)$$

Where H is the matrix representative of the Hamiltonian, and E a diagonal matrix of eigenvalues. The corresponding molecular orbitals are given by,

$$\phi = \chi C \quad (2-II2)$$

Now on the transformation to the new basis $\{\eta_i\}$, we find,

$$\phi = \chi S^{-\frac{1}{2}} C \quad (2-II3)$$

On replacing C in equation (2-III) by $S^{-\frac{1}{2}} C$ we obtain the simple eigenvalue equation, (compare with equation (2-8)),

$$H' C = C E \quad (2-II4)$$

where H' is the new matrix representative of the Hamiltonian,

$$H' = S^{-\frac{1}{2}} H S^{-\frac{1}{2}} \quad (2-II5)$$

This new form of H must be remembered in the calculation of resonance integrals, β_{pq}^c , for the Hückel and SCF schemes. The wave functions in the matrix element are not pure atomic orbitals, but their orthogonalized derivatives.

The evaluation of $S^{-\frac{1}{2}}$ can be achieved by a matrix expansion technique, (I08), or alternatively by subjecting $S^{-\frac{1}{2}}$ to a diagonalizing unitary transform, finding the inverse root of the transform, and then reverting to the original basis. If we use the former method, and neglect terms higher than first order in the overlap matrix, then,

$$S^{-\frac{1}{2}} \approx [1] - \frac{1}{2} S \quad (2-II6)$$

and hence,

$$\eta_i \approx \chi_i - \frac{1}{2} \sum_{j, j \neq i} S_{ij} \quad (2-II7)$$

These orthogonalized atomic orbitals contain in general a negative "cusp" on each neighbouring nucleus. The cusps however occupy only a small volume of space, and the overall effect of the transformation to Löwdin orbitals from atomic orbitals, apart from the orthogonalization, is to compress each atomic orbital more tightly about its nucleus.

Thus there is no implied restriction in expanding the molecular orbitals as linear combinations of orthogonal functions instead of real atomic orbitals, as they form equivalent sets. However, we must always transform H into the new basis. Using these Löwdin orbitals Paradejordi,(I09), has compared the results of evaluating the many centre integrals for the normal $2p_z$ $\langle a,b | c,d \rangle$ and Löwdin orbitals, $\langle \underline{a}, \underline{b} | \underline{c}, \underline{d} \rangle$ for trans-Butadiene. The comparison is shown in Table 8.

Table 8.

| Löwdin Orbitals | ev. | Atomic Orbitals | ev. |
|---|-------|-------------------------------|-------|
| $\langle \underline{a}, \underline{a} \underline{a}, \underline{a} \rangle$ | 17.28 | $\langle a, a a, a \rangle$ | 16.92 |
| $\langle \underline{b}, \underline{b} \underline{b}, \underline{b} \rangle$ | 17.57 | $\langle b, b b, b \rangle$ | 16.92 |
| $\langle \underline{a}, \underline{a} \underline{b}, \underline{b} \rangle$ | 9.01 | $\langle a, a b, b \rangle$ | 9.23 |
| $\langle \underline{b}, \underline{b} \underline{c}, \underline{c} \rangle$ | 8.63 | $\langle b, b c, c \rangle$ | 8.69 |
| $\langle \underline{a}, \underline{a} \underline{a}, \underline{b} \rangle$ | -.06 | $\langle a, a a, b \rangle$ | 3.60 |
| $\langle \underline{b}, \underline{b} \underline{a}, \underline{b} \rangle$ | -.08 | $\langle b, b a, b \rangle$ | 3.60 |
| $\langle \underline{a}, \underline{b} \underline{b}, \underline{c} \rangle$ | .01 | $\langle a, b b, c \rangle$ | .63 |
| $\langle \underline{a}, \underline{b} \underline{c}, \underline{d} \rangle$ | -.01 | $\langle a, b c, d \rangle$ | .46 |

It is seen that while the two centre integrals change little, the three and four centre integrals are markedly effected. A similar comparison has been made between the two orbital sets for Benzene by McWeeny,(I10). Leroy,(I11), has shown that the usual Pariser-Parr treatment and that using Löwdin orthogonalized atomic orbitals give similar results for Alternant Hydrocarbons. However it was found less satisfactory with hetero-atomic systems such as Pyridine and Pyrrole. These orbitals have also been used by McWeeny in

non-empirical calculations on conjugated systems, (II0).

Finally, if it is accepted we are not using "ordinary" atomic orbitals in the SCF treatment it must always be remembered that this is so when any attempt is made in interpreting basis coefficients. Strictly a new change in basis functions by an appropriate transform is necessary before any conclusions based on the normal atomic orbital basis set are made. In the semi-empirical SCF treatment we do not need to specify the exact form of our basis set. However in non-empirical calculations where the zero differential overlap approximation is not valid, (II9), we must make a choice of basis. Slater atomic orbitals are often used, but atomic Hartree-Fock SCF orbitals have been used also, (II2). Attempts have been made in the non-empirical treatment to determine the best distorted atomic orbitals using simple model systems, (II3), (II4). However all these problems are circumvented, if not forgotten, in the relatively simple semi-empirical method.

(I3) The Parameters.

(a) Introduction.

In the semi-empirical Pople-Pariser-Parr approximation it will be seen, on neglection of differential overlap, there are three parameters needed to construct the F matrix. They are the valence state ionization energy, I_P^π , introduced by the use of the Goeppert-Mayer and Sklar potential, the core resonance integrals, β_{pq}^c , and the two electron integrals over our basis set, γ_{pq} .

The introduction of these parameters as semi-empirical quantities usually enables us to obtain wave functions giving reasonable agreement with experimental observations. The use of the three parameters as semi-empirical rather than calculated ones is necessitated by the poor agreement obtained between experimental values of the integrals, $\langle pp|rr\rangle$, estimated spectroscopically, and their theoretical values found using Slater atomic orbitals. The methods used to obtain values for these parameters are now discussed briefly, for a more rigorous treatment see references (I20) and (I25).

(b) The Valence State Ionization Energy, I_c^π .

This was introduced as a result of the method used to obtain the core potential, H_c^c . If we take Carbon as an example, I_c^π represents the energy difference between the two valence states $C^+(V_3)$ and $C(V_4)$, (69),

$$I_c^\pi = E[C^+(V_3)] - E[C(V_4)] \quad (2-II8)$$

The value of I_c^π can be estimated if the ionization potential,

I_c of the Carbon atom in its ground state is known,

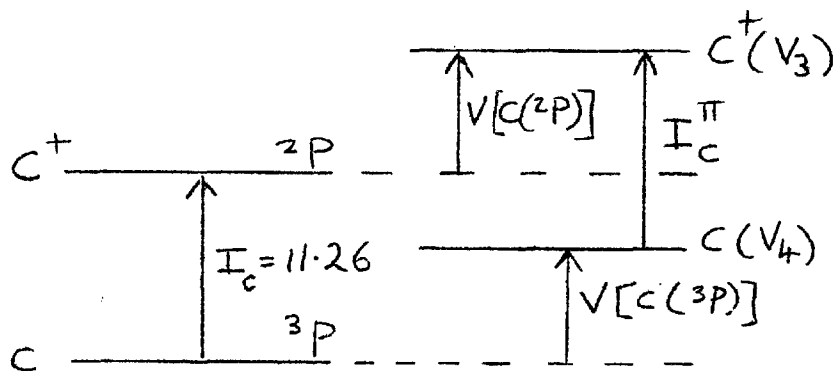
$$I_c = E[C^+(2P)] - E[C(3P)] \quad (2-II9)$$

together with the valence state promotion energies, V ,

$$V[C^+] = E[C^+(V_3)] - E[C^+(2P)]$$

$$V[C] = E[C(V_4)] - E[C(3P)]$$

This can be shown diagrammatically,



The experimental value $I_c = 11.26$ ev. for the ionization of gaseous Carbon is given.

The valence state energy $E[V_3]$ and $E[V_4]$ can be expressed in terms of observed spectroscopic values, and as Moffitt showed, (II5), using experimental results, (II6),

$$V[C^+(V_3)] = 8.42 \quad V[C(V_4)] = 8.26$$

Hence, $I_c^\pi = I_c + V[C^+(V_3)] - V[C(V_4)] = 11.42$ ev.

This result is just for Carbon, but using data tabulated by Pritchard and Skinner, (II7), or Hinze and Jaffe, (II8), other values for hetero-atoms can be found.

(c) The Core Resonance Integrals, β_{pq}^c .

These integrals, $\beta_{pq}^c = \langle \chi_p | H^c | \chi_q \rangle$, are treated in the Pople-Pariser-Parr method as empirical parameters, and varied to give the best possible "fit" for a given set of

I_p^π and $\langle pp|qq \rangle$ additional parameters. For two non-bonding atoms p, q , we require, $\beta_{pq}^c = 0.$

The best set of values of β_{pq}^c to fit an experimental property is, of course, dependent on the methods used to evaluate I_p^π and $\langle pp|qq \rangle$ so quite a range of β_{pq}^c is to be expected. For Benzene Pople and Pariser, (I06) found the optimum value was -2.39 ev., and it is to be anticipated that most treatments using the Pople-Pariser-Parr method will use values of β_{c-c}^c near this. The variation of β_{pq}^c with interatomic distance for a given atomic pair is often given as ,

$$\frac{\beta_{pq}^c(r_1)}{\beta_{pq}^c(r_2)} = \frac{S_{pq}(r_1)}{S_{pq}(r_2)} \quad (2-I2I)$$

This equation however re-introduces the problem of the basis set, the question is, do we calculate the overlap S_{pq} using Slater atomic orbitals or SCF atomic orbitals. Hence the β_{pq}^c have still to be fixed empirically .

The β_{pq}^c mentioned have only been considered as being between two Carbon atoms, for hetero-atomic links other suitable values have to be arrived at, (I66), (I67).

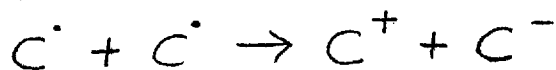
These are often quoted in units of β_{c-c}^c , and usually these core integrals have a rather insecure theoretical basis, and are best regarded as empirical parameters to be fitted to experiment. In the section on results we shall see how the values of β_{pq}^c fall in a relatively small range, and that SCF calculations

are not very sensitive to their reasonable variation. Hückel wave functions are more sensitive, (I20).

(d) The Two Centre Coulomb Integrals; $\langle pp|rr\rangle$.

First we consider the special case of these, $\langle pp|pp\rangle$, which are only one centre forms.

These were obtained semi-empirically by Pariser and Parr, (I06), who considered the reaction, involving two Carbon radical atoms,



If the cores are assumed unchanged in the reaction the energy change should be $\langle pp|pp\rangle$ for the $2p_z$ atomic orbitals. Thus,

$$\langle pp|pp\rangle = I_P^{\pi} - E_P \quad (2-I22)$$

where I_P^{π} is the valence state ionization energy and E_P the electron affinity of the valence state of atom P .

This method applies for atoms other than Carbon, but it is very interesting to compare the value obtained for $\langle pp|pp\rangle$ in the case of Carbon with the theoretical value, obtained using Slater atomic orbitals. It is found that $\langle pp|pp\rangle$ empirical = 10.84ev., whilst the theoretical value = 16.93ev., (I22).

This discrepancy between theory and spectroscopic values suggests either the Slater orbitals used are inaccurate, or, more likely, that the electron correlation possible in the ion results in much reduced electron repulsions.

If we accept an empirical value for $\langle pp|pp\rangle$, it is necessary also to chose an appropriate method to obtain $\langle pp|qq\rangle$.

These two centre integrals have a classical analogue, the repulsion between two charge distributions appropriate to the $2p_z$ π - orbitals. This simplified model is often used in their approximation. In Ethylene Pariser and Parr used a theoretical value of $\langle pp|qq \rangle = 9.25\text{ev.}$, and this is regarded as much too high.

Various approximations are possible for $\langle pp|qq \rangle$, (69), and it has been found that usually calculations are relatively insensitive to which ever method is used. In the calculations presented later the Mataga and Nishimoto approximation was used, (I24);

$$\langle pp|qq \rangle = \frac{14.40}{R_{pq} + \tau} \quad (2\text{-I23})$$

With R_{pq} in Å units, and

$$\tau = \frac{14.40}{\frac{1}{2} \{ (I_p - E_p) + (I_q - E_q) \}} \quad (2\text{-I24})$$

All the semi-empirical methods, except the simple $1/(R_{pq})$ approximation go smoothly into the value of $\langle pp|pp \rangle$ at $R_{pq} = 0$.

The need for these semi-empirical inter-electronic integrals arises chiefly from the inadequacy of atomic orbitals available. As only such inaccurate wave functions are readily accessible for individual atoms, the use of such functions in molecules must lead to inevitably less accurate results, (I23).

Now we have all the necessary prescriptions for the generation of the \mathbb{F} matrix, and can solve the self-consistent problem. Thus we must consider further the nature

and application of the self-consistent model in the deduction of molecular properties.

(I4) Closed Shell SCF Molecular Properties.

(a) Ground State Properties.

With the use of the Pople-Pariser-Parr method to solve the Roothaan equations the SCF antisymmetrized total wave function of the closed shell ground state, Ψ_0 , is found. The form of Ψ_0 is given in equation (2-43).

Hence the ground state energy of the π -electrons may be obtained, $E_0 = \langle \Psi_0 | H | \Psi_0 \rangle$, using the usual expression for our Hamiltonian as shown in equation (2-49). This latter expression can be written in matrix form as,

$$E_0 = \frac{1}{2} \text{Tr} \{ P [H + F] \} \quad (2-I25)$$

P is the charge and bond-order matrix, (see equation(2-99)),

$$P = 2 C^{\dagger} C \quad (2-I26)$$

F is the Hartree-Fock matrix, equation (2-I00) and (2-I01), the elements of the core integral matrix, H , are given in equations (2-I03).

It is interesting to compare the total energy expression, E_0 , to that of the individual Hartree-Fock orbital energy parameters, ϵ_k . If we return to the effective eigenvalue equation for orbital ϕ_k , equation (2-7I),

$$\left(H^c + \sum_{e=1}^n (2J_e - K_e) \right) \phi_k = \epsilon_k \phi_k \quad (2-I27)$$

J_e and K_e are the Coulomb and Exchange operators which have been previously defined. Then we find,

$$\int \phi_k (H^c + \sum_e [z J_{ke} - K_{ke}]) \phi_k d\tau = \epsilon_k \quad (2-I28)$$

and,
$$\epsilon_k = \epsilon_k^c + \sum_{e=1}^n (z J_{ke} - K_{ke}) \quad (2-I29)$$

Hence;
$$E_0 = \sum_{k=1}^n (\epsilon_k^c + \epsilon_k) \quad (2-I30)$$

This shows clearly the interdependence of all the electrons in the system. Only the total energy of the system as represented by the many electron antisymmetrized wave function has meaning. The nearest it is possible to get to an individual electron energy is the set of parameters, $\{\epsilon_k\}$, representing the energy of the various electrons in the field of the core and the other electrons. To obtain the total energy we sum over all ϵ_k and add ϵ_k^c to allow for the "other" electron in each orbital, in this way no interactions are counted twice. This is the reason for referring to "orbitals" rather than to "levels" in many electron systems treated using SCF methods.

It is also valid here to comment on the nature of the "Virtual Orbitals", that is those orbitals, ϕ_k , where $k > n$. The meaning of these virtual orbitals can be understood by considering equation (2-I29), with $k > n$, then the sum over e includes no terms of the type, $(z J_{kl} - K_{kl})$.

Hence, the function, ϕ_k , corresponds to an electron moving in the field of the core and $2n$ other electrons, but not itself contributing to the potential field. Thus the virtual orbitals are not self-consistent in that they minimise electron repulsions, as they are not included in the Hartree-Fock effective Hamiltonian.

It should be noted in the π -approximation E_0 represents the total energy of the system of $2n$ π -electrons moving in the field of the core of σ -electrons and nuclei. The energy clearly does not represent the total electronic energy of the molecule, and is indirectly sensitive to the σ -core density via the π - σ coupling term, G_{σ} , see equation (2-39).

Having obtained a self-consistent ground state it is of value to know the way in which the electrons are distributed over the molecule, and how strong the π -bonds are between bonded atoms. This information is contained in the charge and bond-order matrix, P , equation (2-I26) and (2-99). The diagonal elements of P ,

$$P_{ii} = 2 \sum_{k=1}^n c_{ki} c_{ki} = q_i \quad (2-I31)$$

give the charges, q_i , localized on the centre, i , as seems conceptually reasonable. Also we note, $\text{Tr}\{P\} = 2n = \sum_i q_i$.

Similarly the π -electron bond-order resulting from electron delocalization between bonded centres i and j is given by,

$$P_{ij} = 2 \sum_K c_{ki} c_{kj} \quad (2-I32)$$

This concept of charges and bond-orders stems largely from the Hückel theory, and has been extensively discussed elsewhere, (I26),(I27),(I10),(I28).

A simple consideration of a two centre orbital in the MO approximation can be used as an illustration of these quantities; with an orbital, $\phi_1 = c_{11}\chi_1 + c_{12}\chi_2$, then,

$$\langle \phi_1 | \phi_1 \rangle = c_{11}^2 + c_{12}^2 + 2c_{11}c_{12}\langle \chi_1 | \chi_2 \rangle \quad (2-I33)$$

The values of $2c_{11}^2$ and $2c_{12}^2$ for the doubly occupied orbital give the charge densities at centres 1 and 2 .

The cross-term $2c_{11}c_{12}$ gives the magnitude of the overlap, $\langle \chi_1 | \chi_2 \rangle$, and hence is a measure of the bond-order. For a pure double bond, such as in Ethylene, $P_{12} = 1$.

In Pople-Pariser-Parr SCF theory the various elements of the \mathbf{P} matrix are open to the same interpretation as the Hückel counterpart, however we must consider how much the basis orbitals used are like any simple undistorted atomic orbital. This problem was discussed in the section on the neglect of differential overlap, and must inevitably raise questions as to the unambiguity of such simple explanations as used in the Hückel approximation. For this reason often the expression "density matrix" is perhaps to be preferred to charge and bond-order matrix. The density matrix* \mathbf{D} is given by, $\mathbf{D} = \frac{\mathbf{P}}{2}$, that is,

$$D_{ij} = \sum_{k=1}^n c_{ki} c_{kj} \quad (2-I34)$$

* See (I28),(I29),(66); many different expressions are termed "density matrices".

If however we assume in the transformation from our non-overlapping set to the real set of atomic orbitals the charges and bond-orders differ little, then the Hückel concept of them can be carried over into the SCF treatment.

As it is now possible to represent the ground state

π -electron charge distribution we can calculate the π -contribution to the permanent dipole-moment of any molecule treated. The expectation value of the dipole-moment of a delocalized wave function of π -electrons can be written as,

$$\mu_e = -e \int \psi_0^* \sum_i \vec{r}_i \psi_0 d\tau \quad (2-135)$$

Since ψ_0 is determinantal in form, we use the rules of determinant algebra, (100), (70), (101), to find,

$$\mu_e = -2e \sum_{i=1}^n \int \phi_i^*(1) \vec{r}_i(1) \phi_i(1) d\tau, \quad (2-136)$$

Where ψ_0 represents the total antisymmetrized ground state wave function, equation(2-43), and \vec{r}_i is the radius vector of the i -th electron. $\{\phi_i\}$ are the SCF molecular orbitals.

If the molecular orbitals are expanded in terms of a M -component orthogonal atomic set, $\{\chi_i\}$, then we find,

$$\mu_e = -2e \sum_i^n \sum_j^m c_{ij} c_{ij}^* \vec{r}_i \quad (2-137)$$

Here we have assumed $\int \chi_j(1) \vec{r}_i(1) \chi_k(1) d\tau = \vec{r}_i \delta_{jk}$ justification of this has been given by Daudel, (67). Recalling our definition of atomic charge q_i , and the P matrix, equation (2-131), we

have,

$$\mu_e = -e \sum_j^m q_j \vec{r}_j \quad (2-138)$$

The total π -dipole moment is thus given by,

$$\vec{\mu}_e = e \sum_{j=1}^m (z_j - q_j) \vec{r}_j \quad (2-I39)$$

with z_j representing the virtual charge of the j -th atom, with its π -bonding electrons removed, and q_j the effective π -density on the j -th atom.

Clearly $\vec{\mu}_e$ is invariant of the choice of origin of the vectors \vec{r}_j , so long as the system is electronically uncharged, for if we write, $\vec{r}_j \rightarrow \vec{r}_j + \Delta\vec{r}$, then,

$$\vec{\mu}_e = e \sum_{j=1}^n (z_j - q_j) \vec{r}_j + e \Delta\vec{r} \sum_{j=1}^n (z_j - q_j) \quad (2-I40)$$

But as $\sum_j (z_j - q_j) = 0$ for a neutral system, the dipole-moment is unchanged. It should be noted such a treatment only calculates the π -contribution to the total moment of the molecule, and the dipoles represented by hetero-atomic σ -bonding are omitted.

It is also possible to calculate many other properties from ground state wave functions, such as magnetic properties, bond-polarizabilities, (I30), (I31), and the reactivity of the various atomic centres to chemical reagents, (I32), (I33). Here, however, our main interest is in the extensively observed and recorded optical properties of conjugated molecules, so these ground state characteristics will not be further discussed and we shall turn to the excited states of our molecular systems.

(b) Excited States.

(i) Introduction.

In this section we shall consider the approximation of non ground-state wave functions using virtual orbitals obtained in the ground-state SCF procedure. The use of these antisymmetrized ground-state orbitals for excited states can be expected to generally give a poorer approximation to the total wave function than that obtained originally for the closed shell ground-state. We cannot expect a state constructed by re-allocating the occupation numbers of SCF orbitals to be still "self-consistent". Within the closed-shell of spin-paired electrons repulsions will be partially minimised, but as soon as we depart from our closed-shell state using the ground-state occupied and virtual orbitals, our new state will certainly not be "self-consistent".

Methods for dealing with excited states in a self-consistent manner, which depend on the complete or partial removal of the spin-pairing constraint, will be discussed later. In this section on excited states both electron affinities and ionization potentials will be considered.

(ii) Ionization Potential and Electron Affinity.

The ionized state of a molecule, which previously had $2n$ bound electrons, and now has $2n-1$ to consider, may be written as a single determinantal wave function where we assume electron pairing in all un-ionized orbitals, then with the loss of an electron from orbital e , with $1 \leq e \leq n$, we have,

$$\Phi' = \frac{1}{\sqrt{(2n-1)!}} \begin{vmatrix} \phi'_1(1) & \bar{\phi}'_1(2) & \dots & \phi'_e & \dots & \bar{\phi}'_n & \bar{\phi}'_n \end{vmatrix} \quad (2-141)$$

Here the orbitals, $\{\phi'\}$, are taken as the new orbitals appropriate to the new molecular state.

The requirement of spin pairing for the doubly occupied orbitals does impose additional restriction on the problem, and is the same approximation as used by Roothaan in obtaining SCF wave functions for certain excited states, (I34). With the use of the less restrictive spin-polarized method, given later, this requirement can be removed, and the spin correlation accounted for. This apparent restriction of electron pairing must however be qualified by observing that, as it will also be seen later, spin-polarized orbitals can be transformed into a set of substantially doubly occupied orbitals, plus the unpaired orbitals. So, once again as in the neglect of differential overlap, our apparently gross assumption can be well justified with the use of more complex theory.

If, as a further simplification, it is proposed that the set, $\{\phi'\}$, are unchanged from the closed shell ground state set, $\{\phi\}$, to a first approximation, then we have, assuming the electron l with spin β is removed, a total state function,

$$\Phi' \approx \Phi = \frac{1}{\sqrt{(2n-1)!}} |\phi_1 \bar{\phi}_1 \dots \phi_l \dots \phi_n \bar{\phi}_n| \quad (2-I42)$$

The removal of an α -spin electron would be equally valid.

Thus we assume the removal of one electron from the molecule

does not markedly change the field experienced by those remaining.

The energy of the ionized state is thus given by,

$$E^+ = \sum_{i, i \neq e}^n 2\varepsilon_i^c + \sum_{i, i \neq e}^n \sum_{j, j \neq e}^n (2J_{ij} - K_{ij}) + \varepsilon_e^c + \sum_{i, i \neq e}^n (2J_{ei} - K_{ei}). \quad (2-I42a)$$

With this ionic state energy, E^+ , and the ground state energy, E_0 , equation (2-49), we can find the ionization potential of the particular electron, e ,

$$I_e = E^+ - E_0 = -\left[\varepsilon_e^c + \sum_{j=1}^n (2J_{ej} - K_{ej})\right] \quad (2-I43)$$

and hence,
$$I_e = -\varepsilon_e \quad (2-I44)$$

where ε_e is the Hartree-Fock "orbital energy", given in equation (2-I27). As for an occupied level $\varepsilon_e < 0$, then I_e is always positive.

Thus the diagonal elements of the Hartree-Fock energy matrix, \mathcal{E} , can be associated with the energy required to remove an electron from the appropriate orbital, assuming such a removal leaves the rest of the $2n-1$ electrons in unaltered orbitals.

With $\ell = n$, we obtain the first ionization potential, the energy required to remove an electron from the highest occupied level. This is a special form of Koopmans Theorem, (I35), and the agreement between the highest occupied orbital energy and ionization potential was observed in early applications of the SCF method, (I36). For a more rigorous discussion of ionization potential than the preceding, see (I37).

Later the validity of this theorem is tested, and further discussed, using SCF wave functions applicable directly to the ionized state, that is we avoid placing $\bar{\Phi}' \approx \bar{\Phi}$.

Finally we must observe that the often poor agreement between highest occupied orbital energies and ionization energies may be appreciably worsened, by \sim 1 e.v., with the consideration of penetration integrals, which are introduced with the use of the Goeppert-Mayer and Sklar core potential, (I39). These integrals are completely ignored in conventional Pople-Pariser-Parr methods. This neglect helps Koopmans Theorem, but it may not be very valid in the case of complete electron removal.

The electron affinity of a molecule may be determined by adding an additional electron to the system of $2n$ electrons already present. The electron is placed in a virtual orbital, K , with $n+1 \leq K \leq m$, where m is the limited basis set, equal to the number of $2p_z$ atomic orbitals in Roothaan's method for π -electrons. These virtual orbitals are obtained using the relations (2-I27) and (2-I29), with $n+1 \leq K \leq m$. As, $1 \leq \ell \leq n$, while $n+1 \leq K \leq m$ in these expressions, the sum over ℓ contains no equal Coulomb and Exchange integrals, thus for our electron in the virtual level we have $2n$ repulsions whilst the doubly occupied orbital electrons have only $2n-1$, (I38). Using the determinant $\bar{\Phi}$ to represent the system of $2n+1$ electrons, made up of ground state orbitals plus one virtual orbital of spin α , we find;

$$\bar{\Phi} = \frac{1}{\sqrt{(2n+1)!}} \left| \phi_1 \bar{\phi}_1 \dots \phi_n \bar{\phi}_n \phi_K \right| \quad (2-I45)$$

Then,

$$E^- = \sum_i^n 2 \epsilon_i^c + \sum_{i,j} (2 J_{ij} - K_{ij}) + \epsilon_K^c + \sum_j (2 J_{jK} - K_{jK}) \quad (2-I46)$$

Thus the electron affinity can be found, using the ground state energy given in equation (2-49),

$$E_K = E^+ - E^0 = \epsilon_K^c + \sum_j (2 J_{jK} - K_{jK}) = \epsilon_K \quad (2-I47)$$

So the electron affinity of the molecule corresponding to the placing of an electron in the K -th virtual orbital may be identified with the Hartree-Fock energy, ϵ_K .

It must be remembered that all the qualifications we used in obtaining the ionization potential also apply to the deduction of electron affinity. The addition of an electron is regarded as leaving unchanged the distribution of the rest, and here, as in the case of the consideration of the ionization potentials, we have omitted from our theory the σ -core. This core may be quite distorted after the removal or addition of a π -electron, (I39).

It is interesting also to see the analogy between the identification of these same properties with the energy levels in the Hückel approximation. In this treatment, which ignores any explicit consideration of electron/electron terms,

these electronic properties can be directly obtained from the magnitude of the energy of the level in question. As is obvious however, the analogy is only formal, and as is to be expected the self-constant field procedure is more revealing in its interpretation of the factors involved.

(iii) Optical Excited States.

Here we are going to consider "optically excited" states, this does not imply all the transitions possible for the electrons may actually be observed. Many optical states may be forbidden on grounds of symmetry or multiplicity.

In the closed shell SCF approximation the virtual orbitals obtained from the F matrix are used to construct excited states. It is hoped that configurations built from these orbitals represent reasonable approximations to the real functions of the excited states, in the absence of a SCF treatment for these states. We shall see how we may improve our excited state built up from ground state orbitals in the next section.

Considering the excitation of an electron from molecular orbital k to e , with $1 \leq k \leq n$ and $n+1 \leq e \leq m$ this situation can be described by either,

$$\frac{1}{\sqrt{2n!}} |\phi_1 \bar{\phi}_1 \dots \phi_k \dots \phi_n \bar{\phi}_n \phi_e| \quad \dots\dots (i)$$

$$\frac{1}{\sqrt{2n!}} |\phi_1 \bar{\phi}_1 \dots \bar{\phi}_k \dots \phi_n \bar{\phi}_n \phi_e| \quad \dots\dots(ii)$$

$$\frac{1}{\sqrt{2n!}} \left| \phi_1 \bar{\phi}_1 \cdots \bar{\phi}_k \cdots \phi_n \bar{\phi}_n \bar{\phi}_e \right| \dots\dots\text{(iii)}$$

$$\frac{1}{\sqrt{2n!}} \left| \phi_1 \bar{\phi}_1 \cdots \phi_k \cdots \phi_n \bar{\phi}_n \phi_e \right| \dots\dots\text{(iv)}$$

Examination of (i) and (ii) shows that they are degenerate, and by combining them two antisymmetric wave-functions for the total state of the molecule can be written, (67),

$$(A) \quad {}^0\psi_1^{k \rightarrow e} = \frac{1}{\sqrt{2n!}} \cdot \frac{1}{\sqrt{2}} \left\{ \left| \phi_1 \bar{\phi}_1 \cdots \phi_k \cdots \bar{\phi}_e \right| - \left| \phi_1 \bar{\phi}_1 \cdots \bar{\phi}_k \cdots \phi_e \right| \right\} \quad (2-I48)$$

$$(B) \quad {}^0\psi_3^{k \rightarrow e} = \frac{1}{\sqrt{2n!}} \cdot \frac{1}{\sqrt{2}} \left\{ \left| \phi_1 \bar{\phi}_1 \cdots \phi_k \cdots \bar{\phi}_e \right| + \left| \phi_1 \bar{\phi}_1 \cdots \bar{\phi}_k \cdots \phi_e \right| \right\} \quad (2-I49)$$

The first of these, ${}^0\psi_1^{k \rightarrow e}$, represents a singlet state, the second a triplet, ${}^0\psi_3^{k \rightarrow e}$, both of these states have zero spin projection on the z-axis; that is $\langle S_z \rangle = 0$. The last state, (B), is degenerate with (iii) and (iv) of our original set, but the latter have spin projection, $\langle S_z \rangle = 1$. Hence we can take either (iii) or (iv) to represent another triplet state,

$$(C) \quad {}^1\psi_3^{k \rightarrow e} = \frac{1}{\sqrt{2n!}} \left| \phi_1 \bar{\phi}_1 \cdots \bar{\phi}_k \cdots \bar{\phi}_e \right| \quad (2-I50)$$

This state is given by a single determinant as shown above, and hence the energy corresponding to the function is easily found;

$$\begin{aligned}
 {}^1E_3^{k \rightarrow e} &= \sum_{i \neq k} 2\varepsilon_i^c + \sum_{i, j, \neq k} (2J_{ij} - K_{ij}) \\
 &+ \varepsilon_k^c + \sum_{j, \neq k} (2J_{jk} - K_{jk}) + \varepsilon_e^c + \sum_{j, \neq k} (2J_{je} - K_{je}) \\
 &\quad + J_{ke} - K_{ke} \quad (2-151)
 \end{aligned}$$

The last two terms, $J_{ke} - K_{ke}$, are the k -electron / j -electron interaction contributions.

For the states with zero spin projection, the energy calculation is not so straight forward, as there are two component determinantal wave functions to consider, and we have off diagonal terms in the Hamiltonian. The singlet state represented by (A) has energy, ${}^1E_1^{k \rightarrow e}$, given by,

$$\begin{aligned}
 {}^1E_1^{k \rightarrow e} &= \frac{1}{(2n)!} \left\{ \langle \phi_1 \bar{\phi}_1 \dots \phi_k \bar{\phi}_e | \sum_i H_i^c + \sum_{i, j > i} \frac{1}{r_{ij}} | \phi_1 \bar{\phi}_1 \dots \phi_k \bar{\phi}_e \rangle \right. \\
 &\quad \left. - \langle \phi_1 \bar{\phi}_1 \dots \phi_k \bar{\phi}_e | \sum_i H_i^c + \sum_{i, j > i} \frac{1}{r_{ij}} | \phi_1 \bar{\phi}_1 \dots \bar{\phi}_k \phi_e \rangle \right\} \quad (2-152)
 \end{aligned}$$

The first term in ${}^1E_1^{k \rightarrow e}$, with the same wave function each side of the Hamiltonian, is just what we would expect to obtain, had a single determinantal representation of the singlet state been used. The second term is off diagonal in the sense that one wave function represents a permutation of the spin coordinates of k and e . We find, using determinant algebra,

$$\begin{aligned}
 &\langle \phi_1 \bar{\phi}_1 \dots \phi_k \bar{\phi}_e | \sum_i H_i^c + \sum_{i, j > i} \frac{1}{r_{ij}} | \phi_1 \bar{\phi}_1 \dots \bar{\phi}_k \phi_e \rangle \\
 &= -K_{ke} \quad (2-153)
 \end{aligned}$$

Thus the energy of singlet state (A) is given by,

$$\begin{aligned}
 {}^0E_1^{k \rightarrow e} &= 2 \sum_{i, \neq k} \varepsilon_i^c + \sum_{i, j, \neq k} (2J_{ij} - K_{ij}) \\
 &+ \varepsilon_k^c + \sum_{j, \neq k} (2J_{kj} - K_{kj}) + \varepsilon_e^c + \sum_{j, \neq k} (2J_{ej} - K_{ej}) + J_{ke} + K_{ke}
 \end{aligned} \tag{2-I54}$$

Of the last two terms, J_{ke} arises out of the Coulomb repulsion, and the Exchange integral K_{ke} is the off diagonal non-classical contribution.

Similarly for the triplet, (B), the total energy is to be represented as ,

$$\begin{aligned}
 {}^0E_3^{k \rightarrow e} &= \langle \phi_1 \bar{\phi}_1 \dots \phi_k \bar{\phi}_k \dots \phi_e \bar{\phi}_e | \sum_i H_i^c + \sum_{i, j > i} \frac{1}{r_{ij}} | \phi_1 \bar{\phi}_1 \dots \phi_k \bar{\phi}_k \dots \phi_e \bar{\phi}_e \rangle \\
 &+ \langle \phi_1 \bar{\phi}_1 \dots \phi_k \bar{\phi}_k \dots \phi_e \bar{\phi}_e | \sum_i H_i^c + \sum_{i, j > i} \frac{1}{r_{ij}} | \phi_1 \bar{\phi}_1 \dots \phi_k \bar{\phi}_k \dots \phi_e \bar{\phi}_e \rangle
 \end{aligned} \tag{2-I55}$$

So for the triplet with $\langle S_z \rangle = 0$ the diagonal term has to be added, and hence we obtain,

$${}^0E_3^{k \rightarrow e} = {}^0E_1^{k \rightarrow e} - 2K_{ke} \tag{2-I56}$$

This energy, ${}^0E_3^{k \rightarrow e}$, is found to be identical with that of the triplet state, ${}^1E_3^{k \rightarrow e}$, the latter having $\langle S_z \rangle = 1$ in units of \hbar .

So in our approximation neglecting spin interactions these states are degenerate, even if they are represented by different antisymmetrized wave functions constructed from the same orbitals. With the ground state energy given in equation (2-49), the excitation energies of the singlet and triplet states may be written;

$$\Delta E_1^{k \rightarrow l} = E_1^{k \rightarrow l} - E_0 = \epsilon_L - \epsilon_K + 2K_{kl} - J_{kl} \quad (2-157)$$

$$\Delta E_3^{k \rightarrow l} = E_3^{k \rightarrow l} - E_0 = E_3^{k \rightarrow l} - E_0 = \epsilon_L - \epsilon_K - J_{kl} \quad (2-158)$$

Where ϵ_L and ϵ_K are the SCF orbital energies. It will be noticed that in this properly antisymmetrized treatment, the triplet state is lower in energy than the singlet for any given transition. This agrees with Hund's rule concerning spin-pairing.

The evaluation of the transition energies requires the calculation of the integrals K_{kl} and J_{kl} to take account of the difference in Exchange and Coulomb forces in the transition to the excited state. This situation is not so simple as in the Hückel approximation where it is only necessary to take the energy difference between the two one electron levels to find the energy required. The fact that the orbitals in the SCF model are one electron does not mean they take no notice of the other electrons, this is the complicating factor.

The use of the virtual orbitals is a poor approximation and this may be improved by a procedure known as Configuration Interaction.

(iv) Configuration Interaction.

As has been stated, using the virtual orbitals obtained from the closed-shell ground state SCF we can only hope to derive very approximate wave functions for the excited

states of the system. Some account must be taken of the fact that the alteration of the occupied electron orbital population does change the potential field the electrons move in .

Any solution for the excited states may be improved by what is termed "Configuration Interaction", (66),(I41),(I42), (I43),(I44). In this method the electronic excited state of a many particle system, ψ_i , is expressed in a linear combination of approximate states, $\{\Phi_j\}$, representing various excited states of the system. The component states, the "configurations", are all expressed in full antisymmetric Slater determinant form, and sometimes even the ground state is also included. Löwdin has showed, (66), how any many electron wave function can be expressed as a sum of Slater determinants, built up from a complete basis set of one electron functions. Thus we have a reasonable basis for the procedure of configuration interaction.

The method corresponds to a re-use of the Variation Principle to optimize the stationary excited states of the system. Thus our total wave function for excited state i can be written as ,

$$\psi_i = \sum_j^N a_{ij} \bar{\Phi}_j \quad (2-159)$$

The set of states, $\{\bar{\Phi}_j\}$, comprising all the N configurations considered are orthogonal, and hence we have $\sum_i |a_{ij}|^2 = 1$, and also as the $\bar{\Phi}_j$ are generally approximate, we would not expect

any $a_{ij}=1$ for $1 \leq j \leq N$, unless a state was unable to mix with others on grounds of symmetry or multiplicity. If it does happen however, the state is invariant under this procedure. The set of improved states, $\{\psi_i\}$, can be obtained by solving the eigenvalue problem;

$$H \mathcal{A} = \epsilon \mathcal{A} \quad (2-160)$$

The matrix of eigenvectors, \mathcal{A} , gives the weights, $\{a_{ij}\}$, of the various basis configurations, Φ_j , in the new state of energy ϵ_i .

Hence we need to know how to evaluate the matrix elements, $\langle \Phi_i | H | \Phi_j \rangle$, where Φ_i and Φ_j represent different excited states. Here we shall confine ourselves to considering singly excited states, singlets and triplets, which will be treated in two separate configuration interactions as they do not interact, because of differing multiplicity. The ground state is not involved in the interaction, as all matrix elements between this state and singly excited states are zero in the SCF approximation. This is Brillouin's theorem, (I45). It will be noted here we are considering exclusively configurations built from ground state SCF orbitals. The interacting configurations could in fact be wave functions obtained in the Hückel approximation, although here we would have to include the ground state in the interaction matrix, (I06). Doubly excited states and multiplicities other than 1 or 3 will be neglected.

It may be anticipated that some $\bar{\Phi}_i$ and $\bar{\Phi}_j$ will not mix on grounds of symmetry, but here we consider the general interaction between the singlet transition $\kappa \rightarrow e$ and $i \rightarrow j$, the respective excited states denoted by ${}^0\bar{\Phi}_1^{\kappa \rightarrow e}$ and ${}^0\bar{\Phi}_1^{i \rightarrow j}$. Any latent symmetry in the two states is ignored.

We have for the singlet configuration functions,

$${}^0\bar{\Phi}_1^{\kappa \rightarrow e} = \frac{1}{\sqrt{2^i}} \cdot \frac{1}{\sqrt{2^{n-i}}} \left\{ |\phi_1 \bar{\phi}_1 \dots \phi_k \bar{\phi}_e| - |\phi_1 \bar{\phi}_1 \dots \bar{\phi}_k \phi_e| \right\} \quad (2-I61)$$

$${}^0\bar{\Phi}_1^{i \rightarrow j} = \frac{1}{\sqrt{2^i}} \cdot \frac{1}{\sqrt{2^{n-i}}} \left\{ |\phi_1 \bar{\phi}_1 \dots \phi_i \bar{\phi}_j| - |\phi_1 \bar{\phi}_1 \dots \bar{\phi}_i \phi_j| \right\}$$

These may be compared with equation (2-I48).

(2-I62)

Hence we obtain,

$$\begin{aligned} \langle {}^0\bar{\Phi}_1^{i \rightarrow j} | H | {}^0\bar{\Phi}_1^{\kappa \rightarrow e} \rangle &= \langle |\phi_1 \bar{\phi}_1 \dots \phi_i \bar{\phi}_j| H | \phi_1 \bar{\phi}_1 \dots \phi_k \bar{\phi}_e \rangle \\ &\quad - \langle |\phi_1 \bar{\phi}_1 \dots \phi_i \bar{\phi}_j| H | \phi_1 \bar{\phi}_1 \dots \bar{\phi}_k \phi_e \rangle \end{aligned} \quad (2-I63)$$

The element of the triplet matrix is likewise given by,

$$\begin{aligned} \langle {}^0\bar{\Phi}_3^{i \rightarrow j} | H | {}^0\bar{\Phi}_3^{\kappa \rightarrow e} \rangle &= \langle |\phi_1 \bar{\phi}_1 \dots \phi_i \bar{\phi}_j| H | \phi_1 \bar{\phi}_1 \dots \phi_k \bar{\phi}_e \rangle \\ &\quad + \langle |\phi_1 \bar{\phi}_1 \dots \phi_i \bar{\phi}_j| H | \phi_1 \bar{\phi}_1 \dots \bar{\phi}_k \phi_e \rangle \end{aligned} \quad (2-I64)$$

In these equations H is the Hamiltonian defined in

equation (2-I7). These matrix elements may be evaluated by

standard methods, (I00), (I0I), (70), and it is found,

$$\langle |\phi_1 \bar{\phi}_1 \dots \phi_i \bar{\phi}_j| H | \phi_1 \bar{\phi}_1 \dots \phi_k \bar{\phi}_e \rangle = \langle ij | ek \rangle - \langle ik | ej \rangle \quad (2-I65)$$

$$\langle |\phi_1 \bar{\phi}_1 \dots \phi_i \bar{\phi}_j| H | \phi_1 \bar{\phi}_1 \dots \bar{\phi}_k \phi_e \rangle = -\langle ij | ek \rangle \quad (2-I66)$$

Thus the singlet and triplet matrix elements are given

by, (I24),

$$\langle {}^0\Phi_1^{i \rightarrow j} | H | {}^0\Phi_1^{k \rightarrow e} \rangle = 2 \langle ij | ek \rangle - \langle ik | ej \rangle \quad (2-I67)$$

$$\langle {}^0\Phi_3^{i \rightarrow j} | H | {}^0\Phi_3^{k \rightarrow e} \rangle = - \langle ik | ej \rangle \quad (2-I68)$$

we define $\langle pq | rs \rangle$ as ,

$$\langle pq | rs \rangle = \iint \phi_p(1) \phi_q^*(1) \frac{1}{r_{12}} \phi_r(2) \phi_s^*(2) d\tau_1 d\tau_2 \quad (2-I69)$$

where the orbitals, $\{\phi_i\}$, are the SCF molecular orbital set.

These are the off diagonal terms, the diagonal elements are

obtained as indicated in the previous section, equations (2-I57)

and (2-I58), and the ground state energy E_0 is taken as the

energy zero. Then our general configuration interaction

matrix elements become;

(i). Singlet.

$$\langle {}^0\Phi_1^{i \rightarrow j} | H | {}^0\Phi_1^{k \rightarrow e} \rangle = 2 \langle ij | ek \rangle - \langle ik | ej \rangle + (\epsilon_e - \epsilon_k) \delta_{ik} \delta_{je} \quad (2-I70)$$

(ii). Triplet.

$$\langle {}^0\Phi_3^{i \rightarrow j} | H | {}^0\Phi_3^{k \rightarrow e} \rangle = - \langle ik | ej \rangle + (\epsilon_e - \epsilon_k) \delta_{ik} \delta_{je} \quad (2-I71)$$

The Hartree-Fock parameters, ϵ_k and ϵ_e , are readily available after diagonalizing the Fock matrix F , but the integrals,

$\langle ij | ek \rangle$ and $\langle ik | ej \rangle$ are not. They can however easily be

obtained in the zero differential overlap approximation .

First the SCF molecular orbitals are expanded in terms of the basis functions, $\{\chi_i\}$, the SCF procedure having determined the optimum expansion coefficients,

$$\begin{aligned} \phi_i &= \sum_p c_{ip} \chi_p & \phi_j &= \sum_q c_{jq} \chi_q \\ \phi_e &= \sum_r c_{er} \chi_r & \phi_k &= \sum_s c_{ks} \chi_s \end{aligned} \quad (2-I72)$$

Thus,

$$\langle ij | ek \rangle = \sum_{p,q,r,s} c_{ip} c_{jq} c_{er} c_{ks} \langle \chi_p \chi_q | \chi_r \chi_s \rangle \quad (2-I73)$$

and,

$$\langle ik | ej \rangle = \sum_{p,q,r,s} c_{ip} c_{jq} c_{er} c_{ks} \langle \chi_p \chi_s | \chi_r \chi_q \rangle \quad (2-I74)$$

Since with zero differential overlap,

$$\langle \chi_p \chi_q | \chi_r \chi_s \rangle = \langle p p | r r \rangle \delta_{pq} \delta_{rs} \quad (2-I75)$$

and with the notation, $\langle p p | r r \rangle = \delta_{pr}$, we obtain,

$$\langle ij | ek \rangle = \sum_{p,r} c_{ip} c_{jr} c_{er} c_{kr} \delta_{pr} \quad (2-I76)$$

$$\langle ik | ej \rangle = \sum_{p,r} c_{ip} c_{jr} c_{er} c_{kr} \delta_{pr} \quad (2-I77)$$

With these expressions, (2-I70), (2-I71), and (2-I76), (2-I77), we can set up our configuration interaction matrix, then, before diagonalization the diagonal elements represent the excitation energies of the configuration interaction basis, $\{\Phi_i\}$.

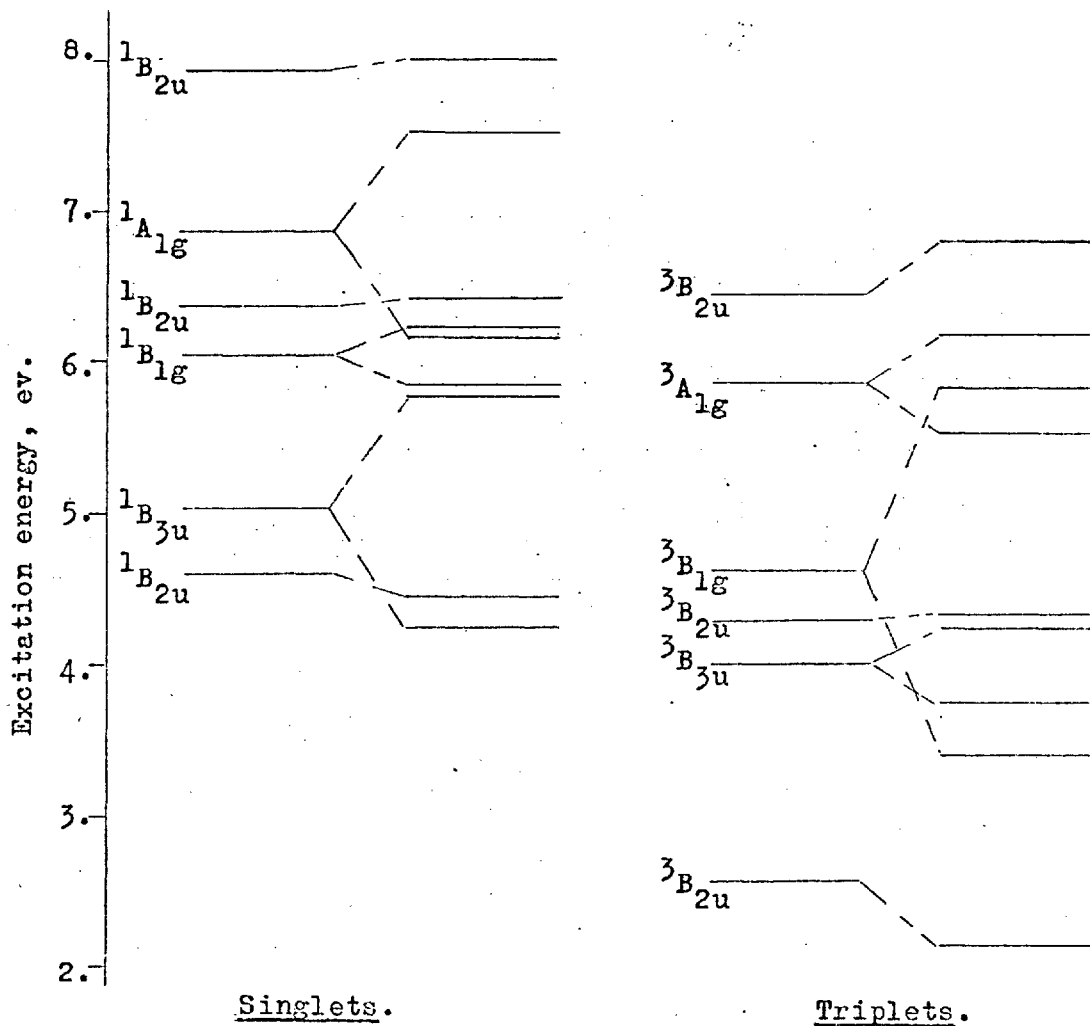
After diagonalization the eigenvalues are the new excitation energies, the eigenvectors showing how much of each configuration

has been included in the state the energy represents. The effect of configuration interaction in Anthracene is shown diagrammatically in Fig.28 .

Following the whole treatment of the optical state, we have first used an antisymmetrized molecular orbital, constructed this orbital to optimum values of the basis set of atomic orbitals in the SCF approximation, and finally used a configuration procedure. Clearly one of the most uncertain steps is the last, the configuration interaction. How many configurations should be used, often the state resulting from a interaction procedure proves to be very slowly convergent as more states are mixed in,(I46). Also we have only given here the treatment of single electron excited states, perhaps higher, especially doubly excited states ought to be included in the process,(I47).

In general, except for simple molecules, we are forced to use a "limited configuration interaction" to improve the wave functions of the optical states. Fortunately the effect of the interaction depends very much on the proximity in energy of the two states. States separated by large differences are little effected, but degenerate states are very strongly effected, this is known as "first order" configuration interaction and presents no convergence problem,(I48). Thus the effect is most important in highly symmetrical molecules, with much degeneracy, less symmetric molecules do not present such problems.

Fig. 28.



The effect of Configuration Interaction in Naphthalene.

Energy is relative to the ground state, with the new states shown on the right of those obtained before the interaction procedure.

Finally it may be noted that configuration interaction is less important the more accurate the initial approximation to the state under investigation is. Thus there is an advantage in using SCF states as starting points rather than Hückel approximations, which are expected to be quite poor guesses at the excited state. Hence, with less inter-state mixing, the results converge much more quickly, and fewer configurations need be included in the interaction matrix.

(v) Intensities of Electronic Transitions.

After using the SCF wave functions to calculate the energy of a transition, it is of great interest, especially when attempting to correlate experimental and theoretical band positions, to calculate the intensity of an electronic transition. This is very important in MO treatments as usually many more transitions are predicted within a certain energy range than are actually experimentally observed, so the number of allowed bands and their intensity becomes vitally significant.

To find the intensity, which is usually expressed experimentally in terms of the "oscillator strength" for a particular transition, we have to evaluate the transition moment, given by, (67),

$$\mu^{k \rightarrow l} = \int \Phi_0^{k \rightarrow l} \cdot \sum_i^n \vec{r}_i \cdot \Phi^0 d\tau \quad (2-178)$$

Where $\Phi_0^{k \rightarrow l}$ represents the excited state, with one electron

in orbital K excited to the orbital ℓ , Φ^0 is the ground state wave function. Both of these are to be taken as the total antisymmetrized wave functions representing the particular states. \vec{r}_i is the radius vector of the i -th electron, all $2n$ π -electrons being included in the sum.

As the ground state, Φ^0 , is a singlet, transitions to other states of higher multiplicity are forbidden, thus all ground state/ triplet transitions are strictly forbidden without consideration of vibrational effects. This does not mean excited triplet/ triplet transitions are forbidden, and these triplet/triplet spectra are being increasingly studied, both theoretically and experimentally, (I49).

Thus for an excited singlet state, $\Phi_1^{K \rightarrow \ell}$, given in equation (2-I48), the intensity of the transition from the ground state may be expressed in terms of the transition dipole, given by;

$$Q^{K \rightarrow \ell} = \frac{1}{\sqrt{2}} \frac{1}{\sqrt{2n!}} \int \{ |\phi_1 \bar{\phi}_1 \dots \phi_K \bar{\phi}_\ell| - |\phi_1 \bar{\phi}_1 \dots \bar{\phi}_K \phi_\ell| \} \sum_i^{2n} \vec{r}_i \frac{1}{\sqrt{2n!}} |\phi_1 \bar{\phi}_1 \dots \phi_n \bar{\phi}_n| \cdot d\tau \quad (2-I79)$$

The first term in front of $\sum_i \vec{r}_i$ represents the appropriate singlet function. With the use of determinant algebra we obtain,

$$Q^{K \rightarrow \ell} = \sqrt{2} \int \phi_K(\mathbb{1}) \vec{r}(\mathbb{1}) \phi_\ell(\mathbb{1}) d\tau, \quad (2-I80)$$

The SCF orbitals ϕ_K and ϕ_ℓ are expressed in terms of a basis set, $\{\chi_i\}$,

$$\phi_K = \sum_P c_{Kp} \chi_p \quad \phi_e = \sum_Q c_{eQ} \chi_Q \quad (2-181)$$

Thus if we assume the components of the set $\{\chi_i\}$ are orthogonal, or on the other hand if we neglect all overlap terms which result from a non-orthogonal set, then,

$$q^{K \rightarrow e} = \sqrt{2} \sum_P c_{Kp} c_{eP} \vec{r}_P \quad (2-182)$$

where \vec{r}_P are the position vectors of the atomic centres, P , and c_{Kp} and c_{eP} are the eigenvectors of the orbitals K and e respectively applicable to the atom P . It is found using the triplet function, $\Phi_3^{0, K \rightarrow e}$, equation (2-149), that zero moment is obtained, as we would expect from symmetry considerations forbidding transitions between states of differing multiplicities.

Having calculated the transition moment and the electronic energy required for the excitation, it is possible to find the experimental parameter, the oscillator strength, $f^{K \rightarrow e}$ given by,

$$f^{K \rightarrow e} = 0.087516 \cdot [q^{K \rightarrow e}]^2 \cdot \Delta E_1^{K \rightarrow e} \quad (2-183)$$

Thus we are in a position to compare both the energies and the intensities of transitions obtained from SCF calculations with experimental values.

The transition moment from the ground state to an excited singlet represented by a series of Slater determinants, as obtained in the configuration interaction procedure, may be

easily obtained by substituting the linear combination of configurations into the expression for $q^{k \rightarrow e}$. The singlet configuration, ${}^0\psi_i$, can be represented as,

$${}^0\psi_i = \sum_j^N a_{ij} {}^0\bar{\phi}_{,j} \quad (2-I84)$$

Where N total configurations are allowed to interact. The coefficients a_{ij} represent the weights of the various singlet components, ${}^0\bar{\phi}_{,j}$. Thus the strength of our mixed transition, i , is given by,

$$Q_i = \sum_j^N a_{ij} q^j \quad (2-I85)$$

with q^j representing the ground state to excited singlet configuration, j , transition dipole.

It will be noticed that after configuration interaction our transition may no longer be represented as a single electron excitation from one orbital to another. The need to express the total wave function of the excited state as an expansion of Slater determinants unfortunately leads to the loss of a simple physical interpretation for the transition. This is an inevitable consequence of attempting to treat many electron problems accurately .

(I5) Comments on the Pople-Pariser-Parr Method.

Here we shall present some general observations on the physical implications and limitations of the closed-shell SCF theory. Many comments will be specific to the

Pople-Pariser-Parr development, but many more will be applicable to the overall concept of the Hartree-Fock self-consistent field approach.

The Elements of the F Matrix.

The following represents an attempt to understand the terms occurring in the Pople-Pariser-Parr formulation of the Hartree-Fock matrix, F , (I46).

(i) The Diagonal Elements, F_{pp} ; these are given by equation (2-100).

The terms in the F matrix are derived using a one electron effective Hamiltonian, H_i , given as,

$$H_i = [H_i^c + \sum_j (2J_j - K_j)]$$
, in the Fock approximation.
 Thus H_i represents the motion of a given electron, i , in the field of the nuclei and the statistical distribution of negative charge of all the other electrons. The ionization term, $-I_p$, is the sum of the kinetic and potential energy of an electron adjacent to nucleus p due to the attraction of the nucleus. The attraction factors, $-\sum_{r \neq p} Z_r \gamma_{pr}$ represent the attractions of all the other nuclei, whilst the repulsive terms, $\sum_{r \neq p} P_{rr} \gamma_{pr}$, give the total repulsions of all the other electrons in the system. This is apparent when we consider that an electron in atomic orbital χ_r would produce a potential $\langle p | 1/r | r \rangle = \gamma_{pr}$, since however there are P_{rr} electrons in orbital χ_r , the repulsion is $P_{rr} \gamma_{pr}$, and we have to sum this over all electrons. Also in this closed-shell approximation

half of the electrons on centre p , $\frac{1}{2}P_{pp}$, will have α -spin and $\frac{1}{2}P_{pp}$, β -spin, this will give rise to the final repulsion term, $\frac{1}{2}P_{pp}\delta_{pp}$.

(ii) The Off-diagonals, F_{pq} ; In the Pople-Pariser-Parr approximation these are given by equation (2-101).

The first parameter, β_{pq}^c , is usually assigned a semi-empirical value in this treatment, it may also be fitted to give the best theoretical/experimental agreement. The significance of this parameter has been discussed by Ruedenburg, (150), and may be illustrated by considering a simple diatomic

π -system, with doubly occupied molecular orbital, ψ , where

$$\psi = c_1 \chi_1 + c_2 \chi_2 \quad (2-186)$$

Here χ_1 and χ_2 are atomic orbitals centred on atom 1 and 2 respectively. c_1 and c_2 are expansion coefficients of the molecular orbital. Then if we assume ψ is real,

$$\psi^2 = c_1^2 \chi_1^2 + 2c_1 c_2 \chi_1 \chi_2 + c_2^2 \chi_2^2 \quad (2-187)$$

The term between the two individual density functions, $c_1^2 \chi_1^2$ and $c_2^2 \chi_2^2$, represents additional electron density in the region where χ_1 and χ_2 overlap. Hence an electron in ψ will be more tightly bound than one would expect from χ_1 and χ_2 atomic binding energies. This extra binding appears in the off-diagonal elements of F as β_{pq}^c . The non-classical exchange term, $-\frac{1}{2}P_{pq}\delta_{pq}$, arises from the repulsion between two like spin-electrons centred at p and q . The $\frac{1}{2}$ occurs as in our closed-shell model α and β .

electrons are equivalent, and electron overlap measured by

P_{pq} , needs multiplying by this factor to give like spin repulsion. This term corresponds to a statement of the Pauli Principle, that two electrons of the same spin cannot simultaneously occupy the same point in space.

(16) Correlation in the Closed-shell Approximation.

The term "electron correlation" is used to describe the tendency of electrons to avoid each other as a result of Coulomb interactions and the interactions between electrons of different spins. This discussion will be essentially concerned with the effect of correlation in the closed-shell model, the open-shell procedures to be discussed later take account of correlation much more explicitly, especially spin effects.

We may define a specific "correlation energy", (66), (73). This is defined as the difference between the energy obtained in the Hartree-Fock approximation and the exact expectation energy obtained from the same specified Hamiltonian. Thus the definition of correlation energy is essentially a non-physical one, experimental comparisons are not involved. The correlation error is incurred by the neglect of ordinary Hartree-Fock methods to include the correlation between electrons with opposite spins. We normally force electrons of anti-parallel spin into the same space orbital, in accordance with the semi-classical Pauli Principle, and also

to ensure a resultant pure spin state using a single determinant wave function. In general the kinetic energy of electrons in the Hartree-Fock scheme is too low, electronic motions are too simple. The effect of including a proper description of correlation is easily obtained using the Virial Theorem, (151); the potential energy of the system is lowered at the expense of the kinetic energy, with an overall energy reduction.

One of the strongest arguments against ordinary Hartree-Fock methods is that they do not treat correlation between particles of different spin types in a proper way, (152). In the study of the most probable electronic configurations in atoms, (73), it has been found electrons of the same spin try to separate out from each other as much as possible. A wave function for a system of like particles with $\frac{1}{2}$ integer spin must be antisymmetric as we have shown. This implies the probability of finding two electrons with the same spins at the same point is zero. Hence like spin electrons try to keep as far apart as possible. The converse is seen to occur for anti-parallel spin electrons, which may occupy the same area of space at the same time. This will of course result in high Coulombic repulsions, but it will not contravene the antisymmetry requirements. Thus we must consider how much correlation is accounted for in the Hartree-Fock scheme, and where improvements are desirable.

In the original Hartree "independent particle" model, the approximate product wave function has the form of equation (2-23). The set of orbitals, $\{\phi_{\alpha}\}$, is determined mainly by the nuclear framework, but there is the very important Coulombic potential term, $1/r_{ij}$, between electrons i and j . The potential becomes large as $r_{ij} \rightarrow 0$, and keeps the electrons apart, forming a "Coulomb Hole". This potential is entirely ignored in this approximation, which includes no Coulomb Hole for either parallel or anti-parallel spin electrons, and gives rise to a correlation error.

If a state is approximated by a Slater determinantal antisymmetrized wave function, the situation is much improved. From considering the properties of the second order density matrix, Löwdin, (152), was able to show the probability density for two particles with the same spin at the same place was zero, at least to second order. Thus using the determinant wave function a "Fermi Hole" is obtained, antisymmetrization itself acts as if there were strong repulsion between particles with the same spin at small separations. This consequence of the generalized Pauli Principle automatically diminishes error due to electron correlation, it does not however mean it is explicitly considered, the degree to which antisymmetrization "relieves" the correlation is uncertain.

We should not however judge the Hartree-Fock method too harshly. The correlation energy is a relatively small

proportion of the total, approximately 1%, so the overall success of the SCF method is not really endangered.

Unfortunately however this 1% will be of the order of 1 eV. per electron pair, and this is not insignificant, small as it is compared to the total electronic energy of the system.

In some cases, when taking differences in energies between two states, the correlation energy may be approximately equal in both cases, and hence apparently good experimental predictions may be made, even in the presence of large correlation errors. The fortuitous cancellation is most likely between two isoelectronic systems with doubly filled orbitals. With states of differing multiplicities no such cancellations can occur.

In the semi-empirical method of Pople-Pariser-Parr, the effects of correlation are masked to a large extent by the optimization of parameters to obtain the best experimental fit possible. As mentioned previously the fact that our total wave function is fully antisymmetrized helps to reduce correlation errors. Also the semi-empirical nature of the two centre Coulomb integrals, largely arrived at from experimental results which include correlation effects of course, is a further compensating factor.

Dewar, (I46), (I53), has discussed the effect of two types of Π -electron correlation on the elements of the Hartree-Fock matrix F .

(i) Vertical Correlation.

This term describes the tendency of two electrons of differing spins to separate partially onto opposite sides of the π -nodal plane. This does not effect the total electronic density, it just gives unequal distributions of

α and β -spin electrons in the two lobes of a $2p_z$ π atomic orbital. In the F matrix, the diagonal term, F_{pp} , is effected by this correlation, which reduces $\frac{1}{2} P_{pp} \delta_{pp}$. The repulsion integral, $\langle pp|pp \rangle$, is reduced by the spin polarization at centre p . The effect of correlation on

$\langle pp|pp \rangle$ was discussed in the section on parameters. The terms $P_{rr} \delta_{rr}$ are uneffected, as the total repulsion of α and β electrons is being considered between the atomic orbitals at p and r , $\langle pp|rr \rangle$.

In the off-diagonal term, β_{pq}^c may be assumed practically invariant as it is a one electron integral.

However correlation will tend to increase the exchange term, $\frac{1}{2} P_{pq} \delta_{pq}$, as the value of $\langle pp|qq \rangle$ between atomic orbitals of the same spin will be greater, the orbitals being more concentrated, and this results in a lowering of the overall total π -energy of the system.

Dewar, (153), has proposed the use of split $2p_z$ orbitals to deal with this correlation, α and β electrons are each assigned to the opposite lobes of the $2p_z$ orbital.

(ii) Horizontal Correlation.

This concerns the tendency for a π -system to lower its energy by alternating α and β spin density along a π -chain. Löwdin, (75), suggested the use of different orbitals for the electrons of differing spin. These molecular orbitals, "Alternate molecular orbitals", (AMO's), introduced a spin separation by artificial means. The best idea, however, seems to use entirely different orbital sets for the α and β -spin electrons, and allow both sets to be varied in a SCF procedure. The execution and result of such a method is considered later.

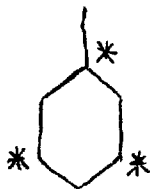
(I7) Alternant Hydrocarbons and the Hückel Approximation.

The reason for discussing the Hückel approximation within a section on one particular type of conjugated molecule will become clear later.

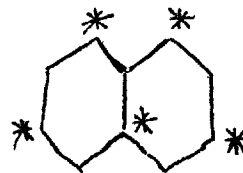
First an "Alternant Hydrocarbon" must be defined. It is merely a hydrocarbon in which the Carbon atoms can be divided into two sets, no two atoms of the same set being directly linked, (I30). If one set is labeled with stars, then no two starred atoms are to be bonded. Some examples of alternant hydrocarbons are shown below.



Butadiene.



Benzyl Radical



Naphthalene.

The molecular orbital for an alternant hydrocarbon with an even number of Carbon atoms assumes a very simple form. This was first deduced from the Hückel theory, but later shown to apply also to the Pople SCF formalism, (I54). The distinctive properties are set out below.

(i) We find in the charge and bond-order matrix that all $P_{pp} = 1$, and all $P_{pq} = 0$ if p and q belong to the same set, starred or unstarred. Also for each occupied molecular orbital, ϕ_m^+ , there corresponds an empty or virtual orbital, ϕ_m^- , with

$$\phi_m^+ = \sum_i c_{mi} \chi_i + \sum_j c_{mj} \chi_j \quad (2-I88)$$

$$\phi_m^- = \sum_i c_{mi} \chi_i - \sum_j c_{mj} \chi_j \quad (2-I89)$$

where i and j refer to atoms in the different sets.

(ii) Singly excited configurations arising from transitions between pairs of related orbitals, ϕ_m^+ and ϕ_m^- , are unique, but remaining transitions appear in degenerate pairs. For

example the transition $\phi_m^+ \rightarrow \phi_n^-$ will be degenerate with

$\phi_n^+ \rightarrow \phi_m^-$, both in the Hückel and SCF approximations.

(iii) For an alternant hydrocarbon the mean of the highest filled and the lowest empty orbital energies is constant. That is the mean of the ionization potential and electron affinity as defined by Koopman's Theorem does not depend on the particular alternant hydrocarbon studied, (I55).

These theoretical deductions explain several properties of alternant hydrocarbons. For example they are non-polar, whilst

non-alternants like Azulene, Fulvene, have appreciable dipole moments. Also it is possible to conclude that substituents have little effect on the lowest $\pi \rightarrow \pi^*$ transitions, (I56), and that there is no change in charge density on the atoms in these transitions, unlike in non-alternants.

Of the first four transitions in an alternant hydrocarbon, from the levels ϕ_{m-1}^+ , ϕ_m^+ to ϕ_m^- , ϕ_{m-1}^- , two are unique, and two degenerate, $\phi_m^+ \rightarrow \phi_{m-1}^-$ and $\phi_{m-1}^+ \rightarrow \phi_m^-$. Analysis by Clar, (I57), shows a first-order configuration interaction splits then into two states, transitions to the lower being partially or completely forbidden, and the transition to the higher levels being correspondingly intense. These observations may be compared with the SCF results obtained for Butadiene, Benzene, and other alternant hydrocarbons.

When applying a SCF treatment to an alternant hydrocarbon we can simplify our Hartree-Fock matrix elements, by using the fact that $P_{pp} = 1$, and find from equations (2-I00) and (2-I01),

$$F_{pp} = -I_p + \frac{1}{2} \langle pp | pp \rangle \quad (2-I90)$$

$$F_{pq} = \beta_{pq}^c - \frac{1}{2} \langle pp | qq \rangle P_{pq} \quad (2-I91)$$

Clearly all diagonal elements have the same value, say α , $F_{pp} = \alpha$, and this α can be associated directly with the Hückel parameter. In the off diagonals of the F matrix, the term $\frac{1}{2} P_{pq} \gamma_{pq}$ is zero whenever p and q belong to the same

set, starred or unstarred, as $P_{pq} = 0$ in this instance. Hence if we neglect β_{pq}^c for non-bonded atoms, and neglect also $\frac{1}{2} P_{pq} \gamma_{pq}$ for P and q separated by more than two bonds, then $F_{pq} = 0$ if P and q are not directly linked.

In alternant hydrocarbons bond lengths and orders do not change very much, so we can write a mean value for $F_{pq} = \beta_{pq}$ corresponding to the Hückel parameter.

Thus we are able to gain some insight into the reason for the relative success of the Hückel method when applied to alternant hydrocarbons, especially for ground state properties. It is possible however to see why care must be taken in considering non-alternants and hetero-atoms in this approximation.

For strongly alternant bond-orders, of the type that usually result from a Hückel-type approximation, a fixed value of β is not justified. The $\frac{1}{2} P_{pq} \gamma_{pq}$ two electron exchange term introduces a positive feed-back increasing strong/weak bond alternation. Thus the Hückel method underestimates bond alternation, allowing too high a degree of electron delocalization, (I46). The application of the Hückel method to non-alternants, and hetero-atomic systems is hence a rather uncertain procedure, but with much parameter variation reasonable results may be obtained, (I58), (I59). With its complete disregard of inter-electronic terms the method gives no singlet/triplet separation, however well it may be possible to reproduce the singlet spectrum using appropriate parameters.

(I8) Spin-Polarized Self-Consistent Field Theory.

(a) Introduction and Derivation of SCF Conditions.

Until now we have only considered the closed-shell self-consistent problem, where all the electrons are spin paired. This is the "Restricted Hartree-Fock" approximation. We are going to examine here a method of assigning α and β -spin electrons into different orbital sets. This allows us to remove the spin pairing constraint, and is known as an "Unrestricted Hartree-Fock" method. This treatment is very important for obtaining self-consistent excited states, and is especially valuable as it explicitly considers an increased degree of electron correlation compared with the restricted approach.

The problems of SCF theory in handling open-shell systems have long been recognized,(I45). The total energy of a molecular state cannot be identified with the expectation value of a single Slater determinant in the case of degenerate configurations,(I29), for example singlets and triplets with $\langle S_z \rangle = 0$. Even if we can write the energy in convenient form, any effective Hamiltonians derived are not unique, and contain off diagonals. The Hartree-Fock Lagrangian energy matrix cannot be diagonalized by any simple transform,(I34).Also the orthogonality condition between excited and ground states cannot be strictly applied,(I60),except sometimes excited states are automatically orthogonal to the ground state for reasons of symmetry,(for example the Benzyl Radical), or multiplicity.

To build an approximate wave function, Φ , depending on the space and spin coordinates of the electrons involved in an open-shell state, we can use a variational approach, with the requisite that Φ has the correct symmetry, and that it is an eigenfunction of the total spin operators S_z and S^2 . If a single determinant is used to represent Φ , often the spin requirements cannot be fulfilled. In such cases we chose a single determinant which is a near eigenvalue of the spin operators, and build a "good" wave function after the variational procedure by the application of a projection operator, to give an eigenfunction of the spin operators.

In the spin-polarized treatment of half closed-shell systems, the α and β -spin electrons are separately assigned to different sets of molecular orbitals. These orbitals, constructed from an atomic orbital basis set, are then optimized using the variational principle, (I52), (I60), (I61), (I62), (I63). The state is represented by a single Slater determinant built from the two orbital sets;

$$\Phi = \frac{1}{\sqrt{(n_\alpha + n_\beta)!}} \cdot \left| \phi_{i_1}^\alpha \phi_{i_2}^\alpha \dots \phi_{i_{n_\alpha}}^\alpha \phi_{j_{n_\alpha+1}}^\beta \dots \phi_{j_{n_\alpha+n_\beta}}^\beta \right|$$

(2-I92)

n_α and n_β are the number of electrons with α and β spin, and the indices, i, j , and, l, m , will be used to refer to α and β -spin orbitals respectively.

The total Π -energy of the system may thus be written;

$$E = \sum_i^{n_\alpha} \epsilon_i^c + \sum_{ij>i}^{n_\alpha} (J_{ij} - K_{ij}) + \sum_i^{n_\alpha} \sum_e^{n_\beta} J_{ie} + \sum_e^{n_\beta} \epsilon_e^c + \sum_{e,m>e}^{n_\beta} (J_{em} - K_{em}) \quad (2-193)$$

It will be noticed that the spin of each molecular orbital is indicated by its subscript,

$$J_{ie} = \iint \phi_i^\alpha \phi_i^{\alpha*} \frac{1}{r_{12}} \phi_e^\beta \phi_e^{\beta*} d\tau_1 d\tau_2 \quad (2-194)$$

The important central term in equation (2-193), summed over α and β -spin orbitals, represents the coupling of the two different orbital sets. It gives the Coulombic repulsion between the two sets of occupied orbitals. There is no exchange term, as the two sets are of different spin.

To obtain our self-consistent conditions we shall proceed in an analogous manner to the derivation followed for the closed-shell problem. Each set of orbitals will be varied separately in the field of the core and the other set. We shall first consider the effect of a first-order variation in the α -orbitals, in the field of the core and β -orbitals. The result may then be generalized to the SCF conditions for the β -spin orbitals also.

Varying the α -orbitals we write,

$$\phi_i^\alpha \rightarrow \phi_i^\alpha + \sum_{K, K \neq i}^N c_{iK} \phi_K^\alpha \quad (2-195)$$

Here $\{\phi_k\}$ represents a "complete" basis set, $N \rightarrow \infty$, and, $1 \leq i \leq n_\alpha$. As we require our α -orbitals to remain orthonormal throughout this first-order variation we find,

$$c_{ik} = -c_{ki} \quad (2-196)$$

with, $1 \leq k \leq n_\alpha$, and, $1 \leq i \leq n_\alpha$. To find the change in energy resulting from this first-order variation, we need the effect of these variations on all the quantities in the total energy expression involving α -orbitals. These are easily derived by substituting the new perturbed orbitals into our equations as in the closed-shell case. Hence we find;

$$\epsilon_i^c \rightarrow \epsilon_i^c + 2 \sum_{k, \neq i}^N c_{ik} \epsilon_{ik}^c + \dots \quad (2-197)$$

$$J_{ij} \rightarrow J_{ij} + 2 \sum_{k, \neq i}^N c_{ik} \epsilon_{jj}^{ik} + 2 \sum_{e, \neq j}^N c_{je} \epsilon_{ie}^{ij} + \dots \quad (2-198)$$

$$K_{ij} \rightarrow K_{ij} + 2 \sum_{k, \neq i}^N c_{ik} \epsilon_{kj}^{ij} + 2 \sum_{e, \neq j}^N c_{je} \epsilon_{ie}^{ij} + \dots \quad (2-199)$$

$$J_{ie} \rightarrow J_{ie} + 2 \sum_{k, \neq i}^N c_{ik} \epsilon_{ee}^{ki} + \dots \quad (2-200)$$

Only first-order terms are retained.

On substitution of these equations into our total energy expression, equation (2-193), and requiring that there should be no energy change for a first-order variation in orbitals,

it is found that,

$$\sum_i^{\eta_\alpha} \sum_{K, K \neq i}^N c_{iK} \left\{ \epsilon_{iK}^c + \sum_j^{\eta_\alpha} [\xi_{jj}^{iK} - \xi_{Kj}^{ij}] + \sum_e^{\eta_\beta} \xi_{ee}^{iK} \right\} = 0 \quad (2-201)$$

If we use the orthonormality condition, given in equation(2-I96), we find that since in general c_{iK} with $\eta_\alpha + 1 \leq K \leq N$ is not zero, then,

$$\left[\epsilon_{iK}^c + \sum_j^{\eta_\alpha} (\xi_{jj}^{iK} - \xi_{Kj}^{ij}) + \sum_e^{\eta_\beta} \xi_{ee}^{iK} \right] = 0 \quad (2-202)$$

With, $1 \leq i, j \leq \eta_\alpha$, and, $\eta_\alpha + 1 \leq K \leq N$.

On rewriting the above equation in terms of core and electron/ electron operators, we obtain,

$$\int \phi_{iK}^{\alpha} \left[H^c + \sum_j^{\eta_\alpha} (J_j^\alpha - K_j^\alpha) + \sum_e^{\eta_\beta} J_e^\beta \right] \phi_i^{\alpha} d\tau = 0 \quad (2-203)$$

Now, proceeding as in the closed-shell formalism, the result of the above operator in square brackets on ϕ_i^{α} can be expressed in terms of the whole basis set, $\{\phi^{\alpha}\}$. With the further use of the SCF requirement, equation (2-202), the set can be limited to η_α terms, and we finally derive, in analogy to equations (2-70) and (2-7I);

$$\left[H^c + \sum_j^{\eta_\alpha} (J_j^\alpha - K_j^\alpha) + \sum_e^{\eta_\beta} J_e^\beta \right] \phi_i^{\alpha} = \sum_K^{\eta_\alpha} \epsilon_{iK} \phi_K^{\alpha} \quad (2-204)$$

The α -set of spin orbitals can now be subjected to a unitary

transformation, eliminating the off diagonal multipliers in the Hartree-Fock energy matrix. Thus we obtain an effective eigenvalue problem,

$$\left[H^c + \sum_j^{n\alpha} (J_j^\alpha - K_j^\alpha) + \sum_l^{n\beta} J_l^\beta \right] \phi_i^\alpha = \epsilon_i^\alpha \phi_i^\alpha = F^\alpha \phi_i^\alpha \quad (2-205)$$

This transformation of the matrix \mathcal{E} to diagonal form was fully discussed in the section on closed-shell SCF theory.

A similar derivation may be followed for the β -spin orbitals, these are varied in the field of the α -orbitals and the core, and we find,

$$\left[H^c + \sum_l^{n\beta} (J_l^\beta - K_l^\beta) + \sum_j^{n\alpha} J_j^\alpha \right] \phi_m^\beta = \epsilon_m^\beta \phi_m^\beta = F^\beta \phi_m^\beta \quad (2-206)$$

Thus we have two eigenvalue problems, coupled together through the Coulomb terms, which have to be solved to self-consistency. The iterative nature of the problem arises as all the Coulomb and exchange operators are functions of the molecular orbital orbital we are using our SCF procedure to obtain.

The general matrix elements of our spin-polarized effective Hamiltonian may be derived on the supposition of a limited basis set, the orthogonalized atomic orbitals of the system. Both the α and β -spin orbitals will be constructed from the same basis. This limited basis corresponds to an extension of Roothaan's procedure for closed-shell states.

Hence, expanding the molecular orbitals in linear combinations of the atomic orbital basis functions, we have;

$$\begin{aligned} \phi_k^\alpha &= \sum_p c_{kp}^\alpha \chi_p & \phi_j^\alpha &= \sum_s c_{js}^\alpha \chi_s \\ \phi_i^\alpha &= \sum_q c_{iq}^\alpha \chi_q & \phi_\ell^\beta &= \sum_u c_{\ell u}^\beta \chi_u \\ \phi_j^\alpha &= \sum_r^+ c_{jr}^\alpha \chi_r & \phi_\ell^\beta &= \sum_v c_{\ell v}^\beta \chi_v \end{aligned} \quad (2-207)$$

with, $1 \leq k, i, j \leq n_\alpha$, $1 \leq \ell \leq n_\beta$, and,

$N \geq p, q, r, s, u, v \geq 1$. Thus the element $\langle \phi_k^\alpha | F^\alpha | \phi_i^\alpha \rangle$

is given by,

$$\begin{aligned} \langle \phi_k^\alpha | F^\alpha | \phi_i^\alpha \rangle &= \sum_{p,q} c_{kp}^\alpha c_{iq}^\alpha \{ \langle \chi_p | H^c | \chi_q \rangle + \\ & \sum_j^{\alpha} \sum_{r,s}^N c_{jr}^\alpha c_{js}^\alpha [\langle pq | rs \rangle - \langle pr | sq \rangle] + \sum_\ell^{\beta} \sum_{u,v}^N c_{\ell u}^\beta c_{\ell v}^\beta \langle pq | uv \rangle \} \end{aligned} \quad (2-208)$$

and;

$$\begin{aligned} F_{pq}^\alpha &= \langle \chi_p | H^c | \chi_q \rangle + \sum_j^{\alpha} \sum_{r,s}^N c_{jr}^\alpha c_{js}^\alpha [\langle pq | rs \rangle - \langle pr | sq \rangle] \\ & + \sum_\ell^{\beta} \sum_{u,v}^N c_{\ell u}^\beta c_{\ell v}^\beta \langle pq | uv \rangle. \end{aligned} \quad (2-209)$$

If the Pople-Pariser-Parr approximations are now introduced;

that is we use the Goeppert-Mayer and Sklar core potential,

ignore all penetration integrals, and assume zero differential

overlap, then we find,

$$\begin{aligned} F_{pp}^\alpha &= -I_p + \sum_\ell^{\beta} c_{\ell p}^\beta c_{\ell p}^\beta \langle pp | pp \rangle \\ & + \sum_{r \neq p}^N \left\{ \sum_{j=1}^{\alpha} c_{jr}^\alpha c_{jr}^\alpha + \sum_\ell^{\beta} c_{\ell r}^\beta c_{\ell r}^\beta - Z_r \right\} \langle pp | rr \rangle \end{aligned}$$

$$F_{pq}^{\alpha} = \beta_{pq}^c - \sum_j^{\eta_{\alpha}} c_{jp}^{\alpha} c_{jq}^{\alpha} \langle pp|qq \rangle \quad (2-2II)$$

Writing, $\langle pp|qq \rangle = \gamma_{pq}$, and with the assumption, $\gamma_{pp} = I_p - E_p$, we may simplify these expressions by the use of α and β -spin bond-order matrices,

$$P_{ij} = \sum_k^{\eta_{\alpha}} c_{ki}^{\alpha} c_{kj}^{\alpha} \quad (2-2I2)$$

$$Q_{ij} = \sum_k^{\eta_{\beta}} c_{ki}^{\beta} c_{kj}^{\beta} \quad (2-2I3)$$

These matrices have the properties, $P^2 = P$, $Q^2 = Q$, and,

$$\text{Tr}\{P\} = \eta_{\alpha}, \text{Tr}\{Q\} = \eta_{\beta}.$$

Hence for equations (2-2I0) and (2-2II) we have;

$$F_{pp}^{\alpha} = -I_p + Q_{pp}(I_p - E_p) + \sum_{r \neq p} (P_{rr} + Q_{rr} - Z_r) \gamma_{pr} \quad (2-2I4)$$

$$F_{pq}^{\alpha} = \beta_{pq}^c - P_{pq} \gamma_{pq} \quad (2-2I5)$$

The analogous definitions for the β -matrix elements are;

$$F_{pp}^{\beta} = -I_p + P_{pp}(I_p - E_p) + \sum_{r \neq p} (Q_{rr} + P_{rr} - Z_r) \gamma_{pr} \quad (2-2I6)$$

$$F_{pq}^{\beta} = \beta_{pq}^c - Q_{pq} \gamma_{pq} \quad (2-2I7)$$

In terms of these two matrices F^{α} and F^{β} we can express

the total π -energy of the system as,

$$E_{\pi} = \frac{1}{2} \text{Tr} \{ P(F^{\alpha} + H) + Q(F^{\beta} + H) \}$$

This should be compared with equation (2-I93). The matrix elements of \mathbb{H} are given in equations (2-I03).

As we have now derived the elements of the two Hartree-Fock matrices, and a matrix expression for the total energy of the system, it is of interest to investigate the physical meaning of the energy parameters, ϵ^α and ϵ^β . If we remove an α -spin electron from occupied orbital a , and assume our SCF orbitals are unchanged in this process, then we can write the total energy of our ionized system as,

$$E_a = \sum_{i, \neq a}^{n\alpha} \epsilon_i^c + \sum_{i, \neq a}^{n\alpha} \sum_{j, \neq a, > i}^{n\alpha} (J_{ij} - K_{ij}) + \sum_{i, \neq a}^{n\alpha} \sum_e^{n\beta} J_{ie} + \sum_e^{n\beta} \epsilon_e^c + \sum_e^{n\beta} \sum_{m, > e}^{n\beta} (J_{em} - K_{em}) \quad (2-219)$$

It will be seen only terms involving $\alpha - \alpha$ and $\alpha - \beta$ interactions are effected in the energy change, the cross term arises from the altered $\alpha - \beta$ Coulomb interaction.

Subtracting from this energy the ground state energy, E_π , given in equation (2-I93), we obtain the "ionization potential" of the electron a ;

$$E_a - E_\pi = - \left\{ \epsilon_a^c + \sum_{j, \neq a}^{n\alpha} (J_{aj} - K_{aj}) + \sum_e^{n\beta} J_{ae} \right\} \quad (2-220)$$

As, however, $J_{aa} = K_{aa}$, we find the right hand side of the equation above corresponds to the Hartree-Fock coefficient ϵ_a^α ;

$$\epsilon_a^\alpha = \epsilon_a^c + \sum_j^{n\alpha} (J_{aj} - K_{aj}) + \sum_e^{n\beta} J_{ae} \quad (2-22I)$$

which can be found from evaluating $\langle \phi_a^\alpha | F^\alpha | \phi_a^\alpha \rangle$.

Thus these coefficients may be identified with orbital energy as in the closed-shell treatment. They represent the total energy required to remove the appropriate electron from the π -system, with no resultant change in the potential field. This is an extension of Koopman's theorem into unrestricted SCF theory. A similar extension is also possible for electron affinities as represented by the unoccupied orbitals.

(b) Spin Properties of Unrestricted Wave Functions.

The spin-polarized method for finding molecular wave functions attempts to improve on conventional Hartree-Fock treatments, whilst still having the physical advantage of assigning electrons to orbitals, (I64), (I65). The use of different orbitals for α and β -spin electrons allows electron correlation, (Dewar's horizontal correlation), to be included to a greater degree than in spin-paired orbitals as used in closed-shell theory. Unfortunately however, the unrestricted wave function is generally not an eigenfunction of the spin operator, S^2 , with an expectation value of ,

$$\langle S^2 \rangle = \frac{1}{4} (n_\alpha - n_\beta)^2 + \frac{1}{2} (n_\alpha + n_\beta) - \text{Tr}(\mathbf{P} \mathbf{Q}) \quad (2-222)$$

but this can be corrected by the application of spin projection

techniques, (I64), (I65).

Before we can consider such procedures we must first obtain the eigenvalues of the spin operator, S^2 , when it operates on a generalized Slater determinant of spin-orbitals. The single electron operator can be written in terms of the projections of the individual electron's spin along the x, y, and z-axis, (67),

$$S^2(k) = S_x^2(k) + S_y^2(k) + S_z^2(k) \quad (2-223)$$

For an assembly of n electrons, the total operators are given by;

$$\begin{aligned} S^2 &= \sum_k^n S^2(k) & S_y^2 &= \sum_k^n S_y^2(k) \\ S_x^2 &= \sum_k^n S_x^2(k) & S_z^2 &= \sum_k^n S_z^2(k) \end{aligned} \quad (2-224)$$

The two possible eigenfunctions $\alpha(k)$ and $\beta(k)$ of the one electron operator, $S_z(k)$, correspond to a projection of $\pm \frac{\hbar}{2}$ for the electron spin of k along the arbitrary z-axis,

$$\begin{aligned} S_z(k) \alpha(k) &= \frac{\hbar}{2} \alpha(k) \\ S_z(k) \beta(k) &= -\frac{\hbar}{2} \beta(k) \end{aligned} \quad (2-225)$$

From the commutation rules for intrinsic spin-momentum we find,

$$\begin{aligned} S_x(k) \alpha(k) &= \frac{\hbar}{2} \beta(k) & S_y(k) \alpha(k) &= \frac{i\hbar}{2} \beta(k) \\ S_x(k) \beta(k) &= \frac{\hbar}{2} \alpha(k) & S_y(k) \beta(k) &= -\frac{i\hbar}{2} \alpha(k) \end{aligned} \quad (2-226)$$

To find the effect of S^2 on a determinantal wave function of n_α α -spin and n_β β -spin orbitals, where, $n_\alpha \geq n_\beta$, it is simpler to use the commutation rules further to re-write

S^2 as;

$$S^2 = (S_x - iS_y)(S_x + iS_y) + \hbar S_z + S_z^2 \quad (2-227)$$

Now we shall evaluate the results of applying these components of S^2 on our determinant of spin-orbitals, given in equation (2-I92).

If we first take S_z , then it has an eigenvalue given by,

$$\langle S_z \rangle = \left\langle \Phi \left| \sum_k^{n_\alpha + n_\beta} S_z(k) \right| \Phi \right\rangle = \sum_{k=1}^{n_\alpha} \langle \Phi | S_z(k) | \Phi \rangle + \sum_{k=n_\alpha+1}^{n_\alpha+n_\beta} \langle \Phi | S_z(k) | \Phi \rangle \quad (2-228)$$

On integration over all space coordinates, and using the rules for the evaluation of matrix elements of single electron operators, (I00), (I0I), (67), we find,

$$\langle S_z \rangle = \sum_{k=1}^{n_\alpha} \langle \alpha(k) | S_z(k) | \alpha(k) \rangle + \sum_{k=n_\alpha+1}^{n_\alpha+n_\beta} \langle \beta(k) | S_z(k) | \beta(k) \rangle \quad (2-229)$$

With the earlier expressions for the single electron operators, (2-225), and since the spin functions are normalized, then,

$$\langle S_z \rangle = \frac{\hbar}{2} (n_\alpha - n_\beta) \quad (2-230)$$

Hence we can write our eigenvalue equation as

$$S_z \cdot \Phi = \frac{\hbar}{2} (n_\alpha - n_\beta) \cdot \Phi \quad (2-231)$$

This leads directly to the result for S_z^2 , since we have;

$$S_z^2 \Phi = S_z (S_z \Phi) = \frac{\hbar^2}{4} (n_\alpha - n_\beta)^2 \cdot \Phi \quad (2-232)$$

Thus we see any single determinant of spin orbitals is forced to be an eigenfunction of S_z and S_z^2 , so long as integral orbital occupation numbers are used. Finally we note that in

later work we shall often write the eigenvalue of S_z as $\langle S_z \rangle$ itself, and use it in units of \hbar , that is, $\langle S_z \rangle = \frac{1}{2}(n_\alpha - n_\beta)$.

Now we have to find the effect of $(S_x - iS_y)(S_x + iS_y)$ on our determinant. If we expand the two operators in terms of one electron components we find,

$$\begin{aligned} (S_x - iS_y) &= \sum_k (S_x(k) - iS_y(k)) \\ (S_x + iS_y) &= \sum_k (S_x(k) + iS_y(k)) \end{aligned} \quad (2-233)$$

and these individual one electron operators are seen to either annihilate or interchange the spin functions,

$$(S_x(k) - iS_y(k)) \alpha(k) = \hbar \beta(k) \quad (S_x(k) + iS_y(k)) \alpha(k) = 0 \quad (2-234)$$

$$(S_x(k) - iS_y(k)) \beta(k) = 0 \quad (S_x(k) + iS_y(k)) \beta(k) = \hbar \alpha(k) \quad (2-235)$$

The effect of $(S_x + iS_y)$ on Φ is given by,

$$(S_x + iS_y) \Phi = \sum_{k=1}^{n_\alpha} (S_x(k) + iS_y(k)) \Phi + \sum_{k=n_\alpha+1}^{n_\alpha+n_\beta} (S_x(k) + iS_y(k)) \Phi \quad (2-236)$$

As the operator annihilates $\alpha(k)$ spin functions the first term gives zero contribution, whilst the $\beta(k)$ functions in the second sum are changed into their opposite spin counterparts,

$$(S_x + iS_y) \Phi = \hbar \sum_{k=n_\alpha+1}^{n_\alpha+n_\beta} \{ \Phi; \beta(k) \rightarrow \alpha(k) \} \quad (2-237)$$

We must now consider the effect of the operator $(S_x - iS_y)$ on this result,

$$\begin{aligned} (S_x + iS_y)(S_x - iS_y) \Phi &= \hbar \sum_{L=1}^{n_\alpha} (S_x(L) - iS_y(L)) \sum_{k=n_\alpha+1}^{n_\alpha+n_\beta} \{ \Phi; \beta(k) \rightarrow \alpha(k) \} \\ &+ \hbar \sum_{L=n_\alpha+1}^{n_\alpha+n_\beta} (S_x(L) - iS_y(L)) \sum_{k=n_\alpha+1}^{n_\alpha+n_\beta} \{ \Phi; \beta(k) \rightarrow \alpha(k) \} \end{aligned} \quad (2-238)$$

The last term just gives $\mathcal{K}^2 n_\beta \Phi$ since $(S_x(L) - iS_y(L))$ annihilates $\beta(L)$, and gives $\mathcal{K} \beta(L)$ after operating on $\alpha(L)$, so only the term for $L=K$ remains, giving back the original determinant;

$$\begin{aligned} & \mathcal{K} \sum_{L=n_\alpha+1}^{n_\alpha+n_\beta} (S_x(L) - iS_y(L)) \sum_{K=n_\alpha+1}^{n_\alpha+n_\beta} \{ \Phi; \beta(K) \rightarrow \alpha(K) \} \\ &= \mathcal{K}^2 \sum_{K=n_\alpha+1}^{n_\alpha+n_\beta} \{ \Phi; \beta(K) \rightarrow \alpha(K), \alpha(K) \rightarrow \beta(K) \} = \mathcal{K}^2 n_\beta \Phi \end{aligned} \quad (2-239)$$

The first term in equation (2-238) is given by,

$$\begin{aligned} & \mathcal{K} \sum_{L=1}^{n_\alpha} (S_x(L) - iS_y(L)) \sum_{K=n_\alpha+1}^{n_\alpha+n_\beta} \{ \Phi; \beta(K) \rightarrow \alpha(K) \} \\ &= \mathcal{K}^2 \sum_{K=n_\alpha+1}^{n_\alpha+n_\beta} \{ \Phi; \beta(K) \rightarrow \alpha(K), \alpha(L) \rightarrow \beta(L) \} \end{aligned} \quad (2-240)$$

Hence we have,

$$(S_x - iS_y)(S_x + iS_y) \Phi = \mathcal{K}^2 \sum_L^{n_\alpha} \sum_K^{n_\beta} P_{LK} \Phi + \mathcal{K}^2 n_\beta \Phi \quad (2-241)$$

where P_{LK} symbolizes the interchange of the spin functions L and K .

Before we can finally determine $\langle S^2 \rangle$ we have to evaluate $\langle \Phi | \sum_{L,K} P_{LK} | \Phi \rangle$, this is most easily achieved by substituting for Φ , using equation (2-192);

$$\begin{aligned} \langle \Phi | \sum_{L,K} P_{LK} | \Phi \rangle &= - \sum_{L,K} \iint \phi_L^\alpha \alpha(1) \phi_K^\beta \beta(2) \cdot P_{LK} \{ \phi_L^\alpha \alpha(1) \phi_K^\beta \beta(2) \} d\tau_{1,2} \\ &= - \sum_{L,K} \left(\int \phi_L^\alpha \phi_K^\beta d\tau_1 \right)^2 \end{aligned} \quad (2-242)$$

This expression, involving the overlap between the α and β -spin molecular orbital sets, may be simplified if these original sets, $\{ \phi_i^\alpha \}$ and $\{ \phi_i^\beta \}$, are transformed into "Corresponding Orbitals"

in the manner of Amos and Hall, (I64), (I65). These new orbitals are given by,

$$\phi_i^{\alpha'} = \sum_k^{n_\alpha} a_{ik} \phi_k^\alpha \quad \phi_j^{\beta'} = \sum_L^{n_\beta} a_{jL} \phi_L^\beta \quad (2-243)$$

As we have seen in the annihilation of the off diagonals in the Hartree-Fock Lagrangian matrix, such a transform leaves all physical quantities unaltered. We chose our transformation such that,

$$\int \phi_i^{\alpha'}(\nu) \phi_j^{\beta'}(\nu) d\nu = T_i \delta_{ij} \quad (2-244)$$

so that we obtain for the right of equation (2-242),

$$\sum_{L,K} \left(\int \phi_L^{\alpha'}(\nu) \phi_K^{\beta'}(\nu) d\nu \right)^2 = \sum_K^{n_\beta} T_K^2 \quad (2-245)$$

Hence our final expression for the ~~eigenvalues~~ ^{expectation} of S^2 in units of \hbar^2 becomes;

$$\langle S^2 \rangle = \frac{1}{4} (n_\alpha - n_\beta)^2 + \frac{1}{2} (n_\alpha + n_\beta) - \sum_K^{n_\beta} T_K^2 \quad (2-246)$$

These $\{T_K^2\}$ are the non-zero eigenvalues of the matrices

PQP and QPQ . P and Q are charge and bond-

order matrices, defined in equations (2-2I2) and (2-2I3).

The sum, $\sum_K T_K^2$, is simply given by $\text{Tr}\{PQ\}$, as $\text{Tr}\{PQ\} = \text{Tr}\{PQP\} = \text{Tr}\{QPQ\}$. The sum may be physically interpreted as the number of doubly occupied orbitals.

Thus a single Slater determinant with $n_\alpha \geq n_\beta$ only represents a pure spin-state if the number of doubly occupied orbitals defined by $\text{Tr}\{PQ\}$ equals n_β .

From diagonalizing PQP and QPQ , as well as obtaining the values of $\{T_K\}$, we can find the eigenvectors of

the corresponding orbitals, $\{\phi_k^{\alpha'}\}$, and, $\{\phi_k^{\beta'}\}$, respectively, with $1 \leq k \leq n_\beta$. These orbitals may be related to the "Natural Orbitals" which diagonalize the first-order density matrix, (I64), (I65),

$$\left. \begin{aligned} \lambda_k &= (\phi_k^{\alpha'} + \phi_k^{\beta'}) / \sqrt{2} (1 + T_k)^{\frac{1}{2}} \\ \nu_k &= (\phi_k^{\alpha'} - \phi_k^{\beta'}) / \sqrt{2} (1 - T_k)^{\frac{1}{2}} \end{aligned} \right\} k = 1, 2, \dots, n_\beta$$

$$\mu_k = \phi_k^{\alpha'} ; k = 1 + n_\beta, \dots, n_\alpha. \quad (2-247)$$

Their respective occupation numbers are $1 + T_k$, $1 - T_k$, and unity, with typical T_k values in the range $0.9 \leq T_k \leq 1$, the $\{\lambda_k\}$ closely resemble a doubly occupied set of orbitals, (I68). Writing, $\Delta_k^2 = \frac{1}{2}(1 - T_k)$, and with our assumption that T_k is nearly unity, $\Delta_k \ll 1$, we find,

$$\begin{aligned} \phi_k^{\alpha'} &\simeq \lambda_k + \Delta_k \nu_k \\ \phi_k^{\beta'} &\simeq \lambda_k - \Delta_k \nu_k \end{aligned} \quad (2-248)$$

Thus the corresponding orbitals are shown to be symmetrically split about the natural orbitals, so long as the value of Δ_k is small.

For orbitals obtained using closed-shell SCF methods we consider our single electron wave functions as being occupied by two electrons, that is we have,

$$\int \Theta_i^{(\alpha)} \Theta_j^{(\beta)} d\tau_i = \delta_{ij} \quad (2-249)$$

where Θ_i and Θ_j are molecular orbitals. Thus no suitable transform is needed to ensure orthogonality between the α and

β -spin orbitals as before. Hence in ordinary closed-shell treatments we do in fact obtain directly corresponding orbitals, and all the $\{T_k\}$ are unity for the doubly occupied functions. Similarly our natural orbitals are also equivalent to the molecular orbitals. Since for these wave functions all $T_k = 1$, we find, $\sum_k^{n_\beta} T_k^2 = n_\beta = \text{Tr} \{P \otimes Q\}$. Thus we have,

$$\langle S^2 \rangle = \frac{1}{4} (n_\alpha - n_\beta)^2 + \frac{1}{2} (n_\alpha - n_\beta) = \langle S_z \rangle (\langle S_z \rangle + 1) \quad (2-250)$$

where $\langle S_z \rangle (\langle S_z \rangle + 1)$ are just the allowed eigenvalues of S^2 .

Thus we see both ground states and excited states constructed from orbitals found in a spin-pairing approximation will automatically be correct eigenfunctions of S^2 . This is why no explicit consideration of spin properties is necessary for either closed-shell SCF or Roothann's Open-Shell method to be discussed later.

Self-consistent wave functions obtained with the spin-polarized scheme generally give states such that $\text{Tr} \{P \otimes Q\} < n_\beta$. Thus such states are not exact eigenfunctions of S^2 and may be regarded as linear combinations of determinants representing electronic configurations of various multiplicities. The major component in this expansion will be that of the state sought, that is with $\langle S^2 \rangle = \langle S_z \rangle (\langle S_z \rangle + 1)$, hence for the state $\bar{\Phi}$ we have,

$$\bar{\Phi} = c_0 \psi_{2S+1} + c_1 \psi_{2S+3} + c_2 \psi_{2S+5} + \dots \quad (2-251)$$

Where, $S = \frac{1}{2} (n_\alpha - n_\beta)$, corresponding to $\langle S_z \rangle$ for the first component wave function, with $\langle S_z \rangle$ measured in units of \hbar .

The eigenvalue, $\langle S^2 \rangle$, of the pure spin state sought, is given by $S(S+1)$. The multiplicity of this state is $2S+1$.

In the mixture of various multiplicities, Φ , the possible values of $\langle S_z \rangle$ for the individual components have the limits, $\frac{1}{2}(n_\alpha + n_\beta) \geq \langle S_z \rangle \geq \frac{1}{2}(n_\alpha - n_\beta)$. The removal of the unwanted components from the wave function, with its consequent improvement, may be achieved by the use of projection operators as proposed by Löwdin, (1969). The operator,

$$A_S = S^2 - S(S+1) \quad (2-252)$$

acting on a mixture of wave functions will annihilate the contribution of the state of multiplicity $2S+1$. Repetition will remove higher energy components, further improving the wave function. The spin eigenfunction $2S+1$ can be chosen exclusively from a mixture of different multiplicities by the use of the projection operator,

$$\Theta_S = \prod_{e, \neq S} \frac{S^2 - e(e+1)}{S(S+1) - e(e+1)} \quad (2-253)$$

This may be seen by considering the effect of the operator on the linear combination of various multiplicities represented by

Φ ;

$$\Theta_S \cdot \Phi = \prod_{e, \neq S} \frac{S^2 - e(e+1)}{S(S+1) - e(e+1)} \left\{ c_0 \psi_{2S+1} + c_1 \psi_{2S+3} + \dots \right\} \quad (2-254)$$

If the product $\prod_{e, \neq S} \{S^2 - e(e+1)\}$ is applied to a component different from ψ_{2S+1} , for which,

$$S^2 \psi_{2S+1} = S(S+1) \psi_{2S+1} \quad (2-255)$$

there must be a factor of zero. For example, with $l = s + 1$, the term $\{S^2 - (s+1)(s+2)\} \psi_{2s+3}$ will be zero as,

$$S^2 \psi_{2s+3} = (s+1)(s+2) \psi_{2s+3} \quad (2-256)$$

Thus the contribution $c_0 \psi_{2s+1}$ may be selected from the series, (2-250).

Amos and Hall, (164), have shown that high multiplicity terms are generally small, $c_0 \gg c_1 \gg c_2 \dots$, and that the component of next highest multiplicity to that required, that is ψ_{2s+3} , is the most contaminating unwanted wave function. Thus the use of a single annihilator;

$$A_s = S^2 - (s+1)(s+2) \quad (2-257)$$

is usually sufficient in place of the full projection, and the improved wave function is given by,

$$\Phi' = A_s \cdot \Phi \quad (2-258)$$

With the application of this single annihilator relatively simple expressions result for the various properties of the new wave function, which is an improved approximation to the exact eigenfunction of S^2 . Only in special cases, where terms of higher multiplicity than $2s+3$ are not involved in our state, Φ , will a single annihilation ensure an exact eigenfunction of S^2 .

The new expectation value of the total π -energy of the molecule represented by the improved wave function, Φ' , is given by;

$$E'_0 = \frac{\int \Phi'^* H \Phi' d\tau}{\int \Phi'^* \Phi' d\tau} = \frac{\int (A_S \Phi)^* H (A_S \Phi) d\tau}{\int (A_S \Phi)^* (A_S \Phi) d\tau} \quad (2-259)$$

One characteristic property of projection operators, (I52), is that $A_S^2 = A_S$. If in addition we assume A_S and θ commute, that is we have $A_S \theta - \theta A_S = 0$. Then we obtain from equation (2-259), where the operator θ is the Hamiltonian,

$$E'_0 = \frac{\int \Phi^* H A_S \Phi d\tau}{\int \Phi^* A_S \Phi d\tau} \quad (2-260)$$

This initial assumption that the annihilator and all operators, θ , it encounters, (including the Hamiltonian), commute, was made by Amos and Hall, (I64), (I65), and results in relatively simple equations for various properties after the single projection. The requirement that θ and A_S commute was removed in a later paper, (I68), but results in much more complex expressions. First we shall review the various equations, obtained on the assumption that $A_S \theta - \theta A_S = 0$,

With the component of next highest multiplicity removed, the improved value of $\langle S^2 \rangle$ is given by,

$$\langle S^2 \rangle' = \langle S^2 \rangle - \frac{1}{\chi} \left\{ (n_\alpha - \text{Tr}\{P\mathcal{Q}\}) \cdot (n_\beta - \text{Tr}\{P\mathcal{Q}\}) + 2 \text{Tr}\{P\mathcal{Q}\} - 2 \text{Tr}\{P\mathcal{Q}P\mathcal{Q}\} \right\} \quad (2-261)$$

where,

$$\chi = (S+1)(S+2) - \langle S^2 \rangle \quad (2-262)$$

The new α and β charge and bond-order matrices, \mathcal{J} and \mathcal{K} , obtained after a single annihilation are,

$$J = P - \frac{1}{\chi} (PQP - \frac{1}{2}PQ - \frac{1}{2}QP) \quad (2-263)$$

$$K = Q - \frac{1}{\chi} (QPQ - \frac{1}{2}QP - \frac{1}{2}PQ) \quad (2-264)$$

The total π -energy is given by,

$$E'_0 = \text{Tr} \{ (J+K) H \} + \frac{1}{2} \text{Tr} \{ JF \} + \frac{1}{2} \text{Tr} \{ KG \} + C \quad (2-265)$$

H is the familiar core integral matrix defined in equation (2-103). In the Pople-Pariser-Parr approximation the F and G matrices have the elements,

$$F_{t,t} = \sum_{u, \neq t} (P_{uu} + Q_{uu}) \gamma_{tu} + Q_{tt} \gamma_{tt}$$

$$F_{s,t} = -P_{st} \gamma_{st} \quad (2-266)$$

$$G_{t,t} = \sum_{u, \neq t} (Q_{uu} + P_{uu}) \gamma_{tu} + P_{tt} \gamma_{tt}$$

$$G_{s,t} = -Q_{st} \gamma_{st} \quad (2-267)$$

The value of C , which is usually small, is given by,

$$C = -\frac{1}{2\chi} \sum_{t,s} (P[P-Q])_{st} \cdot ([P-Q]Q)_{ts} \gamma_{ts} \quad (2-268)$$

With these equations, (2-261) to (2-268), we can evaluate spin-densities, charges and energy for a π wave function subjected to a single annihilation.

These expressions all depend on the idempotent and commuting character of A_S . In a later paper, however, Amos and Synder, (168), showed that A_S did not always commute with an operator, Θ , $A_S \Theta - \Theta A_S \neq 0$, and that A_S was

not exactly idempotent, with $A_S^2 \neq A_S$, (I68), (I70).

Discarding their previous assumption of an idempotent and commuting A_S , they were able to obtain new more accurate expressions for the calculation of the charge and bond-order matrices after a single annihilation. These are;

$$\begin{aligned} \mathcal{N} \mathcal{J} = & \{ A^2 - 2A \cdot \text{Tr}\{P\uparrow\downarrow\} + n_\alpha n_\beta - n_\beta - N \cdot \text{Tr}\{P\uparrow\downarrow\} \\ & + 3 \text{Tr}\{P\uparrow\downarrow\} + 2 \text{Tr}^2\{P\uparrow\downarrow\} - 2 \cdot \text{Tr}\{P\uparrow\downarrow P\uparrow\downarrow\} \} P \\ & + (n_\alpha - \text{Tr}\{P\uparrow\downarrow\}) Q + Q P Q \\ & + (N - 4 \text{Tr}\{P\uparrow\downarrow\} - 3 + 2A) P Q P \\ & + (P\uparrow\downarrow + Q P) \cdot (2 \text{Tr}\{P\uparrow\downarrow\} - n_\alpha + 1 - A) \\ & - 2(P\uparrow\downarrow P\uparrow\downarrow + Q P Q P) + 4 P Q P Q P \end{aligned} \quad (2-269)$$

The normalization, \mathcal{N} , is given by,

$$\begin{aligned} \mathcal{N} = & A^2 - 2A \cdot \text{Tr}\{P\uparrow\downarrow\} + n_\alpha n_\beta - N \cdot \text{Tr}\{P\uparrow\downarrow\} \\ & + 2 \text{Tr}\{P\uparrow\downarrow\} + 2 \text{Tr}^2\{P\uparrow\downarrow\} - 2 \text{Tr}\{P\uparrow\downarrow P\uparrow\downarrow\} \end{aligned} \quad (2-270)$$

where,

$$A = n_\beta - 2(\langle S_z \rangle + 1) \quad (2-271)$$

and N is the total number of electrons, $n_\alpha + n_\beta$.

The analogous expression for the β -spin electron matrix, K , is obtained by interchanging ($P \leftrightarrow Q$) and ($n_\alpha \leftrightarrow n_\beta$), in equations (2-269) and (2-270).

The improved approximation to the eigenvalue of S^2 as a result of the single annihilation may be obtained from,

$$\langle S^2 \rangle' = \frac{\langle S^6 \rangle - 2(\langle S_z \rangle + 1)(\langle S_z \rangle + 2)\langle S^4 \rangle + (\langle S_z \rangle + 1)^2(\langle S_z \rangle + 2)^2\langle S^2 \rangle}{\langle S^4 \rangle - 2(\langle S_z \rangle + 1)(\langle S_z \rangle + 2) + (\langle S_z \rangle + 1)^2(\langle S_z \rangle + 2)^2} \quad (2-272)$$

Where;

$$\langle S^2 \rangle = B - \text{Tr}\{P \otimes Q\} \quad (2-273)$$

$$\begin{aligned} \langle S^4 \rangle &= B^2 + n_\alpha n_\beta + 2(\text{Tr}\{P \otimes Q\} - \text{Tr}\{P \otimes Q P \otimes Q\}) \\ &\quad - (2B + N - 2) \cdot \text{Tr}\{P \otimes Q\} \end{aligned} \quad (2-274)$$

$$\begin{aligned} \langle S^6 \rangle &= B^3 + B n_\alpha n_\beta + n_\alpha n_\beta (2B + N - 2) \\ &\quad - (3B^2 + 3B(N-2) + (N-2)^2 + n_\alpha n_\beta + 4(n_\alpha - 1)(n_\beta - 1)) \text{Tr}\{P \otimes Q\} \\ &\quad + 2(3B + 3N - 10) (\text{Tr}^2\{P \otimes Q\} - \text{Tr}\{P \otimes Q P \otimes Q\}) \\ &\quad - 6(\text{Tr}^3\{P \otimes Q\} - 3\text{Tr}\{P \otimes Q\} \cdot \text{Tr}\{P \otimes Q P \otimes Q\} + 2\text{Tr}\{P \otimes Q P \otimes Q P \otimes Q\}) \end{aligned} \quad (2-275)$$

With,

$$B = n_\beta + \langle S_z \rangle (\langle S_z \rangle + 1) \quad (2-276)$$

When the annihilator encounters the Hamiltonian it does commute with it exactly, and the only error in the energy obtained using equation (2-269) instead of (2-259) arises from the fact that A_S is not exactly idempotent. However it has been shown that the error involved in assuming an idempotent A_S is of the order, $(E_S - E_{S+2}) C_{S+2}^2$, which is generally quite small. Thus the expression for the total energy after a single annihilation, (2-265) is still reasonably accurate.

The evaluation of equation (2-269) to find the matrices

J

and \mathbb{K} after a single annihilation involves much numerical work, but the improved approximation does give appreciably different results than those obtained in the simpler approach, equations (2-263) and (2-264).

Thus we can now calculate spin-projected results for the bond-orders, charge and spin densities, and total $\overline{\Pi}$ - energies of open-shell states that can be represented as single determinants. The importance of the spin projection varies between molecules, as will be seen in the results section. In few cases can it be said to be inconsequential. Adams, (I7I), commented that such projection was especially necessary to produce meaningful results for spin-related properties. Also the single annihilation ensures that the final wave function is a close approximation to an eigenfunction of S^2 , and thus circumvents a basic objection to the unprojected results for spin-polarized functions.

The minimization of the total $\overline{\Pi}$ -energy of a molecular state using a spin-polarized wave function which is not an exact eigenfunction of S^2 for the state, followed by spin projection is clearly a compromise. It would be better to use an exact eigenfunction of S^2 , say $\Theta_s \overline{\Phi}$, in minimizing the total energy with the Hartree-Fock equations. Such methods "Extended Hartree-Fock" procedures, give improved wave functions as we vary only the desired component in reaching a self-consistent state. In the method we have discussed the energy is minimized with respect to an impure wave function. As, however,

the main contribution to the "mixed" function is always the one we require, $C_0 \gg C_1 \gg C_2 \dots$, the selection of an eigenfunction of S^2 from the final multiplet is not a bad approximation.

Finally we note the importance of accurate spin-projection using a single annihilator. The simpler treatment assuming an idempotent and commuting annihilator gives unsatisfactory results in many cases as we shall see in some results found by both methods. The inadequacy of the simpler method is especially apparent when applied to SCF ground states. The accurate procedure markedly changes spin densities, represented by J and K , however the total bond-order matrix, $(J+K)$, is practically invariant between the two levels of approximation.

(c) Some Comments on the Spin-Polarized Method.

It seems pertinent to include a few general observations on the spin-polarized method here.

An important point to note is its advantage over both the closed-shell, and Roothaan's open-shell methods in relaxing the electron spin-pairing constraint. In the treatment of radicals the method seems especially superior, (I72), a high degree of electron correlation is taken explicitly into account. Experimental results often indicate negative spin-densities, that is apparent contributions of spin-density by closed-shell electrons, and the spin-polarized method is the only treatment to predict these simply, (I72), (I73), (I74).

These spin-densities are directly obtained from the diagonal elements of the α and β electron bond-order matrices, P and Q , and after projection, J , K ;

$$\sigma_i = (P_{ii} - Q_{ii}) \frac{1}{2\langle S_z \rangle} \quad (2-277)$$

$$f_i = (J_{ii} - K_{ii}) \frac{1}{2\langle S_z \rangle} \quad (2-278)$$

σ_i , represent the unprojected results, f_i the projected ones. $\langle S_z \rangle$ is the total z-axis spin projection of the state, for example, a radical, $\langle S_z \rangle = \frac{1}{2}$, whilst for a quartet, $\langle S_z \rangle = 3/2$.

Other methods have been used to calculate spin-densities. The Valence Bond treatment can be used to give quite good results,(I73), and the Hückel approximation has been frequently applied,(I76),(I77). Roothaan's open-shell method gives reasonable results,although this method like the more primitive Hückel approach, does not take spin-correlation directly into account and can only give positive spin-densities, as all closed-shell electrons are fully paired.

A point not yet considered is the effect of a lone π -electron on the σ -core. It would be reasonable to assume a degree of induced polarization in the σ -core due to the π -electron. Attempts have been made to include this polarization,(I78),(I79), but it is a rather uncertain effect.

Although we have been considering the spin-polarized method as applied to none closed-shell states, $n_\alpha \neq n_\beta$, the

method could equally well be used on a closed-shell ground state. Here we would expect some α and β -spin separation, as this would lead to a lower ground state energy. This spin-polarized state however does not have the full molecular symmetry, and we find after the use of an accurate annihilation, that the final pure spin state has no variations in spin-density. In fact the orbitals are exactly those we would have obtained from the spin-paired closed-shell SCF procedure. Hence the spin-polarized ground states obtained by Dewar, (53), must be viewed with this in mind, as the appropriate wave functions are not eigenfunctions of S^2 . If these functions were improved by a projection operator in the manner previously discussed, we would anticipate no resultant spin-densities or energy reductions. This will be illustrated by results in a later section.

Finally we must always remember the single annihilator technique used is only valid so long as, Δ , equation (2-247), is small. With $\Delta \gtrsim 0.3$ the procedure gives inconsistent results, and the annihilation fails to produce a close approximation to an eigenfunction of S^2 . As we shall see when discussing the results obtained for various molecules, Δ is usually small, only becoming large for ground state systems, which as we have just commented, need not be treated in this spin-polarized manner.

(I9) The Open-Shell Self-Consistent Theory of Roothaan.

(a) The SCF Equations.

This open-shell procedure represents another method of obtaining self-consistent wavefunctions for excited states, and may be used successfully on more molecular states than the previously discussed spin-polarized treatment. Roothaan considered the closed-shell and open-shell orbitals as forming two sets, with the closed-shell orbitals each containing two electrons. This spin-pairing is an added restriction on our wave function similar to that imposed in the Hartree-Fock treatment of fully closed-shell states. Normally the problem of the Lagrangian cross-multipliers between the two sets of open and closed-shell orbitals cannot be easily solved. Roothaan, however, showed how this difficulty could be circumvented for molecular states whose energy could be written in a certain general form. Here we shall follow a derivation of the Roothaan method very similar to that used in the evaluation of both the closed-shell and spin-polarized SCF Hamiltonians.

The total wave function for the system is represented as a general sum of antisymmetrized products, each containing a doubly occupied closed-shell core, $\{\phi_c\}$, and a partially occupied open-shell chosen from the set, $\{\phi_o\}$. The final wave function may be written as a combined set of orbitals, $\{\Phi\} = \{\phi_c, \phi_o\}$. The set $\{\Phi\}$ is assumed orthogonal, thus the sub-sets, $\{\phi_c\}$ and $\{\phi_o\}$ are normalized, and mutually orthogonal. The basis of the derivation is writing the total

expectation energy of the state as,

$$E = 2 \sum_K \epsilon_K^c + \sum_{K,L} (2J_{KL} - K_{KL})$$

$$+ f \left[2 \sum_m \epsilon_m^c + f \sum_{m,n} (2aJ_{mn} - bK_{mn}) + 2 \sum_{k,m} (2J_{km} - K_{km}) \right] \quad (2-279)$$

Where a , b , f , are specific constants depending on the state under consideration. In this expression, and throughout the following theoretical development K and L refer to doubly occupied orbitals in the closed-shell; m and n refer to single electron open-shell orbitals; i and j refer to any orbitals. The number f represents the fractional occupation of the open-shell, the number of available open-shell orbitals divided into those actually occupied. Only those states whose energy can be expressed as shown in equation (2-279) may be treated with this self-consistent procedure. Thus excited singlets and triplets with $\langle S_z \rangle = 0$, are not included in the theory.

For all our use $f = .5$, $a = 1$, $b = 2$.; we have half closed open-shells, with all the unpaired electrons having parallel spins. This covers all excited triplets, (With $\langle S_z \rangle = 1$), and a doublet state with a single open-shell electron. Thus the total energy becomes;

$$E = 2 \sum_K \epsilon_K^c + \sum_{K,L} (2J_{KL} - K_{KL})$$

$$+ \sum_m \epsilon_m^c + \sum_{m,n > m} (J_{mn} - K_{mn}) + \sum_{k,m} (2J_{km} - K_{km}) \quad (2-280)$$

The last term gives the open-shell/closed-shell interactions. Now to obtain our SCF equations we shall vary first the closed-shell orbitals in the field of the open-shell and the core, then turn to the open-shell, and examine it's stability to a slight variation in the field of the core and the closed-shell.

(i) Closed-Shell_Variation.

The only two energy terms changed in equation (2-279) by a first order variation in the closed-shell orbital set, $\{\phi_c\}$,

$$\phi_K \rightarrow \phi_K + \sum_{j, \neq K}^N c_{Kj} \phi_j \quad (2-281)$$

are;

$$\sum_K^{n_c} 2\varepsilon_K^c + \sum_{K,L}^{n_c} (2J_{KL} - K_{KL}) + 2f \sum_{K,m}^{n_c, n_o} (2J_{K_m} - K_{K_m})$$

The first order variation in an occupied closed-shell orbital is expanded in terms of a complete set, including the $\{\phi_c\}$ and $\{\phi_o\}$ sets. Hence to maintain orthonormality we require,

$$c_{Kj} = -c_{jK} \quad (2-282)$$

with, $1 \leq j \leq n_c + n_o$, and, $1 \leq K \leq n_c$.

Applying this first order variation to the energy terms given;

$$\begin{aligned} \varepsilon_K^c &\rightarrow \varepsilon_K^c + 2 \sum_{i, \neq K}^N c_{Ki} \varepsilon_{Ki}^c + \dots \\ J_{KL} &\rightarrow J_{KL} + 2 \sum_{i, \neq K}^N c_{Ki} \int_{LL}^{Ki} + 2 \sum_{j, \neq L}^N c_{Lj} \int_{jL}^{KK} + \dots \\ K_{KL} &\rightarrow K_{KL} + 2 \sum_{i, \neq K}^N c_{Ki} \int_{iL}^{KL} + 2 \sum_{j, \neq L}^N c_{ej} \int_{Kj}^{KL} + \dots \end{aligned}$$

$$J_{km} \rightarrow J_{km} + 2 \sum_{j, \neq k}^N c_{kj} \xi_{mm}^{kj} + \dots$$

$$K_{km} \rightarrow K_{km} + 2 \sum_{j, \neq k}^N c_{kj} \xi_{mK}^{jm} + \dots$$

(2-283)

Thus for a zero first order change in energy we require,

$$\begin{aligned} \sum_K 4 \sum_{i, \neq K} c_{Ki} \epsilon_{Ki}^c + \sum_{K, L} \left\{ 2 \left[2 \sum_{i, \neq K} c_{Ki} \xi_{LL}^{Ki} + 2 \sum_{j, \neq L} c_{Lj} \xi_{jL}^{KK} \right] \right. \\ \left. - \left[2 \sum_{i, \neq K} c_{Ki} \xi_{iL}^{KL} + 2 \sum_{j, \neq L} c_{Lj} \xi_{Kj}^{KL} \right] \right\} \\ + 2f \sum_{K, m} \left[4 \sum_{j, \neq K} c_{Kj} \xi_{mm}^{Kj} - 2 \sum_{j, \neq K} c_{Kj} \xi_{mK}^{jm} \right] = 0 \end{aligned} \quad (2-284)$$

and hence;

$$\begin{aligned} \sum_{i, \neq K} \sum_K c_{Ki} \left\{ \epsilon_{Ki}^c + \sum_L \left[2 \xi_{LL}^{Ki} - \xi_{iL}^{KL} \right] \right. \\ \left. + f \sum_m \left[2 \xi_{mm}^{Ki} - \xi_{mK}^{im} \right] \right\} = 0 \end{aligned} \quad (2-285)$$

However with the requirement expressed in equation (2-282),

in general,

$$\begin{aligned} \epsilon_{Ki}^c + \sum_L \left[2 \xi_{LL}^{Ki} - \xi_{iL}^{KL} \right] \\ + f \sum_m \left[2 \xi_{mm}^{Ki} - \xi_{mK}^{im} \right] = 0 \end{aligned} \quad (2-286)$$

with, $n_0 + n_c + 1 \leq i \leq N$; $1 \leq K, L \leq n_c$; and, $1 \leq m \leq n_0$.

Re -writing this equation we have;

$$\int \phi_i \left[H^c + \sum_L (2J_L - K_L) + f \sum_m (2J_m - K_m) \right] \phi_K d\tau = 0 \quad (2-287)$$

The result of the above operator,

$$H^c + \sum_L (2J_L - K_L) + f \sum_m (2J_m - K_m) \quad (2-288)$$

on one of the closed-shell set can be expanded in terms of the complete set;

$$\left[H^c + \sum_L (2J_L - K_L) + f \sum_m (2J_m - K_m) \right] \phi_K = \sum_{j=1}^N \epsilon_{Kj} \phi_j \quad (2-289)$$

Hence;

$$\langle \phi_i | H^c + \sum_L (2J_L - K_L) + f \sum_m (2J_m - K_m) | \phi_K \rangle = \epsilon_{Ki} \quad (2-290)$$

But from our SCF conditions we have $\epsilon_{Ki} = 0$ for, $1 \leq K \leq n_c$, $n_o + n_c + 1 \leq i \leq N$, thus we finally obtain;

$$\left[H^c + \sum_L (2J_L - K_L) + f \sum_m (2J_m - K_m) \right] \phi_K = \sum_i^{n_c + n_o} \epsilon_{Ki} \phi_i \quad (2-291)$$

(ii) Open-Shell Variation.

To derive the self-consistent equations for the open-shell orbitals in the field of the core and the closed-shell electrons, we need to consider the effect of a first order variation in the orbitals on the terms in the total energy expression,

$$f \left[\sum_m 2\epsilon_m^c + f \sum_{m,n} (2a J_{mn} - b K_{mn}) + 2 \sum_{K,m} (2J_{Km} - K_{Km}) \right]$$

Writing our first order variation as ,

$$\phi_m \rightarrow \phi_m + \sum_{i, \neq m}^N c_{mi} \phi_i \quad (2-292)$$

$\{\phi_i\}$ are members of the complete set, and from the orthogonality requirements we find,

$$c_{mi} = -c_{im} \quad (2-293)$$

for, $1 \leq i \leq n_o + n_c$, and, $1 \leq m \leq n_o$. The effect of this first order variation in the energy terms is;

$$\begin{aligned} E_m^c &\rightarrow E_m^c + 2 \sum_{i, \neq m} c_{mi} E_{mi}^c + \dots \\ J_{mn} &\rightarrow J_{mn} + 2 \sum_{i, \neq m} c_{mi} \xi_{nn}^{mi} + 2 \sum_{j, \neq n} c_{nj} \xi_{nj}^{mn} + \dots \\ K_{mn} &\rightarrow K_{mn} + 2 \sum_{i, \neq m} c_{mi} \xi_{in}^{mn} + 2 \sum_{j, \neq n} c_{nj} \xi_{nj}^{mn} + \dots \\ J_{km} &\rightarrow J_{km} + 2 \sum_{i, \neq m} c_{mi} \xi_{mi}^{kk} + \dots \\ K_{km} &\rightarrow K_{km} + 2 \sum_{i, \neq m} c_{mi} \xi_{km}^{ik} + \dots \end{aligned} \quad (2-294)$$

Requiring there be no energy change for this variation we have,

$$\begin{aligned} 4f \left\{ \sum_m \sum_{i, \neq m} c_{mi} E_{mi}^c + f \sum_{m, n} \left[a \sum_{i, \neq m} c_{mi} \xi_{nn}^{mi} + \sum_{j, \neq n} c_{nj} \xi_{nj}^{mn} \right] - \frac{g}{2} \left[\sum_{i, \neq m} c_{mi} \xi_{in}^{mn} + \sum_{j, \neq n} c_{nj} \xi_{mj}^{mn} \right] \right. \\ \left. + \sum_{k, m} \left[2 \sum_{i, \neq m} c_{mi} \xi_{mi}^{kk} - \sum_{i, \neq m} c_{mi} \xi_{km}^{ik} \right] \right\} = 0 \end{aligned} \quad (2-295)$$

Thus we find finally;

$$f \sum_m \sum_{i \neq m} c_{mi} \left\{ \epsilon_{mi}^c + f \sum_n (2a \xi_{nn}^{mi} - b \xi_{in}^{mn}) + \sum_k (2 \xi_{mi}^{kk} - \xi_{km}^{ik}) \right\} = 0 \quad (2-296)$$

From the orthonormality conditions applying to the coefficients given in equation (2-293), we have in general,

$$f \left\{ \epsilon_{mi}^c + f \sum_n (2a \xi_{nn}^{mi} - b \xi_{in}^{mn}) + \sum_k (2 \xi_{mi}^{kk} - \xi_{km}^{ik}) \right\} = 0 \quad (2-297)$$

with, $n_0 + n_c + 1 \leq i \leq N$; $1 \leq m, n \leq n_0$; and, $1 \leq k \leq n_c$.

Proceeding analogously to the closed-shell development,

equations (2-289) to (2-29I), we find;

$$f \left[H^c + \sum_k (2J_k - K_k) + f \sum_n (2a J_n - b K_n) \right] \phi_m = \sum_e^{n_c} \epsilon_{me} \phi_e + \sum_n^{n_0} \epsilon_{mn} \phi_n \quad (2-298)$$

where the effective Hamiltonian is,

$$\left[H^c + \sum_k (2J_k - K_k) + f \sum_n (2a J_n - b K_n) \right] \quad (2-299)$$

(iii) Transformation into an Effective Eigenvalue Problem.

As we have seen in the derivation of the self-consistent equations for both the closed and open-shell orbitals we have the problem of the Lagrangian multipliers, $\{\epsilon_{me}\}$ and $\{\epsilon_{mn}\}$. Here we have multipliers involving both open and closed-shells, and as the two sets of orbitals can only be transformed within themselves,

$$\phi'_c = \phi_c \cdot U_c \quad \phi'_o = \phi_o \cdot U_o \quad (2-300)$$

we cannot diagonalize the Lagrangian matrix completely using such a single unitary transform as we did for the closed-shell and spin-polarized methods. We can only diagonalize the open or closed-shell coefficients separately, no general transform is available to totally diagonalize our \mathcal{E} matrix.

Hence Roothaan devised a method to solve this problem, and to obtain a pseudo-eigenvalue equation for both the open and closed-shell cases. This is now given, but first we must define some new operators, Coulomb and exchange terms;

$$\begin{aligned} J_c &= \sum_K J_K & J_o &= f \sum_m J_m \\ K_c &= \sum_K K_K & K_o &= f \sum_m K_m \\ J_T &= J_o + J_c & K_T &= K_o + K_c \end{aligned} \quad (2-301)$$

and coupling operators, between the closed and open-shells;

$$\begin{aligned} L_i \phi &= \langle \phi_i | J_o | \phi \rangle \phi_i + \langle \phi_i | \phi \rangle J_o \phi_i \\ m_i \phi &= \langle \phi_i | K_o | \phi \rangle \phi_i + \langle \phi_i | \phi \rangle K_o \phi_i \\ L_c &= \sum_K L_K & L_o &= f \sum_m L_m \\ m_c &= \sum_K m_K & m_o &= f \sum_m m_m \\ L_T &= L_c + L_o & m_T &= m_o + m_c \end{aligned}$$

Hence we can now write our closed and open-shell equations as,

$$[H^c + 2J_c - K_c + 2J_o - K_o] \phi_k = \sum_L \epsilon_{kL} \phi_L + \sum_n \epsilon_{kn} \phi_n \quad (2-303)$$

$$f[H^c + 2J_c - K_c + 2\alpha J_o - \beta K_o] \phi_m = \sum_L \epsilon_{mL} \phi_L + \sum_n \epsilon_{mn} \phi_n \quad (2-304)$$

If we multiply equation (2-303) by ϕ_m^* , and (2-304) by ϕ_k^* we obtain, on integration,

$$\langle \phi_m | H^c + 2J_c - K_c + 2J_o - K_o | \phi_k \rangle = \epsilon_{km} \quad (2-305)$$

$$f \langle \phi_k | H^c + 2J_c - K_c + 2\alpha J_o - \beta K_o | \phi_m \rangle = \epsilon_{mk} \quad (2-306)$$

The Lagrangian matrix ϵ is Hermitian however, so $\epsilon_{km} = \epsilon_{mk}$, hence from multiplying (2-305) by $\frac{-f}{1-f}$ and (2-306) by $\frac{1}{1-f}$, on adding we find,

$$\epsilon_{mk} = -f \langle \phi_m | 2\alpha J_o - \beta K_o | \phi_k \rangle \quad (2-307)$$

where, $\alpha = \frac{1-a}{1-f}$, and, $\beta = \frac{1-g}{1-f}$. For the closed-shell equation we can express the Lagrangians of the open-shell as,

$$\sum_n \epsilon_{kn} \phi_n = -f \sum_n \phi_n \langle \phi_k | 2\alpha J_o - \beta K_o | \phi_n \rangle \quad (2-308)$$

and using the coupling operators defined earlier we find,

$$\sum_n \epsilon_{kn} \phi_n = - (2\alpha L_o - \beta M_o) \phi_k \quad (2-309)$$

Similarly we can show,

$$\sum_L \epsilon_{mL} \phi_L = -f (2\alpha L_c - \beta M_c) \phi_m \quad (2-310)$$

Thus for our open and closed-shell equations, (2-304) and (2-303), we can now write, after the addition of (2-310) and (2-309), respectively ;

$$\begin{aligned} [H^c + 2J_c - K_c + 2J_o - K_o + 2\alpha L_o - \beta m_o] \phi_K \\ = F^c \phi_K = \sum_L \epsilon_{KL} \phi_L \end{aligned} \quad (2-311)$$

and,

$$\begin{aligned} f[H^c + 2J_c - K_c + 2\alpha J_o - \beta K_o + 2\alpha L_c - \beta m_c] \phi_m \\ = f F^o \phi_m = \sum_n \epsilon_{mn} \phi_n \end{aligned} \quad (2-312)$$

F^c and F^o are the new closed and open shell effective Hamiltonians, defined in these equations, and do not exactly correspond to the original operators, (2-288) and (2-299).

Now we can use the available unitary transforms, given in equation (2-300), to diagonalize the open and closed-shell \mathcal{E} matrices, and obtain our eigenvalue problems;

$$F^c \phi_K = \epsilon_K \cdot \phi_K \quad (2-313)$$

$$F^o \phi_m = \frac{\epsilon_m}{f} \cdot \phi_m = \epsilon'_m \phi_m \quad (2-314)$$

There is little analogy between ϵ_K and ϵ'_m and the closed-shell SCF orbital energies. When we find the eigenvalues of the F^c and F^o operators, the first n_c of F^c refer to occupied closed-shell orbitals. For F^o , the valid eigenvalues are those belonging to the roots beginning $n_c + 1$ through to $n_o + n_c$, the orbitals lower than $n_c + 1$ might be expected to resemble the closed-shell ones as F^c and F^o are quite similar.

There would be an obvious advantage in reducing the solution of the system F^c and F^o to a single eigenvalue problem. This is indeed possible if we add to the closed-shell equation,

$$[2\alpha(L_c - J_o) - \beta(m_c - K_o)]\phi_K = \sum_L \phi_L \xi_{KL} \quad (2-315)$$

where we derive ξ_{KL} using the operators previously defined;

$$\xi_{KL} = \sum_L \langle \phi_L | 2\alpha J_o - \beta K_o | \phi_K \rangle \quad (2-316)$$

Hence we find,

$$[F^c + 2\alpha(L_c - J_o) - \beta(m_c - K_o)]\phi_K = \sum_L \epsilon_{KL} \phi_L + \sum_L \xi_{KL} \phi_L \quad (2-317)$$

and,

$$F\phi_K = \sum_L (\epsilon_{KL} + \xi_{KL}) \phi_L \quad (2-318)$$

where;

$$F = H^c + 2J_T - K_T + 2\alpha(L_T - J_o) - \beta(m_T - K_o) \quad (2-319)$$

Thus an eigenvalue is finally obtained,

$$F\phi_K = \epsilon_K \phi_K \quad (2-320)$$

where \mathcal{E} represents a column matrix, as we have diagonalized $\{\mathcal{E} + \mathcal{S}\}$ with an appropriate transform.

Similarly, if we add to the open-shell Hamiltonian

F^o , defined in equation (2-312), the equation,

$$[2\alpha(L_o - fJ_o) - \beta(m_o - fK_o)]\phi_m = \sum_n \phi_n \xi_{nm} \quad (2-321)$$

with,

$$\xi_{nm} = f \langle \phi_m | 2\alpha J_o - \beta K_o | \phi_n \rangle \quad (2-322)$$

we obtain the same form for our total Hamiltonian as in the closed-shell case,

$$F = F^{\circ} + 2\alpha(L_0 - fJ_0) - \beta(M_0 - fK_0) \quad (2-323)$$

and if we diagonalize the open-shell matrix, $\mathcal{E} + \mathcal{S}$, we obtain the same eigenvalue problem as before,

$$F \phi_m = \epsilon_m \phi_m \quad (2-324)$$

Thus to find all our orbitals we need to solve;

$$F \phi = \mathcal{E} \phi \quad (2-325)$$

\mathcal{E} is a diagonal matrix of eigenvalues. The set, $\{\phi\}$, satisfying this equation is equivalent to $\{\phi_m\}$ and $\{\phi_L\}$ satisfying F° and F^c , the two sets being related by a unitary transform. Also the eigenvalues \mathcal{E} will in general be different from \mathcal{E}° and \mathcal{E}^c . These values of $\{\mathcal{E}\}$ cannot be identified in any way with orbital energy in the Koopman approximation. The total energy for the system is given by,

$$E = \sum_K (H_K + \epsilon_K) + f \sum_m (H_m + \epsilon_m) - f \sum_{k,m} (2\alpha J_{km} - \beta K_{km}) - f^3 \sum_{m,n} (2\alpha J_{mn} - \beta K_{mn}) \quad (2-326)$$

As we have now formulated the open-shell SCF procedure, we must consider what basis functions and approximations we are going to use to obtain F in tractable form.

(b) Open-Shell SCF Matrix Elements.

In the Roothaan approximation used here we expand the basis functions, $\{\phi_i\}$, which are the molecular orbitals of the system, in terms of an orthogonalized atomic orbital set;

$$\phi_i = \sum_p c_{ip} \chi_p = c_i \chi \quad (2-327)$$

We assume orthogonality, hence;

$$c_i^+ c_j = \delta_{ij} \quad (2-328)$$

For convenience we normalize the vector c_i to half the number of electrons contained in the orbital i it represents,

$$\begin{aligned} c_k^+ c_l &= \delta_{kl} & c_k^+ c_m &= 0 \\ c_m^+ c_n &= f \delta_{mn} \end{aligned} \quad (2-329)$$

Roothaan derived the expression for the open-shell Hartree-Fock Hamiltonian as, (I34),

$$F = H + P - Q + R \quad (2-330)$$

with the corresponding eigenvalue problem;

$$F c_i = \epsilon_i c_i \quad (2-331)$$

The component matrices of F , equation (2-330), are defined as follows;

H is the core integral term, and in the Goeppert-Mayer and Sklar approximation may be obtained from equations (2-I03).

P is given by,

$$P = (2J - K) D^T \quad (2-332)$$

where D^T refers to the total density matrix,

$$D^T = D^c + D^o \quad (2-333)$$

with;

$$D_{ij}^c = \sum_k C_{ki} C_{kj} \quad (2-334)$$

$$D_{ij}^o = \sum_m C_{mi} C_{mj} \quad (2-335)$$

We note also that,

$$D^o D^c = 0$$

J and K are supermatrices, with elements defined by;

$$J_{pq:rs} = \langle pq | rs \rangle \quad (2-336)$$

$$K_{pq:rs} = \langle ps | rq \rangle \quad (2-337)$$

Hence the elements of P are given by,

$$P_{pq} = \sum_{r,s} (2 \langle pq | rs \rangle - \langle ps | rq \rangle) D_{sr}^T \quad (2-338)$$

With the Pople-Pariser-Parr approximation we neglect differential overlap, and obtain;

$$P_{pp} = \sum_{r \neq p} 2 \langle pp | rr \rangle D_{rr}^T + \langle pp | pp \rangle D_{pp}^T \quad (2-339)$$

$$P_{pq} = - \langle pp | qq \rangle D_{pq}^T \quad (2-340)$$

Q is closely analogous to P ;

$$Q = (2\alpha J - \beta K) D^o \quad (2-24I)$$

and with neglect of differential overlap we find;

$$Q_{pp} = 2\alpha \sum_{r \neq p} \langle pp | rr \rangle D_{rr}^o + (2\alpha - \beta) D_{pp}^o \langle pp | pp \rangle \quad (2-342)$$

$$Q_{pq} = -\beta \langle pp | qq \rangle D_{pq}^o \quad (2-343)$$

R . In the zero overlap approximation we have,

$$R = D^T Q + Q D^T \quad (2-344)$$

and hence;

$$R_{pq} = \sum_r D_{pr}^T Q_{rq} + \sum_r Q_{pr} D_{rq}^T \quad (2-345)$$

$$R_{pp} = 2 \sum_r D_{pr}^T Q_{rp} \quad (2-346)$$

Thus we have all the matrix elements necessary to evaluate F . After obtaining the required degree of self-consistency in the iterative process , we can find the total energy , with;

$$E = \text{Tr} \left\{ (H + F) D_T - Q (D^c + f D^o) \right\} \quad (2-347)$$

(c) Comments on Roothaan's Open-Shell Method.

The open-shell procedure of Roothaan is simpler in execution than the spin-polarized method. We do not have to iterate two coupled Hamiltonians to self-consistency as in the latter . The use of spin-pairing in the closed-shell orbitals facilitates this, in the spin-polarized method all the spin-orbitals have different spatial dependence, as well as opposite spin functions.

The restriction of spin-pairing does, however, result in the introduction of a correlation error. This spin correlation is relieved to a certain extent by using an antisymmetrized wave function, but it is certainly not explicitly

accounted for.

Wave functions obtained with Roothaan's procedure are automatically eigenfunctions of S^2 , and so we do not need to consider any spin-projection techniques to obtain a valid state function.

As well as being numerically simpler than the spin-polarized method, the Roothaan procedure has the advantage of converging for states which have un-occupied orbitals at lower energies, (these are virtual orbitals), than the highest unpaired electron. The spin-polarized method could not be persuaded to converge in such circumstances.

(20) Self-Consistent Wave Functions for Polymeric Systems.

In this discussion of π -electronic polymer wave functions, we shall limit ourselves to one-dimensional chains of conjugated monomers. Such macromolecules are clearly analogous to one-dimensional crystals, and we use solid-state theory to calculate the energy levels and wave functions of the system. We shall only consider the delocalization of the π -electrons, the σ -core of each monomer will not be explicitly involved, although it may be allowed for by the use of semi-empirical parameters.

The important simplifying factor in any one-dimensional linear array of identical molecules is the translational symmetry present in such a structure. We shall deal only with perfectly periodic systems, in which a repeated

unit cell can be defined. We shall neglect "end-effects", assuming our polymer to contain a large number of monomers. The simple LCAO-MO Crystal Orbital method will be used, and the Pople-Pariser-Parr approximations introduced to simplify the final equations. We only take into account "nearest-neighbour" interactions between the monomers.

Representing the one electron polymer wave function as $\Psi_{p,\ell}$, we have an eigenvalue problem of the type,

$$F \Psi_{p,\ell} = E_{\ell}(\rho) \Psi_{p,\ell} \quad (2-348)$$

Where F is some effective Hamiltonian, for either Hückel or SCF approximations, (I66). ρ indicates the wave number of the Bloch orbital, and ℓ is the band-index. If N is the number of unit cells, and n the number of atoms with $2p_z$ orbitals per cell, then for these integers we have,

$1 \leq \rho \leq N$, and, $1 \leq \ell \leq n$. This approximation of the crystal orbitals, $\Psi_{p,\ell}$, by delocalized Bloch functions allows complete electron exchange over the whole polymer.

If we expand the orbital $\Psi_{p,\ell}$ in a linear combination of the atomic orbitals of the whole polymer, (I80), then,

$$\Psi_{p,\ell} = \sum_m^N \sum_j^n c_{p,\ell:m,j} \chi_{mj} \quad (2-349)$$

In this π -electron approximation χ_{mj} represents the $2p_z$ orbital of the j -th atom in the m -th unit cell. From the

translational symmetry of the one-dimensional chain, with \vec{a} as the primitive translation vector, we can write;

$$\chi_{mj} = \chi_j (\vec{r}_j - m \vec{a}) \quad (2-350)$$

where \vec{r}_j is the distance from the j -th atom in the first unit cell, thus,

$$\Psi_{p,\ell} = \sum_m \sum_j c_{p,\ell:mj} \chi_j (\vec{r}_j - m \vec{a}) \quad (2-351)$$

We now use the Born-Von Karman Boundary Condition, joining our "infinite" chain at the first and the last elementary cell. Thus we have a cyclic chain, and;

$$\Psi_{p,\ell}(\vec{r}) = \Psi_{p,\ell}(\vec{r} + N \vec{a}) \quad (2-352)$$

This means our wave function must have the same value after

N translations. Using this we derive the Bloch condition, (181);

$$c_{p,\ell:mj} = \exp\left(\frac{2\pi i m p}{N}\right) c_{p,\ell:j} \quad (2-353)$$

As N is very large, we can introduce a continuous variable,

k , such that,

$$k = \frac{2\pi p}{N} \quad (2-354)$$

with, $0 \leq k \leq 2\pi$. Hence we find;

$$c_{p,\ell:mj} = \exp(i k m) c_{p,\ell:j} \quad (2-355)$$

Altering our notation, as p is a function of k , we can write,

$$c_{p,\ell:m,j} = \exp(i k m) c_{\ell,j}(k) \quad (2-356)$$

and our polymer wave function is represented as ,

$$\Psi_{\ell}(k) = \sum_m^N \sum_j^n c_{\ell,j}(k) \cdot \exp(ikm) \chi_{mj} \quad (2-357)$$

If we consider the derivation of a general matrix element obtained from an effective Hamiltonian F , we multiply the equation;

$$F \sum_{m,j} c_{\ell,j}(k) \exp(ikm) \chi_{mj} = E_{\ell}(k) \sum_{m,j} c_{\ell,j}(k) e^{ikm} \chi_{mj} \quad (2-358)$$

by say $\chi_{m'j'} e^{-ikn'}$ on both sides, and integrate;

$$\sum_{m,j} c_{\ell,j}(k) e^{ik(m-m')} \langle \chi_{m'j'} | F | \chi_{mj} \rangle = E_{\ell}(k) \sum_{m,j} c_{\ell,j}(k) e^{ik(m-m')} \langle \chi_{m'j'} | \chi_{mj} \rangle \quad (2-359)$$

Assuming an orthogonalized basis of atomic orbitals we find,

$$\sum_{m,j} c_{\ell,j}(k) e^{ik(m-m')} \langle \chi_{m'j'} | F | \chi_{mj} \rangle = E_{\ell}(k) c_{\ell,j'}(k) \quad (2-360)$$

But the sum,

$$\sum_m e^{ik(m-m')} \langle \chi_{m'j'} | F | \chi_{mj} \rangle = F'_{jj'}(k) \quad (2-361)$$

is independent of m' , so we can write, with $F'_{jj'}$ representing the "lattice sum" term,

$$\sum_j c_{\ell,j}(k) F'_{jj'}(k) = E_{\ell}(k) c_{\ell,j'}(k) \quad (2-362)$$

So we have reduced our series of $N \times n$ secular equations to just the set n , which we can evaluate to find our eigenvectors. Clearly in a SCF procedure, we use these to build a new F' matrix, and continue iterations until self-consistency.

Ladik and co-workers have obtained expressions for the SCF matrix elements, $F_{jj}'(\mathbf{k})$, using the LCAO-MO and nearest neighbour approximations, with a limited basis set of n atomic orbitals as in the Roothaan method, (182).

With the Pople-Pariser-Parr approximation it is found, (183);

$$\begin{aligned}
 F_{LL}(\mathbf{k}) = & -I_L + \frac{1}{2} P_{LL} (I_L - E_L) \\
 & + \sum_{s \neq L}^n (P_{ss} - Z_s) \gamma_{Ls} + \sum_s^n (P_{ss} - Z_s) (\gamma_{Ls}^+ + \gamma_{Ls}^-) \\
 & + \beta_{LL}^+ e^{i\mathbf{k}} + \beta_{LL}^- e^{-i\mathbf{k}} - \frac{1}{2} P_{LL}^+ \gamma_{LL}^+ e^{i\mathbf{k}} - \frac{1}{2} P_{LL}^- \gamma_{LL}^- e^{-i\mathbf{k}}
 \end{aligned}
 \tag{2-363}$$

and the off diagonal elements are,

$$\begin{aligned}
 F_{Ls}(\mathbf{k}) = & \beta_{Ls}^c - \frac{1}{2} P_{Ls} \gamma_{Ls} - \frac{1}{2} P_{Ls}^+ \gamma_{Ls}^+ e^{i\mathbf{k}} \\
 & - \frac{1}{2} P_{Ls}^- \gamma_{Ls}^- e^{-i\mathbf{k}} + \beta_{Ls}^+ e^{i\mathbf{k}} + \beta_{Ls}^- e^{-i\mathbf{k}}
 \end{aligned}
 \tag{2-364}$$

In these expressions;

$$\beta_{Ls}^{\pm} = \int \chi_L^*(\vec{r}_L - j\vec{a}) \cdot H^c \chi_s(\vec{r}_s - (j \pm 1)\vec{a}) d\tau
 \tag{2-365}$$

$$\begin{aligned}
 \gamma_{Ls}^{\pm} = & \iint \chi_L^*(1; \vec{r}_L - j\vec{a}) \chi_L(1; \vec{r}_L - j\vec{a}) \cdot \frac{1}{r_{12}} \\
 & \chi_s^*(2; \vec{r}_s - (j \pm 1)\vec{a}) \chi_s(2; \vec{r}_s - (j \pm 1)\vec{a}) d\tau_1 d\tau_2
 \end{aligned}
 \tag{2-366}$$

Where $\chi_L(\vec{r} - j\vec{a})$ is the atomic orbital centred on the L -th atom of the j -th elementary unit cell. These quantities represent interactions between nearest neighbours, and hence the

superscript + or - indicates interaction with a cell on the right(+), or the unit cell on the left(-). Thus with β^{\pm} and γ^{\pm} matrices representing the inter-unit cell interactions, the intra-unit cell interactions arise as the familiar terms in the Pople-Pariser-Parr molecular SCF method. For our helical polymers we have, $\beta_{LS}^+ = \beta_{SL}^-$, and $\gamma_{LS}^+ = \gamma_{SL}^-$, the two matrices giving the resonance binding and Coulomb-exchange terms between each cell and its neighbours. In the Hückel approximation the F matrix elements are much simpler, (I84),(I85).

The bond-order matrices are defined as,

$$P_{L,S} = \frac{1}{\pi} \sum_{\tau} \int_0^{2\pi} C_{\tau L}^*(k) C_{\tau S}(k) dk. \quad (2-367)$$

$$P_{L,S}^{\pm} = \frac{1}{\pi} \sum_{\tau} \int_0^{2\pi} C_{\tau L}^*(k) C_{\tau S}(k) e^{\pm ik} dk. \quad (2-368)$$

All the elements of P^0 and P^{\pm} are real, and whilst the first is symmetric, $P_{LS} = P_{SL}$, we find for the inter-unit cell interaction matrices, $P_{LS}^+ = P_{SL}^-$. As we see in the definitions of P and P^{\pm} we need to know $C_{\ell}(k)$ for any band ℓ , in order to perform the integration over k . Our eigenvalue problem,

$$F(k) C_{\ell}(k) = E_{\ell}(k) C_{\ell}(k) \quad (2-369)$$

must thus either be solved for $E_{\ell}(k)$ with C_{ℓ} derived as an

analytic function of K , or we can solve for various values of K , and interpolate for results between established points. This latter is the only possibility considered here, so the integrals in P and P^\pm , equations (2-367) and (2-368), become numerical integrals.

The complex eigenvalue problem can be solved by partitioning the matrix F into real and imaginary parts, then;

$$\begin{bmatrix} \text{Real}(F) & -\text{Imag}(F) \\ \text{Imag}(F) & \text{Real}(F) \end{bmatrix} \begin{bmatrix} U_\ell \\ V_\ell \end{bmatrix} = \epsilon_\ell \begin{bmatrix} U_\ell \\ V_\ell \end{bmatrix} \quad (2-370)$$

Where F , U , V , and ϵ_ℓ are all functions of K .

$U_\ell(k)$ is the real and $V_\ell(k)$ the imaginary component of the complex column vector, $C_\ell(k)$. The eigenvalue problem dimensioned $2n \times 2n$ is degenerate, the roots $\epsilon_\ell(k)$ arising in pairs, with respective eigenvectors $U_\ell + iV_\ell$, and $i(U_\ell + iV_\ell)$, or $-i(U_\ell + iV_\ell)$. Hence we can express an element of $C_\ell(k)$ as, $C_{\ell i}(k) = U_{\ell i}(k) + iV_{\ell i}(k)$, the i indicating the matrix element.

If we cycle the process, after an initial choice of

P and P^\pm , and provide the parameters, \mathcal{I} , \mathcal{E} , \mathcal{Z} , \mathcal{O} , \mathcal{O}^\pm , \mathcal{B} , \mathcal{B}^\pm , we can thus obtain the energy band structure of a one dimensional polymer. The \mathcal{O}^\pm matrix is easily constructed if we know the geometry of the polymer, but the inter-molecular resonance terms in \mathcal{B}^\pm must be evaluated more carefully. We require to know the overlap terms between the

$2p_z$ orbitals on the atoms in the different unit cells. This will be discussed in more detail when the results of some calculations are presented

CHAPTER III.

Four Semi-empirical SCF Computer Programs.

(I) Introduction.

In this chapter four computer programs are presented for the solution of π -electron self-consistent field problems. These programs represent precise and complete procedures for solving the many sets of equations and individual relations encountered in the previous chapter. The language used to express these algorithms is the electronic computer code, FORTRAN IV. After the FORTRAN source program has been compiled into basic machine instructions, all that is required to examine a particular molecule, or set of molecules, in the programmed approximation is the appropriate input data. Thus the systematic study of a whole series of conjugated molecules, or the effect of parameter variations on a single molecule, may be readily achieved.

As all the programs are written in the semi-empirical Pople-Pariser-Parr approximation they are relatively simple, and require little input data. The main block of data for a given molecule is common to all the first three programs, the last program, treating polymers, requires special consideration. This data block is sandwiched between cards supplying additional control information concerning the execution of a particular program.

This common data is first the geometric matrix, R,

specifying interatomic distances. Then follow the ionization potential, I , electron affinity, E , and virtual charge, Z , for the constituent atoms. Finally the Hückel matrix of core integrals, H , $H_{pq} = \langle \chi_p | H | \chi_q \rangle$, is required. Typical values of these parameters were discussed in chapter II, and individual quantities may be obtained from chapter IV.

In reading the symmetrical doubly dimensioned matrices, H and R , only the elements of the upper triangle are required. Most data is read as one item per card, the use of such an uneconomic format is to facilitate rapid data preparation and checking.

The Mataga and Nishimoto approximation has been used for all Coulomb integrals, (I24), although some programs have options for multiplying these values by constant coefficients.

The matrix diagonalization and eigenvector routines were obtained from the IBM-Share Library at Imperial College, (I86), (I87). These routines have been modified to various extents, and in the case of degenerate roots, the gradients method is used to give orthogonal vectors, (I88), (I89).

It should be noted that the first three programs are all dimensioned for molecules of 30 constituent π -electron atoms or less. The polymer program only treats polymers composed of monomers with up to 20 atoms per unit cell. The variable identifiers used in discussing data input are in general those used within the programs, although this may not always be the case,

as frequently overwriting is necessary to economize on storage space.

In the following description of input forms, all matrices have their size specified in brackets, for example $H(N,N)$, and $Z(N)$. Also all formats are indicated for individual variables, and variable lists. Input enclosed in slashes, for example, $/H(N,N)/$, represents a whole sequence of data cards, the absence of slashes implies a single input card.

In the next sections the programs are presented. It is hoped that they will prove useful to others who are interested in conjugated systems. Such users may of course wish to introduce their own modifications and improvements.

(2) The Closed-Shell SCF Program, with Configuration Interaction for Excited States.

This program treats closed-shell ground-state conjugated molecules in the self-consistent spin-paired Pople-Pariser-Parr approximation, outlined in sections (II) to (I4) of chapter II. Configuration interaction is used to obtain excited states.

Hückel orbitals are utilized as the starting point of the SCF iterations, directed at finding the self-consistent doubly occupied ground-state orbitals. The orbitals are found to a degree of consistency determined by the variation in the elements of the bond-matrix, P , between successive iterations. The total π -energy of the system is calculated at each SCF iteration, indicating the convergence of the state.

When a self-consistent state has been achieved, or the program has run out of its specified number of SCF iterations, the π -contribution to the dipole moment of the molecule is calculated, and the excited singlet and triplet states found. These single electron excited states are found both with and without configuration interaction, (see section (I4b) of chapter II). The degree of interaction invoked is determined by the input control cards, NU and NL. In addition the intensities of the electronic transitions are calculated, (see section (I4b) of chapter II).

The input data is now specified in the required sequence, with a description of the various options available.

NI,(I3): This control card is used in subroutine RITE to label any write statements to be compiled. Usually, however, as shown in the following program the title is read in execution time as an item of data.

Program Title,(Free Format): The contents of this card are printed at the head of the computer printout. This serves to identify a particular program.

N,(I3): This is the number of π -donating atoms in the molecule, with the restriction, $N \leq 30$.

NIT,(I3): The maximum number of SCF iterations allowed.

If matrix P has not converged to the required extent after NIT iterations, the program prints out all results, and then reads N2, (see later); usually $NIT \leq I2$.

NF,(I3): The number of doubly occupied orbitals, half the total number of electrons.

NU,(I3): Upper limit of virtual orbitals to be included in the configuration interaction. Orbitals are labelled from the lowest upwards. We require $NU \leq N$, and an additional restriction is given below.

NL,(I3): Lower limit of configuration interaction; with restrictions, $NF \geq NL \geq I$, and $(NF-NL+I)*(NU-NF) \leq 30$.

CONV,(F20.8): Convergence requirement. Program regards a self-consistent state as being achieved when successive P matrices do not differ by more than CONV for all corresponding elements, that is,

$$\left| P_{ij}^n - P_{ij}^{n+1} \right| \leq \text{CONV} \quad 1 \leq i, j \leq N$$

A typical value of CONV is 0.001.

/R(N,N),AI(N),E(N),Z(N),H(N,N)/,(F20.8): This is the block data common to all the first three programs. Only the upper triangles of the geometric matrix, R, and the Hückel matrix, H, are read. For example the matrix R is presented as; $R_{11}, R_{12} \dots R_{1N}$; $R_{22}, R_{23}, \dots R_{2N}$; $R_{33}, \dots R_{3N}$; and so on, a total of $N(N+1)/2$ cards.

N2,(I3): This is the final card read by the program, after either stopping because NIT iterations were exceeded, or a SCF state obtained. If $N2=1$, the program restarts, reading in another set of data. When $N2 \neq 1$, computation ends.

\$IBFTC DECK1 DECK

DECK1 - EFN SOURCE STATEMENT - IFN(S) -

DIMENSION AI(30),E(30),Z(30),BETA(30,30),GAMA(30,30),
1 EN(30),P(30,30),Q(30,30),F(30,30),C(30,30),H(30,30),AA(30,30)
2 ,COORDX(30),COORDY(30),COORDZ(30)

C MOLECULE,CLOSED SHELL SCF

1 READ(5,2) N1

C N1 LABELS THE TITLE REQUIRED

CALL RITE(N1)

READ(5,2) N

C N LABELS NUMBER OF ATOMS IN MOLECULE

READ(5,2) NIT

2 FORMAT(I3)

READ(5,2) NF

C NUMBER OF FILLED LEVELS

READ(5,2) NU

READ(5,2) NL

READ(5,4) CONV

DO 3 I=1,N

DO 3 J=1,N

READ(5,4) C(I,J)

3 C(J,I)=C(I,J)

C C IS THE GEOMETRIC MATRIX

4 FORMAT(F20.8)

READ(5,4) (AI(I),I=1,N)

READ(5,4) (E(I),I=1,N)

READ(5,4) (Z(I),I=1,N)

DO 5 I=1,N

DO 5 J=1,N

READ(5,4) H(I,J)

BETA(I,J)=H(I,J)

BETA(J,I)=H(I,J)

5 H(J,I)=H(I,J)

DO 6 I=1,N

6 BETA(I,I)=0.0

CALL XYZ(C,COORDX,COORDY,COORDZ,N)

WRITE(6,7)

7 FORMAT(14H HUCKEL MATRIX, //)

DO 8 I=1,N

8 WRITE(6,9) (H(I,J),J=1,N)

9 FORMAT(12F8.3)

WRITE(6,10)

10 FORMAT(1H ,///,21H IONIZATION POTENTIAL, //)

WRITE(6,9) (AI(I),I=1,N)

WRITE(6,11)

11 FORMAT(1H ,///,18H ELECTRON AFFINITY, //)

WRITE(6,9) (E(I),I=1,N)

WRITE(6,12)

12 FORMAT(1H ,///,14H R(I,J) MATRIX, //)

DO 13 I=1,N


```
13 WRITE(6,9) (C(I,J),J=1,N)
   WRITE(6,902)
902 FORMAT(1H ,///,9H X COORDS,/)
   WRITE(6,9) (COORDX(I),I=1,N)
   WRITE(6,903)
903 FORMAT(1H ,///,9H Y COORDS,/)
   WRITE(6,9) (COORDY(I),I=1,N)
   WRITE(6,900)
900 FORMAT(1H ,///,9H Z COORDS,/)
   WRITE(6,9) (COORDZ(I),I=1,N)
   WRITE(6,14)
14 FORMAT(1H ,///,17H RESONANCE MATRIX,/)
   DO 15 I=1,N
15 WRITE(6,9) (BETA(I,J),J=1,N)
   WRITE(6,16)
16 FORMAT(1H ,///,23H NUMBER OF PI ELECTRONS,/)
   WRITE(6,9) (Z(I),I=1,N)
   CALL COUL(AI,E,C,GAMA,N)
   C   GAMA(I,J) MATRIX
   CALL CALBM(H,P,C,EN,N,NF)
   C   HUCKEL APPROX CHARGE AND BOND ORDER
   WRITE(6,800)
800 FORMAT(1H ,///,21H HUCKEL APPROXIMATION,/)
   WRITE(6,26)
   WRITE(6,19) (EN(I),I=1,N)
19 FORMAT(1H ,10F10.5)
   WRITE(6,27)
   DO 801 I=1,N
801 WRITE(6,19) (C(I,J),J=1,N)
   WRITE(6,17)
17 FORMAT(1H ,///,29H CHARGE AND BOND ORDER MATRIX,/)
   DO 18 I=1,N
18 WRITE(6,19) (P(I,J),J=1,N)
   WRITE(6,802)
802 FORMAT(1H ,///,15H SCF PROPERTIES,/)
   WRITE(6,803) CONV
803 FORMAT(1H ,18H CONV REQUIREMENT=,F10.5,/)
   DO 20 L=1,NIT
   CALL FMAT(AI,E,P,Z,GAMA,BETA,N,F)
   C   CALCULATES THE F MATRIX
   CALL RECAL(F,Q,N,NF)
   C   RECALCULATES P AS Q
   IF(L.EQ.NIT) GO TO 100
   DO 21 I=1,N
   DO 21 J=1,N
21 IF(ABS(P(I,J)-Q(I,J)).GT.CONV) GO TO 82
100 WRITE(6,22) L
22 FORMAT(1H ,///,22H NUMBER OF ITERATIONS=,I3,/)
   WRITE(6,23)
23 FORMAT(15H FINAL P MATRIX,/)
```

```
DO 24 I=1,N
24 WRITE(6,19) (Q(I,J),J=1,N)
CALL DEGEN(EN,F,C,N,N)
WRITE(6,26)
26 FORMAT(1H ,///,12H EIGENVALUES,/)
WRITE(6,19) (EN(I),I=1,N)
WRITE(6,27)
27 FORMAT(1H ,///,13H EIGENVECTORS,/)
DO 28 I=1,N
28 WRITE(6,19) (C(I,J),J=1,N)
FEN=TOTEN(F,Q,AI,BETA,Z,GAMA,N)
WRITE(6,998) FEN
998 FORMAT(1H ,///,17H TOTAL PI-ENERGY=,F9.4,/)
CALL SING(C,EN,GAMA,NF,N,NU,NL,COORDX,COORDY,COORDZ)
CALL TRIP(C,EN,GAMA,NF,N,NU,NL)
CALL DIPOLE(Q,COORDX,COORDY,COORDZ,N)
GO TO 31
82 DO 32 I=1,N
DO 32 J=1,N
32 P(I,J)=Q(I,J)
20 CONTINUE
31 READ(5,2) N2
C N2=1 FOR ANOTHER MOLECULE
C N2 .NE.1 FOR STOP
IF(N2.EQ.1) GO TO .1
STOP
END
```

\$IBFTC DECK4

DECK4 - EFN SOURCE STATEMENT - IFN(S) -

```
SUBROUTINE CALBM(H,P,CH,EN,N,NF)
DIMENSION H(30,30),P(30,30),CH(30,30),EN(30)
CALL DEGEN(EN,H,CH,N,N)
DO 2 I=1,N
DO 2 J=1,N
P(I,J)=0.0
DO 2 K=1,NF
2 P(I,J)=P(I,J)+2.0*CH(K,I)*CH(K,J)
RETURN
END
```

\$IBFTC DECK3

DECK3 - EFN SOURCE STATEMENT - IFN(S) -

```
SUBROUTINE COUL(AI,E,R,GAMA,N)
DIMENSION AI(30),E(30),R(30,30),GAMA(30,30)
DO 1 I=1,N
DO 1 J=1,N
1 GAMA(I,J)=1.0/((R(I,J)/14.41)+(2.0/(AI(I)-E(I)+AI(J)-E(J))))
RETURN
END
```

\$IBFTC DECK5

DECK5 - EFN SOURCE STATEMENT - IFN(S) -

```
SUBROUTINE FMAT(AI,E,P,Z,GAMA,BETA,N,F)
DIMENSION AI(30),E(30),P(30,30),Z(30),GAMA(30,30),
1 BETA(30,30),F(30,30)
DO 1 I=1,N
F(I,I)=0.0
DO 2 J=1,N
IF(I.EQ.J) GO TO 2
F(I,J)=BETA(I,J)-0.5*P(I,J)*GAMA(I,J)
F(I,I)=F(I,I)+(P(J,J)-Z(J))*GAMA(I,J)
2 CONTINUE
1 F(I,I)=F(I,I)-AI(I)+0.5*P(I,I)*(AI(I)-E(I))
RETURN
END
```

\$IBFTC DECK6

DECK6 - EFN SOURCE STATEMENT - IFN(S) -

```
SUBROUTINE RECAL(F,Q,N,NF)
DIMENSION F(30,30),Q(30,30),EN(30),C(30,30)
CALL DEGEN(EN,F,C,N,NF)
DO 2 I=1,N
DO 2 J=1,N
Q(I,J)=0.0
DO 2 K=1,NF
2 Q(I,J)=Q(I,J)+C(K,I)*C(K,J)*2.0
RETURN
END
```

\$IBFTC SCNFIG

SCNFIG - EFN SOURCE STATEMENT - IFN(S) -

```
SUBROUTINE SING(C,E,GAMA,NF,N,NU,NL,COORDX,COORDY,COORDZ)
DIMENSION C(30,30),E(30),GAMA(30,30),G(30,30),CC(30,30),
1 EC(30),COORDX(30),COORDY(30),COORDZ(30),QX(30),QY(30),QZ(30)
WRITE(6,1)
1 FORMAT(1H ,///,30H SINGLET EXCITATION PROPERTIES,/,
129H NO CONFIGURATION INTERACTION,/)
WRITE(6,2)
2 FORMAT(11H TRANSITION,5X,7H ENERGY,5X,18H TRANSITION DIPOLE,
15X,6H ALPHA,5X,5H BETA,6X,13H OSC STRENGTH,/)
NFP1=NF+1
M1=0
NG=(NF-NL+1)*(NU-NF)
IF(NG.GT.30) GO TO 100
DO 3 I=NL,NF
DO 3 J=NFP1,NU
M1=M1+1
M=0
DO 4 K=NL,NF
DO 4 L=NFP1,NU
M=M+1
G(M,M)=ELEMENT(I,J,K,L,GAMA,C,N)+(E(J)-E(I))*DELTA(I,K)
1 *DELTA(J,L)
IF(I.EQ.K.AND.J.EQ.L) GO TO 50
GO TO 4
50 QX(M)=DIMOM(COORDX,C,I,J,N)
QY(M)=DIMOM(COORDY,C,I,J,N)
QZ(M)=DIMOM(COORDZ,C,I,J,N)
Q2=2.0*(QX(M)*QX(M)+QY(M)*QY(M)+QZ(M)*QZ(M))
W1=QY(M)
W2=QZ(M)
ALPHA=ATAN(W1,W2)*57.2958
BETA=ATAN(QX(M)/SQRT(QZ(M)*QZ(M)+QY(M)*QY(M)))*57.2958
F=0.0875161*Q2*G(M,M)
WRITE(6,5) I,J,G(M,M),Q2,ALPHA,BETA,F
5 FORMAT(3H ,I2,1H ,I2,4X,1PE13.5,5X,1PE13.5,8X,0PF7.2,3X,0PF7
1.2,6X,E13.5,/)
4 CONTINUE
3 CONTINUE
WRITE(6,6)
6 FORMAT(1H ,///,31H WITH CONFIGURATION INTERACTION,/)
WRITE(6,2)
CALL DEGEN(EC,G,CC,NG,NG)
DO 7 J=1,NG
QX1=0.0
QY1=0.0
QZ1=0.0
DO 8 I=1,NG
QX1=QX1+CC(J,I)*QX(I)
QY1=QY1+CC(J,I)*QY(I)
```

```
8 QZ1=QZ1+CC(J,I)*QZ(I)
  Q2=2.0*(QX1*QX1+QY1*QY1+QZ1*QZ1)
  ALPHA=PATAN(QY1,QZ1)*57.2958
  BETA=ATAN(QX1/SQRT(QZ1*QZ1+QY1*QY1))*57.2958
  F=0.0875161*Q2*EC(J)
  WRITE(6,9) J,EC(J),Q2,ALPHA,BETA,F
9  FORMAT(4H      ,I2,6X,1PE13.5,5X,1PE13.5,8X,0PF7.2,3X,0PF7.2,
  16X,E13.5,/)
7  CONTINUE
  WRITE(6,10)
10  FORMAT(1H ,///,22H CONFIGURATION VECTORS,/)
  DO 11 I=1,NG
11  WRITE(6,12) (CC(I,J),J=1,NG)
12  FORMAT(1H ,12F9.5)
100 RETURN
  END
```

\$IBFTC ELMT

ELMT - EFN SOURCE STATEMENT - IFN(S) -

```
REAL FUNCTION ELMENT(I,J,K,L,GAMA,C,N)
DIMENSION C(30,30),GAMA(30,30)
ELMENT=0.0
DO 1 JP=1,N
DO 1 JR=1,N
1  ELMENT=ELMENT-(C(I,JP)*C(K,JP)*C(J,JR)*C(L,JR)-
1  2.0*C(L,JP)*C(K,JP)*C(J,JR)*C(I,JR))*GAMA(JP,JR)
RETURN
END
```

\$IBFTC DIP

DIP - EFN SOURCE STATEMENT - IFN(S) -

```
REAL FUNCTION DIMOM(COORD,C,I,K,N)
DIMENSION COORD(30),C(30,30)
DIMOM=0.0
DO 1 J=1,N
1  DIMOM=DIMOM+C(I,J)*C(K,J)*COORD(J)
RETURN
END
```

\$IBFTC DFN

DFN - EFN SOURCE STATEMENT - IFN(S) -

```
REAL FUNCTION DELTA(I,J)
DELTA=1.0
IF(I.NE.J) DELTA=0.0
RETURN
END
```

\$IBFTC TCNFIG

TCNFIG - EFN SOURCE STATEMENT - IFN(S) -

```
SUBROUTINE TRIP(C,E,GAMA,NF,N,NU,NL)
DIMENSION C(30,30),E(30),GAMA(30,30),T(30,30),CT(30,30),EC(30)
WRITE(6,1)
1 FORMAT(1H ,///,30H TRIPLET EXCITATION PROPERTIES,/,
129H NO CONFIGURATION INTERACTION,/)
WRITE(6,2)
2 FORMAT(11H TRANSITION,5X,7H ENERGY,/)
NFP1=NF+1
NG=(NF-NL+1)*(NU-NF)
IF(NG.GT.30) GO TO 100
M1=0
DO 3 I=NL,NF
DO 3 J=NFP1,NU
M1=M1+1
M=0
DO 3 K=NL,NF
DO 3 L=NFP1,NU
M=M+1
T(M1,M)=TELMNT(I,J,K,L,GAMA,C,N)+(E(J)-E(I))*DELTA(I,K)
1*DELTA(J,L)
IF(I.EQ.K.AND.J.EQ.L) GO TO 4
GO TO 3
4 WRITE(6,5) I,J,T(M1,M)
5 FORMAT(3H ,I2,1H,,I2,4X,1PE13.5,/)
3 CONTINUE
WRITE(6,6)
6 FORMAT(1H ,///,31H WITH CONFIGURATION INTERACTION,/)
CALL DEGEN(EC,T,CT,NG,NG)
WRITE(6,2)
DO 7 J=1,NG
WRITE(6,8) J,EC(J)
8 FORMAT(4H ,I2,6X,1PE13.5,/)
7 CONTINUE
WRITE(6,9)
9 FORMAT(1H ,///,22H CONFIGURATION VECTORS,/)
DO 10 I=1,NG
10 WRITE(6,11) (CT(I,J),J=1,NG)
11 FORMAT(1H ,I2F9.5)
100 RETURN
END
```

\$IBFTC TEL

TEL - EFN SOURCE STATEMENT - IFN(S) -

```
REAL FUNCTION TELMNT(I,J,K,L,GAMA,C,N)
DIMENSION C(30,30),GAMA(30,30)
TELMNT=0.0
DO 1 JP=1,N
DO 1 JR=1,N
1 TELMNT=TELMNT-C(I,JP)*C(K,JP)*C(J,JR)*C(L,JR)*GAMA(JP,JR)
RETURN
END
```

\$IBFTC PAT

PAT - EFN SOURCE STATEMENT - IFN(S) -

```
REAL FUNCTION PATAN(Y,X)
PATAN=ABS(ATAN(Y/X))
IF(X.LT.0.0.AND.Y.GT.0.0) PATAN=3.14159-PATAN
IF(X.LT.0.0.AND.Y.LT.0.0) PATAN=PATAN+3.14159
IF(X.GT.0.0.AND.Y.LT.0.0) PATAN=6.28318-PATAN
RETURN
END
```

\$IBFTC TEN

TEN - EFN SOURCE STATEMENT - IFN(S) -

```
REAL FUNCTION TOTEN(F,P,AI,BETA,Z,GAMA,N)
DIMENSION F(30,30),P(30,30),AI(30),BETA(30,30),Z(30)
1,GAMA(30,30)
C CALCULATES THE TOTAL ENERGY FOR A CLOSED SHELL GROUND STATE
TOTEN=0.0
DO 1 I=1,N
X=0.0
DO 2 J=1,N
IF(I.EQ.J) GO TO 2
TOTEN=TOTEN+P(I,J)*(BETA(J,I)+F(J,I))
X=X+Z(J)*GAMA(J,I)
2 CONTINUE
1 TOTEN=TOTEN+P(I,I)*(F(I,I)-X-AI(I))
TOTEN=0.5*TOTEN
RETURN
END
```

\$IBFTC JL8

JL8 - EFN SOURCE STATEMENT - IFN(S) -

SUBROUTINE XYZ(R,X,Y,Z,N)

DIMENSION R(30,30),X(30),Y(30),Z(30)

C CALCULATES THE ATOMIC COORDINATES X,Y, AND Z, FROM THE
C INTERATOMIC DISTANCE MATRIX,R.

X(1)=0.

Y(1)=0.

Z(1)=0.

X(2)=0.

Y(2)=0.

Z(2)=R(1,2)

X(3)=0.

W1=R(1,3)*R(1,3)

W2=R(2,3)*R(2,3)

W3=R(1,2)*R(1,2)

Z(3)=(W1-W2+W3)/(2.*R(1,2))

Y(3)=SQRT(W1-Z(3)*Z(3))

DO 1 I=4,N

S1=R(I,1)*R(I,1)

S2=R(I,2)*R(I,2)

S3=R(I,3)*R(I,3)

Z(I)=(Z(2)*Z(2)+S1-S2)/(2.*Z(2))

Y(I)=(Y(3)*Y(3)+(Z(I)-Z(3))*(Z(I)-Z(3))-(Z(I)-Z(2))*

1 (Z(I)-Z(2))+S2-S3)/(2.*Y(3))

1 X(I)=0.

XMAX =0.

DO 11 I=4,N

W4=R(I,1)*R(I,1)-Y(I)*Y(I)-Z(I)*Z(I)

IF(W4.LT.0.0) W4=1.0E-20

X(I)=SQRT(W4)

IF(X(I).GT.XMAX) J=I

IF(X(I).GT.XMAX) XMAX=X(I)

11 CONTINUE

DO 12 I=4,N

IF(I.EQ.J) GO TO 12

W5=R(I,J)*R(I,J)

W6=W5-(Y(I)-Y(J))*(Y(I)-Y(J))-(Z(I)-Z(J))*(Z(I)-Z(J))

W7=W6-(X(I)-X(J))*(X(I)-X(J))

W8=W6-(X(I)+X(J))*(X(I)+X(J))

W9=W7*W7

W10=W8*W8

IF(W10.LT.W9) X(I)=-X(I)

12 CONTINUE

RETURN

END

\$IBFTC DIPOL

DIPOL - EFN SOURCE STATEMENT - IFN(S) -

```
SUBROUTINE DIPOLE(P,X,Y,Z,CZ,N)
DIMENSION P(30,30),X(30),Y(30),Z(30),CZ(30)
DIX=0.0
DIY=0.0
DIZ=0.0
DO 1 I=1,N
ALPHA=CZ(I)-P(I,I)
DIX=DIX+ALPHA*X(I)
DIY=DIY+ALPHA*Y(I)
1 DIZ=DIZ+ALPHA*Z(I)
DIX=DIX*4.8
DIY=DIY*4.8
DIZ=DIZ*4.8
DIT=SQRT(DIX*DIX+DIY*DIY+DIZ*DIZ)
ALPHA=ATAN(DIY/DIZ)*57.2958
BETA=ATAN(DIX/SQRT(DIZ*DIZ+DIY*DIY))*57.2958
WRITE(6,2)
2 FORMAT(1H ,///,33H PI CONTRIBUTION TO DIPOLE MOMENT,/)
WRITE(6,3) DIX,DIY,DIZ
3 FORMAT(1H ,8H MOMENTS,3H X=,F7.3,4X,3H Y=,F7.3,4X,3H Z=,F7.3,/)
WRITE(6,4) DIT,ALPHA,BETA
4 FORMAT(1H ,14H TOTAL MOMENT=,F7.3,10X,7H ALPHA=,F7.2,10X
1 ,6H BETA=,F7.2,/)
RETURN
END
```

\$IBFTC DECK2 DECK

DECK2 - EFN SOURCE STATEMENT - IFN(S) -

```
SUBROUTINE RITE(N)
DIMENSION CHAR(12)
READ(5,1) (CHAR(I),I=1,12)
1 FORMAT(12A6)
WRITE(6,2) (CHAR(I),I=1,12)
2 FORMAT(1H1,1H ,12A6,/)
RETURN
END
```

DG3

EFN

SOURCE STATEMENT

IFN(S)

```

SUBROUTINE DEGEN(EIG,F,C,N,NF)
DIMENSION EIG(30),F(30,30),C(30,30),V(30),A(30,30),IX(30)
1,Z(30)
DO 1 I=1,N
IX(I)=0
DO 1 J=1,N
C(I,J)=0.0
1 A(I,J)=F(I,J)
CALL HESSEN(A,N)
CALL QREIG(A,N,EIG)
NM1=N-1
A(1,1)=0.0
DO 2 I=1,NM1
IP1=I+1
IF(ABS(EIG(I)-EIG(IP1)).GT.0.001) GO TO 2
A(1,1)=A(1,1)+1.0
IX(I)=1
IX(IP1)=1
2 CONTINUE
IF(A(1,1).LT.0.5) GO TO 3
DO 4 I=1,NF
IF(IX(I).EQ.1) GO TO 4
Y=EIG(I)
CALL VCTR(F,V,N,Y)
DO 5 J=1,N
5 C(I,J)=V(J)
4 CONTINUE
WB=F(1,1)
IF(F(1,1).GT.0.01) GO TO 15
DO 16 I=1,N
16 F(I,I)=F(I,I)+1.0
15 W=F(1,1)
F(1,1)=F(1,1)*1.01
WA=F(1,1)
DO 6 I=1,N
DO 6 J=1,N
6 A(I,J)=F(I,J)
CALL HESSEN(A,N)
CALL QREIG(A,N,Z)
DO 7 I=1,NF
IF(IX(I).EQ.0) GO TO 7
Y=Z(I)
CALL VCTR(F,V,N,Y)
F(1,1)=W
CALL COV(I,V,IX,A,C,F,N,NF)
F(1,1)=WA
DO 9 J=1,N
9 C(I,J)=V(J)
IX(I)=0
    
```

```
7 CONTINUE
  F(1,1)=WB
  IF(WB.GT.0.01) GO TO 10
  DO 18 I=2,N
18 F(I,1)=F(I,1)-1.0
  GO TO 10
  3 DO 11 I=1,NF
  Y=EIG(I)
  CALL VCTR(F,V,N,Y)
  DO 12 J=1,N
12 C(I,J)=V(J)
11 CONTINUE
10 RETURN
  END
```

LIB-TC CV DECK

CV - EFN SOURCE STATEMENT - IFN(S) -

```
SUBROUTINE COV(I,V,IX,A,C,F,N,NF)
DIMENSION V(30),IX(30),A(30,30),C(30,30),F(30,30)
A(5,2)=0.2
NITER=40
CALL OTH(I,V,C,A,IX,N,NF)
A(5,3)=0.0
DO 5 L=1,NITER
  DO 2 J=1,N
  A(4,J)=0.0
  DO 2 K=1,N
2 A(4,J)=A(4,J)+F(J,K)*V(K)
  A(5,1)=0.0
  DO 3 J=1,N
3 A(5,1)=A(5,1)+V(J)*A(4,J)
  DO 4 J=1,N
4 V(J)=V(J)-A(5,2)*(A(4,J)-A(5,1)*V(J))
  DO 7 J=1,N
  IF(ABS(V(J)-A(6,J)).GT.0.000005) GO TO 8
7 CONTINUE
  CALL OTH(I,V,C,A,IX,N,NF)
  GO TO 9
8 A(5,3)=A(5,3)+1.0
  IF(A(5,3).GT.4.2) CALL OTH(I,V,C,A,IX,N,NF)
  IF(A(5,3).GT.4.2) A(5,3)=0.0
  DO 10 J=1,N
10 A(6,J)=V(J)
5 CONTINUE
9 RETURN
  END
```

OTC DECK

OTC - EFN SOURCE STATEMENT - IFN(S) -

```
SUBROUTINE DTH(I,V,C,A,IX,N,NF)
DIMENSION V(30),C(30,30),A(30,30),IX(30)
DO 1 J=1,NF
  IF(IX(J).EQ.1) GO TO 1
  A(2,J)=0.0
  DO 2 K=1,N
    2 A(2,J)=A(2,J)+V(K)*C(J,K)
  1 CONTINUE
  DO 3 J=1,NF
    IF(IX(J).EQ.1) GO TO 3
    DO 4 K=1,N
      4 V(K)=V(K)-A(2,J)*C(J,K)
    3 CONTINUE
    A(3,1)=0.0
    DO 5 J=1,N
      5 A(3,1)=A(3,1)+V(J)*V(J)
      A(3,1)=SQRT(A(3,1))
    DO 6 J=1,N
      6 V(J)=V(J)/A(3,1)
  RETURN
END
```

\$IBFTC QRCN

QRCN - EFN SOURCE STATEMENT - IFN(S) -

```
C PROGRAM TO CALL QR TRANSFORMATION, MAXIMUM ITER IS 50.
SUBROUTINE QREIG(A,M,ROOTR)
DIMENSION A(30,30),ROOTR(30),ROOTI(30)
IPRNT=0
N = M
N50=N
IF(IPRNT) 80,81,80
80 WRITE (6,104)
81 ZERO = 0.0
JJ=1
177 XNN=0.0
XN2=0.0
AA = 0.0
B = 0.0
C = 0.0
DD = 0.0
R=0.0
SIG=0.0
ITER = 0
17 IF(N-2) 13,14,12
13 IF(IPRNT) 82,83,82
```

```
82 WRITE (6,105)A(1,1)
83 ROOTR(1) = A(1,1)
   ROOTI(1) = 0.0
   1 M50=N50-1
   DO 505 K50=1,M50
     K1=K50+1
     DO 505 J50=K1,N50
       IF(ROOTR(K50).LT.ROOTR(J50)) GO TO 505
504 X1=ROOTR(K50)
   ROOTR(K50)=ROOTR(J50)
   ROOTR(J50)=X1
505 CONTINUE
   RETURN
14 JJ=-1
   12 X = (A(N-1,N-1) - A(N,N))*2
   S = 4.0*A(N,N-1)*A(N-1,N)
   ITER = ITER + 1
   IF(X .EQ. 0.0 .OR. ABS(S/X) .GT. 1.0E-8) GO TO 15
16 IF(ABS(A(N-1,N-1))-ABS(A(N,N))) 32,32,31
   31 E = A(N-1,N-1)
   G = A(N,N)
   GO TO 33
   32 G = A(N-1,N-1)
   E = A(N,N)
   33 F = 0.
   H = 0.
   GO TO 24
15 S = X + S
   X = A(N-1,N-1) + A(N,N)
   IF(S) 18,19,19
19 SQ=SQRT(S)
   F=0.0
   H=0.0
   IF (X) 21,21,22
21 E=(X-SQ)/2.0
   G=(X+SQ)/2.0
   GO TO 24
22 G=(X-SQ)/2.0
   E=(X+SQ)/2.0
   GO TO 24
18 F = SQRT(-S)/2.0
   E=X/2.0
   G=E
   H=-F
24 IF(JJ) 28,70,70
70 D = 1.0E-10*(ABS(G) + F)
   IF(ABS(A(N-1,N-2)) .GT. D) GO TO 26
26 IF(IPRNT) 84,85,84
84 WRITE (6,105)E,F, ITER
   WRITE (6,105)G,H
85 ROOTR(N) = E
   ROOTI(N) = F
```

```
ROOTR(N-1) = G
ROOTI(N-1) = H
N=N-2
IF(JJ) 1,177,177
26 IF(ABS(A(N,N-1)) .GT. 1.0E-10*ABS(A(N,N))) GO TO 50
29 IF(IPRNT) 86,87,86
86 WRITE (6,105)A(N,N), ZERO, ITER
87 ROOTR(N) = A(N,N)
   ROOTI(N) = 0.0
   N=N-1
   GO TO 177
50 IF(ABS(ABS(XNN/A(N,N-1))-1.0)-1.0E-6) 63,63,62
62 IF(ABS(ABS(XN2/A(N-1,N-2))-1.0)-1.0E-6) 63,63,700
63 VQ=ABS(A(N,N-1))-ABS(A(N-1,N-2))
   IF (ITER-15) 53,164,64
164 IF(VQ) 165,165,166
165 R = A(N-1,N-2)**2
   SIG = 2.0*A(N-1,N-2)
   GO TO 60
166 R = A(N,N-1)**2
   SIG = 2.0*A(N,N-1)
   GO TO 60
64 IF(VQ) 67,67,66
66 IF(IPRNT) 88,88,88
88 WRITE (6,107)A(N-1,N-2)
   GO TO 84
67 IF(IPRNT) 89,87,89
89 WRITE (6,107)A(N,N-1)
   GO TO 86
700 IF(ITER .GT. 50) GO TO 63
   IF(ITER .GT. 5 ) GO TO 53
701 Z1= ((E-AA)**2+(F-B)**2)/(E*E+F*F)
   Z2= ((G-C)**2+(H-DD)**2)/(G*G+H*H)
   IF(Z1-0.25) 51,51,52
51 IF(Z2-0.25) 53,53,54
53 R=E*G-F*H
   SIG=E+G
   GO TO 60
54 R=E*E
   SIG=E+E
   GO TO 60
52 IF(Z2-0.25) 55,55,601
53 R=G*G
   SIG=G+G
   GO TO 60
601 R = 0.0
   SIG = 0.0
60 XNN=A(N,N-1)
   XN2=A(N-1,N-2)
   CALL QRT(A,N,R,SIG,D)
   AA=E
   B=F
   C=G
   DD=H
```

```

GO TO 12
104 FORMAT(////1X, 9HREAL PART 6X 14HIMAGINARY PART, 25X
1 13HTAKEN AS ZERO 6X 4HITER //)
105 FORMAT(1X,E15.8,3X,E15.8, 42X I3)
107 FORMAT(56X E13.8)
END

```

SIBFTC HESS

HESS - EFN SOURCE STATEMENT - IFN(S) -

C SUBROUTINE TO PUT MATRIX IN UPPER HESSENBERG FORM.

```

SUBROUTINE HESSEN(A,M)
DIMENSION A(30,30),B(50)
DOUBLE PRECISION SUM
IF (M - 2) 30,30,32
32 DO 40 LC = 3,M
N = M - LC + 3
N1 = N - 1
N2 = N - 2
NI = N1
DIV = ABS(A(N,N-1))
DO 2 J=1,N2
IF(ABS(A(N,J))- DIV) 2,2,1
1 NI = J
DIV = ABS(A(N,J))
2 CONTINUE
IF(DIV) 3,40,3
3 IF(NI - N1) 4, 7,4
4 DO 5 J = 1,N
DIV = A(J,NI)
A(J,NI) = A(J,N1)
5 A(J,N1) = DIV
DO 6 J = 1,M
DIV = A(NI,J)
A(NI,J) = A(N1,J)
6 A(N1,J) = DIV
7 DO 26 K = 1, N1
26 B(K) = A(N,K)/A(N,N-1)
DO 45 J = 1,M
SUM = 0.0
IF (J - N1) 46,43,43
46 IF(B(J)) 41,43,41
41 A(N,J) = 0.0
DO 42 K = 1,N1
A(K,J) = A(K,J) - A(K,N1)*B(J)
42 SUM = SUM + A(K,J)*B(K)
GO TO 45
43 DO 44 K = 1,N1
44 SUM = SUM + A(K,J)*B(K)
45 A(N1,J) = SUM
40 CONTINUE
30 RETURN
END

```

\$IBFTC *QRT

*QRT - EFN SOURCE STATEMENT - IFN(S) -

```
SUBROUTINE QRT(A,N,R,SIG,D)
DIMENSION A(30,30),PSI(2),G(3)
N1 = N - 1
IA = N - 2
IP = IA
IF(N-3) 101,10,60
60 DO 12 J = 3,N1
    J1 = N - J
    IF(ABS(A(J1+1,J1))-D) 10,10,11
11 DEN = A(J1+1,J1+1)*(A(J1+1,J1+1)-SIG)+A(J1+1,J1+2)*A(J1+2,J1+
1-1))+R
    IF(DEN) 61,12,61
61 IF(ABS(A(J1+1,J1)*A(J1+2,J1+1)*(ABS(A(J1+1,J1+1)+A(J1+2,J1+2)
1-SIG)+ABS(A(J1+2,J1+2)))/DEN)-D) 10,10,12
12 IP=J1
10 DO 14 J=1,IP
    J1=IP-J+1
    IF(ABS(A(J1+1,J1))-D) 13,13,14
14 IQ=J1
13 DO 100 I=IP,N1
    IF(I-IP) 16,15,16
15 G(1)=A(IP,IP)*(A(IP,IP)-SIG)+A(IP,IP+1)*A(IP+1,IP)+R
    G(2)=A(IP+1,IP)*(A(IP,IP)+A(IP+1,IP+1)-SIG)
    G(3)=A(IP+1,IP)*A(IP+2,IP+1)
    A(IP+2,IP)=0.0
    GO TO 19
16 G(1)=A(I,I-1)
    G(2)=A(I+1,I-1)
    IF(I-IA) 17,17,18
17 G(3)=A(I+2,I-1)
    GO TO 19
18 G(3)=0.0
19 XK = SIGN(SQRT(G(1)**2 + G(2)**2 + G(3)**2), G(1))
22 IF(XK) 23,24,23
23 AL=G(1)/XK+1.0
    PSI(1)=G(2)/(G(1)+XK)
    PSI(2)=G(3)/(G(1)+XK)
    GO TO 25
24 AL=2.0
    PSI(1)=0.0
    PSI(2)=0.0
25 IF(I-IQ) 26,27,26
26 IF(I-IP) 29,28,29
28 A(I,I-1)=-A(I,I-1)
    GO TO 27
29 A(I,I-1)=-XK
27 DO 30 J=1,N
    IF(I-IA) 31,31,32
31 C=PSI(2)*A(I+2,J)
```



```
GO TO 33
32 C=0.0
33 E=AL*(A(I,J)+PSI(1)*A(I+1,J)+C)
   A(I,J)=A(I,J)-E
   A(I+1,J)=A(I+1,J)-PSI(1)*E
   IF(I-IA) 34,34,30
34 A(I+2,J)=A(I+2,J)-PSI(2)*E
30 CONTINUE
   IF(I-IA) 35,35,36
35 L=I+2
   GO TO 37
36 L=N
37 DO 40 J=IQ,L
   IF(I-IA) 38,38,39
38 C=PSI(2)*A(J,I+2)
   GO TO 41
39 C=0.0
41 E=AL*(A(J,I)+PSI(1)*A(J,I+1)+C)
   A(J,I)=A(J,I)-E
   A(J,I+1)=A(J,I+1)-PSI(1)*E
   IF(I-IA) 42,42,40
42 A(J,I+2)=A(J,I+2)-PSI(2)*E
40 CONTINUE
   IF(I-N+3) 43,43,100
43 E=AL*PSI(2)*A(I+3,I+2)
   A(I+3,I)=-E
   A(I+3,I+1)=-PSI(1)*E
   A(I+3,I+2)=A(I+3,I+2)-PSI(2)*E
100 CONTINUE
101 RETURN
   END
```

\$IBFTC RWVCTR

RWVCTR - EFN SOURCE STATEMENT - IFN(S) -

```
SUBROUTINE VCTR(AX,V,N,XY)
DIMENSION AX(30,30),A(30,30),V(30)
ALPHA=XY
DO 501 I51=1,N
DO 501 J51=1,N
501 A(I51,J51)=AX(I51,J51)
A(1,1)=A(1,1)-ALPHA
6 DO 15 I=2,N
A(I,I)=A(I,I)-ALPHA
70 II=I-1
7 DO 15 J=1,II
8 IF (A(I,J))9,15,9
9 IF (ABS (A(J,J))-ABS (A(I,J)))11,10,10
10 R=A(I,J)/A(J,J)
GO TO 130
11 R=A(J,J)/A(I,J)
DO 12 K=1,N
C=A(J,K)
A(J,K)=A(I,K)
12 A(I,K)=C
130 JJ=J+1
13 DO 14 K=JJ,N
14 A(I,K)=A(I,K)-R*A(J,K)
15 CONTINUE
C=A(N,N)
V(N)=1.
DO 29 I=2,N
JJ=N-I+1
R=0.
II=N-I+2
DO 25 K=II,N
25 R=R+A(JJ,K)*V(K)
IF (ABS (A(JJ,JJ))-1.0E-10)27,27,28
27 V(JJ)=1.
C=0.
DO 26 J=II,N
26 V(J)=0.
GO TO 29
28 V(JJ)=(C-R)/A(JJ,JJ)
29 CONTINUE
X50=0.0
DO 502 J52=1,N
502 X50=X50+V(J52)*V(J52)
X51=SQRT(X50)
DO 503 J53=1,N
503 V(J53)=V(J53)/X51
RETURN
END
```

(3) The Spin-Polarized SCF Program, with Spin Projection.

This program calculates SCF spin-polarized wave functions for half closed-shell states of molecules and radicals as discussed in section (I8) of chapter II . In addition to the theoretical limitation of the method to states which can be represented by a single determinant, it is found to be a non-convergent procedure for occupation numbers involving "holes" in the electronic population of the two spin-orbital sets. These "holes" are unoccupied virtual orbitals at lower orbital energies than the highest occupied spin orbital.

From a starting point of the spin-paired SCF closed-shell orbitals, the program iterates the two sets of coupled α and β -spin orbitals to a pre-determined degree of consistency. The total π -energy of the molecule is calculated at each iteration.

The use of a spin projection routine on this SCF state is controlled by an input data card. The results of these various approximations are printed out at the conclusion of each step.

Special procedures are included to help the iterations converge, one of these is a subroutine VSORT . This routine sorts the vectors from successive iterations so as to ensure electrons are always assigned to the intended orbital, even if in the SCF procedure they may chance to become energetically unfavourable. The input data is now detailed.

N33, ICV, ICON, (3I3): These three control integers are all punched on the same card. N33 controls the use of the spin-polarizing routine PURV, which is only called if $N33=5$. Subroutine PURV serves to alternate α and β -spin density in the input bond matrices P^α and P^β , and is used to obtain spin-polarized ground-states. For non-ground state use $N33 \neq 5$. If ICV=I, the routine VSORT is by-passed, with $ICV \neq I$, it is used after every iteration. ICON controls the spin-projection routine, with $ICON=2$ only the simple projection is used, (see page 248). If $ICON=3$, both simple and accurate projections are performed, and the set of "corresponding orbitals" found. With $ICON=I$, only the projected results are obtained.

Title Card, (Free Format): This is read as in program (2).

N, (I3): The number of atoms in the molecule, $N \leq 30$.

NIT, (I3): Maximum number of SCF iterations, typically $NIT \leq 50$.

GN, CONVG, DVC, (3F20.8): GN controls the approximation used for the Coulomb integrals. These are given the value of GN times the Mataga and Nishimoto approximation. Normally $GN=I$. CONVG is the convergence criterion. For a self-consistent state we require simultaneously,

$$\left| (P_{ij}^n) - (P_{ij}^{n+1}) \right| \leq \text{CONVG}$$

$$\left| (P_{ij}^n) - (P_{ij}^{n+1}) \right| \leq \text{CONVG}$$

Usually we have $\text{CONVG}=0.001$.

DVC controls the degree of feed-back for successive bond-matrices used as input for the SCF iterations. A typical value would be 0.3.

/R(N,N),AI(N),E(N),Z(N),H(N,N)/,(F20.8): These are defined in the previous program.

/ANA(N)/,(F20.8): This matrix specifies the α -orbital occupation numbers, counting from the lowest occupied upwards.

Thus $ANA(i)=1$ if ϕ_i^α is occupied, otherwise $ANA(i)=0$.

/ANB(N)/,(F20.8): The β -occupation matrix, assigned as ANA above.

N5,(I3): If $N5=5$, the program restarts on a new set of input data, after concluding the SCF procedure on the first set of molecular data. Otherwise, if $N5=1$, the program stops.

When $N5 \neq 2$ or 5 , a new set of occupation numbers, ANA and ANB, are read, and another excited state treated.

\$IBFTC DECK4 DECK

DECK4 - EFN SOURCE STATEMENT - IFN(S) -

```
DIMENSION AI(30),E(30),Z(30),ANA(30),ANB(30),BETA(30,30),
1  GAMA(30,30),ENA(30),PA(30,30),PB(30,30),FA(30,30),
2  FB(30,30),QA(30,30),QB(30,30),C(30,30),H(30,30),
3  CH(30,30),CA(30,30),CB(30,30)
4  ,X(30,30),CF(30,30)
C MOLECULE OPEN SHELL LCAO.MD.SCF.
208 READ(5,984) N33,ICV,ICON
984 FORMAT(3I3)
C N33 LABELS TITLE REQUIRED
CALL RITE(N33)
500 READ(5,1) N
C N GIVES THE NUMBER OF ATOMS IN THE MOLECULE
1  FORMAT(I3)
READ(5,1)NIT
READ(5,900) GN,CONVG,DVC
900 FORMAT(3F20.8)
N5=1
DO 2 I=1,N
DO 2 J=I,N
READ(5,3) PA(I,J)
2  PA(J,I)=PA(I,J)
3  FORMAT(F20.8)
READ(5,3) (AI(I),I=1,N)
READ(5,3) (E(I),I=1,N)
READ(5,3) (Z(I),I=1,N)
DO 9 I=1,N
DO 9 J=I,N
READ(5,3) H(I,J)
BETA(I,J)=H(I,J)
BETA(J,I)=H(I,J)
9  H(J,I)=H(I,J)
C READ THE HUCKEL MATRIX
C RESONANCE INTEGRAL MATRIX
DO 10 I=1,N
10 BETA(I,I)=0.0
WRITE(6,23)
23 FORMAT(14H HUCKEL MATRIX,/)
DO 24 I=1,N
24 WRITE(6,301) (H(I,J),J=1,N)
301 FORMAT(12F8.3)
WRITE(6,51)
51 FORMAT(1H ,///,21H IONIZATION POTENTIAL,/)
WRITE(6,301) (AI(I),I=1,N)
WRITE(6,52)
52 FORMAT(1H ,///,18H ELECTRON AFFINITY,/)
WRITE(6,301) (E(I),I=1,N)
WRITE(6,56)
56 FORMAT(1H ,///,14H R(I,J) MATRIX,/)
```

```
DO 57 I=1,N
57 WRITE(6,301) (PA(I,J),J=1,N)
WRITE(6,58)
58 FORMAT(1H ,///,17H RESONANCE MATRIX,/)
DO 59 I=1,N
59 WRITE(6,301) (BETA(I,J),J=1,N)
WRITE(6,53)
53 FORMAT(1H ,///,23H NUMBER OF PI ELECTRONS,/)
WRITE(6,301) (Z(I),I=1,N)
CALL COUL(AI,E,PA,GAMA,N)
DO 753 I=1,N
DO 753 J=1,N
753 GAMA(I,J)=GN*GAMA(I,J)
WRITE(6,754) GN
754 FORMAT(1H ,///,13H GAMA FACTOR=,F6.3,/)
C
800 READ(5,3) (ANA(I),I=1,N)
READ(5,3) (ANB(I),I=1,N)
WRITE(6,54)
54 FORMAT(1H ,///,17H ALPHA OCCUPATION,/)
WRITE(6,301) (ANA(I),I=1,N)
WRITE(6,55)
55 FORMAT(1H ,///,16H BETA OCCUPATION,/)
WRITE(6,301) (ANB(I),I=1,N)
WRITE(6,901)
901 FORMAT(1H ,///,31H CLOSED SHELL SCF APPROXIMATION,/)
IF(N5.NE.1) CALL PUTIN(CH,PA,PB,ANA,ANB,N)
IF(N5.NE.1) GO TO 581
CALL SCFCS(H,BETA,GAMA,AI,E,Z,FA,CA,CB,PA,PB,ANA,ANB,ENA,N)
IF(N33.EQ.5) CALL PURV(PA,PB,N)
DO 902 I=1,N
DO 902 J=1,N
902 CH(I,J)=CA(I,J)
581 WRITE(6,60)
60 FORMAT(1H ,///,10H PA MATRIX,/)
DO 61 I=1,N
61 WRITE(6,302) (PA(I,J),J=1,N)
302 FORMAT(1H ,10F10.5)
WRITE(6,62)
62 FORMAT(1H ,///,10H PB MATRIX,/)
DO 63 I=1,N
63 WRITE(6,302) (PB(I,J),J=1,N)
WRITE(6,903)
903 FORMAT(1H ,///,19H SPIN POLARIZED SCF,/)
DO 11 L=1,NIT
VC=1.0-DVC*FLOAT(L)
IF(VC.LT.0.0)VC=0.0
VCM=1.0-VC
```

```
CONV=VCM*CONVG
CALL FMAT(AI,E,PA,PB,Z,GAMA,BETA,N,FA,FB)
C F MATRICES ALPHA AND BETA
CALL RECAL(FA,QA,ANA,N,CA,X,CF,ICV)
CALL RECAL(FB,QB,ANB,N,CB,X,CF,ICV)
C RECALCULATES P MATRICES AS QA AND QB
PEN=POLEN(FA,FB,QA,QB,AI,BETA,Z,GAMA,N)
WRITE(6,757) PEN
757 FORMAT(1H ,///,17H TOTAL PI ENERGY=,F10.4,/)
IF(L.EQ.NIT) GO TO 81
DO 13 I=1,N
DO 13 J=1,N
13 IF(ABS(PA(I,J)-QA(I,J)).GT.CONV.OR.
1 ABS(PB(I,J)-QB(I,J)).GT.CONV) GO TO 91
WRITE(6,904) CONV
904 FORMAT(1H ,//,28H METHOD HAS CONVERGED, CONV=,F8.5,/)
81 WRITE(6,31) L
31 FORMAT(1H ,///,22H NUMBER OF ITERATIONS=,I3,///)
WRITE(6,16)
16 FORMAT(16H FINAL PA MATRIX,/)
DO 64 I=1,N
64 WRITE(6,302) (QA(I,J),J=1,N)
WRITE(6,17)
17 FORMAT(1H ,///,16H FINAL PB MATRIX,/)
DO 65 I=1,N
65 WRITE(6,302) (QB(I,J),J=1,N)
WRITE(6,905)
905 FORMAT(1H ,//,29H CHARGE AND BOND-ORDER MATRIX,/)
DO 906 I=1,N
DO 906 J=1,N
906 C(I,J)=QA(I,J)+QB(I,J)
DO 907 I=1,N
907 WRITE(6,302) (C(I,J),J=1,N)
WRITE(6,908)
908 FORMAT(1H ,///,5H ATOM,10X,13H SPIN DENSITY,10X,
115H CHARGE DENSITY,/)
DO 909 I=1,N
X(1,1)=QA(I,1)-QB(I,1)
WRITE(6,755) I,X(1,1),C(I,1)
755 FORMAT(1H ,I3,14X,F8.5,14X,F8.5,/)
909 CONTINUE
CALL DEGEN(ENA,FA,C,N,N)
CALL VSORT(C,CA,X,CF,ENA,N,ICV)
WRITE(6,69)
69 FORMAT(1H ,///,18H ALPHA EIGENVALUES,/)
WRITE(6,302) (ENA(I),I=1,N)
WRITE(6,70)
70 FORMAT(1H ,///,19H ALPHA EIGENVECTORS,/)
```



```
DO 71 I=1,N
71 WRITE(6,302) (C(I,J),J=1,N)
   CALL DEGEN(ENA,FB,C,N,N)
   CALL VSORT(C,CB,X,CF,ENA,N,ICV)
   WRITE(6,72)
72 FORMAT(1H ,///,17H BETA EIGENVALUES,/)
   WRITE(6,302) (ENA(I),I=1,N)
   WRITE(6,73)
73 FORMAT(1H ,///,18H BETA EIGENVECTORS,/)
   DO 74 I=1,N
74 WRITE(6,302) (C(I,J),J=1,N)
   CALL SPIN(QA,QB,PA,PB,FA,FB,CA,CB,C,CF,H,X,BETA,AI,E,Z,GAMA,
1N,ICON,ANA,ANB)
   GO TO 205
91 DO 32 I=1,N
   DO 32 J=1,N
   PA(I,J)=VC*PA(I,J)+VCM*QA(I,J)
32 PB(I,J)=VC*PB(I,J)+VCM*QB(I,J)
11 CONTINUE
205 READ(5,1) N5
   IF(N5.EQ.5) GO TO 208
   IF(N5.EQ.1) GO TO 751
   WRITE(6,752)
752 FORMAT(1H ,///,14H EXCITED STATE,/)
   GO TO 800
751 STOP
END
```

\$IBFTC SPP DECK

SPP - EFN SOURCE STATEMENT - IFN(S) -

```
SUBROUTINE SPIN(QA,QB,PA,PB,FA,FB,CA,CB,C,CF,H,X,BETA,AI,E,Z,
1 GAMA,N,ICON,ANA,ANB)
DIMENSION QA(30,30),QB(30,30),PA(30,30),PB(30,30),FA(30,30),
1 FB(30,30),CA(30,30),CB(30,30),C(30,30),CF(30,30),H(30,30)
1 ,X(30,30),BETA(30,30),AI(30),E(30),Z(30),GAMA(30,30)
1 ,ANA(30),ANB(30)
Q=0.0
P=0.0
DO 1 I=1,N
P=P+ANA(I)
1 Q=Q+ANB(I)
PPQ=P+Q
PMQ=ABS(P-Q)
```

```
SZ=PMQ*0.5
SM=SZ*(SZ+1.0)
I=IFIX(PMQ)+1
WRITE(6,2)
2 FORMAT(1H ,///,31H****SPIN PROJECTION ROUTINE****,/)
WRITE(6,3) I,SZ,SM
3 FORMAT(23H MULTIPLICITY OF STATE=,I2,10X,21H Z-SPIN COMPONENT
1F5.2,/,25H SPIN OF PURE STATE,(S2)=,F5.2,/)
CALL AMAT(QA,QB,FA,N)
C STORES (PQ) IN FA
T=SECTR(FA,N)
C T=TRACE(PQ)
SM=0.25*PMQ*PMQ+0.5*PPQ-T
WRITE(6,4) SM
4 FORMAT(23H UNPROJECTED SPIN,(S2)=,F9.6,/)
WRITE(6,5)
5 FORMAT(27H SIMPLIFIED SPIN PROJECTION,/)
DO 6 I=1,N
DO 6 J=1,N
6 X(I,J)=FA(I,J)
CALL AMAT(FA,X,FB,N)
C STORES(PQPQ) IN FB
T2=SECTR(FB,N)
C T2=TRACE(PQPQ)
X(1,1)=(SZ+1.0)*(SZ+2.0)-SM
SM=SM-((P-T)*(Q-T)+2.0*(T-T2))/X(1,1)
WRITE(6,7) SM
7 FORMAT(23H AFTER PROJECTION,(S2)=,F9.6,/)
CALL AMAT(FA,QA,CA,N)
CALL AMAT(QB,FA,CB,N)
CALL AMAT(QB,QA,CF,N)
C CA=(PQP) CB=(QPQ) CF=(QP)
DO 8 I=1,N
DO 8 J=1,N
PA(I,J)=QA(I,J)-(CA(I,J)-0.5*(FA(I,J)+CF(I,J)))/X(1,1)
PA(J,I)=PA(I,J)
PB(I,J)=QB(I,J)-(CB(I,J)-0.5*(FA(I,J)+CF(I,J)))/X(1,1)
8 PB(J,I)=PB(I,J)
C PA AND PB ARE NEW SPIN PROJECTED MATRICES
WRITE(6,9)
9 FORMAT(29H SPIN PROJECTED BOND MATRICES,/)
WRITE(6,10)
10 FORMAT(11H ALPHA SPIN,/)
DO 11 I=1,N
11 WRITE(6,12) (PA(I,J),J=1,N)
12 FORMAT(10F10.6)
WRITE(6,13)
13 FORMAT(1H ,///,10H BETA SPIN,/)
DO 14 I=1,N
14 WRITE(6,12) (PB(I,J),J=1,N)
```

```
DO 15 I=1,N
DO 15 J=I,N
H(I,J)=PA(I,J)+PB(I,J)
15 H(J,I)=H(I,J)
WRITE(6,16)
16 FORMAT(1H ,//,16H TOTAL BOND MATRIX,//)
DO 17 I=1,N
17 WRITE(6,12) (H(I,J),J=1,N)
CALL SPWRT(PA,PB,H,X,N)
CALL PROJEN(BETA,AI,E,Z,GAMA,QA,QB,FA,PA,PB,X,H,C,N)
IF(ICCN.EQ.2) GO TO 26
WRITE(6,18)
18 FORMAT(37H****MORE ACCURATE SPIN PROJECTION****,//)
X(1,2)=P
IF(P.GT.Q) X(1,2)=Q
X(1,2)=X(1,2)+SZ*(SZ+1.0)
C X(1,2)=A
X(1,3)=X(1,2)*X(1,2)
C X(1,3)=A*A
T3=TRACE(FB,FA,N)
C T3=TRACE(PQPQPQ)
X(1,4)=X(1,2)-T
C X(1,4)=S*S
X(1,5)=X(1,3)+P*Q+2.0*(T*T-T2)-T*(2.0*X(1,2)+PPQ-2.0)
C X(1,5)=S*S*S*S
X(1,6)=X(1,3)*X(1,2)+X(1,2)*P*Q+P*Q*(2.0*X(1,2)+PPQ-2.0)
X(1,6)=X(1,6)-T*(3.0*X(1,3)+3.0*X(1,2)*(PPQ-2.0)+(PPQ-2.0)*
1 (PPQ-2.0)+P*Q+4.0*(P-1.0)*(Q-1.0))
X(1,6)=X(1,6)+2.0*(3.0*X(1,2)+3.0*PPQ-10.0)*(T*T-T2)
X(1,6)=X(1,6)-6.0*(T*T*T-3.0*T2*T+2.0*T3)
C X(1,6)=S*S*S*S*S*S
X(1,7)=(SZ+1.0)*(SZ+2.0)
X(1,8)=X(1,7)*X(1,7)
SM=X(1,6)-2.0*X(1,7)*X(1,5)+X(1,8)*X(1,4)
SM=SM/(X(1,5)-2.0*X(1,7)*X(1,4)+X(1,8))
WRITE(6,19) SM
19 FORMAT(23H AFTER PROJECTION,(S2)=,F9.6,//)
CALL AMAT(QB,CA,H,N)
CALL AMAT(FB,QA,C,N)
CALL AMAT(H,QB,PB,N)
C H=(QPQP) C=(PQPQP) PB=QPQPQ
X(1,2)=X(1,2)-SZ*(SZ+1.0)-2.0*(SZ+1.0)
X(1,3)=X(1,2)*X(1,2)
C NEW A AND A*A VALUES
X(2,1)=X(1,3)+P*Q+T*(3.0+2.0*T-2.0*X(1,2)-PPQ)
C X(2,1)=A*A+PQ+TRACE(PQ)(3-2TRACE(PQ)-2A-N)
X(2,2)=PPQ-4.0*T-3.0+2.0*X(1,2)
C X(2,2)=N-4TRACE(PQ)-3+2A
X(2,3)=2.0*T+1.0-X(1,2)
```

```
C      X(2,3)=2TRACE(PQ)+1-A
      X(2,4)=X(1,3)+P*Q+T*(2.0+2.0*T-2.0*X(1,2)-PPQ)
C      X(2,4)=A*A+PQ+TRACE(PQ)(2+2TRACE(PQ)-2A-N)
      T3=SECTR(H,N)
C      T3=TRACE(QPQPQ)
      DO 21 I=1,N
      DO 21 J=I,N
      C(I,J)=4.0*C(I,J)+QA(I,J)*(X(2,1)-Q-2.0*T2)
      C(I,J)=C(I,J)+(P-T)*QB(I,J)+CB(I,J)
      C(I,J)=C(I,J)+X(2,2)*CA(I,J)+(FA(I,J)+CF(I,J))*(X(2,3)-P)
      C(I,J)=C(I,J)-2.0*(FB(I,J)+H(I,J))
      C(I,J)=C(I,J)/(X(2,4)-2.0*T2)
      C(J,I)=C(I,J)
      PB(I,J)=4.0*PB(I,J)+QB(I,J)*(X(2,1)-P-2.0*T3)
      PB(I,J)=PB(I,J)+(Q-T)*QA(I,J)+CA(I,J)
      PB(I,J)=PB(I,J)+X(2,2)*CB(I,J)+(FA(I,J)+CF(I,J))*(X(2,3)-Q)
      PB(I,J)=PB(I,J)-2.0*(H(I,J)+FB(I,J))
      PB(I,J)=PB(I,J)/(X(2,4)-T3*2.0)
      PB(J,I)=PB(I,J)
21 CONTINUE
C      C AND PB ARE NEW DENSITY MATRICES
      WRITE(6,9)
      WRITE(6,10)
      DO 22 I=1,N
22 WRITE(6,12) (C(I,J),J=1,N)
      WRITE(6,13)
      DO 23 I=1,N
23 WRITE(6,12) (PB(I,J),J=1,N)
      DO 24 I=1,N
      DO 24 J=I,N
      PA(I,J)=C(I,J)+PB(I,J)
24 PA(J,I)=PA(I,J)
      WRITE(6,16)
      DO 25 I=1,N
25 WRITE(6,12) (PA(I,J),J=1,N)
      CALL SPWRT(C,PB,PA,X,N)
      CALL PROJEN(BETA,AI,E,Z,GAMA,QA,QB,FA,C,PB,X,PA,H,N)
      IF(ICON.EQ.3) CALL EQQB(CA,CB,QA,QB,PA,PB,N,AI)
26 RETURN
      END
```

\$IBFTC SW DECK

SW - EFN SOURCE STATEMENT - IFN(S) -

```
SUBROUTINE SPWRT(PA,PB,H,X,N)
DIMENSION PA(30,30),PB(30,30),X(30,30),H(30,30)
WRITE(6,1)
```

```
1 FORMAT(1H ,//,5H ATOM,10X,13H SPIN DENSITY,10X,15H CHARGE
1 DENSITY,/)
DO 2 I=1,N
```

```
X(1,2)=PA(I,I)-PB(I,I)
WRITE(6,3) I,X(1,2),H(I,I)
```

```
2 CONTINUE
```

```
3 FORMAT(1H ,I3,14X,F8.5,14X,F8.5,/)
RETURN
```

```
END
```

\$IBFTC AM DECK

AM - EFN SOURCE STATEMENT - IFN(S) -

```
SUBROUTINE AMAT(A,B,C,N)
DIMENSION A(30,30),B(30,30),C(30,30)
```

```
DO 1 I=1,N
```

```
DO 1 J=1,N
```

```
C(I,J)=0.0
```

```
DO 1 K=1,N
```

```
1 C(I,J)=C(I,J)+A(I,K)*B(K,J)
```

```
RETURN
```

```
END
```

\$IBFTC TRC DECK

TRC - EFN SOURCE STATEMENT - IFN(S) -

```
REAL FUNCTION TRACE(A,B,N)
```

```
DIMENSION A(30,30),B(30,30)
```

```
TRACE=0.0
```

```
DO 1 I=1,N
```

```
DO 1 J=1,N
```

```
1 TRACE=TRACE+A(I,J)*B(J,I)
```

```
RETURN
```

```
END
```

\$IBFTC HKL DECK

HKL - EFN SOURCE STATEMENT - IFN(S) -

```
SUBROUTINE HUCK(H,NE,CA,ENA,PA,N)
DIMENSION H(30,30),CA(30,30),ENA(30),PA(30,30)
CALL DEGEN(ENA,H,CA,N,NE)
DO 1 I=1,N
DO 1 J=1,N
PA(I,J)=0.0
DO 1 K=1,NE
1 PA(I,J)=PA(I,J)+CA(K,I)*CA(K,J)*2.0
RETURN
END
```

\$IBFTC DECK1 DECK

DECK1 - EFN SOURCE STATEMENT - IFN(S) -

```
SUBROUTINE COUL(AI,E,R,GAMA,N)
DIMENSION AI(30),E(30),R(30,30),GAMA(30,30)
C EQUATION 8 ,MONOMER,OPEN SHELL
DO 1 I=1,N
DO 1 J=1,N
1 GAMA(I,J)=1.0/(((R(I,J)/14.41)+(2.0/(AI(I)-E(I)+AI(J)
1-E(J))))))
RETURN
END
```

\$IBFTC PT DECK

PT - EFN SOURCE STATEMENT - IFN(S) -

```
SUBROUTINE PUTIN(CH,PA,PB,ANA,ANB,N)
DIMENSION CH(30,30),PA(30,30),PB(30,30),ANA(30),ANB(30)
DO 1 I=1,N
DO 1 J=1,N
PA(I,J)=0.0
PB(I,J)=0.0
DO 1 K=1,N
PA(I,J)=PA(I,J)+CH(K,I)*CH(K,J)*ANA(K)
1 PB(I,J)=PB(I,J)+CH(K,I)*CH(K,J)*ANB(K)
RETURN
END
```

\$IBFTC DECK3 DECK

DECK3 - EFN SOURCE STATEMENT - IFN(S) -

```
SUBROUTINE FMAT(AI,E,PA,PB,Z,GAMA,BETA,N,FA,FB)
DIMENSION AI(30),E(30),PA(30,30),PB(30,30),Z(30),
1 GAMA(30,30),BETA(30,30),FA(30,30),FB(30,30)
C EQUATIONS 3 AND 4 ,OPEN SHELL MOLECULE
DO 2 I=1,N
FA(I,I)=0.0
FB(I,I)=0.0
DO 1 J=1,N
IF(I.EQ.J) GO TO 1
FA(I,J)=BETA(I,J)-PA(I,J)*GAMA(I,J)
FB(I,J)=BETA(I,J)-PB(I,J)*GAMA(I,J)
FA(I,I)=FA(I,I)+GAMA(I,J)*(PA(J,J)+PB(J,J)-Z(J))
FB(I,I)=FB(I,I)+GAMA(I,J)*(PB(J,J)+PA(J,J)-Z(J))
1 CONTINUE
FA(I,I)=FA(I,I)-AI(I)+PB(I,I)*(AI(I)-E(I))
2 FB(I,I)=FB(I,I)-AI(I)+PA(I,I)*(AI(I)-E(I))
RETURN
END
```

\$IBFTC POL DECK

POL - EFN SOURCE STATEMENT - IFN(S) -

```
REAL FUNCTION POLEN(FA,FB,PA,PB,AI,BETA,Z,GAMA,N)
DIMENSION FA(30,30),FB(30,30),PA(30,30),PB(30,30),AI(30),
1 Z(30),BETA(30,30),GAMA(30,30)
POLEN=0.0
DO 1 I=1,N
X=0.0
DO 2 J=1,N
IF(I.EQ.J) GO TO 2
POLEN=POLEN+PA(J,I)*(FA(I,J)+BETA(I,J))+PB(J,I)*(FB(I,J)+
1 BETA(I,J))
X=X+Z(J)*GAMA(J,I)
2 CONTINUE
1 POLEN=POLEN+PA(I,I)*(FA(I,I)-X-AI(I))+PB(I,I)*(FB(I,I)-X-
AI(I))
POLEN=0.5*POLEN
RETURN
END
```

\$IBFTC PVT DECK

PVT - EFN SOURCE STATEMENT - IFN(S) -

```
SUBROUTINE PURV(PA,PB,N)
DIMENSION PA(30,30),PB(30,30)
WRITE(6,1)
1 FORMAT(1H ,//,26H PA AND PB ANTISYMMETRIZED,/)
DO 2 I=1,N,2
PA(I,I)=PA(I,I)*1.3
2 PB(I,I)=PB(I,I)*0.7
DO 3 I=2,N,2
PB(I,I)=PB(I,I)*1.3
3 PA(I,I)=PA(I,I)*0.7
RETURN
END
```

\$IBFTC DECK6 DECK

DECK6 - EFN SOURCE STATEMENT - IFN(S) -

```
SUBROUTINE RITE(N)
DIMENSION CHAR(12)
READ(5,1) (CHAR(I),I=1,12)
1 FORMAT(12A6)
WRITE(6,2) (CHAR(I),I=1,12)
2 FORMAT(1H1,1H ,12A6,///)
RETURN
END
```

\$IBFTC STRC DECK

STRC - EFN SOURCE STATEMENT - IFN(S) -

```
REAL FUNCTION SECTR(A,N)
DIMENSION A(30,30)
SECTR=0.0
DO 1 I=1,N
1 SECTR=SECTR+A(I,I)
RETURN
END
```


\$IBFTC PJE DECK

PJE - EFN SOURCE STATEMENT - IFN(S) -

```
SUBROUTINE PROJEN(BETA, AI, E, Z, GAMA, QA, QB, FA, PA, PB, X, H, C, N)
DIMENSION BETA(30,30), AI(30), E(30), Z(30), GAMA(30,30), QA(30,30),
1 QB(30,30), FA(30,30), PA(30,30), PB(30,30), X(30,30), H(30,30),
2 C(30,30)
DO 1 I=1, N
C(I, I)=0.0
DO 2 J=1, N
IF(I.EQ.J) GO TO 2
C(I, I)=C(I, I)-Z(J)*GAMA(I, J)
C(I, J)=BETA(I, J)
2 CONTINUE
1 C(I, I)=C(I, I)-AI(I)
X(1,3)=TRACE(H, C, N)
DO 3 I=1, N
H(I, I)=0.0
C(I, I)=0.0
DO 4 J=1, N
IF(I.EQ.J) GO TO 4
C(I, I)=C(I, I)+(QA(J, J)+QB(J, J))*GAMA(I, J)
C(I, J)=-QB(I, J)*GAMA(I, J)
H(I, J)=-QA(I, J)*GAMA(I, J)
4 CONTINUE
H(I, I)=C(I, I)+QB(I, I)*(AI(I)-E(I))
3 C(I, I)=C(I, I)+QA(I, I)*(AI(I)-E(I))
X(1,3)=X(1,3)+0.5*(TRACE(PA, H, N)+TRACE(PB, C, N))
X(1,4)=0.0
DO 5 I=1, N
DO 6 J=1, N
IF(I.EQ.J) GO TO 6
X(1,4)=X(1,4)+(QA(I, J)-FA(I, J))*(FA(J, I)-QB(J, I))*GAMA(I, J)
6 CONTINUE
5 X(1,4)=X(1,4)+(QA(I, I)-FA(I, I))*(FA(I, I)-QB(I, I))*(AI(I)-E(I))
X(1,4)=0.5*X(1,4)/X(1,1)
WRITE(6,7) X(1,4)
7 FORMAT(1H ,//, 17H CORRECTION TERM=, F10.6, //)
X(1,3)=X(1,3)-X(1,4)
WRITE(6,8) X(1,3)
8 FORMAT(34H TOTAL ENERGY WITH SPIN PROJECTED=, F12.6, //)
RETURN
END
```

\$IBFTC COBO DECK

COBO - EFN SOURCE STATEMENT - IFN(S) -

```

SUBROUTINE EQOB(CA,CB,QA,QB,PA,PB,N,EIG)
DIMENSION CA(30,30),CB(30,30),QA(30,30),QB(30,30),PA(30,30)
1  PB(30,30),EIG(30)
C  CA=(PCP)      CB=QPQ
DO 1 I=1,N
DO 1 J=1,N
1  QA(I,J)=CA(I,J)
CALL HESSEN(QA,N)
CALL QREIG(QA,N,EIG)
DO 2 I=1,N
2  QA(I,I)=EIG(I)
K=N+1
QB(1,1)=0.0
DO 3 I=1,N
J=K-I
EIG(I)=QA(J,J)
IF(EIG(I).GT.1.0E-5) QB(1,1)=QB(1,1)+1.0
3  CONTINUE
J=IFIX(QB(1,1))
WRITE(6,4)
4  FORMAT(1H ,///,34H CORRESPONDING ORBITAL COEFFICENTS,/)
WRITE(6,5)
5  FORMAT(8H ORBITAL,10X,10H C-O COEFF,10X,6H DELTA,/)
DO 6 I=1,J
QB(3,I)=EIG(I)
QB(1,1)=SQRT(EIG(I))
QB(1,2)=0.5*(1.0-QB(1,1))
IF(QB(1,2).LT.1.0E-10) QB(1,2)=1.0E-10
QB(1,2)=SQRT(QB(1,2))
WRITE(6,7) I,QB(1,1),QB(1,2)
6  CONTINUE
7  FORMAT(1H ,3X,I2,15X,F6.4,12X,F6.4,/)
WRITE(6,8)
8  FORMAT(1H ,///,10H ALPHA C-O,/)
DO 9 I=1,J
W=QB(3,I)
CALL VCTR(CA,EIG,N,W)
WRITE(6,10) (EIG(K),K=1,N)
10  FORMAT(10F10.6)
9  CONTINUE
WRITE(6,11)
11  FORMAT(1H ,///,9H BETA C-O,/)
DO 12 I=1,J
W=QB(3,I)
CALL VCTR(CB,EIG,N,W)
WRITE(6,10) (EIG(K),K=1,N)
12  CONTINUE
RETURN
END
```

\$IBFTC SOTVCT DECK

SOTVCT - EFN SOURCE STATEMENT - IFN(S) -

```
SUBROUTINE VSORT(C,CH,X,CF,ENA,N,ICV)
DIMENSION C(30,30),CH(30,30),X(30,30),CF(30,30),
1 ENA(30),ENAF(30),IM(30)
IF(ICV.EQ.1) GO TO 13
DO 1 M=1,N
DO 1 I=1,N
X(M,I)=0.0
DO 1 J=1,N
1 X(M,I)=X(M,I)+CH(I,J)*C(M,J)
DO 2 M=1,N
IM(M)=1
DO 2 J=2,N
IF(X(M,J).LE.X(M,1))GO TO 2
X(M,1)=X(M,J)
IM(M)=J
2 CONTINUE
IY=0
DO 3 I=1,N
3 IY=IY+IM(I)
IZ=N*(N+1)/2
IF(IY.EQ.IZ) GO TO 15
NM1=N-1
DO 10 I=1,NM1
IPI=I+1
DO 10 J=IPI,N
IF(IM(I).EQ.IM(J)) GO TO 11
10 CONTINUE
11 IF(X(I,1).GE.X(J,1)) GO TO 12
IM(I)=IZ-IY+IM(I)
GO TO 13
12 IM(J)=IZ-IY+IM(J)
13 IY=0
DO 14 I=1,N
14 IY=IY+IM(I)
IF(IY.EQ.IZ) GO TO 15
WRITE(6,16)
16 FORMAT(13H DOUBLE DEGEN,/)
15 DO 6 I=1,N
K=IM(I)
ENAF(K)=ENA(I)
DO 6 J=1,N
6 CF(K,J)=C(I,J)
DO 7 I=1,N
ENA(I)=ENAF(I)
DO 7 J=1,N
7 C(I,J)=CF(I,J)
18 RETURN
END
```

\$IBFTC DG3 DECK

DG3 - EFN SOURCE STATEMENT - IFN(S) -

```
SUBROUTINE DEGEN(EIG,F,C,N,NF)
DIMENSION EIG(30),F(30,30),C(30,30),V(30),A(30,30),IX(30),Z(30)
DO 1 I=1,N
IX(I)=0
DO 1 J=1,N
C(I,J)=0.0
1 A(I,J)=F(I,J)
CALL HESSEN(A,N)
CALL QREIG(A,N,EIG)
NM1=N-1
A(1,1)=0.0
DO 2 I=1,NM1
IP1=I+1
IF(ABS(EIG(I)-EIG(IP1)).GT.0.001) GO TO 2
A(1,1)=A(1,1)+1.0
IX(I)=1
IX(IP1)=1
2 CONTINUE
IF(A(1,1).LT.0.5) GO TO 3
DO 4 I=1,NF
IF(IX(I).EQ.1) GO TO 4
Y=EIG(I)
CALL VCTR(F,V,N,Y)
DO 5 J=1,N
5 C(I,J)=V(J)
4 CONTINUE
WB=F(1,1)
IF(F(1,1).GT.0.01) GO TO 15
DO 16 I=1,N
16 F(I,I)=F(I,I)+1.0
15 W=F(1,1)
F(1,1)=F(1,1)*1.01
WA=F(1,1)
DO 6 I=1,N
DO 6 J=1,N
6 A(I,J)=F(I,J)
CALL HESSEN(A,N)
CALL QREIG(A,N,Z)
DO 7 I=1,NF
IF(IX(I).EQ.0) GO TO 7
Y=Z(I)
CALL VCTR(F,V,N,Y)
F(1,1)=W
CALL COV(I,V,IX,A,C,F,N,NF)
F(1,1)=WA
DO 9 J=1,N
9 C(I,J)=V(J)
IX(I)=0
```

```
7 CONTINUE
  F(1,1)=WB
  IF(WB.GT.0.01) GO TO 10
  DO 18 I=2,N
18 F(I,I)=F(I,I)-1.0
  GO TO 10
 3 DO 11 I=1,NF
  Y=EIG(I)
  CALL VCTR(F,V,N,Y)
  DO 12 J=1,N
12 C(I,J)=V(J)
11 CONTINUE
10 RETURN
  END
```

\$IBFTC CV DECK

CV - EFN SOURCE STATEMENT - IFN(S) -

```
  SUBROUTINE COV(I,V,IX,A,C,F,N,NF)
  DIMENSION V(30),IX(30),A(30,30),C(30,30),F(30,30)
  A(5,2)=0.2
  NITER=40
  CALL OTH(I,V,C,A,IX,N,NF)
  A(5,3)=0.0
  DO 5 L=1,NITER
  DO 2 J=1,N
  A(4,J)=0.0
  DO 2 K=1,N
 2 A(4,J)=A(4,J)+F(J,K)*V(K)
  A(5,1)=0.0
  DO 3 J=1,N
 3 A(5,1)=A(5,1)+V(J)*A(4,J)
  DO 4 J=1,N
 4 V(J)=V(J)-A(5,2)*(A(4,J)-A(5,1)*V(J))
  DO 7 J=1,N
  IF(ABS(V(J)-A(6,J)).GT.0.000005) GO TO 8
 7 CONTINUE
  CALL OTH(I,V,C,A,IX,N,NF)
  GO TO 9
 8 A(5,3)=A(5,3)+1.0
  IF(A(5,3).GT.4.2) CALL OTH(I,V,C,A,IX,N,NF)
  IF(A(5,3).GT.4.2) A(5,3)=0.0
  DO 10 J=1,N
10 A(6,J)=V(J)
 5 CONTINUE
 9 RETURN
  END
```

\$IBFTC DECK5 DECK

DECK5 - EFN SOURCE STATEMENT - IFN(S) -

```
SUBROUTINE RECAL(F,Q,AN,N,CH,X,CF,ICV)
DIMENSION F(30,30),Q(30,30),AN(30),ENA(30),C(30,30),CH(30,30)
1  ,X(30,30),CF(30,30)
C  RECALCULATES P FROM F EIGENVECTORS RETURNS AS Q
CALL DEGEN(ENA,F,C,N,N)
CALL VSORT(C,CH,X,CF,ENA,N,ICV)
DO 2 I=1,N
DO 2 J=1,N
Q(I,J)=0.0
DO 2 K=1,N
2 Q(I,J)=Q(I,J)+AN(K)*C(K,I)*C(K,J)
DO 3 I=1,N
DO 3 J=1,N
3 CH(I,J)=C(I,J)
RETURN
END
```

\$IBFTC OTC DECK

OTC - EFN SOURCE STATEMENT - IFN(S) -

```
SUBROUTINE OTH(I,V,C,A,IX,N,NF)
DIMENSION V(30),C(30,30),A(30,30),IX(30)
DO 1 J=1,NF
IF(IX(J).EQ.1) GO TO 1
A(2,J)=0.0
DO 2 K=1,N
2 A(2,J)=A(2,J)+V(K)*C(J,K)
1 CONTINUE
DO 3 J=1,NF
IF(IX(J).EQ.1) GO TO 3
DO 4 K=1,N
4 V(K)=V(K)-A(2,J)*C(J,K)
3 CONTINUE
A(3,1)=0.0
DO 5 J=1,N
5 A(3,1)=A(3,1)+V(J)*V(J)
A(3,1)=SQRT(A(3,1))
DO 6 J=1,N
6 V(J)=V(J)/A(3,1)
RETURN
END
```

\$IBFTC QRCN DECK

QRCN - EFN SOURCE STATEMENT - IFN(S) -

C PROGRAM TO CALL QR TRANSFORMATION, MAXIMUM ITER IS 50.

SUBROUTINE QREIG(A,M,ROOTR)

DIMENSION A(30,30),ROOTR(30),ROOTI(30)

IPRNT=0

N = M

N50=N

IF(IPRNT) 80,81,80

80 WRITE (6,104)

81 ZERO = 0.0

JJ=1

177 XNN=0.0

XN2=0.0

AA = 0.0

B = 0.0

C = 0.0

DD = 0.0

R=0.0

SIG=0.0

ITER = 0

17 IF(N-2) 13,14,12

13 IF(IPRNT) 82,83,82

82 WRITE (6,105)A(1,1)

83 ROOTR(1) = A(1,1)

ROOTI(1) = 0.0

1 M50=N50-1

DO 505 K50=1,M50

K1=K50+1

DO 505 J50=K1,N50

IF(ROOTR(K50).LT.ROOTR(J50)) GO TO 505

504 X1=ROOTR(K50)

ROOTR(K50)=ROOTR(J50)

ROOTR(J50)=X1

505 CONTINUE

RETURN

14 JJ=-1

12 X = (A(N-1,N-1) - A(N,N))**2

S = 4.0*A(N,N-1)*A(N-1,N)

ITER = ITER + 1

IF(X .EQ. 0.0 .OR. ABS(S/X) .GT. 1.0E-8) GO TO 15

16 IF(ABS(A(N-1,N-1))-ABS(A(N,N))) 32,32,31

31 E = A(N-1,N-1)

G = A(N,N)

GO TO 33

32 G = A(N-1,N-1)

E = A(N,N)

33 F = 0.

H = 0.

GO TO 24

```
15 S = X + S
   X = A(N-1,N-1) + A(N,N)
   IF(S) 18,19,19
19 SQ=SQRT(S)
   F=0.0
   H=0.0
   IF (X) 21,21,22
21 E=(X-SQ)/2.0
   G=(X+SQ)/2.0
   GO TO 24
22 G=(X-SQ)/2.0
   E=(X+SQ)/2.0
   GO TO 24
18 F = SQRT(-S)/2.0
   E=X/2.0
   G=E
   H=-F
24 IF(JJ) 28,70,70
20 D = 1.0E-10*(ABS(G) + F)
   IF(ABS(A(N-1,N-2)) .GT. D) GO TO 26
28 IF(IPRNT) 84,85,84
84 WRITE (6,105)E,F, ITER
   WRITE (6,105)G,H
85 ROOTR(N) = E
   ROOTI(N) = F
   ROOTR(N-1) = G
   ROOTI(N-1) = H
   N=N-2
   IF(JJ) 1,177,177
26 IF(ABS(A(N,N-1)) .GT. 1.0E-10*ABS(A(N,N))) GO TO 50
29 IF(IPRNT) 86,87,86
86 WRITE (6,105)A(N,N), ZERO, ITER
87 ROOTR(N) = A(N,N)
   ROOTI(N) = 0.0
   N=N-1
   GO TO 177
50 IF(ABS(ABS(XNN/A(N,N-1))-1.0)-1.0E-6) 63,63,62
62 IF(ABS(ABS(XN2/A(N-1,N-2))-1.0)-1.0E-6) 63,63,700
63 VQ=ABS(A(N,N-1))-ABS(A(N-1,N-2))
   IF (ITER-15) 53,164,64
164 IF(VQ) 165,165,166
165 R = A(N-1,N-2)**2
   SIG = 2.0*A(N-1,N-2)
   GO TO 60
166 R = A(N,N-1)**2
   SIG = 2.0*A(N,N-1)
   GO TO 60
64 IF(VQ) 67,67,66
66 IF(IPRNT) 88,85,88
88 WRITE (6,107)A(N-1,N-2)
```



```
GO TO 84
67 IF(IPRNT) 89,87,89
89 WRITE (6,107)A(N,N-1)
GO TO 86
700 IF(ITER .GT. 50) GO TO 63
IF(ITER .GT. 5 ) GO TO 53
701 Z1= ((E-AA)**2+(F-B)**2)/(E+E+F*F)
Z2= ((G-C)**2+(H-DD)**2)/(G*G+H*H)
IF(Z1-0.25) 51,51,52
51 IF(Z2-0.25) 53,53,54
53 R=E*G-F*H
SIG=E+G
GO TO 60
54 R=E+E
SIG=E+E
GO TO 60
52 IF(Z2-0.25) 55,55,601
55 R=G*G
SIG=G+G
GO TO 60
601 R = 0.0
SIG = 0.0
60 XNN=A(N,N-1)
XN2=A(N-1,N-2)
CALL QRT(A,N,R,SIG,D)
AA=E
B=F
C=G
DD=H
GO TO 12
104 FORMAT(////1X, 9HREAL PART 6X 14HIMAGINARY PART, 26X
1 13HTAKEN AS ZERO 6X 4HITER //)
105 FORMAT(1X,E15.8,3X,E15.8, 42X I3)
107 FORMAT(56X E13.8)
END
```

\$IBFTC *QRT DECK

*QRT - EFN SOURCE STATEMENT - IFN(S) -

```

SUBROUTINE QRT(A,N,R,SIG,D)
DIMENSION A(30,30),PSI(2),G(3)
N1 = N - 1
IA = N - 2
IP = IA
IF(N-3) 101,10,60
60 DO 12 J = 3,N1
    J1 = N - J
    IF(ABS(A(J1+1,J1))-D) 10,10,11
11 DEN = A(J1+1,J1+1)*(A(J1+1,J1+1)-SIG)+A(J1+1,J1+2)*A(J1+2,
    J1+1)+R
    IF(DEN) 61,12,61
61 IF(ABS(A(J1+1,J1)*A(J1+2,J1+1)*(ABS(A(J1+1,J1+1)+A(J1+2,J
    1+2)
    I-SIG)+ABS(A(J1+3,J1+2)))/DEN)-D) 10,10,12
12 IP=J1
10 DO 14 J=1,IP
    J1=IP-J+1
    IF(ABS(A(J1+1,J1))-D) 13,13,14
14 IQ=J1
13 DO 100 I=IP,N1
    IF(I-IP) 16,15,16
15 G(1)=A(IP,IP)*(A(IP,IP)-SIG)+A(IP,IP+1)*A(IP+1,IP)+R
    G(2)=A(IP+1,IP)*(A(IP,IP)+A(IP+1,IP+1)-SIG)
    G(3)=A(IP+1,IP)*A(IP+2,IP+1)
    A(IP+2,IP)=0.0
    GO TO 19
16 G(1)=A(I,I-1)
    G(2)=A(I+1,I-1)
    IF(I-IA) 17,17,18
17 G(3)=A(I+2,I-1)
    GO TO 19
18 G(3)=0.0
19 XK = SIGN(SQRT(G(1)**2 + G(2)**2 + G(3)**2), G(1))
22 IF(XK) 23,24,23
23 AL=G(1)/XK+1.0
    PSI(1)=G(2)/(G(1)+XK)
    PSI(2)=G(3)/(G(1)+XK)
    GO TO 25
24 AL=2.0
    PSI(1)=0.0
    PSI(2)=0.0
25 IF(I-IQ) 26,27,26
26 IF(I-IP) 29,28,29
28 A(I,I-1)=-A(I,I-1)
```

```
GO TO 27
29 A(I,I-1)=-XK
27 DO 30 J=I,N
   IF(I-IA) 31,31,32
31 C=PSI(2)*A(I+2,J)
   GO TO 33
32 C=0.0
33 E=AL*(A(I,J)+PSI(1)*A(I+1,J)+C)
   A(I,J)=A(I,J)-E
   A(I+1,J)=A(I+1,J)-PSI(1)*E
   IF(I-IA) 34,34,30
34 A(I+2,J)=A(I+2,J)-PSI(2)*E
30 CONTINUE
   IF(I-IA) 35,35,36
35 L=I+2
   GO TO 37
36 L=N
37 DO 40 J=IQ,L
   IF(I-IA) 38,38,39
38 C=PSI(2)*A(J,I+2)
   GO TO 41
39 C=0.0
41 E=AL*(A(J,I)+PSI(1)*A(J,I+1)+C)
   A(J,I)=A(J,I)-E
   A(J,I+1)=A(J,I+1)-PSI(1)*E
   IF(I-IA) 42,42,40
42 A(J,I+2)=A(J,I+2)-PSI(2)*E
40 CONTINUE
   IF(I-N+3) 43,43,100
43 E=AL*PSI(2)*A(I+3,I+2)
   A(I+3,I)=-E
   A(I+3,I+1)=-PSI(1)*E
   A(I+3,I+2)=A(I+3,I+2)-PSI(2)*E
100 CONTINUE
101 RETURN
   END
```

\$IBFTC HESS DECK

HESS - EFN SOURCE STATEMENT - IFN(S) -

C SUBROUTINE TO PUT MATRIX IN UPPER HESSENBERG FORM.

SUBROUTINE HESSEN(A,M)
DIMENSION A(30,30),B(50)
DOUBLE PRECISION SUM
IF (M - 2) 30,30,32

32 DO 40 LC = 3,M

N = M - LC + 3

N1 = N - 1

N2 = N - 2

NI = N1

DIV = ABS(A(N,N-1))

DO 2 J=1,N2

IF(ABS(A(N,J))- DIV) 2,2,1

1 NI = J

DIV = ABS(A(N,J))

2 CONTINUE

IF(DIV) 3,40,3

3 IF(NI - N1) 4, 7,4

4 DO 5 J = 1,N

DIV = A(J,NI)

A(J,NI) = A(J,N1)

5 A(J,N1) = DIV

DO 6 J = 1,M

DIV = A(NI,J)

A(NI,J) = A(N1,J)

6 A(N1,J) = DIV

7 DO 26 K = 1, N1

26 B(K) = A(N,K)/A(N,N-1)

DO 45 J = 1,M

SUM = 0.0

IF (J - N1) 46,43,43

46 IF(B(J)) 41,43,41

41 A(N,J) = 0.0

DO 42 K = 1,N1

A(K,J) = A(K,J) - A(K,N1)*B(J)

42 SUM = SUM + A(K,J)*B(K)

GO TO 45

43 DO 44 K = 1,N1

44 SUM = SUM + A(K,J)*B(K)

45 A(N1,J) = SUM

40 CONTINUE

30 RETURN

END

SV - EFN SOURCE STATEMENT - IFN(S) -

```

SUBROUTINE VCTR(AX,V,N,XY)
DIMENSION AX(30,30),A(30,30),V(30)
VNR=1.0
ALPHA=XY
DO 501 I51=1,N
DO 501 J51=1,N
501 A(I51,J51)=AX(I51,J51)
A(1,1)=A(1,1)-ALPHA
6 DO 15 I=2,N
A(I,I)=A(I,I)-ALPHA
70 II=I-1
7 DO 15 J=1,II
8 IF (A(I,J))9,15,9
9 IF (ABS (A(J,J))-ABS (A(I,J)))11,10,10
10 R=A(I,J)/A(J,J)
GO TO 130
11 R=A(J,J)/A(I,J)
DO 12 K=1,N
C=A(J,K)
A(J,K)=A(I,K)
12 A(I,K)=C
130 JJ=J+1
13 DO 14 K=JJ,N
14 A(I,K)=A(I,K)-R*A(J,K)
15 CONTINUE
C=A(N,N)
V(N)=1.0
DO 29 I=2,N
JJ=N-I+1
R=0.0
II=N-I+2
DO 25 K=II,N
25 R=R+A(JJ,K)*V(K)
IF (ABS (A(JJ,JJ))-1.0E-10)27,27,28
27 V(JJ)=1.0
C=0.0
DO 26 J=II,N
26 V(J)=0.0
GO TO 29
28 V(JJ)=(C-R)/A(JJ,JJ)
29 CONTINUE
X50=0.0
DO 502 J52=1,N
502 X50=X50+V(J52)*V(J52)
X51=SQRT(X50/VNR)
DO 503 J53=1,N
503 V(J53)=V(J53)/X51
RETURN
END

```

#IBFTC SCS DECK

SCS - EFN SOURCE STATEMENT - IFN(S) -

```

SUBROUTINE SCFCS(H,BETA,GAMA,AI,E,Z,FA,CA,CB,PA,PB,ANA,
1 ANB,ENA,N)
DIMENSION H(30,30),BETA(30,30),GAMA(30,30),AI(30),E(30),
1 FA(30,30),CA(30,30),CB(30,30),PA(30,30),PB(30,30),Z(30)
2 ANA(30),ANB(30),ENA(30)
NIT=5
W=0.0
DO 1 I=1,N
1 W=W+ANA(I)+ANB(I)
W=W*0.5
NF=IFIX(W)
CALL HUCK(H,NF,CA,ENA,PA,N)
DO 3 L=1,NIT
DO 4 I=1,N
FA(I,1)=0.0
DO 5 J=1,N
IF(L.EQ.J) GO TO 5
FA(I,J)=BETA(I,J)-0.5*PA(I,J)*GAMA(I,J)
FA(I,I)=FA(I,I)+(PA(J,J)-Z(J))*GAMA(I,J)
5 CONTINUE
4 FA(I,I)=FA(I,I)-AI(I)+0.5*PA(I,I)*(AI(I)-E(I))
IF(L.EQ.NIT) NF=N
CALL DEGEN(ENA,FA,CA,N,NF)
IF(L.EQ.NIT) GO TO 7
DO 6 I=1,N
DO 6 J=1,N
PA(I,J)=0.0
DO 6 K=1,NF
6 PA(I,J)=PA(I,J)+CA(K,I)*CA(K,J)*2.0
3 CONTINUE
7 DO 8 I=1,N
DO 8 J=1,N
CB(I,J)=CA(I,J)
PA(I,J)=0.0
PB(I,J)=0.0
DO 8 K=1,N
PA(I,J)=PA(I,J)+CA(K,I)*CA(K,J)*ANA(K)
8 PB(I,J)=PB(I,J)+CA(K,I)*CA(K,J)*ANB(K)
RETURN
END
```

(4) A Program of Roothaan's Open-Shell Procedure .

This program obtains self-consistent wave functions for half closed-shell states using the technique introduced by Roothaan. This method which was fully discussed in section (I9) of Chapter II, may be used for a greater variety of excited molecular states than the spin-polarized method. Empty virtual orbitals of lower energy than the highest occupied open-shell orbital usually cause no trouble.

With this procedure some difficulty may be experienced in obtaining convergent results for some particular molecular states. However, with the judicious use of the input feed-back control, DVC, (see later), convergency may usually be achieved.

The starting point of the SCF iterations is the closed-shell SCF orbital set of the particular molecule, and self-consistent results are assumed to have been reached when the bond matrix, P, has converged to the required degree. The total Π -energy is calculated at every iteration, and after obtaining a self-consistent state, or running out of iterations, the results are printed out.

The form of input to the program is very similar to the previous program discussed.

NI, (I3): This integer may be used to label various write statements in the subroutine RITE, but it is frequently redundant, as the program title is read from the next card.

Title Card,(Free Format): Columns 1 to 72 of this card are used to head the print out .

N,(I3): The number of atoms in the molecule; $N \leq 30$.

NIT,(I3): Maximum number of SCF iterations, usually $NIT \leq 50$.

If NIT iterations are reached before convergence, results are printed out and N2 read.

A,B,FR,GM,(4F10.5): The first three of these correspond to Roothaan's a,b, and f ,(see page 259) . GM specifies the multiple of the Mataga-Nishimoto Coulomb integrals to be used. Normally $GM=1$. ; and for all triplet and doublet states, $A=1$. , $B=2$. , and $FR=0.5$.

/R(N,N),AI(N),E(N),Z(N),H(N,N)/,(F20.8): This is the usual block of input data.

/ANC(N)/,(F20.8): This matrix provides the closed-shell occupation numbers, counting from the lowest energy upwards. That is $ANC(i) = 1$. if ϕ_i is doubly occupied , otherwise it is zero.

/ANO(N)/,(F20.8): The open-shell occupation numbers. $ANO(i)=1$. for all occupied open-shells, otherwise it is zero.

CONV,DVC,(2F20.5): The first variable is the convergence criterion, normally $CONV=0.001$. For convergence we have the same condition as the closed-shell SCF program, in section (2) . A typical value of DVC is 0.3, but if difficulty with convergence is experienced, values as low as 0.05 may be tried.

N2,(I3): This control integer is read at the end of the program. If $N2 \neq 2$ the program stops , if $N2=2$ another set of ANC and ANO

matrices are read in, with a new CONV,DVC card; thus a new excited state may be treated.

\$IBFTC DK1 DECK

DK1 - EFN SOURCE STATEMENT - IFN(S) -

```

DIMENSION AI(30),E(30),Z(30),BETA(30,30),GAMA(30,30),EN(30),
1 DO(30,30),DC(30,30),DT(30,30),C(30,30),AA(30,30),
2 QO(30,30),QC(30,30)
3 ,H(30,30),AND(30),ANC(30),P(30,30),Q(30,30),F(30,30)
4 ,CH(30,30)

```

C RCOOHAANS OPEN SHELL SCF

```
READ(5,1) N1
```

C LABELS TITLE REQUIRED

```
CALL RITE(N1)
```

1 FORMAT(I3)

```
READ(5,1) N
```

C NUMBER OF ATOMS IN MOLECULE

```
READ(5,1) NIT
```

C MAX. NO. ITERATIONS

```
READ(5,29) A,B,FR,GM
```

C RCOOHAANS A,B,F, AND THE GAMA FACTOR

29 FORMAT(4F10.5)

```
N2=1
```

```
A1=(1.0-A)/(1.0-FR)
```

```
B1=(1.0-B)/(1.0-FR)
```

C RCOOHAANS ALPHA AND BETA

```
DO 2 I=1,N
```

```
DO 2 J=I,N
```

```
READ(5,3) C(I,J)
```

2 C(J,I)=C(I,J)

C GEOMETRIC MATRIX READ AS C

3 FORMAT(F20.8)

```
READ(5,3) (AI(I),I=1,N)
```

```
READ(5,3) (E(I),I=1,N)
```

```
READ(5,3) (Z(I),I=1,N)
```

C IONIZATION POTENTIAL, AFFINITY, VIRTUAL CHARGE

```
DO 4 I=1,N
```

```
DO 4 J=I,N
```

```
READ(5,3) H(I,J)
```

```
BETA(I,J)=H(I,J)
```

```
BETA(J,I)=H(I,J)
```

4 H(J,I)=H(I,J)

C RESONANCE AND HUCKEL MATRICES

```
WRITE(6,30) A,B,FR
```

30 FORMAT(1H ,///,22H RCOOHAAN COEFFICIENTS,5X,3H A=,F6.3,

```
15X,3H B=,F6.3,5X,3H F=,F6.3,///)
```

```
WRITE(6,6)
```

6 FORMAT(14H HUCKEL MATRIX,///)

```
DO 7 I=1,N
```

7 WRITE(6,8) (H(I,J),J=1,N)

8 FORMAT(12F8.3)

```
WRITE(6,9)
```

9 FORMAT(1H ,///,21H IONIZATION POTENTIAL,///)

```
WRITE(6,8) (AI(I),I=1,N)
WRITE(6,10)
10 FORMAT(1H ,///,18H ELECTRON AFFINITY,/)
WRITE(6,8) (E(I),I=1,N)
WRITE(6,11)
11 FORMAT(1H ,///,14H R(I,J) MATRIX,/)
DO 12 I=1,N
12 WRITE(6,8) (C(I,J),J=1,N)
WRITE(6,13)
13 FORMAT(1H ,///,23H NUMBER OF PI ELECTRONS,/)
WRITE(6,8) (Z(I),I=1,N)
CALL COUL(AI,E,C,GAMA,N)
DO 93 I=1,N
DO 93 J=1,N
93 GAMA(I,J)=GAMA(I,J)*GM
C REPULSION EXCHANGE MATRIX
54 READ(5,3) (ANC(I),I=1,N)
READ(5,3) (ANO(I),I=1,N)
C OPEN AND CLOSED SHELL OCCUPATIONS
READ(5,60) CONV,DVC
CONV2=CONV
60 FORMAT(2F20.5)
WRITE(6,14)
14 FORMAT(1H ,///,24H CLOSED SHELL OCCUPATION,/)
WRITE(6,8) (ANC(I),I=1,N)
WRITE(6,15)
15 FORMAT(1H ,///,22H OPEN SHELL OCCUPATION,/)
WRITE(6,8) (ANO(I),I=1,N)
IF(N2.EQ.2) CALL PUTIN(CH,P,DO,DC,ANO,ANC,N)
IF(N2.EQ.2) GO TO 70
CALL SCFCS(H,BETA,GAMA,AI,E,Z,F,C,P,DO,DC,EN,ANO,ANC,N,CH)
70 WRITE(6,16)
16 FORMAT(1H ,///,21H CLOSED SHELL SCF APPROXIMATION,/)
IF(N2.NE.1) GO TO 55
WRITE(6,17)
17 FORMAT(1H ,//,12H EIGENVALUES,/)
WRITE(6,18) (EN(I),I=1,N)
18 FORMAT(1H ,10F10.5)
WRITE(6,19)
19 FORMAT(1H ,///,13H EIGENVECTORS,/)
DO 20 I=1,N
20 WRITE(6,18) (C(I,J),J=1,N)
55 WRITE(6,21)
21 FORMAT(1H ,///,29H CHARGE AND BOND ORDER MATRIX,/)
DO 22 I=1,N
22 WRITE(6,18) (P(I,J),J=1,N)
WRITE(6,23)
23 FORMAT(1H ,///,28H CLOSED SHELL DENSITY MATRIX,/)
DO 24 I=1,N
24 WRITE(6,18) (DC(I,J),J=1,N)
WRITE(6,25)
```

```
25 FORMAT(1H ,///,26H OPEN SHELL DENSITY MATRIX,/)
   DO 26 I=1,N
26 WRITE(6,18) (DO(I,J),J=1,N)
   WRITE(6,27)
27 FORMAT(1H ,///,26H OPEN SHELL SCF PROPERTIES,/)
   DO 28 L=1,NIT
   VC=1.0-DVC*FLOCAT(L)
   IF(VC.LT.0.0) VC=0.0
   VCM=1.0-VC
   CONV=CONV2*VCM
   CALL FMAT(AI,E,Z,DO,DC,GAMA,N,BETA,A1,B1,AA,F)
   C RETURNS THE F MATRIX
   CALL RECAL(F,N,ANO,ANC,QO,QC,Q,C,EN)
   C RECALCULATES THE DENSITY MATRICES
   ENERGY=ENGY(BETA,AI,Z,GAMA,F,QO,QC,AA,FR,N)
   WRITE(6,50) ENERGY
50 FORMAT(1H ,/,17H TOTAL PI-ENERGY=,F11.5,/)
   IF(L.EQ.NIT) GO TO 31
   DO 32 I=1,N
   DO 32 J=1,N
32 IF(ABS(P(I,J)-Q(I,J)).GT.CONV) GO TO 33
   WRITE(6,90) CONV
90 FORMAT(1H ,//,28H METHOD HAS CONVERGED, CONV=,F8.5,/)
31 WRITE(6,34) L
34 FORMAT(1H ,///,22H NUMBER OF ITERATIONS=,I3,/)
   WRITE(6,35)
35 FORMAT(15H FINAL P MATRIX,/)
   DO 36 I=1,N
36 WRITE(6,18) (Q(I,J),J=1,N)
   WRITE(6,23)
   DO 37 I=1,N
37 WRITE(6,18) (QC(I,J),J=1,N)
   WRITE(6,25)
   DO 38 I=1,N
38 WRITE(6,18) (QO(I,J),J=1,N)
   WRITE(6,91)
91 FORMAT(1H ,///,5H ATOM,10X,13H SPIN DENSITY,10X,
115H CHARGE DENSITY,/)
   DO 39 I=1,N
   QO(I,I)=2.0*QO(I,I)
   WRITE(6,92) I,QO(I,I),Q(I,I)
92 FORMAT(1H ,I3,14X,F8.5,14X,F8.5,/)
   ANO(I)=0.0
39 ANC(I)=1.0
   CALL ENVEC(F,N,ANO,ANC,C,EN)
   WRITE(6,17)
   WRITE(6,18) (EN(I),I=1,N)
   WRITE(6,19)
   DO 40 I=1,N
40 WRITE(6,18) (C(I,J),J=1,N)
```

```
GO TO 41
33 DO 42 I=1,N
DO 42 J=1,N
P(I,J)=VC*P(I,J)+VCM*Q(I,J)
DO(I,J)=VC*DO(I,J)+VCM*QO(I,J)
42 DC(I,J)=VC*DC(I,J)+VCM*QC(I,J)
28 CONTINUE
41 READ(5,1) N2
IF(N2.EQ.2) GO TO 51
GO TO 52
51 WRITE(6,53)
53 FORMAT(1H ,////,18H SCF FOR NEW STATE,////)
GO TO 54
52 STOP
END
```

LIBRIC ENT DECK

ENT - EFN SOURCE STATEMENT - IFN(S) -

```
SUBROUTINE ENVEC(F,N,AND,ANC,C,EIG)
DIMENSION F(30,30),AND(30),ANC(30),C(30,30),EIG(30),V(30)
X=1.0/SQRT(2.0)
NF=0
DO 1 I=1,N
IF(AND(I).GT.C.1.OR.ANC(I).GT.C.1) NF=I
1 CONTINUE
IR=1
CALL SDEC(EIG,F,C,N,NF,IR)
IF(IR.GT.1) GO TO 2
DO 3 I=1,NF
IF(AND(I).LT.C.1.AND.ANC(I).LT.C.1) GO TO 3
Y=EIG(I)
IF(ANC(I).GT.C.1) CALL SVCIR(F,V,N,Y,1.0)
IF(AND(I).GT.C.1) CALL SVCIR(F,V,N,Y,0.5)
DO 4 J=1,N
4 C(I,J)=V(J)
3 CONTINUE
GO TO 5
2 DO 6 I=1,NF
IF(AND(I).LT.C.1) GO TO 6
DO 7 J=1,N
7 C(I,J)=C(I,J)*X
6 CONTINUE
5 RETURN
END
```

E1BFTC DGS DECK

DGS - EFN SOURCE STATEMENT - IFN(S) -

```
SUBROUTINE SDEG(EIG,F,C,N,NF,IR)
DIMENSION EIG(30),F(30,30),C(30,30),V(30),A(30,30),IX(30),Z(30)
DO 1 I=1,N
  IX(I)=0
DO 1 J=1,N
  C(I,J)=0.0
1 A(I,J)=F(I,J)
  CALL HESSEN(A,N)
  CALL QREIG(A,N,EIG)
  NMI=N-1
  IR=1
DO 2 I=1,NMI
  IP1=I+1
  IF(ABS(EIG(I)-EIG(IP1)).GT.0.001) GO TO 2
  IR=IR+1
  IX(I)=1
  IX(IP1)=1
2 CONTINUE
  IF(IR.EQ.1) GO TO 10
DO 4 I=1,NF
  IF(IX(I).EQ.1) GO TO 4
  Y=EIG(I)
  CALL SVCTR(F,V,N,Y,1.0)
DO 5 J=1,N
5 C(I,J)=V(J)
4 CONTINUE
  WB=F(1,1)
  IF(F(1,1).GT.0.01) GO TO 15
DO 16 I=1,N
16 F(I,1)=F(1,1)+1.0
15 W=F(1,1)
  F(1,1)=F(1,1)*1.01
  WA=F(1,1)
DO 6 I=1,N
DO 6 J=1,N
6 A(I,J)=F(I,J)
  CALL HESSEN(A,N)
  CALL QREIG(A,N,Z)
DO 7 I=1,NF
  IF(IX(I).EQ.0) GO TO 7
  Y=Z(I)
  CALL SVCTR(F,V,N,Y,1.0)
  F(1,1)=W
  CALL CUV(I,V,IX,A,C,F,N,NF)
  F(1,1)=WA
DO 9 J=1,N
9 C(I,J)=V(J)
  IX(I)=0
```

```
7 CONTINUE
  F(1,1)=WB
  IF(WB.GT.0.01) GO TO 10
  DO 18 I=2,N
18 F(1,I)=F(1,I)-1.0
10 RETURN
  END
```

8IBFTC CV DECK

CV - EFN SOURCE STATEMENT - IFN(S) -

```
SUBROUTINE COV(I,V,IX,A,C,F,N,NF)
  DIMENSION V(30),IX(30),A(30,30),C(30,30),F(30,30)
  A(5,2)=0.2
  NITER=40
  CALL OIH(I,V,C,A,IX,N,NF)
  A(5,3)=0.0
  DO 5 L=1,NITER
  DO 2 J=1,N
  A(4,J)=0.0
  DO 2 K=1,N
2 A(4,J)=A(4,J)+F(J,K)*V(K)
  A(5,1)=0.0
  DO 3 J=1,N
3 A(5,1)=A(5,1)+V(J)*A(4,J)
  DO 4 J=1,N
4 V(J)=V(J)-A(5,2)*(A(4,J)-A(5,1)*V(J))
  DO 7 J=1,N
  IF(ABS(V(J)-A(6,J)).GT.0.000005) GO TO 8
7 CONTINUE
  CALL OTH(I,V,C,A,IX,N,NF)
  GO TO 9
8 A(5,3)=A(5,3)+1.0
  IF(A(5,3).GT.4.2) CALL OTH(I,V,C,A,IX,N,NF)
  IF(A(5,3).GT.4.2) A(5,3)=0.0
  DO 10 J=1,N
10 A(6,J)=V(J)
5 CONTINUE
9 RETURN
  END
```

\$IBFTC OTC DECK

OTC - EFN SOURCE STATEMENT - IFN(S) -

```
SUBROUTINE OTH(I,V,C,A,IX,N,NF)
DIMENSION V(30),C(30,30),A(30,30),IX(30)
DO 1 J=1,NF
IF(IX(J).EQ.1) GO TO 1
A(2,J)=0.0
DO 2 K=1,N
2 A(2,J)=A(2,J)+V(K)*C(J,K)
1 CONTINUE
DO 3 J=1,NF
IF(IX(J).EQ.1) GO TO 3
DO 4 K=1,N
4 V(K)=V(K)-A(2,J)*C(J,K)
3 CONTINUE
A(3,1)=0.0
DO 5 J=1,N
5 A(3,1)=A(3,1)+V(J)*V(J)
A(3,1)=SQRT(A(3,1))
DO 6 J=1,N
6 V(J)=V(J)/A(3,1)
RETURN
END
```

\$IBFTC RCL DECK

RCL - EFN SOURCE STATEMENT - IFN(S) -

```
SUBROUTINE RECAL(F,N,ANO,ANC,QO,QC,Q,C,EIG,CH)
DIMENSION F(30,30),ANC(30),ANO(30),QO(30,30),QC(30,30),
1 C(30,30),EIG(30),Q(30,30)
CALL ENVEC(F,N,ANO,ANC,C,EIG)
DO 1 I=1,N
DO 1 J=1,N
QO(I,J)=0.0
QC(I,J)=0.0
DO 2 K=1,N
QC(I,J)=QC(I,J)+C(K,I)*C(K,J)*ANC(K)
2 QO(I,J)=QO(I,J)+C(K,I)*C(K,J)*ANO(K)
1 Q(I,J)=2.0*(QC(I,J)+QO(I,J))
RETURN
END
```


SIBFTC SCS DECK

SCS - EFN SOURCE STATEMENT - IFN(S) -

```
SUBROUTINE SCFCS(H,BETA,GAMA,AI,E,Z,F,C,P,DO,DC,EN,AND,ANC,N,CH)
DIMENSION H(30,30),BETA(30,30),GAMA(30,30),AI(30),E(30),Z(30),
1 F(30,30),C(30,30),P(30,30),DO(30,30),DC(30,30),EN(30),
2 AND(30),ANC(30),XO(30),XC(30)
3 ,CH(30,30)
NIT=5
W=0.0
DO 1 I=1,N
XO(I)=0.0
XC(I)=0.0
1 W=W+ANC(I)*2.0+AND(I)
W=W*0.5
NF=IFIX(W)
DO 2 I=1,NF
2 XC(I)=1.0
CALL HUCK(H,XO,XC,N,NF,EN,C,P)
DO 3 L=1,NIT
DO 4 I=1,N
F(I,I)=0.0
DO 5 J=1,N
IF(I.EQ.J) GO TO 5
F(I,J)=BETA(I,J)-0.5*P(I,J)*GAMA(I,J)
F(I,I)=F(I,I)+(P(J,J)-Z(J))*GAMA(I,J)
5 CONTINUE
4 F(I,I)=F(I,I)-AI(I)+0.5*P(I,I)*(AI(I)-E(I))
IF(L.LT.NIT) CALL ENVEC(F,N,XO,XC,C,EN)
IF(L.EQ.NIT) GO TO 10
DO 6 I=1,N
DO 6 J=1,N
P(I,J)=0.0
DO 6 K=1,NF
6 P(I,J)=P(I,J)+C(K,I)*C(K,J)*2.0
3 CONTINUE
10 NFP1=NF+1
DO 11 I=NFP1,N
11 XC(I)=1.0
CALL ENVEC(F,N,XO,XC,C,EN)
7 DO 8 I=1,N
DO 8 J=1,N
CH(I,J)=C(I,J)
DO(I,J)=0.0
DC(I,J)=0.0
DO 9 K=1,N
DO(I,J)=DO(I,J)+C(K,I)*C(K,J)*AND(K)*0.5
9 DC(I,J)=DC(I,J)+C(K,I)*C(K,J)*ANC(K)
8 P(I,J)=2.0*(DC(I,J)+DO(I,J))
RETURN
END
```

\$IBFTC PT DECK

PT - EFN SOURCE STATEMENT - IFN(S) -

```
SUBROUTINE PUTIN(CH,P,DO,DC,AND,ANC,N)
DIMENSION CH(30,30),P(30,30),DO(30,30),DC(30,30),AND(30),ANC(30)
DO 1 I=1,N
DO 1 J=1,N
DO(I,J)=0.0
DC(I,J)=0.0
DO 2 K=1,N
DO(I,J)=DO(I,J)+CH(K,I)*CH(K,J)*AND(K)*0.5
2 DC(I,J)=DC(I,J)+CH(K,I)*CH(K,J)*ANC(K)
1 P(I,J)=2.0*(DC(I,J)+DO(I,J))
RETURN
END
```

\$IBFTC HLE DECK

HLE - EFN SOURCE STATEMENT - IFN(S) -

```
SUBROUTINE HUCK(H,XD,XC,N,NF,EN,C,P)
DIMENSION H(30,30),XD(30),XC(30),EN(30),C(30,30),P(30,30)
CALL ENVEC(H,N,XD,XC,C,EN)
DO 1 I=1,N
DO 1 J=1,N
P(I,J)=0.0
DO 1 K=1,NF
1 P(I,J)=P(I,J)+C(K,I)*C(K,J)*2.0
RETURN
END
```

\$IBFTC DECK2 DECK

DECK2 - EFN SOURCE STATEMENT - IFN(S) -

```
SUBROUTINE RITE(N)
DIMENSION CHAR(12)
READ(5,1) (CHAR(I),I=1,12)
1 FORMAT(12A6)
WRITE(6,2) (CHAR(I),I=1,12)
2 FORMAT(1H1,1H,12A6,///)
RETURN
END
```

\$IBFTC FMF DECK

FMF - EFN SOURCE STATEMENT - IFN(S) -

```
SUBROUTINE FMAT(AI,E,Z,DO,DC,GAMA,N,BETA,A1,B1,Q,F)
DIMENSION AI(30),E(30),Z(30),DO(30,30),DC(30,30),GAMA(30,30)
1  ,BETA(30,30),AA(30,30)
2  ,Q(30,30),F(30,30)
DO 1 I=1,N
Q(I,I)=0.0
DO 2 J=1,N
IF(I.EQ.J) GO TO 2
Q(I,J)=-GAMA(I,J)*DO(I,J)*B1
Q(I,I)=Q(I,I)+DO(J,J)*GAMA(I,J)
2 CONTINUE
1 Q(I,I)=Q(I,I)*A1*2.0+(2.0*A1-B1)*(AI(I)-E(I))*DO(I,I)
DO 3 I=1,N
F(I,I)=0.0
DO 4 J=1,N
F(I,I)=F(I,I)+(DO(I,J)+DC(I,J))*Q(J,I)+Q(I,J)*(DO(J,I)+DC(J,I))
IF(I.EQ.J) GO TO 4
F(I,J)=0.0
DO 5 K=1,N
5 F(I,J)=F(I,J)+(DO(I,K)+DC(I,K))*Q(K,J)+Q(I,K)*(DO(K,J)+DC(K,J))
F(I,J)=F(I,J)+BETA(I,J)-Q(I,J)-GAMA(I,J)*(DO(I,J)+DC(I,J))
F(I,I)=F(I,I)+GAMA(I,J)*(2.0*(DO(J,J)+DC(J,J))-Z(J))
4 CONTINUE
3 F(I,I)=F(I,I)-AI(I)-Q(I,I)+(AI(I)-E(I))*(DO(I,I)+DC(I,I))
RETURN
END
```

\$IBFTC CL DECK

CL - EFN SOURCE STATEMENT - IFN(S) -

```
SUBROUTINE COUL(AI,E,R,GAMA,N)
DIMENSION AI(30),E(30),R(30,30),GAMA(30,30)
DO 1 I=1,N
DO 1 J=1,N
1 GAMA(I,J)=1.0/((R(I,J)/14.41)+(2.0/(AI(I)-E(I)+AI(J)-E(J))))
RETURN
END
```

QRCN - EFN SOURCE STATEMENT - IFN(S) -

C PROGRAM TO CALL QR TRANSFORMATION, MAXIMUM ITER IS 50.

SUBROUTINE QREIG(A,M,ROOTR)
 DIMENSION A(30,30),ROOTR(30),ROOTI(30)

IPRNT=0

N = M

N50=N

IF(IPRNT) 80,81,80

80 WRITE (6,104)

81 ZERO = 0.0

JJ=1

177 XNN=0.0

XN2=0.0

AA = 0.0

B = 0.0

C = 0.0

DD = 0.0

R=0.0

SIG=0.0

ITER = 0

17 IF(N-2) 13,14,12

13 IF(IPRNT) 82,83,82

82 WRITE (6,105)A(1,1)

83 ROOTR(1) = A(1,1)

ROOTI(1) = 0.0

1 M50=N50-1

DO 505 K50=1,M50

K1=K50+1

DO 505 J50=K1,N50

IF(ROOTR(K50).LT.ROOTR(J50)) GO TO 505

504 X1=ROCTR(K50)

RCOTR(K50)=RCOTR(J50)

ROOTR(J50)=X1

505 CONTINUE

RETURN

14 JJ=-1

12 X = (A(N-1,N-1) - A(N,N))*2

S = 4.0*A(N,N-1)*A(N-1,N)

ITER = ITER + 1

IF(X .EQ. 0.0 .OR. ABS(S/X) .GT. 1.0E-8) GO TO 15

16 IF(ABS(A(N-1,N-1))-ABS(A(N,N))) 32,32,31

31 E = A(N-1,N-1)

G = A(N,N)

GO TO 33

32 G = A(N-1,N-1)

E = A(N,N)

33 F = 0.

H = 0.

GO TO 24

```
15 S = X + S
   X = A(N-1,N-1) + A(N,N)
   IF(S) 18,19,19
19 SQ=SQRT(S)
   F=0.0
   H=0.0
   IF (X) 21,21,22
21 E=(X-SQ)/2.0
   G=(X+SQ)/2.0
   GO TO 24
22 G=(X-SQ)/2.0
   E=(X+SQ)/2.0
   GO TO 24
18 F = SQRT(-S)/2.0
   E=X/2.0
   G=E
   H=-F
24 IF(JJ) 28,70,70
70 D = 1.0E-10*(ABS(G) + F)
   IF(ABS(A(N-1,N-2)) .GT. D) GO TO 26
28 IF(IPRNT) 84,85,84
84 WRITE (6,105)E,F, ITER
   WRITE (6,105)G,H
85 ROOTR(N) = E
   RCOTI(N) = F
   ROOTR(N-1) = G
   RCOTI(N-1) = H
   N=N-2
   IF(JJ) 1,177,177
26 IF(ABS(A(N,N-1)) .GT. 1.0E-10*ABS(A(N,N))) GO TO 50
29 IF(IPRNT) 86,87,86
86 WRITE (6,105)A(N,N), ZERO, ITER
87 ROOTR(N) = A(N,N)
   ROOTI(N) = 0.0
   N=N-1
   GO TO 177
50 IF(ABS(ABS(XNN/A(N,N-1))-1.0)-1.0E-6) 63,63,62
62 IF(ABS(ABS(XN2/A(N-1,N-2))-1.0)-1.0E-6) 63,63,700
63 VQ=ABS(A(N,N-1))-ABS(A(N-1,N-2))
   IF (ITER-15) 53,164,64
164 IF(VQ) 165,165,166
165 R = A(N-1,N-2)**2
   SIG = 2.0*A(N-1,N-2)
   GO TO 60
166 R = A(N,N-1)**2
   SIG = 2.0*A(N,N-1)
   GO TO 60
64 IF(VQ) 67,67,66
66 IF(IPRNT) 88,85,88
88 WRITE (6,107)A(N-1,N-2)
```

```

GO TO 84
67 IF(IPRNT) 89,87,89
89 WRITE (6,107)A(N,N-1)
GO TO 86
700 IF(ITER .GT. 50) GO TO 63
IF(ITER .GT. 5 ) GO TO 53
701 Z1= ((E-AA)**2+(F-B)**2)/(E*E+F*F)
Z2= ((G-C)**2+(H-DD)**2)/(G*G+H*H)
IF(Z1-0.25) 51,51,52
51 IF(Z2-0.25) 53,53,54
53 R=E*G-F*H
SIG=E+G
GO TO 60
54 R=E*E
SIG=E+E
GO TO 60
52 IF(Z2-0.25) 55,55,601
55 R=G*G
SIG=G+G
GO TO 60
601 R = 0.0
SIG = 0.0
60 XNN=A(N,N-1)
XN2=A(N-1,N-2)
CALL QRT(A,N,R,SIG,D)
AA=E
B=F
C=G
DD=H
GO TO 12
104 FORMAT(////1X, 9HREAL PART 6X 14HIMAGINARY PART, 26X
1 13HTAKEN AS ZERO 6X 4HITER //)
105 FORMAT(1X,E15.8,3X,E15.8, 42X I3)
107 FORMAT(56X E13.8)
END

```

\$IBFTC *QRT DECK

*QRT - EFN SOURCE STATEMENT - IFN(S) -

```

SUBROUTINE QRT(A,N,R,SIG,D)
DIMENSION A(30,30),PSI(2),G(3)
N1 = N - 1
IA = N - 2
IP = IA
IF(N-3) 101,10,60
60 DO 12 J = 3,N1
J1 = N - J
IF(ABS(A(J1+1,J1))-D) 10,10,11
11 DEN = A(J1+1,J1+1)*(A(J1+1,J1+1)-SIG)+A(J1+1,J1+2)*A(J1+2,J1
1+1)

```

```
IF(DEN) 61,12,61
61 IF(ABS(A(J1+1,J1)*A(J1+2,J1+1)*(ABS(A(J1+1,J1+1)+A(J1+2,J1+2)
1-SIG)+ABS(A(J1+3,J1+2)))/DEN)-D) 10,10,12
12 IP=J1
10 DO 14 J=1,IP
    J1=IP-J+1
    IF(ABS(A(J1+1,J1))-D) 13,13,14
14 IQ=J1
13 DO 100 I=IP,N1
    IF(I-IP) 16,15,16
15 G(1)=A(IP,IP)*(A(IP,IP)-SIG)+A(IP,IP+1)*A(IP+1,IP)+R
    G(2)=A(IP+1,IP)*(A(IP,IP)+A(IP+1,IP+1)-SIG)
    G(3)=A(IP+1,IP)*A(IP+2,IP+1)
    A(IP+2,IP)=0.0
    GO TO 19
16 G(1)=A(I,I-1)
    G(2)=A(I+1,I-1)
    IF(I-IA) 17,17,18
17 G(3)=A(I+2,I-1)
    GO TO 19
18 G(3)=0.0
19 XK = SIGN(SQRT(G(1)**2 + G(2)**2 + G(3)**2), G(1))
22 IF(XK) 23,24,23
23 AL=G(1)/XK+1.0
    PSI(1)=G(2)/(G(1)+XK)
    PSI(2)=G(3)/(G(1)+XK)
    GO TO 25
24 AL=2.0
    PSI(1)=0.0
    PSI(2)=0.0
25 IF(I-IQ) 26,27,26
26 IF(I-IP) 29,28,29
28 A(I,I-1)=-A(I,I-1)
    GO TO 27
29 A(I,I-1)=-XK
27 DO 30 J=I,N
    IF(I-IA) 31,31,32
31 C=PSI(2)*A(I+2,J)
    GO TO 33
32 C=0.0
33 E=AL*(A(I,J)+PSI(1)*A(I+1,J)+C)
    A(I,J)=A(I,J)-E
    A(I+1,J)=A(I+1,J)-PSI(1)*E
    IF(I-IA) 34,34,30
34 A(I+2,J)=A(I+2,J)-PSI(2)*E
30 CONTINUE
    IF(I-IA) 35,35,36
35 L=I+2
    GO TO 37
36 L=N
```

```
37 DO 40 J=IQ,L
   IF(I-IA) 38,38,39
38 C=PSI(2)*A(J,I+2)
   GO TO 41
39 C=0.0
41 E=AL*(A(J,I)+PSI(1)*A(J,I+1)+C)
   A(J,I)=A(J,I)-E
   A(J,I+1)=A(J,I+1)-PSI(1)*E
   IF(I-IA) 42,42,40
42 A(J,I+2)=A(J,I+2)-PSI(2)*E
40 CONTINUE
   IF(I-N+3) 43,43,100
43 E=AL*PSI(2)*A(I+3,I+2)
   A(I+3,I)=-E
   A(I+3,I+1)=-PSI(1)*E
   A(I+3,I+2)=A(I+3,I+2)-PSI(2)*E
100 CONTINUE
101 RETURN
   END
```

\$IBFTC ENY DECK

ENY - EFN SOURCE STATEMENT - IFN(S) -

```
REAL FUNCTION ENGY(BETA,AI,Z,GAMA,F,DO,DC,Q,FR,N)
DIMENSION BETA(30,30),AI(30),Z(30),GAMA(30,30),F(30,30)
1 ,DO(30,30),DC(30,30),Q(30,30)
ENGY=0.0
DO 1 I=1,N
X=0.0
DO 2 J=1,N
IF(I.EQ.J) GO TO 2
ENGY=ENGY+(BETA(I,J)+F(I,J))*(DO(J,I)+DC(J,I))-
1 Q(I,J)*(DC(J,I)+FR*DO(J,I))
X=X+GAMA(I,J)*Z(J)
2 CONTINUE
1 ENGY=ENGY+(F(I,I)-X-AI(I))*(DO(I,I)+DC(I,I))-
1 Q(I,I)*(DC(I,I)+FR*DO(I,I))
RETURN
END
```


\$IBFTC HESS DECK

HESS - EFN SOURCE STATEMENT - IFN(S) -

C SUBROUTINE TO PUT MATRIX IN UPPER HESSENBERG FORM.

SUBROUTINE HESSEN(A,M)

DIMENSION A(30,30),B(50)

DOUBLE PRECISION SUM

IF (M - 2) 30,30,32

32 DO 40 LC = 3,M

N = M - LC + 3

N1 = N - 1

N2 = N - 2

NI = N1

DIV = ABS(A(N,N-1))

DO 2 J=1,N2

IF(ABS(A(N,J))- DIV) 2,2,1

1 NI = J

DIV = ABS(A(N,J))

2 CONTINUE

IF(DIV) 3,40,3

3 IF(NI - N1) 4, 7,4

4 DO 5 J = 1,N

DIV = A(J,NI)

A(J,NI) = A(J,N1)

5 A(J,N1) = DIV

DO 6 J = 1,M

DIV = A(NI,J)

A(NI,J) = A(N1,J)

6 A(N1,J) = DIV

7 DO 26 K = 1, N1

26 B(K) = A(N,K)/A(N,N-1)

DO 45 J = 1,M

SUM = 0.0

IF (J - N1) 46,43,43

46 IF(B(J)) 41,43,41

41 A(N,J) = 0.0

DO 42 K = 1,N1

A(K,J) = A(K,J) - A(K,N1)*B(J)

42 SUM = SUM + A(K,J)*B(K)

GO TO 45

43 DO 44 K = 1,N1

44 SUM = SUM + A(K,J)*B(K)

45 A(N1,J) = SUM

40 CONTINUE

30 RETURN

END

\$IBFTC SV DECK

SV - EFN SOURCE STATEMENT - IFN(S) -

```
SUBROUTINE SVCTR(AX,V,N,XY,VN)
DIMENSION AX(30,30),A(30,30),V(30)
VNR=VN
ALPHA=XY
DO 501 I51=1,N
DO 501 J51=1,N
501 A(I51,J51)=AX(I51,J51)
A(1,1)=A(1,1)-ALPHA
6 DO 15 I=2,N
A(I,I)=A(I,I)-ALPHA
70 II=I-1
7 DO 15 J=1,II
8 IF (A(I,J))9,15,9
9 IF (ABS (A(J,J))-ABS (A(I,J)))11,10,10
10 R=A(I,J)/A(J,J)
GO TO 130
11 R=A(J,J)/A(I,J)
DO 12 K=1,N
C=A(J,K)
A(J,K)=A(I,K)
12 A(I,K)=C
130 JJ=J+1
13 DO 14 K=JJ,N
14 A(I,K)=A(I,K)-R*A(J,K)
15 CONTINUE
C=A(N,N)
V(N)=1.
DO 29 I=2,N
JJ=N-I+1
R=0.
II=N-I+2
DO 25 K=II,N
25 R=R+A(JJ,K)*V(K)
IF (ABS (A(JJ,JJ))-1.0E-10)27,27,28
27 V(JJ)=1.
C=0.
DO 26 J=II,N
26 V(J)=0.
GO TO 29
28 V(JJ)=(C-R)/A(JJ,JJ)
29 CONTINUE
X50=0.0
DO 502 J52=1,N
502 X50=X50+V(J52)*V(J52)
X51=SQRT(X50/VNR)
DO 503 J53=1,N
503 V(J53)=V(J53)/X51
RETURN
END
```

(5) The Polymer SCF Program.

This program calculates the π -electron Bloch wave functions and energy-band structures of a one-dimensional polymer constructed from conjugated monomers. Only nearest-neighbour π -electron interactions are considered between adjacent monomers, and the Pople-Pariser-Parr approximations used as in the previous molecular programs. All Coulomb integrals, both within and between unit cells, are approximated in the manner of Mataga and Nishimoto. This procedure, whose basis was discussed in section (20) of chapter II, was originally designed for the particular problem of helical polymers composed of nucleotide bases. However, the method may clearly be used on any one-dimensional polymer with a defined repeating unit cell.

The program requires additional data compared to those discussed previously. As well as the intra-molecular parameters, inter-molecular data is also required to account for the interactions between the constituent molecules in the polymer. This data is given by additional geometric and resonance integrals.

The Bloch orbitals and energy-bands of the polymer are determined as functions of a wave number, k , where $0 \leq k \leq 2\pi$. The number of k intervals is left to the discretion of the program user, who must remember the additional execution time imposed by a large number of intervals. When the wave function for the various k values has been found, the monomer bond matrix, P ,

can be obtained using numerical integration . These bond matrices are checked between successive iterations for convergency, with a pre-set criterion of 0.001 for all elements in sequential iterates. For a SCF state some results are printed out, whilst others are stored on magnetic tape.

It will be noted much of the program is written in the complex mode, the eigenvalue problem being solved by partition as previously discussed, (see page 279). The subroutine FMOD is used to account for the H-bonds in the particular polymer investigated, and is not a general option.

The input data for this program is less easy to define than in the cases of the last three programs. Since the program uses appreciable amounts of computer time in reaching self-consistency ,(2 hours for an IBM 7090/I401, with 11 k intervals and a 20 atom unit cell), results of runs which did not reach a SCF state are stored on tape for future use by the program. Thus all tape manipulation is a function of the individual program, tape reel, and stage in attainment of self-consistency. Here initial guesses at P and P^{\pm} are read from cards, but at later stages in convergence they would usually be read directly from tape. The tape storing the results of the last run which had not yet reached self-consistency.

Thus it is felt appropriate to leave individual users to construct their own input/output forms, utilizing the following program as a basis. The input data required will now be listed.

NI,(I3): This is a title label, and also serves to control tape instructions.

N,(I3): The number of atoms per unit cell, $N \leq 20$.

NK,(I3): The number of k intervals, normally 11 for $N=20$.

NIT,(I3): Maximum number of iterations, if this is reached before a self-consistent state results are stored on tape.

NF,(I3): Half the number of electrons per unit cell.

/AI(N),E(N),Z(N)/,(F20.8): See previous programs. These are the parameters of the individual atoms in each unit cell.

/GAMA(N,N),GAMAP(N,N),BETA(N,N),BETAP(N,N),CP(N,N),CPP(N,N)/,(F20.8):

These are all read by a subroutine and represent the matrices,

$R, R^+, \beta, \beta^+, P, P^+$, respectively. Any future user should be able to feed in this data to the main program using a subroutine of his or her own, reading their own data format.

\$IBFTC KBAND

KBAND - EFN SOURCE STATEMENT - IFN(S) -

```
1 DIMENSION BA(40,40),EIG(40),GAMA(20,20),GAMAP(20,20),
  BETA(20,20),BETAP(20,20),Z(20),AI(20),E(20)
  COMPLEX CP(20,20),CPP(20,20),CF(20,20),CQ(20,20),CQP(20,20),
  1 CC(20,20)
C LADIKS SCF
C K BAND STRUCTURE OF A POLYMER
  READ(5,1) N1
C N1 LABELS THE TITLE REQUIRED
  CALL RUB(N1)
  CALL UDATE(CP,AI)
  CALL RITE(N1)
  READ(5,1) N
C N LABELS THE NUMBER OF ATOMS IN THE MOLECULE
  1 FORMAT(I3)
  READ(5,1) NK
C NK=NUMBER OF K INTERVALS
  READ(5,1) NIT
C NIT = MAX ITERATIONS
  READ(5,1) NF
C NF=NUMBER OF FILLED SHELLS
  READ(5,2) (AI(I),I=1,N)
  READ(5,2) (E(I),I=1,N)
  READ(5,2) (Z(I),I=1,N)
  2 FORMAT(F20.8)
  CALL DATA(GAMA,GAMAP,BETA,BETAP,CP,CPP)
C READS DATA GAMA=R,GAMAP=RP
  WRITE(6,3)
  3 FORMAT(1H ,///,11H INPUT DATA,/)
  WRITE(6,4)
  4 FORMAT(1H ,///,12H R(O) MATRIX,/)
  DC 5 I=1,N
  5 WRITE(6,6) (GAMA(I,J),J=1,N)
  6 FORMAT(1H ,20F5.2)
  WRITE(6,7)
  7 FORMAT(1H ,///,12H R(+) MATRIX,/)
  DC 8 I=1,N
  8 WRITE(6,6) (GAMAP(I,J),J=1,N)
  WRITE(6,9)
  9 FORMAT(1H ,///,15H BETA(O) MATRIX,/)
  DC 10 I=1,N
  10 WRITE(6,6) (BETA(I,J),J=1,N)
  WRITE(6,11)
  11 FORMAT(1H ,///,15H BETA(+) MATRIX,/)
  DC 12 I=1,N
  12 WRITE(6,6) (BETAP(I,J),J=1,N)
  WRITE(6,39)
  39 FORMAT(1H ,///,12H P(O) MATRIX,/)
  DC 40 I=1,N
```

```
40 WRITE(6,41) (CP(I,J),J=1,N)
41 FORMAT(1H ,16F7.4)
   WRITE(6,13)
13  FORMAT(1H ,///,21H IONIZATION POTENTIAL,/)
   WRITE(6,14) (AI(I),I=1,N)
14  FORMAT(1H ,18F6.2)
   WRITE(6,15)
15  FORMAT(1H ,///,18H ELECTRON AFFINITY,/)
   WRITE(6,14) (E(I),I=1,N)
   WRITE(6,16)
16  FORMAT(1H ,///,23H NUMBER OF PI ELECTRONS,/)
   WRITE(6,14) (Z(I),I=1,N)
   CALL COUL(GAMA,GAMAP,AI,E,N)
   FNK=FLOAT(NK)
   H=2.0/(FNK-1.0)
   PIH=6.28318/(FNK-1.0)
   DO 17 L=1,NIT
-  DO 19 JK=1,NK
   AK=PIH*FLCAT(JK-1)
   CALL CFMAT(CP,CPP,GAMA,GAMAP,BETA,BETAP,Z,AI,E,AK,N,CF)
   CALL FMOD(CF)
   CALL CPADD(CF,CQ,CQP,JK,NK,NF,N,AK,H)
19  CONTINUE
   IF(L.EQ.NIT) GO TO 34
   DO 21 I=1,N
   DO 21 J=1,N
   P=REAL(CP(I,J))
   Q=REAL(CQ(I,J))
21  IF(ABS(P-Q).GT.0.001) GO TO 22
34  WRITE(6,23) L
23  FORMAT(1H ,///,31H NUMBER OF ITERATIONS FOR SCF =,I3,/)
   WRITE(6,24)
24  FORMAT(1H ,///,12H P(0) MATRIX,/)
-  DO 25 I=1,N
25  WRITE(6,41) (CQ(I,J),J=1,N)
   WRITE(6,27)
27  FORMAT(1H ,///,12H P(+) MATRIX,/)
   DO 28 I=1,N
28  WRITE(6,41) (CQP(I,J),J=1,N)
   WRITE(6,29)
29  FORMAT(1H ,///,22H ENERGY BAND STRUCTURE,/)
-  DO 30 JK=1,NK
   AK=PIH*FLCAT(JK-1)
   CALL CFMAT(CQ,CQP,GAMA,GAMAP,BETA,BETAP,Z,AI,E,AK,N,CF)
   CALL FMOD(CF)
   CALL CQREIG(CF,N,EIG,BA)
   CALL CVCTR(BA,CC,N,N,EIG)
   CALL TAPED(AK,CF,CC,EIG,CQ,CQP,JK,NK)
   WRITE(6,31) AK
```

```
31 FORMAT(1H ,//,3H K=,F10.6,//)
   WRITE(6,32) (EIG(J),J=1,N)
32 FORMAT(1H ,1P8E13.5)
30 CONTINUE
   GC TO 38
22 DC 33 I=1,N
   DC 33 J=1,N
   CP(I,J)=CQ(I,J)
33 CPP(I,J)=CQP(I,J)
17 CONTINUE
38 STOP
   END
```

\$IBFTC TPE

```
TPE      -   EFN  SOURCE STATEMENT  -   IFN(S)  -
SUBROUTINE TAPED(AK,CF,CC,EIG,CQ,CQP,JK,NK)
DIMENSION EIG(20)
COMPLEX CF(20,20),CC(20,20),CQ(20,20),CQP(20,20)
WRITE(7) AK
WRITE(7) CF
WRITE(7) EIG
WRITE(7) CC
IF(JK.NE.NK) GO TO 1
WRITE(7) CQ
WRITE(7) CQP
REWIND 7
1 RETURN
END
```

\$IBFTC FM

```
FM      -   EFN  SOURCE STATEMENT  -   IFN(S)  -
SUBROUTINE FMDC(CF)
COMPLEX CF(20,20)
LADIK CORRECTIONS FOR POLY-AT
CF(1,1)=CF(1,1)-0.478
CF(10,10)=CF(10,10)+0.478
CF(11,11)=CF(11,11)+0.478
CF(18,18)=CF(18,18)-0.478
RETURN
END
```


JL6

- EFN SOURCE STATEMENT - IFN(S) -

```
SUBROUTINE DATA(R,RP,B,BP,CP,CPP)
DIMENSION R(20,20),RP(20,20),B(20,20),BP(20,20),P(20,20)
COMPLEX CP(20,20),CPP(20,20)
M=10
N=20
K=M+1
DC 1 I=1,M
1 READ(5,2) (R(I,J),J=1,M)
2 FORMAT(10F5.2)
DC 3 I=1,M
3 READ(5,2) (R(I,J),J=K,N)
DC 4 I=K,N
4 READ(5,2) (R(I,J),J=1,M)
DC 5 I=K,N
5 READ(5,2) (R(I,J),J=K,N)
DC 6 I=1,N
DC 6 J=1,N
6 IF(J.LT.I) R(I,J)=R(J,I)
DC 7 I=1,M
7 READ(5,2) (RP(I,J),J=1,M)
DC 8 I=1,M
8 READ(5,2) (RP(I,J),J=K,N)
DC 9 I=K,N
9 READ(5,2) (RP(I,J),J=1,M)
DC 10 I=K,N
10 READ(5,2) (RP(I,J),J=K,N)
DC 11 I=1,M
11 READ(5,2) (B(I,J),J=1,M)
DC 12 I=1,M
12 READ(5,2) (B(I,J),J=K,N)
DC 13 I=K,N
13 READ(5,2) (B(I,J),J=1,M)
DC 14 I=K,N
14 READ(5,2) (B(I,J),J=K,N)
DC 15 I=1,N
DC 15 J=1,N
15 IF(J.LT.I) B(I,J)=B(J,I)
DC 16 I=1,M
16 READ(5,2) (BP(I,J),J=1,M)
DC 17 I=1,M
17 READ(5,2) (BP(I,J),J=K,N)
DC 18 I=K,N
18 READ(5,2) (BP(I,J),J=1,M)
DC 19 I=K,N
19 READ(5,2) (BP(I,J),J=K,N)
DC 20 I=1,M
20 READ(5,2) (P(I,J),J=1,M)
DC 21 I=1,M
```

```
21 READ(5,2) (P(I,J),J=K,N)
   DC 22 I=K,N
22 READ(5,2) (P(I,J),J=1,M)
   DC 23 I=K,N
23 READ(5,2) (P(I,J),J=K,N)
   DC 24 I=1,N
   DC 24 J=1,N
24 IF(J.LT.I) P(I,J)=P(J,I)
   DC 100 I=1,N
   DO 100 J=1,N
   B(I,J)=-2.39*B(I,J)
   BP(I,J)=-2.39*BP(I,J)
   CP(I,J)=CMPLX(P(I,J),0.0)
100 CPP(I,J)=(0.0,0.0)
   RETURN
   END
```

\$IBFTC TITLE

TITLE - EFN SOURCE STATEMENT - IFN(S) -

```
SUBROUTINE RITE(N)
  DIMENSION CHAR(8)
  DATA (CHAR(I),I=1,8)/6H POLY ,6HADENIN,6HE-THYM,6HINE
,16H 28FEB,6HLADIKS,6H DATA,6H /
  IND=2
  WRITE(6,1)
1  FORMAT(1H1,21H POLY ADENINE-THYMINE,///)
  WRITE(7) IND
  WRITE(7) CHAR
  RETURN
  END
```

\$IBFTC COULI DECK

COULI - EFN SOURCE STATEMENT - IFN(S) -

```
SUBROUTINE COUL(GAMA,GAMAP,AI,E,N)
  DIMENSION GAMA(20,20),GAMAP(20,20),AI(20),E(20)
  DO 1 I=1,N
  DO 1 J=1,N
  X=2.0/(AI(I)-E(I)+AI(J)-E(J))
  GAMA(I,J)=1.0/((GAMA(I,J)/14.41)+X)
1  GAMAP(I,J)=1.0/((GAMAP(I,J)/14.41)+X)
  RETURN
  END
```

\$IBFTC UD

UD - EFN SOURCE STATEMENT - IFN(S) -

```
SUBROUTINE UDATE(CP,AI)
DIMENSION CHAR(8),AI(20)
COMPLEX CP(20,20)
READ(7) IND
READ(7) CHAR
DO 1 I=1,21
READ(7) AK
READ(7) CP
READ(7) AI
READ(7) CP
1 CONTINUE
READ(7) CP
READ(7) CP
RETURN
END
```

\$IBFTC CFMT DECK

CFMT - EFN SOURCE STATEMENT - IFN(S) -

```
SUBROUTINE CFMAT(CP, CPP, GAMA, GAMAP, BETA, BETAP, Z, AI, E, AK, N, CF)
DIMENSION GAMA(20,20), GAMAP(20,20), BETA(20,20), BETAP(20,20),
1 Z(20), AI(20), E(20)
COMPLEX CP(20,20), CPP(20,20), CF(20,20), CX, CY
CX=CEXP(CMPLX(0.0, AK))
CY=CEXP(CMPLX(0.0, -AK))
RZ=2.0*COS(AK)
DO 1 I=1, N
CF(I, I)=(0.0, 0.0)
DO 2 J=1, N
X=1.0
IF(I.EQ.J) X=0.0
2 CF(I, I)=CF(I, I)+(CP(J, J)-Z(J))*(GAMAP(I, J)+GAMAP(J, I)+
1 X*GAMA(I, J))
1 CF(I, I)=CF(I, I)-AI(I)+0.5*CP(I, I)*(AI(I)-E(I))
1 +RZ*(BETAP(I, I)-0.5*CPP(I, I)*GAMAP(I, I))
NMI=N-1
DO 3 I=1, NMI
IP1=I+1
DO 3 J=IP1, N
CF(I, J)=BETA(I, J)-0.5*CP(I, J)*GAMA(I, J)+
1 CX*(BETAP(I, J)-0.5*CPP(I, J)*GAMAP(I, J))
1 +CY*(BETAP(J, I)-0.5*CPP(J, I)*GAMAP(J, I))
3 CF(J, I)=CONJG(CF(I, J))
RETURN
END
```

\$IBFTC PADDI DECK

PADDI - EFN SOURCE STATEMENT - IFN(S) -

```
SUBROUTINE CPADD(CF,CP,CPP,JK,NK,NF,N,AK,H)
DIMENSION BA(40,40),ROOTR(40)
COMPLEX CF(20,20),CC(20,20),CP(20,20),CPP(20,20),CX,X
CALL CQREIG(CF,N,ROOTR,BA)
CALL CVCTR(BA,CC,N,NF,ROOTR)
IF(JK.EQ.1) GO TO 5
IF(JK.EQ.NK) GO TO 6
CX=CEXP(CMPLX(0.0,AK))
DO 14 I=1,N
DO 14 J=I,N
X=(0.0,0.0)
DO 1 K=1,NF
1 X=X+CONJG(CC(K,I))*CC(K,J)
CP(I,J)=CP(I,J)+X
CPP(I,J)=CPP(I,J)+X*CX
14 CP(J,I)=CONJG(CP(I,J))
DO 20 I=2,N
IM1=I-1
DO 20 J=1,IM1
X=(0.0,0.0)
DO 2 K=1,NF
2 X=X+CONJG(CC(K,I))*CC(K,J)
20 CPP(I,J)=CPP(I,J)+X*CX
GO TO 7
5 DO 9 I=1,N
DO 9 J=I,N
CP(I,J)=(0.0,0.0)
DO 8 K=1,NF
8 CP(I,J)=CP(I,J)+CONJG(CC(K,I))*CC(K,J)
CP(I,J)=0.5*CP(I,J)
CP(J,I)=CP(I,J)
CPP(I,J)=CP(I,J)
9 CPP(J,I)=CP(I,J)
GO TO 7
6 DO 10 I=1,N
DO 10 J=I,N
X=(0.0,0.0)
DO 11 K=1,NF
11 X=X+CONJG(CC(K,I))*CC(K,J)
CP(I,J)=(CP(I,J)+X*0.5)*H
CP(J,I)=CP(I,J)
10 CPP(I,J)=(CPP(I,J)+X*0.5)*H
DO 12 I=2,N
IM1=I-1
DO 12 J=1,IM1
X=(0.0,0.0)
DO 13 K=1,NF
13 X=X+CONJG(CC(K,I))*CC(K,J)
```

```
12 CPP(I,J)=(CPP(I,J)+X*0.5)*H
7 RETURN
END
```

\$IBFTC BISH

BISH - EFN SOURCE STATEMENT - IFN(S) -

```
SUBROUTINE RUB(N1)
DIMENSION CHAR(8),EIG(20)
COMPLEX CC(20,20)
CALL FGLD(7)
READ(7) IND
READ(7) CHAR
READ(7) AK
READ(7) CC
READ(7) EIG
READ(7) CC
READ(7) X
RETURN
END
```

\$IBFTC CQRGN DECK

CQRGN - EFN SOURCE STATEMENT - IFN(S) -

```
C PROGRAM TO CALL QR TRANSFORMATION, MAXIMUM ITER IS 50.
SUBROUTINE CQREIG(FC,M,ROOTR,BA)
DIMENSION A(40,40),ROOTR(40),BA(40,40),ROOTI(40)
COMPLEX FC(20,20)
IPRNT=0
N=M*2
N50=N
DO 800 I=1,M
DO 800 J=1,M
X1=REAL(FC(I,J))
BA(I,J)=X1
A(I,J)=X1
IPM=I+M
JPM=J+M
BA(IPM,JPM)=X1
A(IPM,JPM)=X1
X1=AIMAG(FC(I,J))
BA(I,JPM)=-X1
A(I,JPM)=-X1
BA(IPM,J)=X1
800 A(IPM,J)=X1
CALL HESSEN(A,N)
IF(IPRNT) 80,81,80
80 WRITE(6,104)
```

```
81 ZERO = 0.0
   JJ=1
177 XNN=0.0
   XN2=0.0
   AA = 0.0
   B = 0.0
   C = 0.0
   DD = 0.0
   R=0.0
   SIG=0.0
   ITER = 0
17 IF(N-2) 13,14,12
13 IF(IPRNT) 82,83,82
82 WRITE (6,105)A(1,1)
83 ROOTR(1) = A(1,1)
   ROOTI(1) = 0.0
   1 M50=N50-1
     DO 802 J=1,M50,2
       JPI=J+1
       DO 802 K=JPI,N50
         IF(ABS(ROOTR(K)-ROOTR(J)).GT.1.0E-4) GO TO 802
         X1=ROOTR(JPI)
         ROOTR(JPI)=ROOTR(K)
         ROOTR(K)=X1
802 CONTINUE
     DO 803 J=1,M
703 ROOTR(J)=ROOTR(2*J-1)
     M50=M-1
     DO 804 J=1,M50
       JPI=J+1
       DO 804 I=JPI,M
         IF(ROOTR(J).LT.ROOTR(I)) GO TO 804
         X1=ROOTR(J)
         ROOTR(J)=ROOTR(I)
         ROOTR(I)=X1
804 CONTINUE
     RETURN
14 JJ=-1
12 X = (A(N-1,N-1) - A(N,N))**2
   S = 4.0*A(N,N-1)*A(N-1,N)
   ITER = ITER + 1
   IF(X .EQ. 0.0 .OR. ABS(S/X) .GT. 1.0E-8) GO TO 15
16 IF(ABS(A(N-1,N-1))-ABS(A(N,N))) 32,32,31
31 E = A(N-1,N-1)
   G = A(N,N)
   GO TO 33
32 G = A(N-1,N-1)
   E = A(N,N)
33 F = 0.
   H = 0.
   GO TO 24
```

```
15 S = X + S
   X = A(N-1,N-1) + A(N,N)
   IF(S) 18,19,19
19 SQ=SQRT(S)
   F=0.0
   H=0.0
   IF (X) 21,21,22
21 E=(X-SQ)/2.0
   G=(X+SQ)/2.0
   GO TO 24
22 G=(X-SQ)/2.0
   E=(X+SQ)/2.0
   GO TO 24
18 F = SQRT(-S)/2.0
   E=X/2.0
   G=E
   H=-F
24 IF(JJ) 23,70,70
70 D = 1.0E-10*(ABS(G) + F)
   IF(ABS(A(N-1,N-2)) .GT. D) GO TO 26
28 IF(IPRNT) 84,85,84
84 WRITE (6,105)E,F, ITER
   WRITE (6,105)G,H
85 ROOTR(N) = E
   ROOTI(N) = F
   ROOTR(N-1) = G
   ROOTI(N-1) = H
   N=N-2
   IF(JJ) 1,177,177
26 IF(ABS(A(N,N-1)) .GT. 1.0E-10*ABS(A(N,N))) GO TO 50
29 IF(IPRNT) 86,87,86
86 WRITE (6,105)A(N,N), ZERO, ITER
87 ROOTR(N) = A(N,N)
   ROOTI(N) = 0.0
   N=N-1
   GO TO 177
50 IF(ABS(ABS(XNN/A(N,N-1))-1.0)-1.0E-6) 63,63,62
62 IF(ABS(ABS(XN2/A(N-1,N-2))-1.0)-1.0E-6) 63,63,700
63 VQ=ABS(A(N,N-1))-ABS(A(N-1,N-2))
   IF (ITER-15) 53,164,64
164 IF(VQ) 165,165,166
165 R = A(N-1,N-2)**2
   SIG = 2.0*A(N-1,N-2)
   GO TO 60
166 R = A(N,N-1)**2
   SIG = 2.0*A(N,N-1)
   GO TO 60
64 IF(VQ) 67,67,66
66 IF(IPRNT) 88,85,88
88 WRITE (6,107)A(N-1,N-2)
   GO TO 84
67 IF(IPRNT) 89,87,89
```

```
89  WRITE (6,107)A(N,N-1)
    GO TO 86
700 IF(ITER .GT. 50) GO TO 63
    IF(ITER .GT. 5 ) GO TO 63
701 Z1=      ((E-AA)**2+(F-B)**2)/(E*E+F*F)
    Z2=      ((G-C)**2+(H-DD)**2)/(G*G+H*H)
    IF(Z1-0.25) 51,51,52
51  IF(Z2-0.25) 53,53,54
53  R=E*G-F*H
    SIG=E+G
    GO TO 60
54  R=E*E
    SIG=E+E
    GO TO 60
52  IF(Z2-0.25) 55,55,601
55  R=G*G
    SIG=G+G
    GO TO 60
601 R = 0.0
    SIG = 0.0
60  XNN=A(N,N-1)
    XN2=A(N-1,N-2)
    CALL QRT(A,N,R,SIG,D)
    AA=E
    B=F
    C=G
    DD=H
    GO TO 12
104 FORMAT(////1X, 9HREAL PART 6X 14HIMAGINARY PART, 26X
1  13HTAKEN AS ZERO 6X 4HITER //)
105 FORMAT(1X,E15.8,3X,E15.8, 42X 13)
107 FORMAT(56X E13.8)
    END
```

\$IBFTC *QRT DECK

*QRT - EFN SOURCE STATEMENT - IFN(S) -

```
SUBROUTINE QRT(A,N,R,SIG,D)
DIMENSION A(40,40),PSI(2),G(3)
N1 = N - 1
IA = N - 2
IP = IA
IF(N-3) 101,10,60
60  DO 12 J = 3,N1
    J1 = N - J
    IF(ABS(A(J1+1,J1))-D) 10,10,11
11  DEN = A(J1+1,J1+1)*(A(J1+1,J1+1)-SIG)+A(J1+1,J1+2)*A(J1
1+2,J1+1)+R
```



```
IF(DEN) 61,12,61
61 IF(ABS(A(J1+1,J1)*A(J1+2,J1+1)*(ABS(A(J1+1,J1+1)+A(J1+2,J1+2)
1-SIG)+ABS(A(J1+3,J1+2)))/DEN)-D) 10,10,12
12 IP=J1
10 DO 14 J=1,IP
    J1=IP-J+1
    IF(ABS(A(J1+1,J1))-D) 13,13,14
14 IQ=J1
13 DO 100 I=IP,N1
    IF(I-IP) 16,15,16
15 G(1)=A(IP,IP)*(A(IP,IP)-SIG)+A(IP,IP+1)*A(IP+1,IP)+R
    G(2)=A(IP+1,IP)*(A(IP,IP)+A(IP+1,IP+1)-SIG)
    G(3)=A(IP+1,IP)*A(IP+2,IP+1)
    A(IP+2,IP)=0.0
    GO TO 19
16 G(1)=A(I,I-1)
    G(2)=A(I+1,I-1)
    IF(I-IA) 17,17,18
17 G(3)=A(I+2,I-1)
    GO TO 19
18 G(3)=0.0
19 XK = SIGN(SQRT(G(1)**2 + G(2)**2 + G(3)**2), G(1))
22 IF(XK) 23,24,23
23 AL=G(1)/XK+1.0
    PSI(1)=G(2)/(G(1)+XK)
    PSI(2)=G(3)/(G(1)+XK)
    GO TO 25
24 AL=2.0
    PSI(1)=0.0
    PSI(2)=0.0
25 IF(I-IQ) 26,27,26
26 IF(I-IP) 29,28,29
28 A(I,I-1)=-A(I,I-1)
    GO TO 27
29 A(I,I-1)=-XK
27 DO 30 J=I,N
    IF(I-IA) 31,31,32
31 C=PSI(2)*A(I+2,J)
    GO TO 33
32 C=0.0
33 E=AL*(A(I,J)+PSI(1)*A(I+1,J)+C)
    A(I,J)=A(I,J)-E
    A(I+1,J)=A(I+1,J)-PSI(1)*E
    IF(I-IA) 34,34,30
34 A(I+2,J)=A(I+2,J)-PSI(2)*E
30 CONTINUE
    IF(I-IA) 35,35,36
35 L=I+2
    GO TO 37
36 L=N
```

```
37 DO 40 J=IQ,L
   IF(I-IA) 38,38,39
38 C=PSI(2)*A(J,I+2)
   GO TO 41
39 C=0.0
41 E=AL*(A(J,I)+PSI(1)*A(J,I+1)+C)
   A(J,I)=A(J,I)-E
   A(J,I+1)=A(J,I+1)-PSI(1)*E
   IF(I-IA) 42,42,40
42 A(J,I+2)=A(J,I+2)-PSI(2)*E
40 CONTINUE
   IF(I-N+3) 43,43,100
43 E=AL*PSI(2)*A(I+3,I+2)
   A(I+3,I)=-E
   A(I+3,I+1)=-PSI(1)*E
   A(I+3,I+2)=A(I+3,I+2)-PSI(2)*E
100 CONTINUE
101 RETURN
   END
```

\$IBFTC CVECT DECK

CVECT - EFN SOURCE STATEMENT - IFN(S) -

```
SUBROUTINE CVCTR(BA,COEFF,M,NF,EIG)
DIMENSION BA(40,40),A(40,40),EIG(40),V(40)
COMPLEX COEFF(20,20),SUM
N=M*2
DO 500 J50=1,NF
ALPHA=EIG(J50)
DO 501 I51=1,N
DO 501 J51=1,N
501 A(I51,J51)=BA(I51,J51)
A(I,1)=A(I,1)-ALPHA
6 DO 15 I=2,N
A(I,I)=A(I,I)-ALPHA
70 II=I-1
7 DO 15 J=1,II
8 IF (A(I,J))9,15,9
9 IF (ABS (A(J,J))-ABS (A(I,J)))11,10,10
10 R=A(I,J)/A(J,J)
GO TO 130
11 R=A(J,J)/A(I,J)
DO 12 K=1,N
C=A(J,K)
A(J,K)=A(I,K)
12 A(I,K)=C
130 JJ=J+1
13 DO 14 K=JJ,N
14 A(I,K)=A(I,K)-R*A(J,K)
15 CONTINUE
```

```
C=A(N,N)
V(N)=1.
DO 29 I=2,N
  JJ=N-I+1
  R=0.
  II=N-I+2
  DO 25 K=II,N
25  R=R+A(JJ,K)*V(K)
  IF (ABS (A(JJ,JJ))-1.0E-10)27,27,28
27  V(JJ)=1.
  C=0.
  DO 26 J=II,N
26  V(J)=0.
  GO TO 29
28  V(JJ)=(C-R)/A(JJ,JJ)
29  CONTINUE
  SUM=(0.0,0.0)
  DO 800 I=1,M
  IPM=I+M
  COEFF(J50,I)=CMPLX(V(I),V(IPM))
800 SUM=SUM+COEFF(J50,I)*CONJG(COEFF(J50,I))
  SUM=CSQRT(SUM)
  DO 801 I=1,M
801 COEFF(J50,I)=COEFF(J50,I)/SUM
500 CONTINUE
  RETURN
  END
```

\$IBFTC HESS DECK

HESS - EFN SOURCE STATEMENT - IFN(S) -

C SUBROUTINE TO PUT MATRIX IN UPPER HESSENBERG FORM.

SUBROUTINE HESSEN(A,M)

DIMENSION A(40,40),B(50)

DOUBLE PRECISION SUM

IF (M - 2) 30,30,32

32 DO 40 LC = 3,M

N = M - LC + 3

N1 = N - 1

N2 = N - 2

NI = N1

DIV = ABS(A(N,N-1))

DO 2 J = 1,N2

IF(ABS(A(N,J))- DIV) 2,2,1

1 NI = J

DIV = ABS(A(N,J))

2 CONTINUE

IF(DIV) 3,40,3

3 IF(NI - N1) 4, 7,4

4 DO 5 J = 1,N

DIV = A(J,NI)

A(J,NI) = A(J,N1)

5 A(J,N1) = DIV

DO 6 J = 1,M

DIV = A(NI,J)

A(NI,J) = A(N1,J)

6 A(N1,J) = DIV

7 DO 26 K = 1, N1

26 B(K) = A(N,K)/A(N,N-1)

DO 45 J = 1,M

SUM = 0.0

IF (J - N1) 46,43,43

46 IF(B(J)) 41,42,41

41 A(N,J) = 0.0

DO 42 K = 1,N1

A(K,J) = A(K,J) - A(K,N1)*B(J)

42 SUM = SUM + A(K,J)*B(K)

GO TO 43

43 DO 44 K = 1,N1

44 SUM = SUM + A(K,J)*B(K)

45 A(N1,J) = SUM

40 CONTINUE

30 RETURN

END

CHAPTER IV.

SOME SELECTED RESULTS OBTAINED WITH THE SCF
SEMI-EMPIRICAL COMPUTER PROGRAMS.

(1) Introduction.

Rather than reproduce all the results obtained with the four semi-empirical computer programs given in the previous Chapter, only a small proportion of them will be presented here. Even the output data quoted for the limited number of π -systems considered here is only a small portion of that obtained from running a program with a particular input. Future workers, with an interest in one molecule, or some aspect of a whole series of molecules, would be well advised to copy and run the programs given in Chapter III, and thus recover the maximum information. For those interested in properties not covered by the programs given, the SCF eigenvectors produced by these programs could be utilized to calculate expectation values for physical operators not included in the original deck structure. Thus such topics as molecular polarizabilities and magnetic properties could be studied.

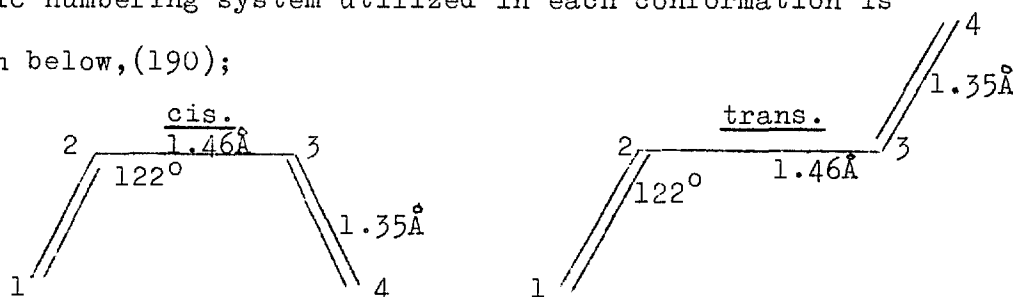
It is hoped that the following results will serve to illustrate various areas of application of the π -electron SCF theory, and reveal the degree of success it is possible to achieve.

(2) Selected Results.

(a) The Butadiene Molecule.

(i) Geometry.

Both the trans and the less stable cis conformations of Butadiene were studied. The molecular geometry, and the atomic numbering system utilized in each conformation is shown below, (190);



(ii) Parameters.

The valence state ionization potential and electron affinity of each constituent Carbon atom were assigned the values of 11.42 and 0.58 ev. respectively, (117), (118). Coulomb integrals were calculated in the Mataga-Nishimoto approximation, (124). The empirical resonance integrals, β_{ij} , were evaluated in a number of ways. The best set, as defined by the closest fit obtained for the first excited singlet, was that suggested by the application of an approximation introduced by I'Haya, (125). These parameters were $\beta_{12} = -2.98$, $\beta_{23} = -2.55$ ev.* and may be compared with the values of Pariser and Parr,

$\beta_{12} = -2.92$, and $\beta_{23} = -1.68$, (106). Yet another set, $\beta_{12} = -2.53$, $\beta_{23} = -2.11$, may be obtained using the overlap criterion,

* This set worked very well for the related molecule, Fulvene, giving a first singlet at 3.16 ev., compared to the experimental value of 3.4 ev..

equation(2-121) , with the Benzene integral, $\beta_{c-c} = -2.39$, and, $R_{c-c} = 1.39 \text{ \AA}$, as a basis.

As these parameters imply , the molecule has more in common with two Ethylene molecules, than with a benzenoid ring structure.

(iii) Ground State Properties.

The results for the closed-shell ground state were obtained using the Closed-Shell SCF program, with input parameters as indicated.

Bond-Orders.

Table 9.

| Isomer | P_{12} | P_{23} |
|--------|----------|----------|
| cis | .9392 | .3435 |
| trans | .9431 | .3325 |

Note how the cis conformation results in a slightly increased degree of electron delocalization compared to the trans form. Both electronic distributions do, however, strongly resemble the classical picture of two double-bonds between atoms 1-2 , and 2-3 . All charges defined by P_{ii} , $1 \leq i \leq 4$, are unity as Butadiene is an Alternant Hydrocarbon.

Orbital Energies.

These are given in ev. in Table 10 , with ϵ_i representing the SCF orbital energy of ϕ_i , ϕ_1 and ϕ_2 are the orbitals

occupied in the ground state. Hence ϕ_3 and ϕ_4 are virtual orbitals.

Table 10.

| Isomer | ϵ_1 | ϵ_2 | ϵ_3 | ϵ_4 |
|--------|--------------|--------------|--------------|--------------|
| cis | -13.2871 | -10.4358 | -1.5642 | 1.2871 |
| trans | -13.3143 | -10.3820 | -1.6180 | 1.3143 |

The identification of ϵ_2 with the first ionization potential using Koopmans theorem is in variance with the experimental value for trans-Butadiene of 9.0 ev.,(191). The results of investigating this discrepancy are given later.

Total π -Energy.

These energies represent the total π -energies of the molecules, in a self-consistent state.

$$E_{\pi}^{\text{cis}} = -79.9996 \text{ ev.}$$

$$E_{\pi}^{\text{trans}} = -79.4242 \text{ ev.}$$

We note from these results an apparent stabilization of the cis form of Butadiene, however this is misleading. We are using only a π -electron approximation, and in addition have omitted atom/atom repulsions from our Hamiltonian. These would all combine to reverse the situation, stabilizing the trans form,(192).

Self-Consistent Eigenvectors.

These are shown in Tables 11 and 12 overleaf.

Table 11.

Cis-Butadiene.

| i | C_{1i} | C_{2i} | C_{3i} | C_{4i} |
|---|----------|----------|----------|----------|
| 1 | .4051 | .5795 | .5795 | .4051 |
| 2 | -.5795 | -.4051 | .4051 | .5795 |
| 3 | .5795 | -.4051 | -.4051 | .5795 |
| 4 | -.4051 | .5795 | -.5795 | .4051 |

Table 12.

Trans-Butadiene.

| i | C_{1i} | C_{2i} | C_{3i} | C_{4i} |
|---|----------|----------|----------|----------|
| 1 | .4085 | .5772 | .5772 | .4085 |
| 2 | -.5772 | -.4085 | .4085 | .5772 |
| 3 | .5772 | -.4085 | -.4085 | .5772 |
| 4 | -.4085 | .5772 | -.5772 | .4085 |

Note:(a) The molecular orbitals are of the form, $\phi_i = \sum_{j=1}^4 c_{ij} \chi_j$,
 where $\{\chi_j\}$ is the atomic orbital basis set.

(b) These orbitals are a good instance of the pairing properties of the occupied and virtual molecular orbital sets, typical of an alternant hydrocarbon, (see section (17) of Chapter II).

(iv) Excited States.

Here we shall confine ourselves to single excited electron states, presenting singlet and triplet results obtained from the Closed-Shell(CS) -SCF-CI program. As well as the essentially spin-paired treatment, both with and without configuration interaction(CI), the two open-shell procedures programmed were used to find excited triplet states. First we give the CS-SCF-CI results.

Table 13.

Cis-Butadiene;no CI..

| Transition | ΔE_s | α_s | f_s | ΔE_t | Symmetry |
|------------|--------------|------------|-------|--------------|----------------|
| 2,3 | 6.04 | 56.9 | .569 | 2.77 | B ₁ |
| 2,4 | 8.44 | 148.7 | .421 | 5.82 | A ₁ |
| 1,3 | 8.44 | 148.7 | .421 | 5.82 | A ₁ |
| 1,4 | 10.84 | 267.1 | .008 | 8.17 | B ₁ |

Note:(a) Subscript 's' denotes singlet, 't' triplet.

(b) ΔE represents the excitation energy required to produce the electronic transition from the molecular ground state.

(c) α_s is the angle which the singlet transition dipole makes with the 1-2 bond. This angle is taken in a direction of rotation in the plane of the molecule such that the atom numbered 3 is included in the arc, $0 \leq \alpha_s \leq 180^\circ$.

(d) f_s is the oscillator strength of the singlet transition, see equation (2-183).

(e) The last column shows the symmetry group of excited state.

Table 14.

Cis-Butadiene; with CI..

| Transition | ΔE_s | α_s | f_s | ΔE_t | Symmetry |
|------------|--------------|------------|-------|--------------|----------------|
| 1 | 6.03 | 56.9 | .568 | 2.23 | B ₁ |
| 2 | 7.61 | - | - | 4.03 | A ₁ |
| 3 | 9.27 | 148.7 | .924 | 7.61 | A ₁ |
| 4 | 10.85 | 196.1 | .001 | 8.71 | B ₁ |

Note; (a) That transitions can no longer be labelled by the re-allocation of a specific electron from the closed-shell into a single virtual orbital after a CI procedure .

(b) Omissions from the table, denoted '-' indicate f_s values less than .0005 .

Table 15.

Trans-Butadiene; no CI ..

| Transition | ΔE_s | α_s | f_s | ΔE_t | Symmetry |
|------------|--------------|------------|-------|--------------|----------------|
| 2,3 | 6.26 | 11. | 1.223 | 2.79 | B _u |
| 2,4 | 8.36 | - | - | 5.84 | A _g |
| 1,3 | 8.36 | - | - | 5.84 | A _g |
| 1,4 | 10.98 | 327. | .296 | 8.27 | B _u |

Table 16.

Trans-Butadiene; with CI. .

| Transition | ΔE_s | α_s | f_s | ΔE_t | Symmetry |
|------------|--------------|------------|-------|--------------|----------------|
| 1 | 6.24 | 12. | 1.174 | 2.21 | B _u |
| 2 | 7.71 | - | - | 3.98 | A _g |
| 3 | 9.02 | - | - | 7.71 | A _g |
| 4 | 11.00 | 153. | .376 | 8.84 | B _u |

These results may be compared with those of Parr and Mulliken,(192), Pariser and Parr,(106), and I'Haya,(125); the figures given here are very similar to those obtained in these references. Experimental results,(191), give the first singlet at 6.0 ev., with the possibility of the next at 7.2 ev. , and thus the theoretical results can be regarded as fairly satisfactory. With a little parameter variation it would be possible to exactly reproduce the first singlet at 6. ev. for the trans form, the most likely experimental conformation of the molecule. The question of the ionization potential of the molecule, which is apparently not represented so well by the same set of parameters will be discussed later.

(v) Self-Consistent Excited Triplet States.

With the identical input parameters as the CS-SCF-CI program various excited triplets of trans-Butadiene were investigated by the open-shell Roothaan and spin-polarized

methods. Detailed results of eigenvectors and orbital energies are not given here for reasons of brevity .

Table 17.

| State | ΔE_t | P_{11} | P_{22} | P_{12} | P_{23} | σ_1 | σ_2 |
|-------------------|--------------|----------|----------|----------|----------|------------|------------|
| 2,4 | 5.83 | .8591 | 1.1402 | .4798 | .1410 | .5000 | .5000 |
| 1,4 | 8.19 | 1.0000 | 1.0000 | .4352 | -.2538 | .2538 | .7462 |
| 2,3 | 2.44 | 1.0000 | 1.0000 | .3853 | .8187 | .8187 | .1813 |
| 1,3 | 5.83 | 1.1402 | .8598 | .4800 | .1402 | .5000 | .5000 |
| 2,3 ^{SP} | 2.45 | 1.0000 | 1.0000 | .3863 | .8174 | .8174 | .1826 |

Note:(a) By the state i,j , the excited triplet formed by the transfer of a paired electron from orbital i to a virtual orbital j is implied.

(b) ΔE_t is the triplet energy relative to the CS-SCF ground state.

(c) P_{11}, P_{22} ; the diagonal elements of the bond matrix give the π -electron charges on atoms 1 and 2 . Those on 3 and 4 follow from symmetry.

P_{12} , P_{23} , are bond orders.

σ_1 , σ_2 , unpaired π -spin density at the atomic centre indicated by the subscript.

(d) The last row of the table gives the results for the first Butadiene triplet obtained with the spin-polarized SCF program. All other results were found with the

Rootaan procedure . No projection of the spin-polarized SCF wave function was necessary, as the molecular symmetry of Butadiene ensured it was a pure spin state.

- (e) The energy of the first triplet calculated by both open-shell methods are in good agreement, and differ only slightly from that obtained in the CS-SCF-CI approximation. All these values, however, seem in variance with other reported values, which are in the range 3. to 4. ev.,(192), (106),(125). Since no experimental data is available it is impossible to decide on the respective merits of any particular result.
- (f) States 2,4 and 1,3 are degenerate, and need splitting by a configuration interaction .All these triplet energies may be compared to those found with the CS-SCF program.

(vi) Spin-Polarized Ground State.

From the form of the spin-polarized effective Hamiltonians employed in deriving a self-consistent spin-polarized state, it may be seen that if the method is used on a ground state molecule, with an even number of electrons, spin-alternation and an overall energy reduction may be obtained for the system.

This spin-alternation has to be introduced artificially into the SCF procedure by the choice of the initial matrices P^α and P^β , otherwise a normal spin-paired ground state ensues..

Such spin-polarized ground-states are not, however,

eigenfunctions of S^2 , and do not have the full molecular symmetry. With the application of a spin projection technique previously discussed, full spin-pairing is re-established in the attainment of a singlet ground state. This state in fact is just the normal closed-shell spin-paired SCF ground state.

This is illustrated by the results now given for trans-Butadiene, obtained using the set of parameters given previously .
Unprojected Results.

$$\langle S^2 \rangle = 0.1735$$

$$E_{\pi} = -79.4390 \text{ ev.}$$

Table 18.

| P_{12} | P_{23} | σ_1 | σ_2 |
|----------|----------|------------|------------|
| .8978 | .3561 | .3110 | -.2396 |

Note:(a) All P_{ii} , $1 \leq i \leq 4$, are unity.

(b) Compare with the closed-shell results.

Table 19.

α -spin orbital energies and eigenvectors.

| i | ϵ_i | C_{i1} | C_{i2} | C_{i3} | C_{i4} |
|-----|--------------|----------|----------|----------|----------|
| 1 | -13.3693 | .4667 | .5401 | .6064 | .3505 |
| 2 | -10.5515 | -.6616 | -.2976 | .5021 | .4708 |
| 3 | -1.4485 | .4708 | -.5021 | -.2976 | .6616 |
| 4 | 1.3693 | -.3505 | .6064 | -.5401 | .4667 |

Table 20.

β -spin orbital energies and eigenvectors.

| i | ϵ_i | C_{i1} | C_{i2} | C_{i3} | C_{i4} |
|---|--------------|----------|----------|----------|----------|
| 1 | -13.3693 | .3505 | .6064 | .5401 | .4667 |
| 2 | -10.5515 | -.4708 | -.5021 | .2976 | .6616 |
| 3 | -1.4485 | .6616 | -.2976 | -.5021 | .4708 |
| 4 | 1.3693 | -.4667 | .5401 | -.6064 | .3505 |

Note:(a) The equivalent sets of orbital energies for α and β electrons.

(b) How the eigenvectors minimize α/β -spin electron interaction.

Projected Results.

These were obtained with the accurate spin-projection routine.

$$\langle S^2 \rangle = 0.0183$$

$$E_{\pi} = -79.4328 \text{ ev.}$$

This energy may be compared with the CS-SCF ground state energy of -79.4242 ev. .

Table 21.

| P_{12} | P_{23} | σ_1 | σ_2 |
|----------|----------|------------|------------|
| .9353 | .3410 | 0.0000 | 0.0000 |

Note:(a) Since $\sigma_1 = \sigma_2 = 0$, we no longer have an alternant spin-state. All electrons are effectively paired .

- (b) P_{12} and P_{23} are very close to their CS-SCF ground state values. Deviations can be ascribed to the inadequacies of the projection technique, and computer round-off errors.

Now the "corresponding orbital" eigenvectors are given. These orbitals are used in a transformation technique associated with the spin projection discussed in Chapter II, see page 244 .

Table 22.

| i | T_i | Δ_i | C_{i1} | C_{i2} | C_{i3} | C_{i4} |
|---|-------|------------|----------|----------|----------|----------|
| 1 | .9853 | .0856 | .4391 | .5274 | .6265 | .3696 |
| | | | .3696 | .6265 | .5274 | .4391 |
| 2 | .9250 | .1937 | -.6802 | -.3195 | .4768 | .4560 |
| | | | -.4560 | -.4768 | .3195 | .6802 |

Note:(a) The corresponding spin-orbital set, $\{\phi'_i\}$, is related to the SCF spin-polarized molecular orbital set, $\{\phi_j\}$, by; $\phi'_i{}^\alpha = \sum_{j=1}^L C_{ij}^\alpha \phi_j^\alpha$, (see page 245) .
 α -corresponding orbital vectors are shown above β eigenvectors .

- (b) The symmetry of the orbitals for a given closed-shell
 (c) Since Δ_2 is appreciable, $\langle S^2 \rangle$ is not reduced more closely to zero.

(b) The Trans-Butadiene Ion, C₄H₄⁺

(i) Geometry.

In the ionization process removing an electron from the Butadiene molecule to form the positive ion, the geometry of the Carbon core was assumed unaltered. Thus the geometry given for the molecule of trans-Butadiene was again used for the ion, and also the atoms were indexed in the same way.

(ii) Parameters.

These were approximated by a technique introduced by I'Haya,(125), which proved successful in predicting the first singlet transition of the molecule. In the treatment of this ion the main objective was to obtain a reasonable value for the first ionization potential of the molecule, using the same methods for the deduction of input parameters as was satisfactory in reproducing the molecular spectra.

This ionization potential, I , was calculated from a comparison of the total molecular π -energy before the removal of the electron, and the π -energy of the ion which results from the loss of an electron. As has been already noted, Koopman's Theorem fails to accurately predict I , giving a value of 10.38 ev., compared to the experimental 9.0 ev.,(191).

In an attempt to improve on this situation, three sets of parameters were used as input for the spin-polarized SCF program, and the results compared. These parameters follow,

Set A: This was the ground state set, $\beta_{12} = -2.98$, $\beta_{23} = -2.55$, $I_i = 11.42$, $E_i = 0.58$. We assumed all parameters unaffected by the loss of an electron.

Set B: This set was chosen employing the method of I'Haya to allow for the change in molecular charge distribution following the complete removal of a π -electron. The new effective charge, (193), of each Carbon atom in the molecule, Z_c , is approximated as $Z_{c0} + \frac{1}{4} \Delta Z$, where Z_{c0} is the effective charge experienced by a 2p electron in a neutral Carbon atom $C^0(sp^3)$.

$\Delta Z = Z_{c+} - Z_{c0}$; Z_{c+} being the effective charge of the Carbon ion $C^+(sp^3)$ for 2p electrons. Thus $\frac{1}{4}$ of an electron is regarded as being removed from each Carbon atom in the ionization process. With $Z_{c0} = 3.25$, and $Z_{c+} = 3.60$, (193), we find $Z_c' = 3.34$. In the ion the screening effect of one electron has been lost, and thus those remaining are correspondingly more strongly bound. The valence state ionization potential of each Carbon core was found using a formula derived from experimental results by Moore, (194),

$$I_i = 3.604 * Z_i^2 - 9.599 * Z_i + 4.5535$$

This gives $I_i = 12.65$ ev., with $Z_i = 3.34$. With the assumption that the one-centre Coulomb integral δ_{pp} was proportional to Z_i , and utilizing the normal Carbon integral to obtain the constant of proportionality, it is found with $Z_i = 3.34$, $\delta_{pp} = 11.13$. Off-diagonal Coulomb integrals were left unchanged in the Mataga-Nishimoto approximation, (124). The new values for the

resonance integrals were found with the overlap criterion of I'Haya,(125), $\beta_{ij} = \frac{1}{2}(I_i + I_j) S_{ij}$. The new orbital overlap matrix, S_{ij} , was obtained with the use of the new effective charges and tables published by Mulliken, et al.,(193).

Thus the values used were $\beta_{12} = -3.07$, $\beta_{23} = -2.60$.

Set C: Whereas Set B consisted of fixed parameters, unaffected by the charge distributions in the ion, this set of parameters was flexible, and varied during the self-consistent procedure. Thus the differential charge distributions in the ion as it approached a SCF state were allowed for. That is the assumption that exactly $\frac{1}{4}$ of an electron was removed from each atomic centre was discarded. Instead, the effective charges of the centres were derived from the empirical relation, $Z_i = -.35 * P_{ii} + 3.60$. This equation was obtained by assuming a linear relationship between atomic π -charge, P_{ii} , and effective charge, Z_i . Hence in the SCF procedure Z_i was re-calculated at the end of each iteration, and from this I_i and β_{ii} for the next iteration were calculated as indicated in data set B. In addition the resonance integrals were re-calculated, the overlap $S_{ij}(Z_i, Z_j)$, being found for the variable effective charges using formulae given by Mulliken,(193). With these flexible parameters the spin-polarized SCF program was iterated to convergence.

Results of these various parameter sets are now presented.

(iii) Results.

Orbital Energies.

Table 23.

| Data | ϵ_1 | ϵ_2 | ϵ_3 | ϵ_4 |
|------|--------------|--------------|--------------|--------------|
| A | -17.709 | -10.123 | -5.624 | -3.399 |
| | -19.055 | -16.576 | -7.710 | -4.354 |
| B | -19.006 | -11.302 | -6.650 | -4.388 |
| | -20.399 | -17.883 | -8.810 | -5.384 |
| C | -18.182 | -10.826 | -6.940 | -5.456 |
| | -19.336 | -17.654 | -9.292 | -6.313 |

Note:(a) The orbital energies, ϵ_i , $1 \leq i \leq 4$, are in ev., with the α -spin eigenvalues in the first row of results for the given data set. The β -spin are those in the second row.

(b) The electron removed to form the ion had α -spin.

(c) Compare the extra binding of the electrons remaining by reference to the ground state orbital energies.

Total π -energies and Ionization Potential of C_4H_6

Table 24.

| Data | π -energy | Ionization Pot. |
|------|---------------|-----------------|
| A | -69.1921 | 10.23 |
| B | -73.378 | 6.05 |
| C | -70.641 | 8.78 |

Note:(a) Agreement between result A , and Koopman's Theorem, which predicts $I = 10.38$ ev. . Thus Koopman's approximation that the wave functions of the electrons remaining are not much altered by the loss of one through ionization remains valid. What is ~~o~~mitted from consideration, and it is vital that it should not be, is that all inter-electron integrals and parameters are changed with the alteration in the effective charge of the Carbon cores.

(b) That the result for data C compares quite well with the experimental value of 9.0 ev. for the ionization potential of trans-Butadiene . Thus it does seem possible, with sufficient care, to use the same parameter prescription for ionization potentials and optical transitions in the semi-empirical approximation, and still obtain reasonable results for both.

Electron Distributions.

Table 25.

| Data | P_{11} | P_{22} | σ_1 | σ_2 | P_{12} | P_{23} |
|------|----------|----------|------------|------------|----------|----------|
| A | .6734 | .8265 | .4758 | .0242 | .6662 | .5612 |
| B | .6752 | .8247 | .4759 | .0241 | .6666 | .5595 |
| C | .7205 | .7794 | .5644 | .0644 | .6378 | .5598 |

Note:(a) The more even charge distribution obtained with the flexible parameters, set C .

- (b) Compare these results with those of Hoyland and Goodman, (107), (139) .
- (c) None of the results represent pure spin eigenfunctions as the spin-projection routine was not yet available when this work was done. This, however, does not effect the validity of the numerical results, for example, the wave function represented by data A has $\langle S^2 \rangle = .8060$. After projection we obtain $\langle S^2 \rangle = .7500$, and the following results;

Table 26.

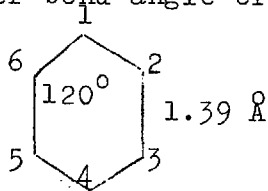
| P_{11} | P_{22} | σ_1 | σ_2 | P_{12} | P_{23} |
|----------|----------|------------|------------|----------|----------|
| .6698 | .8302 | .4411 | .0590 | .6747 | .5649 |

These show little deviation from those given in the in the previous table , Table 25 . Any energy changes incurred by projection would be in the direction of improving the fit of the experimental ionization potential obtained with data C .

(c) Benzene.

(i) Geometry.

The length of the Carbon-Carbon bond was taken as 1.39 \AA , with an inter-bond angle of 120° .



(ii) Parameters.

The valence state ionization potentials and electron affinities of the Carbon cores were given the values, 11.42 and 0.58 ev. , respectively. Data set A , utilizing the Mataga-Nishimoto Coulomb integrals and a Carbon-Carbon resonance integral , $\beta_{C-C} = -2.39$, duplicated results obtained by Mataga and Nishimoto with the same parameters, (124). This acted as a valuable check for all the procedures embodied in the CS-SCF program.

To investigate the dependence of optical transitions on input parameters , the program was re-run with only the resonance integrals changed, and re-allocated the value of -2.30 . This was data set B . In addition the effect of multiplying the two-centre integrals obtained in the Mataga-Nishimoto approximation by a constant factor of 1.2 was studied with data C . All other data was left unaltered .

Also the dependence of the results on the degree of configuration interaction invoked was investigated, and conflicting results found for the lowest Benzene triplet state.

(iii) Results.

As Benzene is an alternant hydrocarbon all π -densities at the atomic centres are unity. Similarly the bond-orders are all identical at $\frac{2}{3}$, determined entirely by the molecular symmetry. In this treatment of the molecule we shall

only consider optical excitations.

Data Set A: No CI.

Table 27.

| Transition | E_s | α_s | f_s | E_t |
|------------|-------|------------|-------|-------|
| 1,4 | 8.74 | - | - | 7.02 |
| 1,5 | 8.77 | - | - | 7.03 |
| 1,6 | 11.49 | - | - | 10.01 |
| 2,4 | 5.94 | 179. | .504 | 4.47 |
| 2,5 | 6.55 | 90. | .560 | 3.63 |
| 2,6 | 8.77 | - | - | 7.03 |
| 3,4 | 6.55 | 270. | .554 | 3.59 |
| 3,5 | 5.94 | 179. | .503 | 4.47 |
| 3,6 | 8.74 | - | - | 7.02 |

Data Set A: With CI.

Table 28.

| Transition | E_s | α_s | f_s | E_t |
|------------|-------|------------|-------|-------|
| 1 | 4.90 | - | - | 2.60 |
| 2 | 6.13 | - | - | 4.03 |
| 3 | 6.95 | 45. | 1.163 | 4.04 |
| 4 | 6.98 | 314. | 1.202 | 4.90 |
| 5 | 8.48 | - | - | 5.56 |
| 6 | 8.50 | - | - | 5.56 |
| 7 | 9.01 | - | - | 8.48 |
| 8 | 9.04 | - | - | 8.50 |
| 9 | 11.49 | - | - | 10.59 |

- Note:(a) For several entries in the table exact degeneracies in optical transitions do not occur where they are expected. This is due to the program failing to handle a problem with degenerate roots accurately.
- (b) Compare these values with the first experimental singlets and triplets of Benzene,(195).

Table 29.

| Transition | Experimental | Theory,data A | M-N,(124) | Symm. |
|------------|--------------|---------------|-----------|-----------|
| Singlet | 4.9 | 4.90 | 4.90 | $1B_{2u}$ |
| | 6.0 | 6.13 | 6.13 | $1B_{1u}$ |
| | 7.0 | 6.96 | 6.96 | $1E_{1u}$ |
| Triplet | 3.8 | 2.60(3.17)* | 3.17 | $3B_{1u}$ |
| | 4.2 | 4.03 | 4.03 | $3E_{1u}$ |
| | 4.9 | 4.90 | 4.90 | $3B_{2u}$ |

* This transition depends strongly on the degree of configuration interaction used. The figure in brackets, the closest to the experimental value, was obtained from considering only the first four excited molecular states. The value of 2.60 ev. is obtained by including all possible singly excited configurations. All other excitations are independent of the degree of interaction used between the two limits given above. Thus a first order interaction seems superior here.

Data Sets B and C .

The results obtained with these parameters are quoted together in order to save space. Only the results after configuration interaction are given, and oscillator strengths are omitted .

Table 30.

| Transition | Data B. | | Data C. | |
|------------|--------------|--------------|--------------|--------------|
| | ΔE_s | ΔE_t | ΔE_s | ΔE_t |
| 1 | 4.73 | 2.40 | 4.93 | 2.08 |
| 2 | 5.95 | 3.86 | 6.41 | 3.88 |
| 3 | 6.76 | 3.86 | 7.36 | 3.90 |
| 4 | 6.79 | 4.72 | 7.43 | 4.92 |
| 5 | 8.21 | 5.29 | 8.73 | 5.23 |
| 6 | 8.22 | 5.29 | 8.77 | 5.24 |
| 7 | 8.75 | 8.21 | 9.37 | 8.73 |
| 8 | 8.76 | 8.22 | 9.41 | 8.77 |
| 9 | 11.11 | 10.24 | 11.19 | 10.87 |

Note:(a) We find the variation of the two centre Coulomb integrals by a factor of 1.2 as in Data C , strongly effects the transition energies. A poor fit of the experimental spectra is obtained.

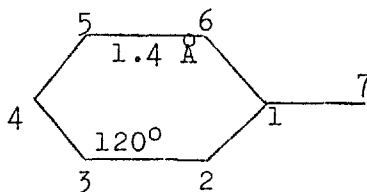
(b) The resonance integrals, given the new value of -2.30 in Data B , alter the optical transitions rather less

severely . However, it seems plain that the choice of parameters is very important, crucially effecting the predicted optical transitions. Thus the whole procedure does appear very sensitive to parameters, and the optimum set is unique .

(d) The Benzyl Radical, C₇H₇[•].

(i) Geometry.

The geometry adopted for this radical in all the calculations whose results are presented here, was that used by Ladik et al.,(196). The length of all Carbon-Carbon bonds was taken as 1.40 Å , and inter-bond angles were assumed to be 120° . The atomic numbering system utilized is shown below.



(ii) Parameters.

The valence state ionization potentials and electron affinities were assigned their usual values of 11.42 and 0.58 ev., respectively. Within the ring, all resonance integrals had the value -2.39 ev., while the 1-7 integral was taken as -2.151 ev., .9 of the ring integrals. The Mataga-Nishimoto approximation was used for the two-centre Coulomb integrals,(124). Data set A uses the normal Mataga-Nishimoto integrals, Data B , 1.5 of these values.

With these parameters both the ground state and excited states of the Benzyl radical were investigated, with both the spin-polarized program, and Roothaan's open-shell procedure .

(iii) Results.

Doublet Ground State.

First we present results obtained with the spin-polarized program.

Table 31.

| Quantity | Data A. | | Data B. | |
|-----------------------|----------|----------|----------|----------|
| | unann | ann | unann | ann |
| σ_1 | .3422 | .1041 | .1361 | .0434 |
| σ_2 | -.4201 | -.2148 | -.1815 | -.1187 |
| σ_3 | .3621 | .1097 | .0940 | .0303 |
| σ_4 | -.3911 | -.1929 | -.1598 | -.0947 |
| σ_7 | -.8352 | -.7010 | -.8014 | -.7720 |
| π -Energy | -177.901 | -177.507 | -224.910 | -224.916 |
| $\langle s^2 \rangle$ | 1.1551 | .8804 | .7903 | .7510 |
| Δ_1 | .1131 | | .0274 | |
| Δ_2 | .2076 | | .0559 | |
| Δ_3 | .2234 | | .0791 | |

Note:(a) The quantities σ_i are spin densities. Δ_i are the corresponding orbital coefficients. The results before annihilation are labelled 'unann' , those after 'ann' .

- (b) The difference in results before and after the use of a single annihilator. This confirms the need for such a technique, especially in view of the particularly poor expectation value of S^2 for the wave function found with Data Set A.
- (c) The high Δ_i values for the corresponding orbitals of Data A, these indicate a poor expectation value for S^2 . Since the Δ_i are quite large, the projection routine is not completely successful in removing all unwanted multiplicities from the wave function.
- (d) These results may be compared directly with those of Ladik, et al., (196), and Berthier, (129).

Table 32.

| Spin Density | Berthier, (129) | | Ladik, (196) | |
|--------------|-----------------|--------|--------------|--------|
| | unann | ann | Data A | Data B |
| σ_1 | .1541 | .1033 | .340 | .140 |
| σ_2 | -.2380 | -.2000 | -.414 | -.186 |
| σ_3 | .1333 | .0899 | .356 | .102 |
| σ_4 | -.2492 | -.2077 | -.386 | -.162 |
| σ_7 | -.6952 | -.6735 | -.840 | -.810 |

Ladik's Data A and Data B correspond to the data similarly labelled in this discussion. The use of 1.5 times the Mataga-Nishimoto integrals in Data B corresponds to the use of Slater type $2p_z$ orbitals in calculating the two centre

integrals.

- (e) Various experimental results are available for the spin-densities in this radical. These are shown in the following table.

Table 33.

| Spin Density | Tolkachev, (197) | Ladik, (196) | |
|--------------|------------------|--------------|-------|
| | | Max. | Min. |
| ρ_1 | - | .144 | .064 |
| ρ_2 | $-.244 \pm .022$ | -.201 | -.187 |
| ρ_3 | - | .068 | .064 |
| ρ_4 | $-.244 \pm .022$ | -.240 | -.223 |
| ρ_7 | $-.733 \pm .044$ | -.639 | -.594 |

As may be seen the results obtained using Data Set A are in quite good agreement with these experimental values. Variations in the experimental spin-densities assigned to the various centres arises from the different possible interpretations of the experimental data. Ladik's data attempts to bracket the likely value within maximum and minimum limits.

Now the results obtained for the doublet ground state with Roothaan's procedure are given, and compared directly with the theoretical values found by Berthier, (129). The study of Benzyl by Berthier was performed without the assumption of zero differential overlap.

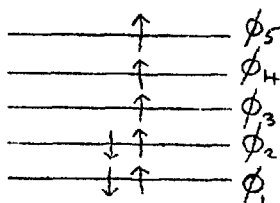
Table 34.

| i | Data A | | Data B | | Berthier | |
|--------|------------|------------|------------|------------|------------|------------|
| | D_{ii}^o | D_{ii}^c | D_{ii}^o | D_{ii}^c | R_{ii}^o | R_{ii}^c |
| 1 | .0000 | .5000 | .0000 | .5002 | .0000 | .4812 |
| 2 | .0505 | .4748 | .0704 | .4646 | .1035 | .4558 |
| 3 | .0000 | .5000 | .0000 | .5003 | .0000 | .4988 |
| 4 | .0283 | .4859 | .0420 | .4787 | .0848 | .4565 |
| 7 | .8707 | .0646 | .8172 | .0914 | .7082 | .1530 |
| Energy | -177.656 | | -224.850 | | - | |

- Note:(a) The matrices D^o and D^c are open and closed-shell density matrices, denoted R^o and R^c in Berthier's notation. The diagonal elements of D^o give the atomic spin-densities directly, this matrix is twice the open-shell density matrix discussed in Chapter II. $2 * D_{ii}^c + D_{ii}^o$, gives the π -electron charge at centre i.
- (b) The total state energies compared with those found with the spin-polarized program. They are very similar.
- (c) Experimental spin densities are not adequately predicted with this procedure of Roothaan. The spin-polarized method seems much more successful.

The Benzyl Quartet State, 4B_2 :

In terms of an orbital occupation diagram, this state can be represented as;



The wave functions corresponding to these orbital populations were calculated in the spin-polarized and Roothaan approximations. First the spin-polarized results are shown, compared to Berthier's theoretical results,

Table 35.

| Quantity | Data A | | Data B | | Berthier | |
|-----------------------|----------|----------|----------|----------|----------|--------|
| | unann | ann | unann | ann | unann | ann |
| σ_1 | .1265 | .0717 | .0756 | .0437 | .0654 | .0527 |
| σ_2 | -.2536 | -.2334 | -.2356 | -.2249 | -.2408 | -.2370 |
| σ_3 | -.2279 | -.2032 | -.1957 | -.1836 | -.1917 | -.1868 |
| σ_4 | .1155 | .0636 | .0458 | .0229 | .0341 | .0249 |
| σ_7 | -.2791 | -.2620 | -.2587 | -.2493 | -.2344 | -.2299 |
| π -Energy | -175.076 | -174.963 | -221.028 | -221.029 | - | - |
| ΔE | 2.82 | 2.54 | 3.88 | 3.89 | - | - |
| $\langle s^2 \rangle$ | 4.0392 | 3.7747 | 3.8336 | 3.7519 | - | - |
| Δ_1 | .1905 | | .0887 | | - | |
| Δ_2 | .1970 | | .1152 | | - | |

Note:(a) Spin-density for this quartet state is defined by

$$\frac{1}{3} * (P_{ii}^{\alpha} - P_{ii}^{\beta}) , \text{ as discussed by Berthier, (129).}$$

(b) ΔE is the state energy relative to the doublet ground state obtained with the same parameters.

Now the results of the application of Roothaan's procedure are given.

Table 36.

| i | Data A | | Data B | | Berthier | |
|---------------|------------------------------|------------------------------|------------------------------|------------------------------|------------------------------|------------------------------|
| | D ^o _{ii} | D ^c _{ii} | D ^o _{ii} | D ^c _{ii} | R ^o _{ii} | R ^c _{ii} |
| 1 | .0000 | .5000 | .0000 | .5000 | .0008 | .4870 |
| 2 | .6122 | .1939 | .6270 | .1865 | .6710 | .1606 |
| 3 | .4983 | .2509 | .4994 | .2504 | .5001 | .2481 |
| 4 | .0311 | .4844 | .0358 | .4822 | .0514 | .4804 |
| 7 | .7453 | .1274 | .7106 | .1447 | .6056 | .2152 |
| π -Energy | -174.326 | | -220.744 | | - | |
| ΔE | 3.33 | | 4.11 | | 3.98 | |

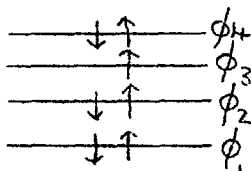
Note:(a) The close correspondence of the results obtained here with those of Berthier.

(b) The total state energies, and the excitation energy, ${}^2B_2 - {}^4B_2$. Berthier obtained 3.98 ev., with the use of a configuration interaction technique.

(c) All atomic π -charges are unity, as the radical is alternant.

Excited Doublet States, 2A_2 :

The first of these may be described by the orbital diagram;

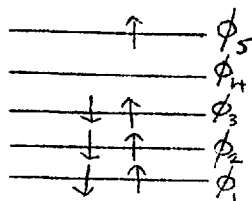


The SCF results for this state when treated with the Roothaan program are shown below.

Table 37.

| i | Data A | | Data B | | Berthier | |
|----------------|------------|------------|------------|------------|------------|------------|
| | D_{ii}^o | D_{ii}^c | D_{ii}^o | D_{ii}^c | R_{ii}^o | R_{ii}^c |
| 1 | .0000 | .5196 | .0000 | .5019 | .0000 | .5128 |
| 2 | .2231 | .3547 | .2434 | .3567 | .2287 | .3406 |
| 3 | .2769 | .2637 | .2566 | .2428 | .2713 | .2400 |
| 4 | .0000 | .5856 | .0000 | .6321 | .0000 | .6432 |
| 7 | .0000 | .6578 | .0000 | .6666 | .0000 | .6827 |
| Π - Energy | -173.688 | | -221.110 | | - | |
| ΔE | 3.97 | | 3.74 | | - | |

A second doublet is possible;



The results for this state are shown on the next page in Table 38., meanwhile the following observations apply to this table as well as Table 37 .

Note:(a) These two states are degenerate in the Roothaan approximation, neglecting differential overlap. Although these states have the same resultant spin-densities, the diagonal closed-shell density matrix elements are not identical . After a configuration interaction procedure Berthier obtains two excited

doublets ,2.76 ev., and ,3.81 ev., which are in accord with experimental data.

- (b) A configuration interaction technique is needed to split the degenerate states obtained here, and predict the optical transitions after the fashion of Berthier.

Table 38.

| i | Data A | | Data B | | Berthier | |
|---------------|------------|------------|------------|------------|------------|------------|
| | D_{ii}^o | D_{ii}^c | D_{ii}^o | D_{ii}^c | R_{ii}^o | R_{ii}^c |
| 1 | .0000 | .4803 | .0000 | .4984 | .0000 | .4278 |
| 2 | .2231 | .4221 | .2436 | .3995 | .2321 | .4184 |
| 3 | .2768 | .4594 | .2564 | .5009 | .2679 | .4925 |
| 4 | .0000 | .4145 | .0000 | .3677 | .0000 | .3272 |
| 7 | .0000 | .3422 | .0000 | .3333 | .0000 | .4233 |
| π -Energy | -173.688 | | -221.110 | | - | |
| ΔE | 3.97 | | 3.74 | | - | |

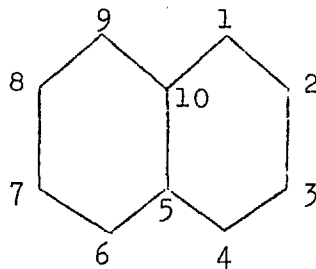
From all these results we are able to draw several conclusions. First as regards spin-densities, it seems clear that the use of 1.5 times the Mataga-Nishimoto two centre integrals by Ladik, et al.,(196) , in predicting spin-densities was only necessitated by their failure to use a spin projection technique . With the use of the single annihilator method, the improved wave functions give quite satisfactory results with the normal unaltered integrals. In fact the spin-polarized results are in good agreement with experiment.

The situation concerning the optical excited states is not so clear, and the results given here seem in variance with those of Berthier. The quartet state, 4B_2 , is of much lower energy in the spin-polarized approximation than in Roothaan's open-shell method. Perhaps this can be attributed to the increased spin correlation allowed by the former, or inadequacies in the energies obtained after the use of a single annihilator.

(e) Naphthalene.

(i) Geometry.

All Carbon-Carbon bonds were assigned a length of 1.40 \AA , with inter-bond angles of 120° . The atomic numbering system utilized is shown below;



(ii) Parameters.

In this alternant hydrocarbon, all Carbon cores were given valence state ionization potentials of 11.42 ev., and electron affinities of 0.58 ev. . Carbon-Carbon bonds were assigned resonance integrals of -2.39 ev., and the Mataga-Nishimoto approximation was used to supply the two centre Coulomb integrals.

(iii) Results.

The following results were obtained with the closed-shell SCF program , with configuration interaction for excited states.

Ground state bond-orders.

These may all be obtained from the following matrix elements, utilizing the molecular symmetry.

$$P_{12} = .7410 \quad P_{23} = .5870 \quad P_{45} = .5399$$

$$P_{5,10} = .5416$$

All charges are unity as the molecule is an alternant hydrocarbon.

Single electron excited states.

The singly excited molecular states are given both before and after configuration interaction, (see Fig. 28).

Table 39.

Naphthalene:No CI.

| Transition | ΔE_s | α_s | f_s | ΔE_t |
|------------|--------------|------------|-------|--------------|
| 3,6 | 6.04 | 279. | .001 | 4.63 |
| 3,7 | 6.86 | 331. | .001 | 5.87 |
| 3,8 | 7.94 | 59. | .558 | 6.46 |
| 4,6 | 5.02 | 330. | .916 | 4.01 |
| 4,7 | 6.36 | 243. | .660 | 4.32 |
| 4,8 | 6.86 | 331. | .001 | 5.87 |
| 5,6 | 4.61 | 239 | .517 | 2.56 |
| 5,7 | 5.02 | 150. | .916 | 4.01 |
| 5,8 | 6.04 | 99. | .001 | 4.63 |

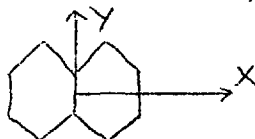
Table 40.

Naphthalene: With CI.

| Transition | ΔE_s | α_s | f_s | Sym. | ΔE_t | Sym. |
|------------|--------------|------------|-------|--------------|--------------|--------------|
| 1 | 4.25 | - | - | ${}^1B_{3u}$ | 2.16 | ${}^3B_{2u}$ |
| 2 | 4.46 | 237. | .254 | ${}^1B_{2u}$ | 3.40 | ${}^3B_{1g}$ |
| 3 | 5.79 | 330. | 2.113 | ${}^1B_{3u}$ | 3.77 | ${}^3B_{3u}$ |
| 4 | 5.84 | - | - | ${}^1B_{1g}$ | 4.25 | ${}^3B_{3u}$ |
| 5 | 6.19 | - | - | ${}^1A_{1g}$ | 4.34 | ${}^3B_{2u}$ |
| 6 | 6.23 | 99. | .001 | ${}^1B_{1g}$ | 5.54 | ${}^3A_{1g}$ |
| 7 | 6.42 | 63. | .698 | ${}^1B_{2u}$ | 5.85 | ${}^3B_{1g}$ |
| 8 | 7.54 | 151. | .002 | ${}^1A_{1g}$ | 6.19 | ${}^3A_{1g}$ |
| 9 | 8.02 | 240. | .984 | ${}^1B_{2u}$ | 6.83 | ${}^3B_{2u}$ |

Note:(a) Typical alternant hydrocarbon spectra, first singlet and triplet are unique , followed by degenerate singlet and triplet transitions which can only be separated with a configuration interaction procedure .

(b) The transitions to states ${}^1B_{3u}$ and ${}^1B_{2u}$ may be predicted as polarized in the X and Y directions respectively from symmetry considerations,



This is confirmed by the transition dipole angles, α_s , for the allowed transitions of these symmetries.

(c) The lower energy singlets and triplets may be directly compared with experimental results, (195), (198), (199).

First the singlets are given.

Table 41.

| Experimental | | Theoretical | | |
|--------------|-------|--------------|-------|-------------|
| ΔE_s | f_s | ΔE_s | f_s | Sym. |
| 3.99 | - | 4.25 | - | $1B_{3u}^*$ |
| 4.35 | - | 4.46 | .25 | $1B_{2u}^*$ |
| 5.62 | 1.7 | 5.79 | 2.11 | $1B_{3u}^e$ |
| 6.51 | .20 | 6.42 | .70 | $1B_{2u}$ |
| 7.41 | .6 | 8.02 | .98 | $1B_{2u}^e$ |

⊕ This assignment is very uncertain, there is a $1A_{1g}$ state at 7.54 ev. .

* Confirmed by polarization studies of McClure, (200).

⊕ Agrees with conclusions of Craig, et al., (201).

As may be seen, the overall prediction is quite satisfactory , especially as no parameter variation has been attempted to further improve the results.

For the triplet states less experimental data is available. This is shown in the following table.

Table 42.

| Experimental ΔE_t | Theoretical | |
|------------------------------|--------------|--------------|
| | ΔE_t | Sym. |
| 2.64 | 2.16 | ${}^3B_{2u}$ |
| 3.72 * | 3.77 | ${}^3B_{3u}$ |
| 4.49 [⊖] | 4.25 | ${}^3B_{3u}$ |
| | 4.34 | ${}^3B_{2u}$ |
| 5.62 [⊕] | 5.54 | ${}^3A_{1g}$ |
| | 5.85 | ${}^3B_{1g}$ |
| 6.27 [⊕] | 6.19 | ${}^3A_{1g}$ |

* Tentative , estimated by Kasha and Nauman ,(198).

⊖ Estimated position , Kleven and Platt ,(199).

⊕ These are from triplet-triplet data obtained by Orloff, (149), who also assigns the 6.27 ev. state a symmetry of ${}^3A_{1g}$.

Once again the fit of experimental results by the theoretical values is reasonable, within the limits of the rather inadequate data available. The first triplet, however, is not predicted very accurately . Attempts were made to improve on this with the two open-shell programs.

Naphthalene First Triplet.

The results of the application of the spin-polarized SCF treatment are given in Table 43. .

Table 43.

| Quantity | unann | ann |
|-----------------------|----------|----------|
| σ_1 | .5183 | .4644 |
| σ_2 | .0905 | .0870 |
| σ_5 | -.2171 | -.1025 |
| Π -Energy | -299.876 | -299.887 |
| ΔE | 2.09 | 2.07 |
| $\langle s^2 \rangle$ | 2.1213 | 2.0057 |
| Δ_1 | .0000 | |
| Δ_2 | .0040 | |
| Δ_3 | .1240 | |
| Δ_4 | .1241 | |

Note:(a) Spin density is here defined as , $P_{ii}^{\alpha} - P_{ii}^{\beta} = \sigma_i$.

- (b) The poor value obtained for the first triplet excitation energy, which has an experimental value of 2.64 , (202). The actual calculated first triplet has very similar energy to that obtained by the configuration interaction procedure just discussed.
- (c) With two centre integrals 1.5 times their Mataga-Nishimoto values , that is nearer their Slater orbital equivalents, the first triplet is found at 2.76 ev. . This value is very satisfactory from the prediction point of view , but the use of such a high multiple of the Coulomb integrals seems very questionable in the semi-empirical

approximation . As we have seen in the case of the Benzyl radical, and for the CS-SCF-CI excited ^{singlet} states of Naphthalene , the normal Mataga-Nishimoto integrals are perfectly adequate. Additional confirmation of this arises from the treatment of the Naphthalene positive and negative ions.

Now the results of a calculation using Roothaan's open-shell technique on the first triplet are given.

Table 44.

| Spin Densities | | | Energy | ΔE_t |
|----------------|-------|-------|----------|--------------|
| .4065 | .0935 | .0000 | -299.566 | 2.39 |

Note:(a) The close similarity with the previous results, Table 43.

(b) The improved value for the first triplet excitation energy.

The bond-orders obtained with the two different methods may also be compared .

Table 45.

| Bond-order element | Spin-polarized | | Roothaan's open-shell |
|--------------------|----------------|-------|-----------------------|
| | unann | ann | |
| P ₁₂ | .4352 | .4368 | .4567 |
| P ₂₃ | .8162 | .8156 | .7990 |
| P ₄₅ | .5657 | .5744 | .5700 |
| P _{10,5} | .4424 | .4487 | .4905 |

All the triplet charge densities are unity .

These results closely resemble those obtained by Amos,(165), and Amos and Synder,(168),(170) . This is to be expected as an identical method with similar input data was used .

(f) The Naphthalene Ions, $C_{10}H_8^+$.

(i) Geometry.

This was assumed identical to that of the ground state molecule given in section (e) .

(ii) Parameters.

In this study of the Naphthalene ions no attempt was made to allow for the differential ionization of the atomic Carbon cores , as was in the investigation of $C_4H_6^+$. The chief objective was the prediction of the spin-densities in the ions , which have been experimentally measured by means of ESR . All parameters used for the ions were identical with those applied to the molecule in previous section.

(iii) Results.

The ions were treated with both the spin-polarized and open-shell Roothaan methods , and the results of both approximations are shown together in Table 46 on the next page. The following notes apply to this table;

Note:(a) The entry in the table ΔE gives the energy of the state relative to the CS-SCF ground state. Thus the ΔE for the negative ion are less than zero, implying

Table 47.

| Quantity | Naphthalene - | | | Naphthalene + | | |
|-----------------------|----------------|----------|----------------|----------------|----------|----------------|
| | Spin-Polarized | | Roothaan OS | Spin-Polarized | | Roothaan OS |
| | unann | ann | | unann | ann | |
| σ_1 | .2889 | .2260 | .1908 | .2894 | .2261 | .1908 |
| σ_2 | .0107 | .0399 | .0592 | .0103 | .0397 | .0591 |
| σ_5 | -.0994 | -.0316 | .0000 | -.0997 | -.0317 | .0000 |
| P_{11} | 1.1637 | 1.1642 | 1.1686 | .8364 | .8358 | .8313 |
| P_{22} | 1.0982 | 1.0969 | 1.0913 | .9018 | .9030 | .9084 |
| P_{55} | .9763 | .9777 | .9802 | 1.0237 | 1.0223 | 1.0200 |
| P_{12} | .5980 | .6010 | .6087 | .5979 | .6009 | .6080 |
| P_{23} | .6857 | .6868 | .6806 | .6858 | .6869 | .6809 |
| P_{45} | .5525 | .5560 | .5534 | .5525 | .5556 | .5531 |
| $P_{10,5}$ | .5066 | .5086 | .5185 | .5065 | .5085 | .5183 |
| π -Energy | -304.553 | -304.591 | -304.415 | -292.555 | -292.568 | -292.414 |
| ΔE | -2.599 | -2.636 | -2.461 | 9.399 | 9.386 | 9.540 |
| $\langle s^2 \rangle$ | .8141 | .7530 | .7500 | .8145 | .7530 | .7500 |
| Δ_1 | .0000 | | - | .0041 | | - |
| Δ_2 | .0040 | | - | .0572 | | - |
| Δ_3 | .0570 | | - | .0750 | | - |
| Δ_4 | .0748 | | - | .0855 | | - |
| Δ_5 | .0852 | | - | - | | - |

lower energy states than those obtained for the molecule. Clearly these ΔE represent the approximate electron affinities of the molecule, with the positive ΔE 's of

the + ion corresponding to the molecular ionization potentials.

- (b) The spin-densities of the two ions evaluated in these separate SCF procedures are very similar. In fact they should be identical as shown by McLachlan,(203), due to the pairing properties of alternant hydrocarbon ion orbitals. Any deviation from equivalence in the results found is due entirely to loss of numerical significance in the execution of the computer program. This equivalence has been experimentally confirmed by De Boer and Weissman,(176), however the two spectra have been shown to be not exactly identical by Carrington,(204) .
- (c) The theoretically calculated spin-densities may be compared with the experimental quantities , and the calculated results of other workers.

Table 47.

| Reference | Experimental result | | | Theoretical result | | |
|---------------------|---------------------|----------|----------|--------------------|--------------|-----------------------------|
| | ρ_1 | ρ_2 | ρ_5 | ρ_1 | ρ_2 | ρ_5 |
| McLachlan (205) | .203 | .076 | -.058 | .222 .211 | .047 .055 | -.037 -.032* |
| Carrington (204) | .218 | .081 | -.098 | - | - | - |
| Amos (165) | - | - | - | .269 .243 | .021 .032 | -.081 -.055 [⊕] |

* Variable β 's used, $\beta(R_{c-c})$. ⊕ Projected results.

(d) The charge densities of the two ions are different, even though the spin distributions are identical. The results given here may be compared with those of other investigations.

Table 48.

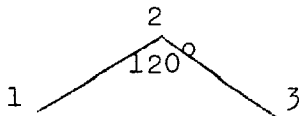
| Reference | Theoretical $C_{10}H_8^+$ | | | Theoretical $C_{10}H_8^-$ | | |
|-----------|---------------------------|----------|----------|---------------------------|----------|----------|
| | P_{11} | P_{22} | P_{55} | P_{11} | P_{22} | P_{55} |
| (107) | .8308 | .8924 | 1.0536 | 1.1732 | 1.1075 | .9385 |
| (165) | .821 | .899 | 1.061 | - | - | - |

(e) The corresponding orbital eigenvectors of these ions as obtained with the spin-polarized program were compared with those published by Amos and Synder, (168), as a check for the program. Amos and Synder used virtually the same input parameters, and the correspondence between the two sets of eigenvectors was very close.

(g) The Allyl Radical.

(i) Geometry.

The radical was assumed planar, with Carbon-Carbon bond-lengths of 1.4 \AA , and an inter-bond angle of 120° .



(ii) Parameters.

These were all assigned their typical hydrocarbon values. The valence state ionization potential and electron affinity were given the values 11.42 and .58 ev., respectively. All resonance integrals between bonded atoms were given the value of -2.39 ev., the Mataga-Nishimoto approximation was used for the Coulomb integrals. This particular investigation was directed at a calculation of spin-densities, to compare with the experimental results.

(iii) Results.

These were all obtained in the spin-polarized approximation.

Table 49.

| Quantity | unann | ann |
|-----------------------|---------|---------|
| σ_1 | .7292 | .5696 |
| σ_2 | -.4584 | -.1392 |
| P_{12} | .6285 | .6758 |
| Π -Energy | -52.152 | -52.086 |
| $\langle S^2 \rangle$ | .9601 | .7500 |
| Δ_1 | .2358 | |

Note:(a) The spin densities are in fair agreement with the experimental results, $\sigma_1 = .58$, $\sigma_2 = -.16$, obtained by Fessenden and Schuler, (206).

(b) The following theoretical results have been found in similar investigations.

Table 50.

| Reference | σ_1 | σ_2 |
|-------------------|------------|------------|
| McLachlan, (205) | .594 | -.187 |
| Brickstock, (207) | .626 | -.252 |

(h) The Nucleotide Bases.

(i) Introduction.

The five nucleotide bases, Uracil, Adenine, Thymine, Guanine and Cytosine, have great biological importance, (167). Hence their electronic structure has been investigated by several authors, using various semi-empirical methods, (167), (166), (208 - 212). In this section results obtained for both the ground state and excited molecular states of these bases are given. The same set of parameters was utilized for all calculations, so numerical results may be directly compared and the degree of equivalence in the approximations studied. The parameters given here could be used as a starting point for the investigation of other groups of hetero-atomic conjugated molecules, the set being re-optimized as necessary.

(ii) Geometry.

The molecular geometries of the five bases were

taken from a paper by Spencer, (213). The atomic indexing system is shown in Fig. 29 .

(iii) Parameters.

The valence state ionization potentials of the constituent atoms of the nucleotide bases are now listed. Their values were taken from references (118) and (117) .

| | | |
|---|--------------------------|-------------------------|
| $\begin{array}{l} \diagup \\ \diagdown \end{array} \text{C} -$ | $I_{\text{C}} = 11.42$ | $E_{\text{C}} = 0.58$ |
| $\begin{array}{l} \diagup \\ \diagdown \end{array} \text{N} - \text{H}$ | $I_{\text{N}} = 29.16$ | $E_{\text{N}} = 14.49$ |
| $\begin{array}{l} \diagup \\ \diagdown \end{array} \text{N}$ | $I_{\text{N}} = 13.83$ | $E_{\text{N}} = 0.48$ |
| $\begin{array}{l} \diagup \\ \diagdown \end{array} \text{C} = \text{O}$ | $I_{\text{O}} = 17.28$ | $E_{\text{O}} = 2.70$ |
| $-\text{C} \equiv \text{H}_3$ | $I_{\text{H}_3} = 13.60$ | $E_{\text{H}_3} = 0.75$ |

The set of resonance integrals used is shown below;

$$\begin{array}{ll} \beta_{\text{C-C}} = -2.39 \text{ ev.} & \beta_{\text{C-H}_3} = 2.*\beta_{\text{C-C}} \\ \beta_{\text{C-O}} = \beta_{\text{C-C}} & \beta_{\text{C-N}} = .8*\beta_{\text{C-C}} \\ \beta_{\text{C-N}} = 1.2*\beta_{\text{C-C}} & \end{array}$$

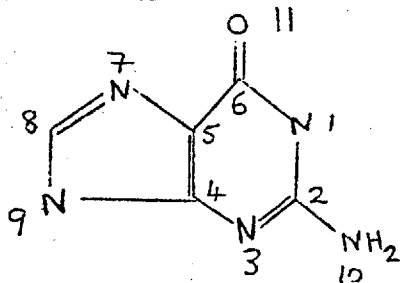
These values differ slightly from those of Ladik and Appel, (210), giving an increased correspondence between the first two experimental singlet excitations of the bases and those found in the CS-SCF-CI approximation.

The Mataga-Nishimoto approximation was used for all two centre Coulomb integrals.

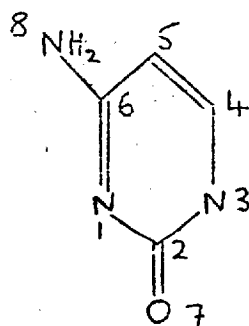
(iv) Results.

Ground-states : The π -electron charge distributions of the ground state bases are shown in Table 51 .

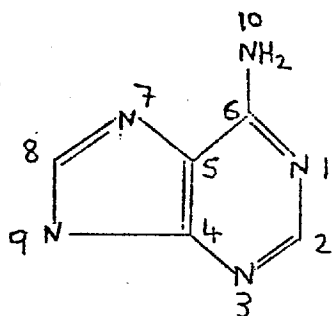
Fig. 29.



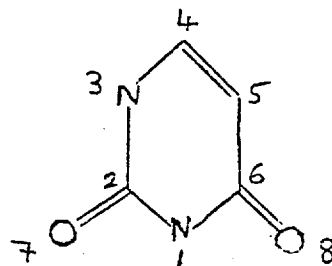
Guanine



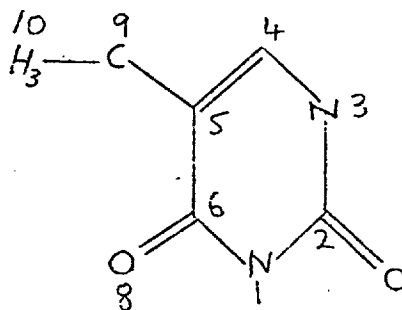
Cytosine



Adenine



Uracil



Thymine

Table 51.

Ground state π -electron distributions in the Nucleotide bases.

| Atom [⊠] | Uracil | Thymine | Cytosine | Guanine | Adenine |
|-------------------|--------|---------|----------|---------|---------|
| 1 | 1.8825 | 1.8826 | 1.1494 | 1.8824 | 1.1444 |
| 2 | .6997 | .7002 | .7319 | .8760 | .9097 |
| 3 | 1.8882 | 1.8875 | 1.8732 | 1.1709 | 1.1361 |
| 4 | .9158 | .9096 | .9187 | .9401 | .9549 |
| 5 | 1.0336 | 1.03998 | 1.0496 | 1.0478 | 1.0356 |
| 6 | .7406 | .7404 | .8616 | .7403 | .9098 |
| 7 | 1.4261 | 1.4249 | 1.4668 | 1.1066 | 1.1284 |
| 8 | 1.4135 | 1.4106 | 1.9489 | .9615 | .9459 |
| 9 | | .9343 | | 1.8678 | 1.8797 |
| 10 | | 1.0703 | | 1.9486 | 1.9556 |
| 11 | | | | 1.4581 | |

⊠ For atomic indexing see Fig. 29.

From this table the similarities in the electronic distributions within the Pyrimidine bases, (Uracil, Thymine, Cytosine), and the Purine bases, (Guanine, Adenine), are evident. These π -densities may be compared with the distributions found in other investigations, (166), (167), (214).

From these ground state π -electron distributions the π -contribution to the total dipole moment of each molecule was calculated, and compared with the theoretical results obtained by Pullman, (215), (216).

Table 52.

| Base | μ_{π} (D) | μ_{π} (D), Pullman. |
|----------|-----------------|---------------------------|
| Uracil | 3.64 | 3.3 |
| Adenine | 1.06 | 2.7 |
| Thymine | 3.62 | 2.8 |
| Cytosine | 4.84 | 5.3 |
| Guanine | 5.06 | 5.7 |

Note:(a) Varying degrees of correspondence between the results obtained here and those found by Pullman, who also calculated the total molecular dipole moments of the bases by including the σ -core contribution, $\mu_{tot} = \mu_{\pi} + \mu_{\sigma}$. With a parameter set specifically designed for the accurate prediction of dipole moments, Pullman obtained moments which were in substantial agreement with experimental values. These parameters were calibrated in Hückel

approximations of simple hetero-atomic molecules.

The data used here was oriented towards a reproduction of the singlet spectra, not the dipole moment of the bases.

- (b) The same sequence is predicted for the magnitude of the molecular π -dipoles of the bases by both sets of results.

Excited States: The singlet excitations calculated with the CS-SCF-CI program are shown in Table 53, and compared to the experimental spectra of the bases, (210), in the same Table. Examining this table an average deviation of .30 ev. between the theoretical and experimental values of the first two singlets of each base is found. This represents a marked improvement over Ladik's mean deviation of .5 ev., (210). In every instance, except for Adenine, each individual calculated transition is a better fit of the experimental value than that obtained by Ladik and Appel, (210). These results may also be compared with those found by Nesbet, (209). Finally it may be noted that as is usual for SCF-CI excited singlet states, the intensity predictions of the transitions are rather unsatisfactory.

The first triplet states of the five bases were investigated with both the spin-polarized and Roothaan open-shell SCF programs. The total π -energies of these states are shown together with the CS-SCF ground state energy in Table 54.

The need for the use of an annihilator to improve the expectation

Table 53.

Excited Singlets of the Nucleotide Bases.

| Base | ΔE_{th} | f_{th} | ΔE_{exp} | f_{exp} |
|----------|-----------------|----------|------------------|-----------|
| Uracil | <u>5.14</u> | .676 | 4.81 | .18 |
| | 5.68 | .062 | | |
| | <u>6.05</u> | .226 | 6.11 | .30 |
| | 6.93 | .011 | | |
| Thymine | <u>5.09</u> | .712 | 4.67 | .18 |
| | 5.64 | .076 | | .37 |
| | <u>6.02</u> | .202 | 5.94 | |
| | 6.71 | .015 | | |
| Cytosine | <u>4.41</u> | .378 | 4.61 | .13 |
| | 5.51 | .053 | | |
| | <u>6.53</u> | .904 | 6.26 | .72 |
| | 6.74 | .080 | | |
| Guanine | <u>4.11</u> | .477 | 4.49 | .20 |
| | <u>5.15</u> | .273 | 5.03 | .27 |
| | 5.88 | .136 | | |
| | 6.07 | .213 | | |
| Adenine | <u>5.00</u> | .003 | 4.75 | .28 |
| | <u>5.35</u> | .467 | 5.99 | .54 |
| | 6.61 | .415 | | |
| | 6.78 | .267 | | |

Table 54.

The first excited triplets of the Nucleotide bases.

| Base | CS - SCF | | Spin - Polarized | | $\langle S^2 \rangle$ | $\langle S^2 \rangle$ Ann | Rootaan | CS-SCF ground-state |
|----------|----------|-----------|------------------|----------|-----------------------|---------------------------|----------|------------------------|
| | No C.I. | With C.I. | Un Ann | Ann | | | SCF | |
| Uracil | -362.652 | -363.228 | -363.276 | -363.244 | 2.12034 | 2.00000 | -363.187 | -364.561 |
| Thymine | -466.424 | -466.908 | -467.092 | -467.053 | 2.12389 | 2.00044 | -466.991 | -468.343 |
| Cytosine | -351.049 | -351.737 | -351.874 | -351.801 | 2.18393 | 2.00186 | -351.497 | -353.248 |
| Guanine | -584.653 | -585.054 | -585.553 | -585.123 | 2.47559 | 2.12267 | -584.843 | -586.829 |
| Adenine | -452.016 | -452.723 | -452.721 | -452.479 | 2.36290 | 2.06404 | -452.622 | -455.436 |

value of the spin-polarized wave functions with the spin operator, S^2 , is made apparent by reference to this table. Even after the application of an annihilator to the SCF wave function, the spin-polarized function of Guanine does not well represent a pure spin state. Configuration Interaction has its usual drastic effect on the CS-SCF results obtained initially with the virtual orbitals. This implies that the use of virtual orbitals in the representation of the molecular excited states is a particularly poor approximation. It will be noted that the spin-polarized method gives lower energy triplet states than Roothaan's method, except in the case of Adenine. This is to be expected, as the former method does not impose spin pairing in the closed π -electron shell. Unfortunately no direct experimental values for these triplet states have been measured to date. There is some evidence for a Uracil triplet at 2.1 -2.2 ev., (212), which agrees most closely with the CS-SCF results for the base, taking the energy found before configuration interaction. All the other approximations give energies of ~ 1.3 ev., except when a restricted four component CI is used, giving 2. ev. .

The SCF charge and spin-densities for the triplet states are given in Tables 55 and 56. From these tables it may be seen that the charge densities of the bases seem reasonably independent of the method applied to find the wave function of the first triplet state. The effect of the single annihilator on the impure spin-polarized wave function's charge density is generally

Table 55.

Triplet π -electron charge densities of the Nucleotide bases.

| Atom | Uracil | | | Thymine | | | Cytosine | | | Guanine | | | Adenine | | |
|------|--------|----------------------|--------|---------|----------------------|--------|----------|----------------------|--------|---------|----------------------|--------|---------|----------------------|--------|
| | SPO | (SPO) _{ann} | ROS | SPO | (SPO) _{ann} | ROS | SPO | (SPO) _{ann} | ROS | SPO | (SPO) _{ann} | ROS | SPO | (SPO) _{ann} | ROS |
| 1 | 1.8975 | 1.8978 | 1.8956 | 1.8970 | 1.8972 | 1.8950 | 1.0542 | 1.0547 | 1.0454 | 1.9140 | 1.9139 | 1.9112 | 1.1332 | 1.1348 | 1.1456 |
| 2 | .6939 | .6937 | .6929 | .6943 | .6942 | .6934 | .8200 | .8101 | .7277 | .9842 | .9814 | .9369 | .9580 | .9563 | .8945 |
| 3 | 1.8894 | 1.8895 | 1.8919 | 1.8896 | 1.8897 | 1.8920 | 1.9001 | 1.8994 | 1.9004 | 1.1224 | 1.1251 | 1.1317 | 1.1025 | 1.1069 | 1.1363 |
| 4 | 1.0350 | 1.0346 | 1.0243 | 1.0359 | 1.0355 | 1.0246 | 1.0536 | 1.0543 | 1.0402 | 1.0115 | 1.0115 | 1.0326 | .9761 | .9736 | .9020 |
| 5 | .9428 | .9409 | .9490 | .9511 | .9495 | .9575 | 1.0038 | 1.0038 | .9754 | .9559 | .9554 | .9319 | .9609 | .9603 | 1.0379 |
| 6 | .9149 | .9109 | .9881 | .9071 | .9028 | .9769 | 1.0028 | 1.0028 | .9893 | .8557 | .8480 | .8788 | .9140 | .9117 | .9044 |
| 7 | 1.4315 | 1.4315 | 1.4353 | 1.4306 | 1.4306 | 1.4341 | 1.2092 | 1.2186 | 1.3639 | 1.0928 | 1.0960 | 1.1166 | 1.1116 | 1.1142 | 1.0590 |
| 8 | 1.1951 | 1.2012 | 1.1230 | 1.1962 | 1.2023 | 1.1273 | 1.9562 | 1.9563 | 1.9577 | .9369 | .9325 | .8833 | .9670 | .9651 | 1.0445 |
| 9 | | | | .9352 | .9351 | .9332 | | | | 1.9217 | 1.9217 | 1.9104 | 1.9278 | 1.9280 | 1.9221 |
| 10 | | | | 1.0631 | 1.0630 | 1.0659 | | | | 1.9568 | 1.9568 | 1.9507 | 1.9489 | 1.9491 | 1.9537 |
| 11 | | | | | | | | | | 1.2482 | 1.2576 | 1.3161 | | | |

Table 56.

Triplet π -electron spin densities of the Nucleotide bases.

| Atom | Uracil | | | Thymine | | | Cytosine | | | Guanine | | | Adenine | | |
|------|--------|----------------------|-------|---------|----------------------|-------|----------|----------------------|-------|---------|----------------------|-------|---------|----------------------|-------|
| | SPO | (SPO) _{ann} | ROS | SPO | (SPO) _{ann} | ROS | SPO | (SPO) _{ann} | ROS | SPO | (SPO) _{ann} | ROS | SPO | (SPO) _{ann} | ROS |
| 1 | -.0062 | -.0006 | .0107 | -.0071 | -.0011 | .0102 | .6247 | .5396 | .5770 | .0208 | .0239 | .0431 | -.1877 | -.0768 | .0001 |
| 2 | -.0041 | -.0012 | .0007 | -.0085 | -.0033 | .0008 | -.3660 | -.1617 | .0214 | .5697 | .4624 | .3375 | .5820 | .4788 | .0452 |
| 3 | .0456 | .0448 | .0429 | .0450 | .0443 | .0429 | .0393 | .0446 | .0505 | -.3491 | -.1562 | .0351 | -.4151 | -.1891 | .0045 |
| 4 | .9031 | .8928 | .8146 | .9031 | .8937 | .8232 | .7719 | .7460 | .8269 | .6772 | .5790 | .5161 | .6760 | .5699 | .0860 |
| 5 | .5959 | .4980 | .1452 | .5694 | .4760 | .1435 | .0220 | .0516 | .1938 | .5397 | .4330 | .3273 | .6342 | .5407 | .0212 |
| 6 | -.2458 | -.0853 | .1563 | -.2519 | -.0901 | .1465 | .2263 | .1949 | .1164 | -.3159 | -.1300 | .1058 | .3018 | .2003 | .0518 |
| 7 | .0025 | .0031 | .0013 | .0076 | .0057 | .0014 | .6666 | .5721 | .2067 | -.3954 | -.1805 | .0074 | -.3099 | -.1325 | .8062 |
| 8 | .7108 | .6484 | .8283 | .7058 | .6416 | .8194 | .0151 | .0129 | .0073 | .5482 | .4005 | .1110 | .6410 | .5461 | .9401 |
| 9 | | | | -.0466 | -.0221 | .0012 | | | | .0521 | .0419 | .0264 | .0551 | .0466 | .0405 |
| 10 | | | | .0830 | .0552 | .0111 | | | | .0289 | .0241 | .0217 | .0226 | .0161 | .0045 |
| 11 | | | | | | | | | | .6238 | .5019 | .4687 | | | |

quite small . With the spin-densities, the contrast between the methods is more marked. Annihilation has an appreciable effect on the spin-polarized orbital spin-densities. Roothaan's method cannot, of course, yield negative spin-densities.

(i) The Nucleotide Base-Pairs, G-C and A-T .

(i) Introduction.

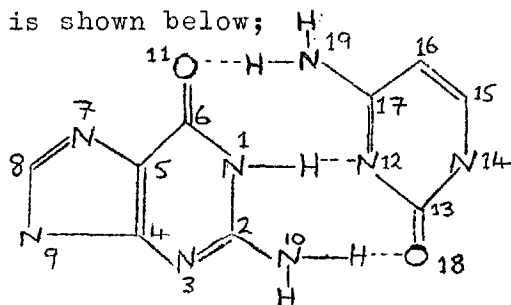
The Hydrogen-bonded base-pairs, Guanine-Cytosine, (G-C), and Adenine-Thymine, (A-T), occur as the basic units of the double-stranded helical model of DNA proposed by Watson and Crick, (217). These base-pairs are planar, and the Hydrogen-bonds linking them determine the relative positions of the component bases. These Hydrogen-bonds are found to be nearly linear, (213), and serve to connect the two π -electron systems of the interacting bases, (216), (166), (167) . The π -electron interaction between these bases may be investigated with the CS-SCF-CI approximation, and some results obtained by this method, and many more found in the Hückel approximation have already been reported, (211), (216), (209), (218).

The results presented here show the effects of the inter-base interactions on the wave functions of the base-pairs and the degree of π -electron re-distribution caused by the pairing. Single electron optical transitions are also discussed.

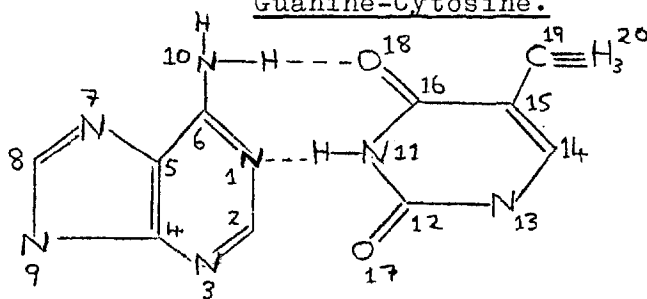
(ii) Parameters.

The geometries of the base-pairs were obtained from

a paper by Spencer, (213), and the atomic numbering system employed is shown below;



Guanine-Cytosine.



Adenine-Thymine.

The valence state ionization potentials and electron affinities of the atoms in the base-pairs were given the same values as in the discussion of the nucleotide bases, section (h) . The set of resonance integrals used here was slightly different from that given in (h), the set corresponding to series (a) of reference (210).

Delocalization of the π -electrons through the Hydrogen-bonds of each base-pair was treated in the manner of Pullmann and Ladik, (166), (219). A resonance integral, $\beta_{X-Y} = .15\beta_{C-C}$, ($\beta_{C-C} = -2.39$ ev.), was assigned to the Hydrogen-bond $X-H \cdots Y$. In addition the appropriate diagonal elements of the Fock matrix, F_{XX} and F_{YY} , were altered by $-.2\beta_{C-C}$ and $+.2\beta_{C-C}$ respectively

at each SCF iteration, ($F_{XX}^1 = F_{XX} - .2\beta_{c-c}$, $F_{YY}^1 = F_{YY} + .2\beta_{c-c}$). All two centre integrals were obtained with the Mataga-Nishimoto approximation.

(iii) Results.

Charge-densities: The SCF π -electron distributions of the two base-pairs are shown compared with those of the free constituent bases in Table 57. The charge-densities of the individual bases were obtained with the same molecular parameters as were used for the base-pairs.

As might have been anticipated, the Hydrogen-bonds only markedly effect the π -electron charges of the atoms directly involved or closely adjacent to the bonds. The total π -electron distributions of the bases are very little effected by their pairing with Hydrogen bonding.

Similarly, the SCF molecular orbitals of the base-pairs preserve to a large degree the independence of the two sets of π -electrons in each base-pair. In spite of the interactions of the paired bases, the single electron states of the base-pairs tend to be localized on one or other of the constituent bases. The base-pair molecular orbitals are sufficiently localized to to be directly comparable with the free base orbitals, and the eigenvectors and eigenvalues are found very similar.

The correspondence of the base-pair and free base orbitals is shown in Table 58, where the orbital energies of the molecules in the base-pairs are compared both before and after pairing.

Table 57.

Atomic π -Charges in G-C and A-T.

| Atom | Paired-bases G-C | Free-bases G+C | Paired-bases A-T | Free-bases A+T |
|------|---------------------|-------------------|---------------------|-------------------|
| 1 | 1.8672 | 1.8865 | 1.2003 | 1.1498 |
| 2 | .8534 | .8697 | .8835 | .9044 |
| 3 | 1.1981 | 1.1861 | 1.1560 | 1.1501 |
| 4 | .9412 | .9531 | .9408 | .9476 |
| 5 | 1.0615 | 1.0515 | 1.0387 | 1.0339 |
| 6 | .7374 | .7623 | .8801 | .9058 |
| 7 | 1.1167 | 1.1174 | 1.1378 | 1.1397 |
| 8 | .9690 | .9635 | .9445 | .9406 |
| 9 | 1.8614 | 1.8614 | 1.8765 | 1.8765 |
| 10 | 1.9316 | 1.9444 | 1.9421 | 1.9518 |
| 11 | 1.4568 | 1.4041 | 1.8840 | 1.8974 |
| 12 | 1.2346 | 1.1706 | .7339 | .7304 |
| 13 | .7278 | .7599 | 1.8966 | 1.8970 |
| 14 | 1.8797 | 1.8809 | .9140 | .9202 |
| 15 | .9007 | .9148 | 1.0469 | 1.0466 |
| 16 | 1.0518 | 1.0525 | .7360 | .7612 |
| 17 | .8110 | .8564 | 1.3774 | 1.3771 |
| 18 | 1.4705 | 1.4193 | 1.4056 | 1.3646 |
| 19 | 1.9297 | 1.9456 | .9328 | .9327 |
| 20 | - | - | 1.0727 | 1.0729 |

Table 58.

The Orbital Energies of G-C and A-T .

| i | ϵ_i^{G-C} | G or C orbital | | A^2 | ϵ_i^{A-T} | A or T orbital | |
|----|--------------------|----------------|---|-------|--------------------|----------------|---|
| | | ϵ_i^k | k | | | ϵ_i^k | k |
| 1 | -17.0474 | -16.9115 | C | .273 | -17.7198 | -17.8780 | T |
| 2 | -16.8222 | -17.2686 | G | .255 | -16.6269 | -16.7150 | A |
| 3 | -16.4640 | -16.6881 | G | .034 | -16.3247 | -16.5301 | T |
| 4 | -15.5301 | -15.9602 | C | .091 | -15.1547 | -15.6331 | A |
| 5 | -15.0484 | -15.7369 | G | .087 | -14.9573 | -15.0011 | T |
| 6 | -13.5820 | -13.4026 | C | .214 | -14.0074 | -13.9909 | T |
| 7 | -13.3848 | -13.5022 | G | .228 | -13.3964 | -13.5652 | A |
| 8 | -12.4147 | -12.5329 | G | .414 | -12.8178 | -12.9574 | T |
| 9 | -12.2624 | -12.3932 | C | .467 | -12.2093 | -12.3134 | A |
| 10 | -11.7009 | -11.7920 | G | .023 | -11.0413 | -11.0066 | T |
| 11 | -10.3505 | -10.1594 | C | .010 | -10.8626 | -10.8967 | A |
| 12 | -9.2545 | -9.3826 | G | .002 | -9.7063 | -9.8464 | A |
| 13 | -2.8998 | -2.7905 | C | - | -2.8325 | -2.8097 | T |
| 14 | -2.3108 | -2.4740 | G | - | -1.7373 | -1.8624 | A |
| 15 | -.9225 | -.9518 | G | - | -1.1962 | -1.2602 | T |
| 16 | -.7113 | -.6401 | C | - | -1.0839 | -1.1186 | A |
| 17 | -.2052 | -.3499 | G | - | .0449 | .0378 | T |
| 18 | 1.1194 | 1.2422 | C | - | .0766 | -.0234 | A |
| 19 | 1.9325 | 1.8297 | G | - | 1.8820 | 1.8538 | T |
| 20 | - | - | - | - | 2.1823 | 2.0982 | A |

The classification of the orbitals as essentially localized on one or other of the molecules in the base-pairs was made entirely as a result of a comparison of the eigenvectors representing the molecular orbitals of the individual bases and base-pairs. The quantity A^2 noted for the occupied orbitals of the pair G-C expresses the degree of delocalization of a particular orbital between the two bases. A^2 for orbital m is defined by $A^2(m) = \sum_i c_{m,i}^2$; where $1 \leq i \leq 11$ for a orbital largely localized on Cytosine, and $12 \leq i \leq 19$ for a Guanine based orbital. Thus $A^2(m)$ is a direct measure of the degree of delocalization of an electron in orbital ϕ_m onto the base it is not mainly localized on. From the values of A^2 shown, there is clearly quite a degree of inter-molecular delocalization induced in the occupied levels by the interactions of the two coupled π -electron systems in the base-pairs. For all the unoccupied orbitals, $A^2(m) < .001$, $13 \leq m \leq 19$.

Total π -Energies: These were calculated both with and without the Hydrogen-bonds, in an attempt to deduce the stabilization energy of the base-pairs in the Hydrogen-bonded situation.

The bonded state is denoted G-C, A-T, and the non-bonded, G+C, and, A+T.

$$\begin{array}{ll} E_{\pi}^{G-C} = -1239.0001 \text{ ev.} & E_{\pi}^{G+C} = -1239.3799 \text{ ev.} \\ E_{\pi}^{A-T} = -1208.3953 \text{ ev.} & E_{\pi}^{A+T} = -1208.6964 \text{ ev.} \end{array}$$

On the basis of these energies alone, the Hydrogen-bonded base-pairs must be regarded as de-stabilized with respect to the

non-bonded component bases held in the same conformation.

This is in direct conflict with Hückel results obtained by Pullman ,(216), who allowed for the base-pair Hydrogen-bonds in the same fashion . Pullman found that the Hydrogen-bonded states were stabilized by several Kcals. in the Hückel approximation , and this has been confirmed by the results of a Hückel treatment not presented here . Hence we have a situation where the Hückel and the SCF approximations are in direct contradiction . This is not surprising , as the two treatments represent entirely different levels of approximation.

The Hückel method ignores all explicit consideration of inter-electronic interaction , while the SCF treatment does attempt to take some degree of electron correlation in account. From SCF treatments of the base pairs both with and without Hydrogen-bonds , it has been shown that most of the inter-base interaction results from the mutual perturbing influence of the two essentially localized π -electron charge distributions on each other . The Hydrogen-bond coupling of the two π -systems has comparatively little significance . Thus a Hückel approximation would seem entirely unsuitable for the investigation of these base-pairs . The π -electron SCF approach seems inappropriate also, since apart from the inadequacies in the description of the Hydrogen-bonds , these bonds themselves represent a very small proportion of the inter-base interactions at separations of several Å . Finally it seems important to comment that the total

π -energies given must be regarded as suspect to a certain degree due to computer round-off errors inherent in such a protracted calculation .

Optical Excitations: These were found with the configuration interaction procedure incorporated in the CS-SCF program.

The first four calculated singlet transitions of the base-pairs are shown in Tables 59 and 60, and they are compared with the free base transitions found with the same parameters.

Table 59.

| Base-pair transition G-C | | | Component base transition | | |
|-----------------------------|--------------|-------|---------------------------|-------|------|
| Trans. | ΔE_s | f_s | ΔE_s | f_s | Base |
| 1 | 3.92 | .504 | 3.93 | .528 | G |
| 2 | 4.42 | .479 | 4.33 | .389 | C |
| 3 | 4.55 | - | - | - | - |
| 4 | 5.05 | .308 | 5.04 | .236 | G |

Table 60.

| Base-pair transition A-T | | | Component base transition | | |
|-----------------------------|--------------|-------|---------------------------|-------|------|
| Trans. | ΔE_s | f_s | ΔE_s | f_s | Base |
| 1 | 4.68 | .023 | 4.57 | .003 | A |
| 2 | 4.96 | .586 | 4.97 | .525 | A |
| 3 | 5.06 | - | - | - | - |
| 4 | 5.45 | .685 | 5.42 | .747 | T |

- Note:(a) The forbidden charge-transfer transitions , transition 3, for both G-C and A-T . These transfers involve the excitation of an electron from an orbital essentially localized on one base to a molecular orbital localized principally on the other. These transitions are hence strongly forbidden , and have no analogue in the single base transitions. All other transitions can be readily identified with the single base excitations , the excitation energies being very similar in the bonded and non-bonded cases.
- (b) The SCF treatment appears inadequate in predicting the expected hypochromic effect for the base-pair transitions, except for the first excitation in G-C . It is felt that the whole question of hypochromism , which has been extensively discussed elsewhere ,(166),(220),(210), is not best treated by an approach such as this . In such big molecules configuration interaction is an uncertain procedure for determining excited states , as for reasons of practical execution ,only such a small number of the total range of configurations can be included . In addition the numerical problem of finding a 20-component eigenvector accurately ,upon which the accuracy of the transition dipole calculated depends, is not easily solved. It would appear again, as in the case of the prediction

of the Hydrogen-bond stabilization , the semi-empirical SCF treatment is not suited to the discussion of such weak interactions.

Finally the base-pair triplets are tabulated,

Table 61.

| Transition | G-C | A-T |
|------------|--------------|--------------|
| | ΔE_t | ΔE_t |
| 1 | 1.82 | 2.21 |
| 2 | 1.93 | 2.73 |
| 3 | 3.43 | 3.61 |
| 4 | 3.51 | 3.95 |

These triplet transitions are very different from those obtained for the constituent bases , being at appreciably higher energies. This is an effect to be expected in larger molecules, for as the electron delocalization increases , the exchange integral, K_{ij} , which separates the singlet and triplet transitions, decreases . In these base-pairs an additional factor tends to further reduce the singlet/triplet separations for the charge-transfer type excitations . These transitions between molecular orbitals essentially localized in different parts of the π -system, will have almost identical singlet and triplet energies. This occurs because K_{ij} tends to zero where the orbitals i and j belong to different weakly interacting π -clusters . The effect

is additional to the reduction of K_{ij} consequent on the increase in molecular size.

From these various results found for the base-pairs, several conclusions may be drawn. First, the constituent molecules in the base-pairs retain a high degree of autonomy, this is indicated by the π -electron distributions and the optical transitions. This independence of the bases is somewhat in variance with the degree of delocalization found in the SCF orbital eigenvectors, (see A^2 in Table 58). It is, however, the most tightly bound electrons which have the greatest degree of delocalization. The higher energy electrons which are directly involved in the optical transitions are more localized.

The second major point to arise from this work is the inadequacy of the MO-SCF description for weakly interacting π -systems, and this is not easily solved without a more 'ab initio' approach to the whole electronic problem.

(j) The Helical Polynucleotides, Poly(G-C), Poly(A-T), and Poly(U).

(i) Introduction.

The band structures of the periodic DNA models, Poly(G-C) and Poly(A-T) have been investigated in the semi-empirical Pople-Pariser-Parr SCF crystal orbital approximation. The theoretical background to this calculation of the SCF Bloch

wave functions of one-dimensional polymers with simple translational symmetry was discussed in Chapter II , section (20). A computer program for performing such calculations was given in Chapter III .

The results found utilizing this delocalized self-consistent model are of general interest in the description of polymeric systems . Here, however, investigation was directed specifically at determining the π -electron energy-band structures of simple analogues of natural DNA , constructed from the base-pairs G-C and A-T . The periodic polynucleotide chains in the models were given the same geometry as the chains in the Watson-Crick stereo-model of DNA B ,(217) , with a translational distance of 3.36 \AA between unit cells, and an inter cell rotation of 36° .

In addition to these stacked base-pairs, the homopoly-nucleotide Poly(U) was studied, both in the SCF crystal orbital scheme , and by the successive stacking of up to five base residues to form a short polymer. This treatment of up to five Uracil molecules in the same conformational relationships as five unit cells in DNA was performed with a modified version of the CS-SCF program .

Finally it should be observed that natural DNA is an aperiodic solid, so the results given here may be of only limited value in the interpretation of the properties of the natural product .

(ii) Parameters.

The parameters necessary for the polymer-SCF program fall into two groups, intermolecular and intramolecular quantities .

The intramolecular parameters of the base-pairs, the valence state ionization potentials and electron affinities, resonance integrals and interatomic distances, were given the same values as in the previous section, where the free base-pairs were considered . The Hydrogen-bonds linking the constituent molecules in the base-pairs were allowed for in the same manner as previously discussed . The intra-base parameters used for Poly(U) were identical to those given in reference ,(210).

The small inter-base resonance integrals, β_{ij}^{\pm} , were the same as those which have been applied in previous Hückel band calculations of periodic DNA models ,(184),(185) . These resonance integrals between neighbouring stacked base-pairs were estimated on the basis of the overlap integrals between the orbitals of the superimposed bases of the model DNA chain,(166), (221) . The smaller integrals between the two components of a base-pair were neglected.

The two centre Coulomb integrals both within the base-pairs and between the base-pairs in the neighbouring unit cells were approximated with the formula of Mataga and Nishimoto, (124) . The inter unit-cell atomic distance matrix required for this, R_{st}^+ , was obtained from the geometry of the B form of DNA,(222).

(iii) Results.

Poly(A-T) and Poly(G-C).

The wave functions of the systems Poly(G-C) and Poly(A-T) reached the required degree of self-consistency in both cases after six iterations of the polymer-SCF program. Eleven K values were taken in the range 0 to 2π , (see page 275), with two of these values representing the limits of K , $K= 0$, and $K = 2\pi$. This number of intervals at which the band energy was derived gave a reasonable compromise between computational accuracy and program execution time. In a test of the program using 11 and 22 K-values for Poly(U) , substantially the same results were produced in both calculations. This is in line with the experience of Ladik, et al.,(223) .

In Tables 62 and 63 the band structures obtained for Poly(A-T) and Poly(G-C) are given . The band widths and limiting energies are shown , together with the K values of the band maximum and minimum . The last column of the Tables lists the corresponding orbital energies of a single A-T and G-C pair respectively , calculated with the CS-SCF program and the same intramolecular parameters .

Figs 30 and 31 give the comparison of the occupied levels of the free nucleotide bases , the base-pairs , and the polymer bands in A-T and G-C respectively .

From the K dependence of the energies of the different bands , with $E_p(K)$ evaluated at 11 K values in the range ,

Table 62.

The band structure of poly(A-T) in eV-s

| Band | Maximum E(K) | K | Minimum E(K) | K | Band Width | A-T base pair levels |
|------|-----------------|----------|-----------------|-------|---------------|-------------------------|
| 1 | -17.491 | π | -18.024 | 0 | 0.532 | -17.720 |
| 2 | -16.292 | π | -16.618 | 0 | 0.326 | -16.627 |
| 3 | -16.142 | π | -16.469 | 0 | 0.327 | -16.325 |
| 4 | -14.985 | $3/5\pi$ | -15.186 | 0 | 0.201 | -15.155 |
| 5 | -14.586 | π | -14.961 | 0 | 0.375 | -14.957 |
| 6 | -13.955 | π | -14.037 | 0 | 0.081 | -14.007 |
| 7 | -13.968 | π | -13.330 | 0 | 0.362 | -13.396 |
| 8 | -12.686 | π | -12.839 | 0 | 0.153 | -12.818 |
| 9 | -11.894 | 0 | -12.107 | π | 0.213 | -12.209 |
| 10 | -11.018 | π | -11.060 | 0 | 0.042 | -11.041 |
| 11 | -10.498 | π | -10.690 | 0 | 0.192 | -10.863 |
| 12 | - 9.316 | 0 | - 9.615 | π | 0.299 | - 9.706 |
| 13 | - 2.767 | 0 | - 2.843 | π | 0.076 | - 2.833 |
| 14 | - 1.465 | 0 | - 1.567 | π | 0.102 | - 1.737 |
| 15 | - 1.175 | π | - 1.222 | 0 | 0.047 | - 1.196 |
| 16 | - 0.793 | 0 | - 0.869 | π | 0.076 | - 0.084 |
| 17 | - 0.102 | π | 0.096 | 0 | 0.006 | 0.045 |
| 18 | 0.321 | 0 | 0.296 | π | 0.024 | 0.077 |
| 19 | 1.787 | 0 | 1.778 | π | 0.008 | 1.882 |
| 20 | 2.471 | π | 2.410 | 0 | 0.060 | 2.182 |

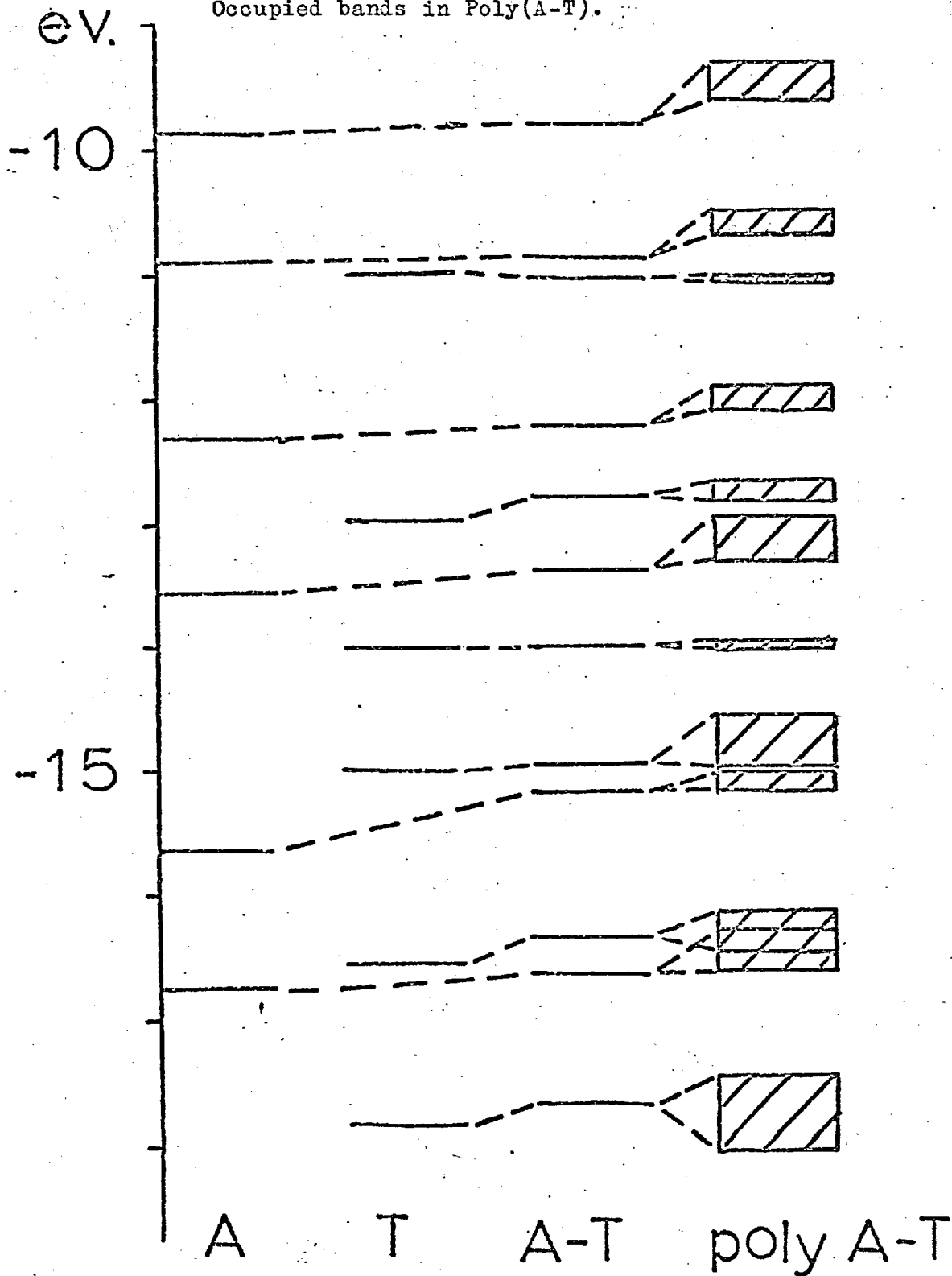
Table 63.

The band structure of poly(G-C) in eV-s

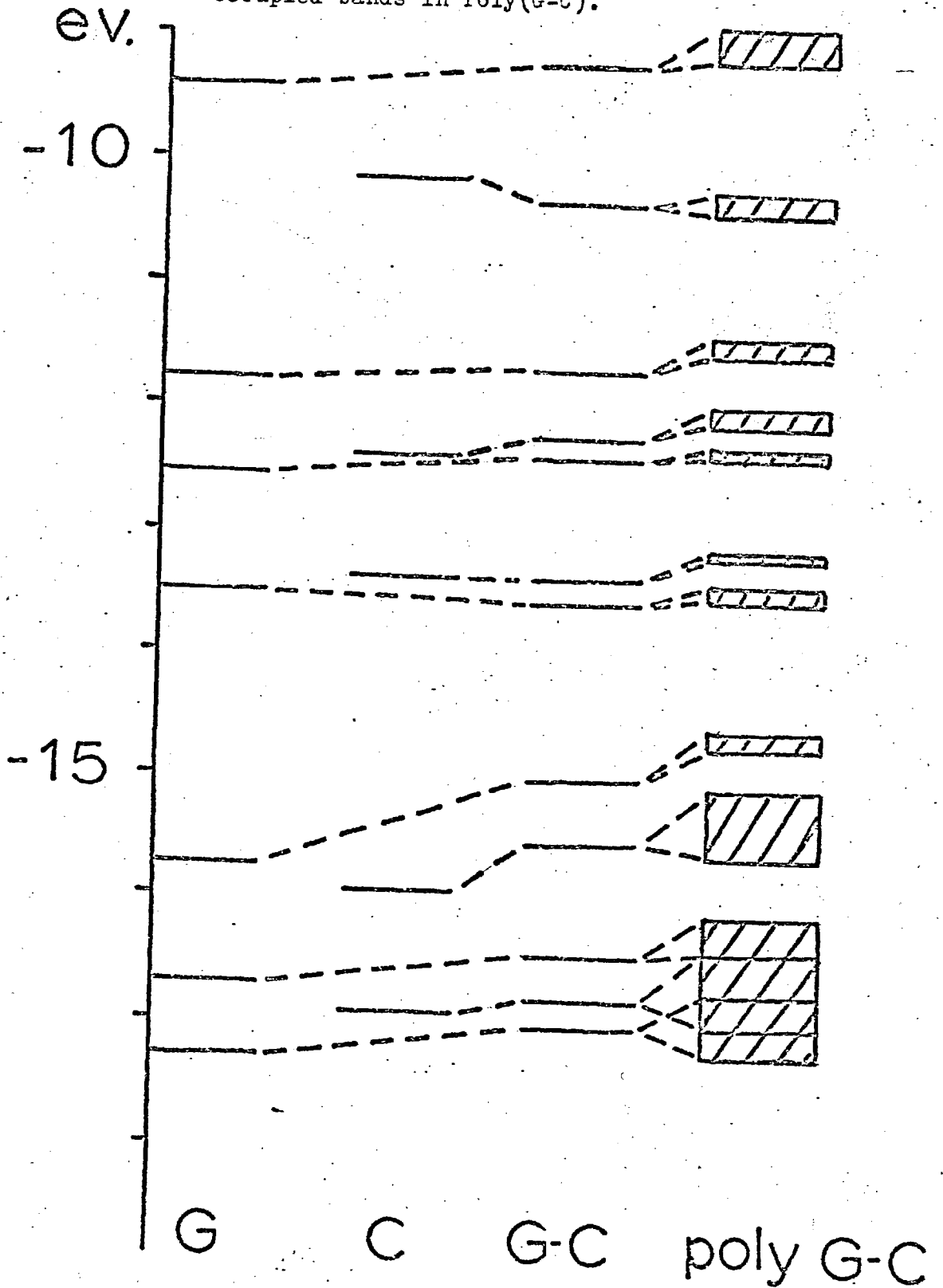
| Band | Maximum E(K) | K | Minimum E(K) | K | Band Width | Molecule G-C level |
|------|-----------------|----------|-----------------|----------|---------------|-----------------------|
| 1 | -16.764 | π | -17.262 | 0 | 0.498 | -17.042 |
| 2 | -16.447 | π | -17.061 | 0 | 0.614 | -16.882 |
| 3 | -16.130 | π | -16.425 | 0 | 0.295 | -16.464 |
| 4 | -15.107 | π | -15.639 | 0 | 0.533 | -15.530 |
| 5 | -14.647 | π | -14.760 | 0 | 0.113 | -15.048 |
| 6 | -13.436 | π | -13.546 | 0 | 0.110 | -13.582 |
| 7 | -13.158 | π | -13.210 | 0 | 0.052 | -13.385 |
| 8 | -12.296 | $4/5\pi$ | -12.408 | 0 | 0.112 | -12.415 |
| 9 | -11.993 | π | -12.141 | 0 | 0.148 | -12.262 |
| 10 | -11.392 | 0 | -11.551 | π | 0.159 | -11.701 |
| 11 | -10.257 | π | -10.348 | 0 | 0.091 | -10.351 |
| 12 | - 8.900 | 0 | - 9.188 | π | 0.288 | - 9.255 |
| 13 | - 2.821 | 0 | - 2.915 | π | 0.094 | - 2.900 |
| 14 | - 2.076 | π | - 2.170 | 0 | 0.093 | - 2.311 |
| 15 | - 0.721 | $3/5\pi$ | - 0.755 | π | 0.035 | - 0.923 |
| 16 | - 0.622 | 0 | - 0.675 | $3/5\pi$ | 0.053 | - 0.711 |
| 17 | 0.026 | 0 | 0.086 | π | 0.112 | - 0.205 |
| 18 | 1.183 | π | 1.169 | 0 | 0.014 | 1.119 |
| 19 | 2.181 | π | 2.152 | 0 | 0.030 | 1.932 |

Fig. 30.

Occupied bands in Poly(A-T).



Occupied bands in Poly(G-C).



$0 \leq K \leq 2\pi$, a Fourier fit for the individual band structures was constructed. The Fourier coefficients,

$$\epsilon_{\ell,0} = \frac{1}{2\pi} \int_0^{2\pi} E_{\ell}(K) dK$$

$$\epsilon_{\ell,n} = \frac{1}{\pi} \int_0^{2\pi} E_{\ell}(K) \cos(nK) dK$$

were calculated, with $1 \leq n \leq 5$. These coefficients are shown in Tables 64 and 65 for Poly(A-T) and Poly(G-C) respectively. In all cases, the smooth curve obtained by substituting these Fourier coefficients in the expression,

$$E_{\ell}(K) = \epsilon_{\ell,0} + \sum_{n=1}^5 \epsilon_{\ell,n} \cos(nK)$$

fitted the computed $E_b(K)$ values very well. This comparison of the Fourier synthesis and the eleven points was achieved with the use of the College's IBM Calcomp incremental plotter, thus all graph plotting was automatic. A sample of the output illustrating the degree of correspondence obtained is shown in Fig 32, the continuous curve represents the Fourier synthesis, and the points the calculated values of $E_b(K)$. The band shown is the highest occupied in Poly(A-T), Band 12.

From the results in Tables 62 and 63 it is clear that the occupied bands in Poly(A-T) and Poly(G-C) have appreciable widths. This justifies the delocalized treatment of the π -electrons of the stacked nucleotide bases.

The forbidden band width between the highest filled

Table 64.

Fourier coefficients for the bands of poly(A-T)

| Band ℓ | $E_{\ell,0}$ | $E_{\ell,1}$ | $E_{\ell,2}$ | $E_{\ell,3}$ | $E_{\ell,4}$ | $E_{\ell,5}$ |
|----------------|--------------|--------------|--------------|--------------|--------------|--------------|
| 1 | -17.756 | -0.266 | -0.002 | 0.000 | 0.000 | 0.000 |
| 2 | -16.452 | -0.163 | -0.003 | -0.000 | 0.000 | -0.000 |
| 3 | -16.312 | -0.163 | 0.006 | -0.000 | 0.000 | -0.000 |
| 4 | -15.043 | -0.087 | -0.053 | -0.012 | 0.005 | 0.008 |
| 5 | -14.823 | -0.196 | 0.054 | 0.013 | -0.005 | -0.008 |
| 6 | -13.994 | -0.041 | -0.003 | -0.000 | 0.000 | -0.000 |
| 7 | -13.164 | -0.180 | 0.015 | -0.001 | -0.000 | 0.000 |
| 8 | -12.777 | -0.072 | 0.013 | -0.004 | 0.001 | -0.001 |
| 9 | -11.978 | 0.102 | -0.022 | 0.004 | -0.001 | 0.001 |
| 10 | -11.039 | -0.021 | -0.000 | 0.000 | 0.000 | 0.000 |
| 11 | -10.595 | -0.096 | 0.001 | 0.000 | -0.000 | 0.000 |
| 12 | - 9.461 | 0.149 | -0.005 | 0.000 | 0.000 | -0.000 |
| 13 | - 2.804 | 0.038 | -0.001 | 0.000 | 0.000 | -0.000 |
| 14 | - 1.515 | 0.051 | -0.001 | 0.000 | -0.000 | 0.000 |
| 15 | - 1.199 | -0.023 | 0.000 | 0.000 | 0.000 | 0.000 |
| 16 | - 0.830 | 0.038 | -0.002 | -0.000 | 0.000 | 0.000 |
| 17 | 0.099 | -0.003 | -0.000 | -0.000 | 0.000 | -0.000 |
| 18 | 0.307 | 0.012 | 0.001 | -0.000 | -0.000 | 0.000 |
| 19 | 1.783 | 0.004 | -0.000 | -0.000 | -0.000 | -0.000 |
| 20 | 2.440 | -0.030 | 0.000 | -0.000 | -0.000 | 0.000 |

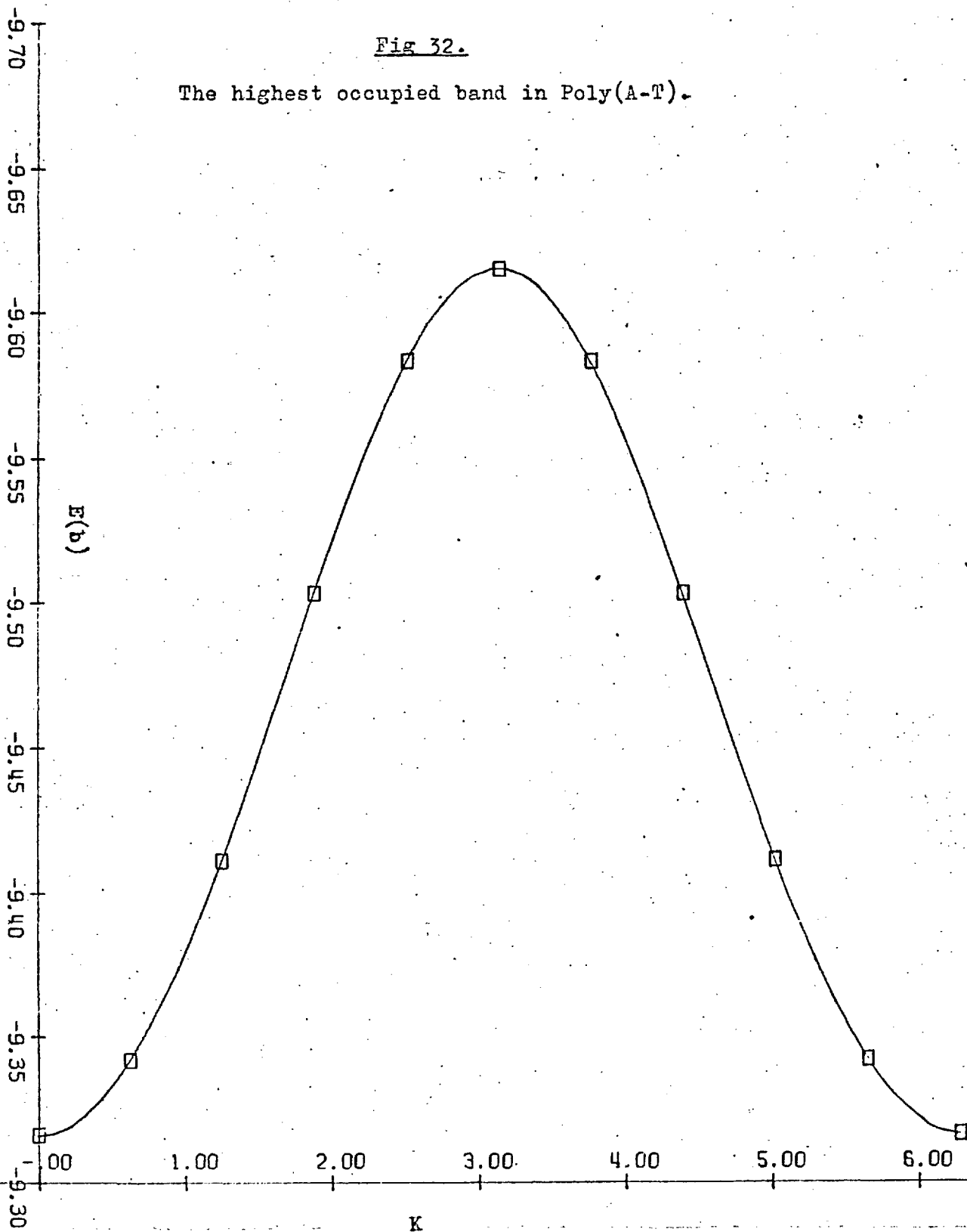
Table 65.

Fourier coefficients for the bands of poly(G-C)

| Band ℓ | $\epsilon_{\ell,0}$ | $\epsilon_{\ell,1}$ | $\epsilon_{\ell,2}$ | $\epsilon_{\ell,3}$ | $\epsilon_{\ell,4}$ | $\epsilon_{\ell,5}$ |
|----------------|---------------------|---------------------|---------------------|---------------------|---------------------|---------------------|
| 1 | -17.002 | -0.248 | -0.012 | -0.001 | 0.000 | 0.000 |
| 2 | -16.761 | -0.310 | 0.008 | 0.003 | -0.001 | 0.000 |
| 3 | -16.289 | -0.145 | 0.011 | -0.003 | 0.001 | -0.000 |
| 4 | -15.378 | -0.266 | 0.006 | 0.000 | -0.000 | 0.000 |
| 5 | -14.696 | -0.057 | -0.008 | 0.001 | -0.000 | 0.000 |
| 6 | -13.487 | -0.055 | -0.004 | 0.000 | 0.000 | -0.000 |
| 7 | -13.190 | -0.026 | 0.006 | -0.000 | -0.000 | 0.000 |
| 8 | -12.333 | -0.054 | -0.022 | 0.001 | 0.001 | -0.000 |
| 9 | -12.095 | -0.072 | 0.029 | -0.002 | -0.001 | -0.000 |
| 10 | -11.460 | 0.078 | -0.011 | 0.002 | -0.000 | 0.000 |
| 11 | -10.303 | -0.046 | 0.001 | 0.000 | 0.000 | 0.000 |
| 12 | -9.042 | 0.144 | -0.002 | 0.000 | 0.000 | 0.000 |
| 13 | -2.866 | 0.047 | -0.002 | 0.000 | 0.000 | 0.000 |
| 14 | -2.124 | -0.047 | 0.001 | -0.000 | 0.000 | -0.000 |
| 15 | -0.733 | 0.007 | -0.015 | 0.002 | 0.001 | -0.001 |
| 16 | -0.655 | 0.022 | 0.013 | -0.002 | -0.001 | 0.001 |
| 17 | -0.031 | 0.056 | 0.001 | -0.000 | -0.000 | -0.000 |
| 18 | 1.176 | -0.007 | 0.000 | -0.000 | -0.000 | 0.000 |
| 19 | 2.167 | -0.015 | -0.000 | -0.000 | -0.000 | -0.000 |

Fig 32.

The highest occupied band in Poly(A-T).



and the lowest empty bands in Poly(A-T) is 6.5 ev., and in Poly(G-C) it is 6. ev. . This gap, however, does not correspond directly to the excitation energy of an electron from the filled band into an empty one . In the treatment of molecular excitations it was seen how additional electron interaction integrals, the Coulomb term, J_{ij} , and the exchange integral, K_{ij} , are needed in the calculation of the transition energy for the excitation of an electron from orbital i to j . With the use of such integrals reasonable predictions of experimental values are possible . For a polymer, clearly both J_{ij} and K_{ij} tend to zero, as the excited electron and the remaining hole are delocalized over the whole of the polymer in the Bloch approximation. The correlation between the hole and the electron is ignored , and it may perhaps be accounted for with the aid of Wannier exciton theory,(8).

The SCF band widths obtained here may be compared with those found in the Hückel approximation , and it is found that the widths are mostly of the same order ,(185) .

Finally it may be noted in Table 66 that the charge distribution of the π -electrons on each monomer of the polynucleotide chain is not appreciably altered from that of the free base-pair.

Poly(U).

This homopolynucleotide was studied from two viewpoints. First the crystal orbital approximation was used to calculate

Table 66.

π -electron charge distributions on Poly(G-C) and Poly(A-T).

| Atom | Poly(G-C) | Free base- pair G-C | Poly(A-T) | Free base- pair A-T |
|------|-----------|------------------------|-----------|------------------------|
| 1 | 1.8730 | 1.8672 | 1.1997 | 1.2003 |
| 2 | .8617 | .8534 | .8768 | .8835 |
| 3 | 1.2034 | 1.1981 | 1.1588 | 1.1560 |
| 4 | .9465 | .9412 | .9386 | .9408 |
| 5 | 1.0517 | 1.0615 | 1.0364 | 1.0387 |
| 6 | .7358 | .7374 | .8832 | .8801 |
| 7 | 1.1182 | 1.1167 | 1.1382 | 1.1378 |
| 8 | .9671 | .9690 | .9491 | .9445 |
| 9 | 1.8624 | 1.8614 | 1.8777 | 1.8765 |
| 10 | 1.9269 | 1.9316 | 1.9416 | 1.9421 |
| 11 | 1.4500 | 1.4568 | 1.8848 | 1.8840 |
| 12 | 1.2229 | 1.2346 | .7326 | .7339 |
| 13 | .7260 | .7278 | 1.8983 | 1.8966 |
| 14 | 1.8778 | 1.8797 | .9226 | .9140 |
| 15 | .9030 | .9007 | 1.0410 | 1.0469 |
| 16 | 1.0587 | 1.0518 | .7346 | .7360 |
| 17 | .8170 | .8110 | 1.3794 | 1.3774 |
| 18 | 1.4699 | 1.4705 | 1.4017 | 1.4056 |
| 19 | 1.9280 | 1.9297 | .9333 | .9328 |
| 20 | | | 1.0716 | 1.0727 |

the band structure as for Poly(G-C) and Poly(A-T), this was the "infinite polymer" treatment. In the second approach, polymers of Uracil consisting of from two to five base residues were examined by treating these "limited polymers" as just one big molecule. In both cases the geometrical relationship between the stacked bases was modelled on the stereochemical structure of natural DNA B, with a translation of 3.36 \AA and a rotation of 36° between neighbouring bases.

The "infinite polymer" was treated with the polymer-SCF program, while the "limited polymer" wave functions were found with a specially modified version of the CS-SCF program. The results obtained for an infinite helical chain of Uracil bases are shown in Tables 67 and 68. The first of these Tables shows the band widths and limits, and compares the bands with the molecular orbital energies. Table 68 gives the coefficients of the Fourier synthesis, which was again very successful in fitting the calculated points. Here only the coefficients up to $n=3$ were required. The results should be compared with Hückel results obtained by Ladik, (184), and also some SCF data published, (223).

After these results for infinite polymers, we turn to the consideration of the polymer analogues, constructed by stacking several Uracil bases together. These small polymers were treated as one large molecule, thus, as for the infinite polymers, complete electron delocalization was allowed.

Table 67.

The π -electron band structure of Poly(U).

| Band b | Maximum | | Minimum | | Band width | Molecular energy |
|-----------|----------|------------------|----------|-------|---------------|---------------------|
| | $E_b(K)$ | K | $E_b(K)$ | K | | |
| 1 | -17.6182 | π | -18.1870 | 0 | .5688 | -17.8171 |
| 2 | -16.4226 | π | -16.6669 | 0 | .2443 | -16.4761 |
| 3 | -14.2060 | $\frac{2}{5}\pi$ | -14.2385 | 0 | .0325 | -14.1911 |
| 4 | -12.9263 | π | -13.0235 | 0 | .0972 | -12.9289 |
| 5 | -11.0654 | π | -11.1077 | 0 | .0423 | -11.0483 |
| 6 | -2.6783 | 0 | -2.7544 | π | .0761 | -2.6838 |
| 7 | -1.1999 | π | -1.2604 | 0 | .0605 | -1.2049 |
| 8 | .4226 | 0 | .4050 | π | .0176 | .4516 |

Table 68.

Fourier coefficients for the Poly(U) bands .

| Band b | $\epsilon_{b,0}$ | $\epsilon_{b,1}$ | $\epsilon_{b,2}$ | $\epsilon_{b,3}$ |
|-----------|------------------|------------------|------------------|------------------|
| 1 | -17.9021 | -.2844 | -.0005 | .0001 |
| 2 | -16.5482 | -.1219 | .0035 | -.0002 |
| 3 | -14.2172 | -.0159 | -.0055 | .0001 |
| 4 | -12.9781 | -.0485 | .0033 | .0000 |
| 5 | -11.0866 | -.0212 | .0001 | .0000 |
| 6 | -2.7157 | .0381 | -.0007 | .0000 |
| 7 | -1.2304 | -.0302 | .0002 | .0000 |
| 8 | .4141 | .0088 | -.0003 | .0000 |

It was of interest to examine to what extent this freedom of π -electron exchange between the bases was utilized by the SCF single electron wave functions. Here, unlike the case in the crystal orbital approximation with Bloch wave functions, excessive delocalization was not imposed by the theoretical treatment applied.

Due to the large size of the effective eigenvalue problem obtained by treating a system of up to five Uracil bases as a single molecule, only ten SCF iterations were allowed in all cases, which usually meant convergence of at least .01 ev. in the orbital energy values between successive iterations.

The maximum and minimum orbital energies found for a given π -electron "band", obtained by the splitting of identical electron states in the formation of the short polymers, are shown in Table 69 together with the band widths for the polymers of five or less Uracil residues. The reason it is possible to assign a particular orbital energy as belonging to a particular "band", is that within the limited polymers the individual base units retain a high degree of autonomy. Individual orbital electron distributions as represented by the appropriate eigenvectors tend to be strongly localized on one or other of the bases. The electrons do not delocalize any further than their nearest neighbours, and manage to retain their molecular identities.

This limited degree of delocalization which the π -electrons have is further reflected by the optical transitions which are

Table 69

Band width in analogues of Poly(U) .

| U | U*U | | U*U*U | | U*U*U*U | | U*U*U*U*U | |
|---------|---------|--------------|---------|--------------|---------|--------------|-----------|--------------|
| | E_i | ΔE_i | E_i | ΔE_i | E_i | ΔE_i | E_i | ΔE_i |
| -17.817 | -17.997 | .281 | -18.069 | .413 | -18.109 | .484 | -18.114 | .542 |
| | -17.715 | | -17.656 | | -17.626 | | -17.571 | |
| -16.476 | -16.579 | .143 | -16.621 | .235 | -16.638 | .281 | -16.635 | .317 |
| | -16.435 | | -16.386 | | -16.356 | | -16.318 | |
| -14.191 | -14.247 | .088 | -14.272 | .160 | -14.262 | .178 | -14.281 | .231 |
| | -14.160 | | -14.112 | | -14.084 | | -14.050 | |
| -12.929 | -12.979 | .066 | -12.989 | .083 | -13.008 | .129 | -13.001 | .160 |
| | -12.913 | | -12.906 | | -12.879 | | -12.841 | |
| -11.048 | -11.141 | .162 | -11.170 | .251 | -11.159 | .273 | -11.178 | .326 |
| | -10.978 | | -10.919 | | -10.886 | | -10.852 | |
| -2.684 | -2.774 | .162 | -2.804 | .252 | -2.796 | .276 | -2.817 | .329 |
| | -2.612 | | -2.552 | | -2.520 | | -2.487 | |
| -1.205 | -1.294 | .152 | -1.263 | .115 | -1.254 | .129 | -1.246 | .131 |
| | -1.142 | | -1.149 | | -1.125 | | -1.115 | |
| .452 | .348 | .182 | .318 | .271 | .330 | .291 | .305 | .348 |
| | .530 | | .589 | | .621 | | .653 | |

- Note: (a) The various polymers are denoted, U, U*U, U*U*U, and so on.
 (b) The limiting energies of the 'bands', E_i are above each other . ΔE_i is the pseudo-band width.
 (c) Compare these bands with those in Table 67 .

shown in Table 70 . The molecular sizes precluded any form of configuration interaction so the virtual levels were used in a straight forward manner to obtain the excitation energies. The electronic transitions could be directly identified with individual transitions occurring in one or other of the base units , and could thus be compared with the free base transitions. The transitions in the polymers were labelled as a result of comparison with the free base excitations. All the "allowed" transitions were very similar to the free base excitations, and hence could be interpreted as transitions between single electron states strongly localized on individual molecules of the polymer. All charge-transfer transitions appeared as "forbidden" excitations, as the degree of electron delocalization was so low in the higher occupied orbitals and the virtual levels. These transitions are not shown in Table 70 .

Thus it would appear that even in a polymer, the inter-base interactions of the π -systems of the Uracil monomers are unable to induce sufficient delocalization in the optical states to give transitions appreciably different to those of the free base . A model with "localized excitations" appears applicable, and the treatment of optical excitations as electronic transitions between energy bands with no electron/hole correlation seems incorrect .

Table 70.

Electronic transitions in stacks of up to five Uracil bases.

| Transition 5,6 | | | Transition 5,7 | | | Transition 4,6 | | | Transition 4,7 | | | N |
|----------------|-------|--------------|----------------|-------|--------------|----------------|-------|--------------|----------------|-------|--------------|---|
| ΔE_s | f_s | ΔE_t | ΔE_s | f_s | ΔE_t | ΔE_s | f_s | ΔE_t | ΔE_s | f_s | ΔE_t | |
| 5.67 | .926 | 2.23 | 6.39 | .065 | 6.09 | 6.88 | .044 | 6.14 | 8.23 | .532 | 5.08 | 1 |
| 5.66 | .894 | 2.31 | 6.24 | .768 | 6.00 | 6.93 | .045 | 6.37 | 8.30 | 1.46 | 5.84 | 2 |
| 5.70 | 1.32 | 2.29 | 6.56 | .064 | 6.25 | 7.19 | .207 | 6.50 | 8.48 | .524 | 5.70 | |
| 5.66 | .858 | 2.41 | 6.36 | .041 | 6.15 | 7.23 | .195 | 6.76 | 8.58 | 1.05 | 6.59 | 3 |
| 5.70 | 1.26 | 2.48 | 6.53 | .643 | 6.31 | 7.42 | .033 | 7.03 | 8.72 | .160 | 7.42 | |
| 5.70 | .899 | 2.30 | 6.61 | .060 | 6.30 | 7.67 | .026 | 7.18 | 9.03 | .374 | 7.01 | |
| 5.67 | .761 | 2.66 | 6.68 | .055 | 6.39 | | | | | | | 4 |
| 5.71 | .756 | 2.65 | 6.70 | .069 | 6.50 | | | | | | | |
| 5.70 | .887 | 2.33 | 6.82 | .026 | 6.68 | | | | | | | |
| 5.72 | 1.01 | 2.94 | 7.00 | .517 | 6.83 | | | | | | | |
| 5.66 | .894 | 2.31 | 7.03 | .026 | 6.86 | 6.92 | .035 | 6.41 | 8.79 | .029 | 7.16 | 5 |
| 5.70 | 1.23 | 2.58 | 7.08 | .375 | 6.95 | 7.41 | .010 | 6.97 | 8.79 | .307 | 7.43 | |
| 5.73 | .790 | 2.61 | 6.65 | .051 | 6.45 | 7.53 | .158 | 7.10 | 9.10 | .291 | 8.01 | |
| 5.80 | .407 | 3.58 | 6.73 | .078 | 6.49 | 7.72 | .007 | 7.49 | 9.04 | .290 | 8.02 | |
| 5.76 | .374 | 3.56 | 6.23 | .050 | 5.99 | 7.78 | .026 | 7.42 | 8.67 | .451 | 6.88 | |

Note:(a) All excitations are given in evs. .

(b) N is the number of monomers in the polymer.

(c) Results are missing for the polymer U*U*U*U due to a computer program fault.

From all this it must not be inferred that no π -electron delocalization occurs between the residues in a polymer of weakly interacting bases such as Poly(U) . As may be seen from Table 70 , the excited singlets and triplets do tend to move to higher energies, and there is evidence for a hypochromic effect, especially in the lowest singlet , which is in agreement with experimental observations,(166) .

Finally it must be remembered that a five residue polymer is a very poor approximation of an infinite one, none of the effects discussed seem to have converged and the results even for five bases stacked together may still be dominated by end-effects . Unfortunately calculations on polymers with more than five monomers were impossible for reasons of computer time.

(3) Comments on the Results.

Most of the individual results which have been presented either speak for themselves, or have been discussed in context . Some generalities may however be made, and several conclusions drawn.

First we may reflect on the results obtained for the polymeric systems of π -conjugated molecules . Unfortunately here we can make no direct appeal to experimental work to confirm our calculations . As we would have expected intuitively , it is predicted that in these polymeric systems of weakly interacting π -conjugated molecules , the constituent

molecular units will retain a high degree of their individuality. Some π -electron delocalization does occur in the lower energy molecular orbitals, but the use of the Bloch crystal orbital approximation may well over emphasize this. Confirmation of this comes from the experimental observation that the spectrum of the DNA chain closely corresponds to that of the superimposed spectra of its nucleotide base constituents. The optical excited states of the chain seem essentially localized. All these comments hinge on the interpretation put upon the results obtained for the polymer analogues, constructed from several stacked repeating base units.

In the assessment of the molecular results much experimental data is readily available, and generally the theoretical values seem in fair agreement with their observed counterparts. Considering the assumptions of zero differential overlap and the π -electron separability, the Pople-Pariser-Parr method achieves outstandingly successful results. The semi-empirical approach succeeds in the accurate prediction of optical spectra and spin-densities for a variety of molecules using the CS-SCF-CI, the spin-polarized or the Roothaan methods. Even reasonable values of the molecular ionization potential may be directly calculated. An excessive degree of parameter variation is not required, and the normally acceptable semi-empirical values of the resonance integrals and two centre integrals give good results for a whole series of

molecules . In one case where other workers have found it necessary to depart from the semi-empirical two centre integrals to reproduce experimental spin densities , it has been shown that this was entirely due to their neglect to ensure that the total molecular wave function was an eigenfunction of S^2 , (196).

The excited triplet states of molecules seem to be poorly predicted by all the techniques used. All methods did, however, tend to give the same value , which was usually too low . Singlet spectra were much easier to predict . It was found that often apparently good results obtained with the CS-SCF-CI method could be effectively ruined by increase in the number of configurations taken in deriving the triplet state.

Before concluding we must acknowledge the degree of equivalence in all these different molecular methods, as witnessed by the similar results often obtained by applying various methods to the same molecular state . The Roothaan and spin-polarized open-shell procedures are very similar , since although the latter does not impose from the outset spin-pairing on the electrons in the closed-shell, it does so eventually in the spin projection routine , used to obtain a "good" eigenfunction of S^2 . In this procedure effective spin-pairing is re-introduced within the closed-shell.

Finally it may be seen that the molecular methods discussed and applied in Chapters II ,III, and IV , represent reasonably sound approaches , which in view of their sweeping

assumptions and often gross neglects, give surprisingly good results. More work is needed in improving the "rigour" with which the molecular problem is approached. A more "ab initio" treatment is required so that the empirical nature of the approach may be replaced with a more deterministic one. The polymer field needs much more investigation, concerning the best model to use, and how to treat excited states. The results presented here are merely preliminaries to the whole electronic problem of weakly interacting systems.

REFERENCES.

- (I) G.Cario & J.Franck, Z. Physik. ,17,202,(1923).
- (2) J.Perrin & Choucroun, C.R. hebd. Seances Acad. Sci.,189,1213,
(1929).
- (3) F.Perrin,Ann. Chim. Physique,17,283,(1932).
- (4) H.Kallman & F.London,Z. physik. Chem.,2,207,(1928).
- (5) Th.Förster, Ann. der Physik ,2,55,(1948).
- (6) Th.Förster,Excitation Transfer, in "Comparative Effects of
Radiation", M.Burton,J.S.Kirby-Smith,& J.L.Magee,eds.(Wiley,N.Y.,
1961),p.300 .
- (7) L.I.Schiff,"Quantum Mechanics", McGraw-Hill,N.Y.,(1955).
- (8) J.S.Avery,Ph.D. Thesis,Imperial College,London University,1965.
- (9) P.O.Löwdin, Biopolymers Symposia ,1,293,(1964).
- (10) D.L.Dexter, J. Chem. Phys.,21,836,(1953).
- (II) J.S.Avery, in "Physical Processes in Radiation Biology",
A.P.,1964.
- (12) W.T.Simpson, Radiation Res.,20,87,(1963).
- (13) M.D.Galanin, Soviet Physics,JETP,1,317,(1955).
- (14) K.B.Eisenthal & S.Seigel, J. Chem.Phys.,41,652,(1964).
- (15) N.F.Mott & I.N.Sneddon,"Wave Mechanics and its Applications",
Dover,N.Y.,1963.
- (16) P.Pringsheim, "Fluorescence and Phosphorescence",Interscience,
N.Y.,1949.
- (17) Th.Förster,"Fluorescence Organischer Verbindungen",
Vandenhoeck & Ruprecht, Göttingen,1951.
- (18) Th.Förster,Z. Electrochem.,53,93,(1949).

- (19) Th.Förster, Disc.Far.Soc.,27,7,(1959).
- (20) W.T.Simpson & D.L.Peterson,J. Chem. Phys.,26,588,(1957).
- (21) E.G.McRae & M.Kasha, in "Physical Processes in Radiation Biology",A.P.,1964.
- (22) M.Kasha, "Classification of Excitons", in "Physical Processes in Radiation Biology",A.P.,1964.
- (23) V.L.Ermoleav & A.N.Terenin,"Pamiati S.I.Vavilova",p.135, Moscow,1952. (Eng. trans: NRC TT-540)
- (24) A.N.Terenin & V.L.Ermoleav, Dokl. Akad. Nauk. SSSR., 85,547,(1952). (Eng. trans: NRC TT-529)
- (25) A.Weinreb, p.44 in "Luminescence of Organic and Inorganic Materials", H.P.Kallman & G.M.Spruch,eds.,Wiley,N.Y.,1962.
- (26) J.Feitelson, J. Chem. Phys. ,44,1497,(1966).
- (27) H.P.Kallmann & M.Furst,Phys. Rev.,79,857,(1950).
- (28) H.W.Leverenz,"An Introduction to Luminescence of Solids", Wiley,N.Y.,1950.
- (29) A.Jablonski, Z.Physik ,13,460,(1931).
- (30) R.K.Swank,L.J.Basile, et al., IRE Trans. Nucl. Sci.,NS-5, 183,(1958).
- (31) D.F.MacDonald,B.J.Dunn,& J.V.Braddock,IRE Trans. Nucl. Sci., NS-7,17,(1960).
- (32) Th.Förster,Z.Naturforsch.,4a,321,(1949).
- (33) R.Livingston,J. Phys. Chem., 61,860,(1957).
- (34) M.Burton & H.Dreeskamp,Disc. Far. Soc. ,27,64,(1959).
- (35) A.Kawski,Ann. der Physik ,8, 116,(1961).
- (36) A.Kawski,Acta Physica Polonica,24,641,(1963).

- (37) M.Inokuti & F.Hirayama, J. Chem. Phys.,43,1978,(1965).
- (38) J.S.Avery & J.C.Packer, "Statistical Aspects of Resonance Energy Transfer", in "The Triplet State",A.B.Zahlan,ed., Cambridge U.P.,1967.
- (39) A.Schmillen,Z. Physik ,135,294,(1953).
- (40) A.Schmillen,"Decay Times of Organic Crystals", in "Luminescence of Organic and Inorganic Materials", H.P.Kallmann & G.W.Spruch, eds.,Wiley,N.Y.,1962.
- (41) W.Kirchhoff,Z. Physik ,116,115,(1940).
- (42) W.Szymanowski,Z.Physik,95,440,(1935).
- (43) E.Bailey & G.Rollenson, J. Chem. Phys.,21,1315,(1953).
- (44) "Symposium on Monte-Carlo Methods",Wiley,N.Y.
- (45) W.H.Melhuish,J. Phys.Chem .,67,1681,(1963).
- (46) A.Weinreb,in "Organic Scintillation Detectors"; Proceedings of the New Mexico Conference, G.H.Daub, et al.,eds,US Gov.Pr.Off..
- (47) R.Hardwick, J. Chem. Phys.,26,323,(1957).
- (48) F.H.Brown,M.Furst,& H.Kallmann,in "Organic Scintillation Detectors",
- (49) E.J.Bowen,Disc. Far. Soc.,27,40,(1959).
- (50) E.J.Bowen, in "Luminescence of Organic and Inorganic Materials",H.P.Kallmann & G.W.Spruch,eds.,Wiley,N.Y.,1962.
- (51) H.Kallmann, "Energy-Transfer Processes",p.342, in "Comparative Effects of Radiation", Wiley,N.Y.,1960.
- (52) J.B.Birks & K.N.Kuchela,Disc. Far. Soc.,27,57,(1959).
- (53) F.H.Brown, M.Furst, & H.Kallmann,Disc. Far. Soc.,27,43,(1959).
- (54) A.Kawski,"Bulletin de l'Academie Polonaise des Sciences", Series des Sceines Math.Astr.et Phys.,VolXII,3,173,(1964).

- (55) A.Kawski & M.Krosnicka, Z. Naturforsch.,20,917,(1965).
- (56) A.Weinreb, J. Chem. Phys.,29,1412,(1958).
- (57) Smoluckowski, Z. Phys. Chem.,92,129,(1917).
- (58) W. Jost , "Diffusion in Solids,Liquids,Gases",A.P.,1960.
- (59) I. Berlmann, in "Luminescence of Organic and Inorganic Materials", H.P.Kallmann & G.W.Spruch, eds.,Wiley,N.Y.,1962.
- (60) A.Terenin & V.Ermolaev,Trans. Far. Soc.,52,1042,(1956).
- (61) C.A.Parker & W.T.Rees, Analyst,85,587,(1960).
- (62) G.K.Rollefson & H.W.Dodgen, J. Chem. Phys.,12,107,(1944).
- (63) J.Lavorel, J. Chem. Phys.,61,864,(1957).
- (64) S.I.Vavilov,"Microstructure of Light",Academie Verlag, Berlin,1954.
- (65) J.B.Birks, in "Organic Scintillation Detectors", Proceedings of the New Mexico Conference, G.H.Daub,et al.,US Gov.Pr.Off..
- (66) P.O.Löwdin,Ann. Rev. Phys. Chem. ,11,(1960)
- (67) R.Daudel,R.Lefebvre,& C.M.Moser,"Quantum Chemistry, Methods and Applications",Interscience,N.Y.,1959.
- (68) M.Born & J.R.Oppenheimer,Ann. Physik ,84,457,(1927).
- (69) K.Ohno,"Notes on Molecular Orbital Calculation of π -Electron Systems", Quantum Chemistry Group,Uppsala,1963.
- (70) D.R.Hartree,"The Calculation of Atomic Structures",Wiley, N.Y.,1957.
- (71) N.Bohr, "Theory of Spectra and Atomic Constitution", Essay 3, "The Structure of the Atom and the Periodic System of the Elements", Cambridge,(1922).
- (72) D.R.Hartree,Proc. Cam. Phil. Soc.,24,89,(1927).
- (73) R.Daudel, Advcs. in Chem. Phys.,1,(1958).

- (74) J.C.Slater, Phys. Rev., 38, 1109, (1931).
- (75) P.O.Löwdin, "Molecular Orbitals in the Exact SCF Theory", in "Molecular Orbitals in Chemistry, Physics and Biology", P.O.Löwdin & B.Pullman, eds., A.P., 1964.
- (76) W.Ritz, J. Reine Angew. Math., 135, 1, (1909).
- (77) H.M.James & A.S.Coolidge, Phys.Rev., 51, 860, (1937)
- (78) R.E.Williamson, Phys. Rev., 62, 538, (1942).
- (79) A.A.Frost, R.E.Kellogg, & E.C.Curtis, Revs. Mod. Phys., 32, 313, (1960).
- (80) R.S.Mulliken, Phys. Rev., 32, 186, 388, 761, (1928).
- (81) V.Fock, Z. Physik, 61, 126, (1930).
- (82) J.C.Slater, Phys. Rev., 35, 509, (1930).
- (83) R.S.Mulliken, J. Chem. Phys., 1, 492, (1933).
- (84) W.Heitler & F. London, Z. Physik, 44, 455, (1927).
- (85) J.R.Platt, et al., "Free-Electron Theory of Conjugated Molecules", Wiley, 1964.
- (86) J.C.Slater, Phys. Rev., 35, 509, (1930).
- (87) N.S.Ham & K.Ruedenberg, J. Chem. Phys., 29, 1199, (1958)
- (88) J.A.Pople, Quart. Rev., 11, 273, (1957).
- (89) E.Hückel, Z. Physik, 70, 204, (1931).
- (90) M.Goeppert-Mayer & A. Sklar, J. Chem. Phys., 6, 645, (1938).
- (91) S.L.Altmann, Proc. Roy. Soc., A210, 327, (1952).
- (92) C.M.Moser, Trans. Far. Soc., 49, 1239, (1953).
- (93) I.G.Ross, Trans. Far. Soc., 48, 973, (1952).
- (94) J.M.Parks & R.G.Parr, J. Chem. Phys., 32, 1657, (1960).

- (95) P.G.Lykos, in "Advances in Quantum Chemistry", Vol 1 ,
P.O.Löwdin, ed., A.P., 1964.
- (96) R.McWeeny & B.T.Sutcliffe, Proc. Roy. Soc., A273, 103, (1963).
- (97) P.G.Lykos & R.G.Parr, J. Chem. Phys., 24, 1166, & 25, 1301, (1956).
- (98) E.T.Stewart, Ph. D. Thesis, Oxford, 1955.
- (99) C.A.Coulson, N.M.March, & S.L.Altmann, Proc. Natl. Acad.
Sci., USA, 38, 372, (1952).
- (100) E.U.Condon & G.H.Shortley, "The Theory of Atomic Spectra",
Cambridge U.P., 1953.
- (101) C.Sandorfy, "Electronic Spectra and Quantum Chemistry",
Prentice-Hall, 1964.
- (102) G. Sansone, "Orthogonal Functions", Interscience, N.Y., 1959.
- (103) C.C.J.Roothaan, Rev. Mod. Phys., 23, 69, (1951).
- (104) M.Goeppert-Mayer & A.L.Sklar, J. Chem. Phys., 6, 645, (1938).
- (105) J.A.Pople, Trans. Far. Soc., 49, 1375, (1953).
- (106) R.Pariser & R.Parr, J. Chem. Phys., 21, 466, 767, (1953).
- (107) J.Hoyland & L.Goodman, J. Chem. Phys., 36, 12, (1962).
- (108) P.O.Löwdin, J. Chem Phys., 18, 365, (1950)
- (109) F.Peradejordi, Compt. Rend., 243, 276, (1963).
- (110) R.McWeeny, Proc. Roy. Soc., A227, 288, (1955).
- (111) G.Leroy, J. Chim. Phys., 60, 1270, (1963).
- (112) J.Katz, et al., J. Chem. Phys., 39, 1683, (1963).
- (113) O.Sovers & W.Kauzman, J. Chem. Phys., 38, 813, (1963)
- (114) R.Breslow & E.Mohacsi, J. Am. Chem. Soc., 85, 431, (1963)
- (115) W.Moffitt, Rept. Prog. Phys., 17, 173, (1954).
- (116) C.E.Moore, "Atomic Energy Levels", Nat. Bur. Stds., USA.

- (117) H.O.Pritchard & H.A.Skinner, Chem. Revs., 55, 786, (1955).
- (118) T.Hinze & J.Jaffe, J. Am. Chem. Soc., 84, 540, (1962).
- (119) C.A.Coulson & L.J.Shard, J. Chem. Phys., 35, 294, (1961).
- (120) I.Fischer-Hjalmars, in "Molecular Orbitals in Chemistry, Physics, and Biology", p.361, A.P., 1964.
- (121) J.Koutecky & J.Paldus, Collect. Czech. Commun., 27, 599, (1962).
- (122) R.G.Parr & B.L.Crawford, J. Chem. Phys., 16, 526, (1948).
- (123) W.E.Moffitt, Proc. Roy. Soc., A210, 224, (1951).
- (124) N.Mataga & K.Nishimoto, Z. Physik. Chem., 13, 140, (1957).
- (125) Y.I'Haya, "Advances in Quantum Chemistry", Vol.1, P.O.Löwdin, ed., A.P., 1964.
- (126) C.A.Coulson, Proc. Roy. Soc., A169, 413, (1939).
- (127) C.A.Coulson & H.C.Longuet-Higgins, Proc. Roy. Soc., 193, 447, 456, & 195, 188, (1948).
- (128) R.McWeeny, Rev. Mod. Phys., 32, 328, (1960).
- (129) G.Berthier, "Self-Consistent Field Methods for Open-Shell Molecules", p.57, in "Molecular Orbitals in Chemistry, Physics, and Biology", P.O.Löwdin & B.Pullman, eds., A.P., 1964.
- (130) C.A.Coulson & H.C.Longuet-Higgins, Proc. Roy. Soc., A191, 39, & A192, 16, (1947).
- (131) B.H.Chirgwin & C.A.Coulson, Proc. Roy. Soc., A291, 196, (1950).
- (132) R.D.Brown, "Molecular Orbital Calculations and Electrophilic Substitution", in "Molecular Orbitals in Chemistry, Physics, and Biology", P.O.Löwdin & B.Pullman, eds., A.P., 1964.
- (133) O.Chalvet, et al., "Application of the Molecular Orbitals to the Study of the Base Strength", in "Molecular Orbitals in Chemistry, Physics and Biology", P.O.Löwdin & B.Pullman, eds., A.P., 1964.

- (134) C.C.J.Roothaan, *Revs. Mod. Phys.*, 32, 179, (1960).
- (135) T.Koopmans, *Physica*, 1, 104, (1933).
- (136) D.H.Hartree, *Proc. Cambridge Phil. Soc.*, 24, 89, (1928).
- (137) G.G.Hall & J.E.Lennard-Jones, *Proc. Roy. Soc.*, A202, 155, (1950).
- (138) R.S.Mulliken, *J. Chim. Phys.*, 46, 497, (1949).
- (139) J.R.Hoyland & L.Goodman, *J. Chem. Phys.*, 33, 946, (1960).
- (140) G.G.Hall, *Trans. Far. Soc.*, 50, 773, (1954).
- (141) H.C.Longuet-Higgins, "Advances in Chem. Phys.", 1, 239, (1958).
- (142) M.Kotani, K.Ohno, & K.Kayama, in "Handbuck der Physik", (1961), S.Flügge, eds., 37, Part 2, Springer, Berlin.
- (143) R.G.Parr, "The Quantum Theory of Molecular Electronic Structure", Benjamin, N.Y., 1963.
- (144) C.A.Coulson & I.Fischer, *Phil. Mag.*, 11, 386, (1949).
- (145) L.Brillouin, "Les Champs 'Self-Consistent' de Hartree et de Fock", Hermann et Cie, Paris, (1934).
- (146) M.J.S.Dewar, *Rev. Mod. Phys.*, 35, 586, (1963).
- (147) D.P.Craig, *Proc. Roy. Soc.*, A200, 474, (1950).
- (148) W.E.Moffitt, *J. Chem. Phys.*, 22, 320, 1820, (1954).
- (149) M.K.Orloff, *J. Chem. Phys.*, 47, 235, (1967).
- (150) K.Ruedenberg, *Rev. Mod. Phys.*, 34, 326, (1962).
- (151) E.A.Hylleraas, "Advances in Quantum Chemistry", Vol 1, P.O.Löwdin, ed., A.P., 1964.
- (152) P.O.Löwdin, *Phys. Rev.*, 97, 1509, (1955).
- (153) M.J.S.Dewar, A.L.H.Chung & N.L.Sabelli, "Electron Correlation in π -Electron Systems"; in "Molecular Orbitals in Chemistry Physics and Biology", P.O.Löwdin & B.Pullman, A.P., 1964.

- (154) J.A.Pople, Proc. Phys. Soc., 68, 81, (1955).
- (155) J.A.Pople & N.S.Hush, Trans. Far. Soc., 51, 600, (1955).
- (156) H.C.Longuet-Higgins & R.G.Sowden, J. Chem. Soc., 1404, (1952).
- (157) A.Clar, "Aromatische Kohlen Wasserstoffe", Springer-Verlag, Berlin, 1941.
- (158) C.W.Wheland & D.E.Mann, J.Chem. Phys., 17, 264, (1949).
- (159) A.Streitwieser, "Molecular Orbital Theory for Organic Chemists", Wiley, N.Y., 1961.
- (160) J.C.Slater, Phys. Rev., 82, 538, (1951).
- (161) J.A.Pople & R.K.Nesbet, J. Chem. Phys., 22, 571, (1954).
- (162) G.Berthier, Compt. Rend. Acad. Sci., 238, 91, (1954).
- (163) G.Berthier, J. Chim. Phys., 51, 363, (1954).
- (164) A.T.Amos & G.G.Hall, Proc. Phys. Soc., A263, 483, (1961).
- (165) A.T.Amos, Mol. Phys., 5, 91, (1962).
- (166) T.A.Hoffmann & J.Ladik, Adv. Chem. Phys., 7, 84, (1964).
- (167) B.Pullman & A.Pullman, "Quantum Biochemistry", Wiley, N.Y., 1963.
- (168) T.Amos & L.Snyder, J. Chem. Phys., 41, 1773, (1964).
- (169) P.O.Löwdin, Phys. Rev., 97, 1509, (1953).
- (170) L.Snyder & T.Amos, J. Am. Chem. Soc., 86, 1647, (1964).
- (171) W.H.Adams, J. Chem. Phys., 39, 23, (1963).
- (172) T.Amos & G.G.Hall, in "Advances in Atomic and Molecular Physics", Vol 1., A.P., 1964.
- (173) H.M.McConnel & D.B.Chesnut, J. Chem. Phys., 27, 984, (1957).
- (174) P.Brovetto & S.Ferroni, Nuovo Cimenta, 5, 142, (1957).
- (175) J.C.Schug, et al., J. Chem. Phys., 37, 330, (1962).

- (176) E.de Boer & S.I.Weissman, J. Am. Chem. Soc.,80,4549,(1958).
- (177) C.A.McDowell, Rev. Mod. Phys.,35,528,(1963).
- (178) R.Hoffmann, J. Chem. Phys.,39,1397,(1963).
- (179) J.W.Moskowitz & M.P.Barnett, J. Chem. Phys.,39,1557,(1963).
- (180) J.Koutecky & R.Zahradnik,Collection Czech. Chem. Commun.,
25,811,(1960).
- (181) J.R.Reitz, Solid State Physics,Vol 1.,A.P.,N.Y.,1955.
- (182) G.Del Re ,J.Ladik, & G.Biczó, Phys. Rev.,155,997.(1967).
- (183) J.Ladik, Acta. Phys. Hung.,18,185,(1965).
- (184) J.Ladik & K.Appel, J. Chem. Phys.,40,2470,(1964).
- (185) J.Ladik & G.Biczó, J. Chem. Phys.,42,1658,(1965).
- (186) F.P.Imad & J.E. Van Ness,"Eigenvalues by the QR-Transform",
IBM-Share Library.
- (187) W.L.Frank,"RWVCTR, Eigenvector Determinator",IBM-Share Library.
- (188) W.Karush, et al.,J. Res. Nat. Bur. Stand.,US,47,45,291,(1951).
- (189) J.H.Wilkinson,"The Algebraic Eigenvalue Problem",Oxford,1965.
- (190) "Tables of Interatomic Distance and Configuration in
Molecules and Ions", Chem. Soc. Pub.,1958.
- (191) R.S.Mulliken, Rev. Mod. Phys.,14,265,(1942).
- (192) R.G.Parr & R.S.Mulliken,J. Chem Phys.,18,1338,(1950).
- (193) R.S.Mulliken,C.A.Rieke,D.Orloff & H.Orloff, J. Chem. Phys.,
17,1248,(1949).
- (194) C.Moore, Nat. Bur. Stands.,US,Circular 467,(1949).
- (195) R.Pariser, J. Chem. Phys.,24,250,(1955).
- (196) J.Ladik, et al.,p.427,"Proceedings of the Conferencè on
some Aspects of Physical Chemistry",Budapest,1966.

- (197) V.A.Tolkachev, et al., Dokl. Akad. Nauk. SSSR., 147, 643, (1962).
- (198) M.Kasha & R.V.Nauman, J. Chem. Phys., 17, 516, (1949).
- (199) H.B.Klevens & J.R.Platt, J. Chem. Phys., 17, 470, (1949).
- (200) D.S.McClure, J. Chem. Phys., 22, 1668, (1954).
- (201) D.Craig, et al., J. Chem. Phys., 22, 1616, (1954).
- (202) D.S.McClure, J. Chem. Phys., 17, 905, (1949).
- (203) A.D.McLachlan, Mol. Phys., 2, 271, (1959).
- (204) A.Carrington, et al., J. Chem. Soc., 947, (1959).
- (205) A.D.McLachlan, Mol. Phys., 3, 233, (1960).
- (206) R.W.Fessenden & R.H.Schuler, J. Chem. Phys., 39, 2147, (1963).
- (207) A.Brickstock, Ph. D. Thesis, Cambridge University, 1954.
- (208) A.Veillard & B.Pullman, J.Theoret. Biol., 4, 37, (1962).
- (209) R.K.Nesbet, Biopolymers Symposia, 1, 129, (1964).
- (210) J.Ladik & K.Appel, Theoret. Chim. Acta , 4, 132, (1966).
- (211) H.Berthod, et al., Theoret. Chim. Acta, 5, 53, (1966).
- (212) H.Berthod, et al., J. Quant. Chem., 1, 123, (1967)
- (213) M.Spencer, Acta Cryst., 12, 59, (1959).
- (214) J.I.Fernandez-Alonso , Advcs. Chem. Phys., 7, 3, (1964).
- (215) H.Berthod & A.Pullman , Biopolymers, 2, 483, (1965).
- (216) B.Pullman , p.237 in "Molecular Biophysics", ed., B.Pullman
& M.Weissbluth , A.P., (1965).
- (217) J.D.Watson & F.H.C.Crick, Nature, 171, 737, (1953), and ,
Proc. Roy. Soc., A223 , 80, (1954).
- (218) J.Ladik & K.Appel, J. Chem. Phys., 40, 2466, (1964).

- (219) A.Pullman & B.Pullman , Biochem. Biophys. Acta,36,343,(1959).
- (220) W. Rhodes & M. Chase , Rev. Mod. Phys.,39,348,(1967) , and,
W.Rhodes , J. Am. Chem. Soc.,83,3609,(1961).
- (221) J.Ladik, Acta Phys. Hung.,11,239,(1960).
- (222) R.Langridge, et al., J. Mol. Biol.,2,38,(1960).
- (223) J.Ladik , D.K.Rai & K.Appel, QB31 ,Quantum Chemistry Group,
Uppsala University,(1966).